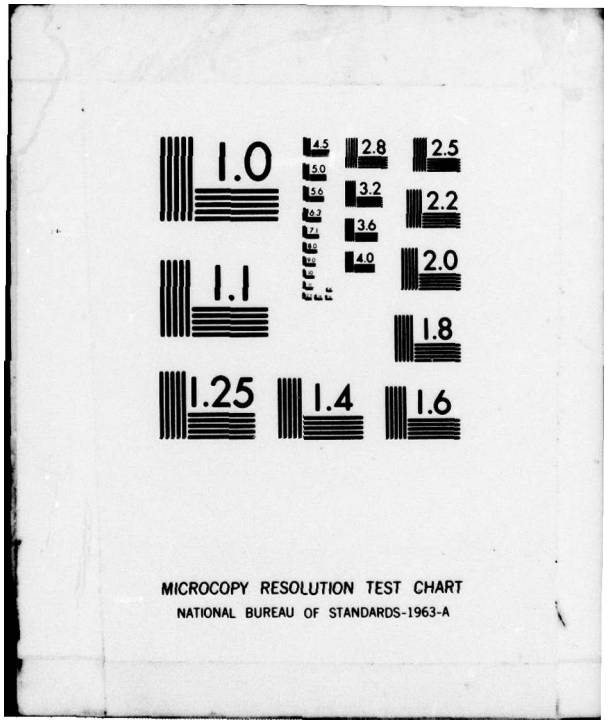
AD-A073 659 UNITED TECHNOLOGIES CORP SUNNYVALE CALIF CHEMICAL SY--ETC F/G 9/1
THE DEVELOPMENT OF IMPROVED NORMAL STRESS TRANSDUCERS FOR PROPE--ETC(U)
JUN 79 E C FRANCIS, R E THOMPSON, W E BRIGGS F04611-75-C-0042

UNCLASSIFIED CSD-2548-FR-VOL-1 AFRPL-TR-79-34-VOL-1 NL

1 OF 3
AD
A073659




1.0
1.1
1.25
1.4
1.6
1.8
2.0
2.2
2.5
2.8
3.2
3.6
4.0
4.5
5.0
5.6
6.3
MICROCOPY RESOLUTION TEST CHART
NATIONAL BUREAU OF STANDARDS-1963-A

AFRPL-TR-79-34

CSD 2548-FR

AD A073659

THE DEVELOPMENT OF IMPROVED NORMAL STRESS TRANSDUCERS FOR PROPELLANT GRAINS

LEVEL II

Volume I

E. C. Francis
R. E. Thompson
W. E. Briggs

Chemical Systems Division
1050 E. Arques
Sunnyvale, CA 94086

June 1979

Final Report for Period March 1975 — December 1978

Approved for Public Release
Distribution Unlimited

DDC FILE COPY

DDC
RECEIVED
SEP 11 1979
A

Prepared for

AIR FORCE ROCKET PROPULSION LABORATORY
DIRECTOR OF SCIENCE AND TECHNOLOGY
AIR FORCE SYSTEMS COMMAND
EDWARDS AIR FORCE BASE, CA 93523

79 09 11 009

NOTICES

When U.S. Government drawings, specifications, or other data are used for any purpose other than a definitely related Government procurement operation, the Government thereby incurs no responsibility nor any obligation whatsoever, and the fact that the Government may have formulated, furnished, or in any way supplied the said drawings, specifications, or other data is not to be regarded by implication or otherwise, or in any manner licensing the holder or any other person or corporation, or conveying any rights or permission to manufacture, use or sell any patented invention that may in any way be related thereto.

FOREWORD

This report was submitted by United Technologies/Chemical Systems Division, Sunnyvale, CA 94086, under contract F04611-75-C-0042, JON 573013 FH with the Air Force Rocket Propulsion Laboratory, Edwards AFB, CA 93523. The report summarizes the technical efforts conducted under this contract from March 1975 to December 1978.

This report has been reviewed by the Information Office/XOJ and is releasable to the National Technical Information Service (NTIS). At NTIS it will be available to the general public, including foreign nations. This technical report has been reviewed and is approved for publication; it is unclassified and suitable for general public release.

Thomas J.C. Chew, Project Manager

Robert L. Geisler, Chief
Propellant Development Branch

FOR THE COMMANDER

Charles R. Cooke, Director
Solid Rocket Division

UNCLASSIFIED

SECURITY CLASSIFICATION OF THIS PAGE (When Date Entered)

REPORT DOCUMENTATION PAGE	READ INSTRUCTIONS BEFORE COMPLETING FORM
1. REPORT NUMBER: AFRPL-TR-79-34-Volume 1	2. GOVT ACCESSION NO. / 3. RECIPIENT'S CATALOG NUMBER
4. TITLE (and Subtitle): THE DEVELOPMENT OF IMPROVED NORMAL STRESS TRANSDUCERS FOR PROPELLANT GRAINS, Volume I.	5. TYPE OF REPORT & PERIOD COVERED: Final Report, for March 1975 - Dec 1978
	6. PERFORMING ORG. REPORT NUMBER: CSD-2548-FR-Vol-1
7. AUTHOR(s): E. C. Francis, R. E. Thompson, W. E. Briggs	8. CONTRACT OR GRANT NUMBER(s): F04611-75-C-0042
9. PERFORMING ORGANIZATION NAME AND ADDRESS: Chemical Systems Division, United Technologies, 1050 E. Arques, Sunnyvale, CA 94086	10. PROGRAM ELEMENT, PROJECT, TASK AREA & WORK UNIT NUMBERS: Program Element 62302 F, Project 5730, Task 13, JON:573013FH
11. CONTROLLING OFFICE NAME AND ADDRESS: Air Force Rocket Propulsion Laboratory, Edwards Air Force Base, CA 93523	12. REPORT DATE: June 1979
	13. NUMBER OF PAGES: 621 Vol. I - 279
14. MONITORING AGENCY NAME & ADDRESS (if different from Controlling Office): 271p.	15. SECURITY CLASS. (of this report): Unclassified
	15a. DECLASSIFICATION/DOWNGRADING SCHEDULE: N/A

16. DISTRIBUTION STATEMENT (of this Report)

Approved for Public Release; Distribution Unlimited

17. DISTRIBUTION STATEMENT (of the abstract entered in Block 20, if different from Report)

18. SUPPLEMENTARY NOTES

19. KEY WORDS (Continue on reverse side if necessary and identify by block number)

Transducer	Finite element analysis
Diaphragm	Stress disturbance
Cantilevered Beam	Axiality
Leadwires	Transducer/propellant interaction factor
Calibration	Zero offset

20. ABSTRACT (Continue on reverse side if necessary and identify by block number)

This report details the CSD effort in the design, analysis, manufacturing, calibration, and embedded use of improved normal stress transducers. Prototype transducers from two different contractors were manufactured and tested as well as final production transducer models. Finite element analysis techniques used for transducer analysis are extensively covered and were used for design optimization and gage interpretation. Results covering gaseous nitrogen calibrations, long term stability, self-heating, diode effects,

DD FORM 1 JAN 73 1473 EDITION OF 1 NOV 65 IS OBSOLETE

UNCLASSIFIED

SECURITY CLASSIFICATION OF THIS PAGE (When Date Entered)

391927

19. KEY WORDS (Continued)

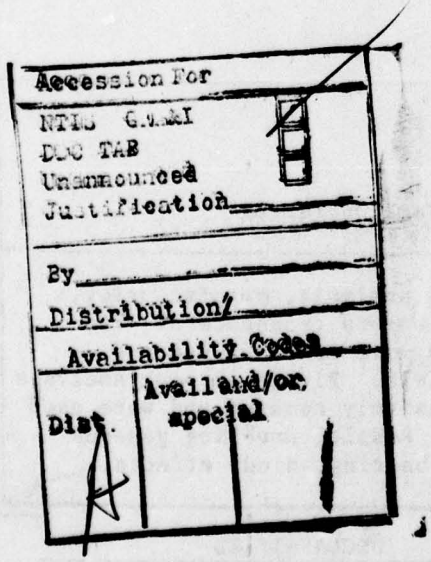
Stress disturbance factor
Constant current
Sensitivity
Semiconductor strain gage
Foil strain gage
Stress transducer
Gage/grain interaction
Full-scale output
EB welding
Glass-to-metal header
Epoxy bond stability
Metal stability
Transducer stability

20. ABSTRACT (Continued)

embedded thermal and pressurization loadings, and mechanical tests are presented and compared with design goals. Detailed manufacturing specifications are presented along with recommended calibration and installation techniques.

The final transducer design is 0.130-in. high with an external prewired compensation package. Stability of the metal and epoxy bond has been optimized by special processing techniques which are presented.

Several significant achievements were obtained during the program. The first computerized design tradeoff curves were generated for stress transducers. Successful electron beam welding of critical components on stress transducers was demonstrated. Transducer measured stress in propellant was verified independently in the tension-compression-shear and TM-1 devices. Transducer response under high rate loading conditions was demonstrated. Agreement between predicted and measured stresses for a thermal loaded solid propellant motor using the thermal-mechanical interaction factor was achieved.



VOLUME I

CONTENTS

Section			Page
1.0	INTRODUCTION		21
	1.1	Design Goals	21
	1.2	Program Outline	31
	1.3	Transducer History Summary	31
		1.3.1 Early Transducer Design - Celesco	31
		1.3.2 Later Transducer Designs - Senso-Metrics	32
		1.3.3 Discussion	37
2.0	STABILITY STUDIES		39
	2.1	Semiconductor Stability	39
	2.2	Epoxy Bond Stability	39
	2.3	Metal Stability	40
	2.4	Experimental Stability Results	44
		2.4.1 Instrumented Cantilevered Beams	44
		2.4.2 Celesco P-95 Transducer 500-Hr Stability Data	77
		2.4.3 Stability Data for Celesco Prototype Transducers	77
		2.4.4 Stability Data for Senso-Metrics Prototype Transducers	80
		2.4.5 Stability Data for Senso-Metrics Production Transducers	80
3.0	FINITE ELEMENT GAGE DESIGN ANALYSIS		85
	3.1	Epoxy Reinforcement Study	85
		3.1.1 Epoxy Thickness	85
		3.1.2 Epoxy Modulus	87
		3.1.3 Surface Roughness	88
	3.2	Optimal External Geometry	89
		3.2.1 Propellant Stress Concentration	90
		3.2.2 Thermal Stress Field Disturbance and Local Stress Change	92
	3.3	Manufacturing Tolerance Study, Preliminary Gage Design	95
	3.4	Diaphragm Thickness Study - Design Considerations	98
4.0	GAGE EXPERIMENTAL RESULTS		106
	4.1	Prototype Transducer Calibrations	106
		4.1.1 Gaseous Nitrogen Calibrations for Celesco Prototype Transducers	106
		4.1.2 Gaseous Nitrogen Calibrations for Senso-Metrics Prototype Transducers	127
		4.1.3 Celesco Prototype Transducers, Self-Heating Studies	133
		4.1.4 Self-Heating Studies for Senso-Metrics Prototype Transducers	134
		4.1.5 Rapid Pressurization Response for Senso-Metrics Prototype Transducer	146

CONTENTS (Continued)

Section			Page
		4.1.6 Tests in Tension/Compression/Shear Device for Senso-Metrics Prototype Transducer	152
	4.2	Production Transducer Calibrations	156
		4.2.1 Gaseous Nitrogen Calibrations for Senso-Metrics Production Transducers	156
		4.2.2 Determination of Stress Disturbance and Propellant-Transducer Interaction Factor	166
		4.2.3 Senso-Metrics Production Transducers, Testing in Tension/Compression/Shear Device	171
		4.2.4 Senso-Metrics Production Transducers in Circular Port TM-1 Motors	187
		4.2.5 Theoretical Thermal Stress Prediction for TM-1 Motor Cooldown	193
5.0	FINITE ELEMENT ANALYSIS OF STRUCTURAL TEST FIXTURES		200
	5.1	Structural Analysis of Celesco Designs	200
		5.1.1 Finite Element Analysis of Celesco Design	205
	5.2	End-Burner Test Fixture for Senso-Metrics, Inc., Transducers	213
		5.2.1 Early Transducer Disturbance and Propellant Interaction Effects	216
	5.3	Shear Fixture	226
		5.3.1 Shear Fixture with Preliminary Gage Design	226
		5.3.2 Tension/Compression/Shear Fixture with Final Gage Design	230
	5.4	Circular Port Grain	233
	5.5	Stress Field Disturbance	236
6.0	COMPARISON OF RESULTS WITH DESIGN GOALS		242
	6.1	Intrinsic Safety and Excitation Voltage	242
	6.2	Frequency Response	242
	6.3	Low Range Transducer Overpressure Ability	243
	6.4	Physical Size	243
	6.5	Operating Temperature Range	243
	6.6	Environmental Protection	244
	6.7	Age and Service Life	244
	6.8	Leadwire Construction	244
	6.9	Cost	245
	6.10	Insensitivity to Out-of-Plane Stresses	245
	6.11	Transducer Accuracy	245
7.0	TRANSDUCER CALIBRATION AND APPLICATION TECHNIQUES		250
	7.1	Hardware Description	250
	7.2	Test Techniques	251
		7.2.1 No-Load Zero Offset Measurements	251
		7.2.2 Pressure Calibration Measurements	251
	7.3	Data Reduction Techniques	255
		7.3.1 No-Load Zero Offset Data Reduction	255

CONTENTS (Continued)

Section		Page
	7.3.2 Pressure Sensitivity Data Reduction	256
	7.4 Stress Transducer Installation Procedure	260
	7.5 Field Measurement of Stress Transducer Output	263
8.0	CONCLUSIONS AND RECOMMENDATIONS	269
	8.1 General Conclusions	269
	8.2 Design Tradeoff and Fabrication Conclusions	270
	8.3 Metal Stability Study Conclusion	271
	8.4 Epoxy Adhesive Conclusion	272
	8.5 Beam Test Conclusions	272
	8.6 Finite Element Analysis Conclusions	273
	8.7 Transducer Application Conclusion	273
	8.8 Recommendations	275
	ABBREVIATIONS	277
	LIST OF SYMBOLS	278

VOLUME II

APPENDIX A:	Celesco Tradeoff Study	A-283
APPENDIX B:	Celesco Transducer Compensation	B-313
APPENDIX C:	Celesco Prototype Transducer Drawings	C-323
APPENDIX D:	Celesco P-95 Transducer 500-Hour Stability Data	D-347
APPENDIX E:	Comparison of 17-4 PH and 15-5 PH Stainless Steel Properties Precipitation Hardenable Stainless Steel	E-381
APPENDIX F:	ARMCO Data - 15-5 PH VAC CE	F-395
APPENDIX G:	Stress in the Transducer Diaphragm Due to Thermal Shock During Heat Treatment	G-419
APPENDIX H:	Plastic Deformation Analysis of Diaphragm for Overpressure Conditions	H-427
APPENDIX I:	Minco Platinum Temperature Sensor Specification and Calibration Tables	I-439
APPENDIX J:	Vishay Resistor Stability Data	J-479
APPENDIX K:	Instrumented Beam Test Procedure and Trouble-shooting Guides	K-499
APPENDIX L:	Epoxy Creep Evaluation Test Uncertainty Analysis	L-513
APPENDIX M:	General Uncertainty Analysis	M-529
APPENDIX N:	Drawings, Processes, Specifications of the 601156 Low Profile Transducer Final Design	N-561

ILLUSTRATIONS

Figure		Page
1	Gage Bond System Modulus and Thickness	25
2	Solid Propellant Thermal Pull-In	27
3	Embedded Transducer Stress Conditions	27
4	Embedded Stress Response vs Propellant Shear Modulus for Older Type Transducer (by Fitzgerald and Hufferd)	28
5	Typical Designs in Rigid End-Burner Fixture	29
6	Development of Improved Normal Stress Transducers for Propellant Grains	33
7	Early in Situ Transducer Designs - Celesco	35
8	Second Generation Stress Transducer - Senso-Metrics, Inc.	35
9	Cross Section of Senso-Metrics Transducer Prototype	36
10	Low Profile Senso-Metrics Stress Transducer	36
11	Low Profile Senso-Metrics Stress Transducer Assembly	37
12	Typical Stress-Strain Curve	41
13	Typical PEL Determination	41
14	Total Creep Curves of 310 Stainless Steel at 85^{o}F	43
15	Total Creep Curves of 310 Stainless Steel at 150^{o}F	43
16	Total Creep Curves of 310 Stainless Steel at 200^{o}F	43
17	Instrumented Constant-Strain Beam	49
18	Beam Test Configuration	49
19	Typical Circuit Diagram, Epoxy Creep Monitoring Test	50
20	Conditioning Ovens for Constant-Strain Beams	50
21	Stress Transducer No-Load Output Data Acquisition System	78
22	Celesco Prototype Transducer Zero Offset History (25-psi Gages)	79

ILLUSTRATIONS (Continued)

Figure		Page
23	Celesco Prorotype Transducer Zero Offset History (2,000-psi Gage)	79
24	Zero Offset Histories for Senso-Metrics Prototype Transducers	81
25	Zero Offset Histories for Senso-Metrics Stress Transducer (Model No. 601156; 2,000-psi, Low Profile Models)	82
26	Zero Offset History for Senso-Metrics Stress Transducer (Model No. 601156; 25-psi, Low Profile Models)	82
27	Zero Offset History for Senso-Metrics Stress Transducer (Model No. 601156; 25-psi, Low Profile Model)	83
28	Zero Offset History for Senso-Metrics Stress Transducer Model No. 601156 (2,000-psi, Low Profile Models)	83
29	Zero Offset History for Senso-Metrics Stress Transducers	84
30	Gage Bond System	86
31	Epoxy Coated Diaphragm Model	86
32	Epoxy Transfer Function Model	88
33	Strain Gradient Through Steel/Epoxy/Silicon for Three Epoxy Moduli	88
34	Surface Roughness Model and Calculated Stresses	89
35	End-Burner Test Vehicle Used for Gage External Geometry Analyses	91
36	External Geometry Analysis Models	91
37	Stress Concentration Factors -$60^{o}/90^{o}$ Design	93
38	Stress Concentrations in Propellant Surrounding Gage and Design Variations for Thermal Loading	93
39	Axial Stress Distribution with and without Gage	94
40	Normal Distribution with and without Gage	94

ILLUSTRATIONS (Continued)

Figure		Page
41	Effect of Gage Geometry on Propellant Stress Disturbance at 1 in.	95
42	Effect of Critical Component Tolerances on Beam Gage Output	97
43	Effect of Weld Joint Tolerances	97
44	Propellant Modulus Interaction vs Diaphragm Thickness - Senso-Metrics Gages (Diaphragm Diameter = 0.125)	98
45	Gage Design Selection Tradeoffs	99
46	Diaghragm Gage Design Curve (0.005-in. Fillet Radius)	100
47	Beam Gage Design Curve (Beam Width = 0.042 in. Except Where Noted)	101
48	Effect of Support Condition on Maximum Diaphragm Stress (Hydrostatic Loading: P = 100; Diaphragm t = 0.0105)	102
49	Effect of Corner Fillet Radius on Diaphragm Stress (Hydrostatic Loading; Diaphragm t = 0.0105)	102
50	Overpressure and Yield Stress Design Curve	104
51	Propellant Interaction vs Diaphragm Thickness	104
52	Diaphragm Thickness Design Curve for Output vs Pressure-to-Yield Limit	105
53	Stress Transducer Calibration and Data Acquisition System	107
54	Celesco Prototype Transducer Dry N_2 Calibration Data (S/N A; 25-psi Flat Diaphragm; Side Exit Leads)	108
55	Celesco Prototype Transducer Dry N_2 Calibration Data (S/N B; 25-psi Flat Diaphragm; Side Exit Leads)	108
56	Celesco Prototype Transducer Dry N_2 Calibration Data (S/N C; 25-psi Flat Diaphragm; Side Exit Leads)	109
57	Celesco Prototype Transducer Dry N_2 Calibration Data (S/N 1; 25-psi Cantilevered Beam; Rear Exit Leads)	109

ILLUSTRATIONS (Continued)

Figure		Page
58	Celesco Prototype Transducer Dry N_2 Calibration Data (S/N 2; 25-psi Cantilevered Beam; Rear Exit Leads)	110
59	Celesco Prototype Transducer Dry N_2 Calibration Data (S/N 1; 2,000-psi Cantilevered Beam; Rear Exit Leads)	110
60	Celesco Prototype Transducer Dry N_2 Calibration Data (S/N A; 2,000-psi Flat Diaphragm; Side Exit Leads)	111
61	Senso-Metrics Prototype Stress Transducer Calibration Data at 5-mA Excitation (S/N 6916; 25-psi Diaphragm Transducer)	129
62	Senso-Metrics Prototype Stress Transducer Calibration Data at 5-mA Excitation (S/N 6917; 25-psi Diaphragm Transducer)	129
63	Senso-Metrics Prototype Stress Transducer Calibration Data at 5-mA Excitation (S/N 6920; 25-psi Cantilevered Beam Transducer)	130
64	Senso-Metrics Prototype Stress Transducer Calibration Data at 5-mA Excitation (S/N 6921; 25-psi Cantilevered Beam Transducer)	130
65	Senso-Metrics Prototype Stress Transducer Calibration Data at 5-mA Excitation (S/N 6918; 25-psi Diaphragm Transducer)	131
66	Senso-Metrics Prototype Stress Transducer Calibration Data at 5-mA Excitation (S/N 6922; 2,000-psi Cantilevered Beam Transducer)	131
67	Celesco Prototype Transducer S/N 1 - 25-psi Cantilevered Beam (Self-Heating Stability Test Without Propellant; Excitation Leadwires Connected Normally)	135
68	Celesco Prototype Tranducer S/N 1 - 25-psi Cantilevered Beam (Self-Heating/Stability Test Without Propellant; Excitation Leadwires Connected Normally)	135
69	Celesco Prototype Transducer S/N 1 - 25-psi Cantilevered Beam (Self-Heating/Stability Test Without Propellant; Excitation Leadwires Connected Normally)	136
70	Celesco Prototype Transducer S/N 1 - 25-psi Cantilevered Beam (Self-Heating/Stability Test Without Propellant; Excitation Leadwires Connected Normally)	136

ILLUSTRATIONS (Continued)

Figure		Page
71	Celesco Prototype Transducer S/N 1 - 25-psi Cantilevered Beam (Self-Heating/Stability Test Without Propellant; Excitation Leadwires Connected Normally)	137
72	Celesco Prototype Transducer S/N 1 - 25-psi Cantilevered Beam (Self-Heating/Stability Test Without Propellant; Excitation Leadwires Reversed)	137
73	Celesco Prototype Transducer S/N 1 - 25-psi Cantilevered Beam (Self-Heating/Stability Test Without Propellant; Excitation Leadwires Reversed)	138
74	Celesco Prototype Transducer S/N A - 2,000-psi Flat Diaphragm (Self-Heating/Stability Test Without Propellant; Excitation Leadwires Connected Normally)	138
75	Celesco Prototype Transducer S/N A - 2,000-psi Flat Diaphragm (Self-Heating/Stability Test Without Propellant; Excitation Leadwires Connected Normally)	139
76	Celesco Prototype Transducer S/N A - 2,000-psi Flat Diaphragm (Self-Heating/Stability Test Without Propellant; Excitation Leadwires Connected Normally)	139
77	Celesco Prototype Transducer S/N A - 2,000-psi Flat Diaphragm (Self-Heating/Stability Test Without Propellant; Excitation Leadwires Connected Normally)	140
78	Celesco Prototype Transducer S/N A - 2,000-psi Flat Diaphragm (Self-Heating/Stability Test Without Propellant; Excitation Leadwires Connected Normally)	140
79	Celesco Prototype Transducer S/N A - 2,000-psi Flat Diaphragm (Self-Heating/Stability Test Without Propellant; Excitation Leadwires Connected Normally)	141
80	Celesco Prototype Transducer S/N A - 2,000-psi Flat Diaphragm (Self-Heating/Stability Test Without Propellant; Excitation Leadwires Reversed)	141
81	Celesco Prototype Transducer S/N A - 2,000-psi Flat Diaphragm (Self-Heating/Stability Test Without Propellant; Excitation Leadwires Reversed)	142
82	Senso-Metrics Transducer S/N 6916 - 25-psi Range (Self-Heating Effects on Bare Gage Bonded in Tension/ Compression/Shear Device; Test Temperature = 163°F)	142

ILLUSTRATIONS (Continued)

Figure		Page
83	Senso-Metrics Transducer S/N 6916 - 25-psi Range (Self-Heating Effects on Bare Gage Bonded in Tension/ Compression/Shear Device; Test Temperature = 72°F)	143
84	Senso-Metrics Transducer S/N 6916 - 25-psi Range (Self-Heating Effects on Bare Gage Bonded in Tension/ Compression/Shear Device; Test Temperature = 1°F)	143
85	Senso-Metrics Transducer S/N 6916 - 25-psi Range (Self-Heating Effects on Bare Gage Bonded in Tension/ Compression/Shear Device; Test Temperature = -68°F)	144
86	Senso-Metrics Transducer S/N 6916 - 25-psi Range (Self-Heating Effects While Embedded in Propellant with Gage Bonded in Tension/Compression/Shear Device; Test Temperature = 155°F)	144
87	Senso-Metrics Transducer S/N 6916 - 25-psi Range (Self-Heating Effects While Embedded in Propellant with Gage Bonded in Tension/Compression/Shear Device; Test Temperature = 66°F)	145
88	Senso-Metrics Transducer S/N 6916 - 25-psi Range (Self-Heating Effects While Embedded in Propellant with Gage Bonded in Tension/Compression/Shear Device; Test Temperature = -11°F)	145
89	Senso-Metrics Transducer S/N 6916 - 25-psi Range (Self-Heating Effects While Embedded in Propellant with Gage Bonded in Tension/Compression/Shear Device; Test Temperature = -54°F)	146
90	Senso-Metrics Transducer S/N 6918 - 2,000-psi Range (Self-Heating Effects on Bare Gage with Gage Bonded in End-Burner Device; Test Temperature = 162°F)	147
91	Senso-Metrics Transducer S/N 6918 - 2,000-psi Range (Self-Heating Effects on Bare Gage with Gage Bonded in End-Burner Device; Test Temperature = 72°F)	147
92	Senso-Metrics Transducer S/N 6918 - 2,000-psi Range (Self-Heating Effects on Bare Gage with Gage Bonded in End-Burner Device; Test Temperature = -1°F)	148
93	Senso-Metrics Transducer S/N 6918 - 2,000-psi Range (Self-Heating Effects on Bare Gage with Gage Bonded in End-Burner Device; Test Temperature = -69°F)	148

ILLUSTRATIONS (Continued)

Figure		Page
94	Transducer/Propellant Test Fixture	149
95	Pressure vs Time for High Rate Pressure Test of the End-Burner Device with Embedded 2,000-psi Transducer	150
96	Pressure vs Time for High Rate Pressure Test of the End-Burner Device with Embedded 2,000-psi Transducer	151
97	Pressure vs Time for High Rate Pressure Test of the End-Burner Device with Embedded 2,000-psi Transducer	151
98	Tension/Compression/Shear Transducer Test Device	152
99	Compression Test Results in Compression/Tension/Shear Device, Preliminary Gage Design	156
100	Senso-Metrics Transducer S/N B381 - 25-psi Calibration Data	158
101	Senso-Metrics Transducer S/N B382 - 25-psi Calibration Data	158
102	Senso-Metrics Transducer S/N B383 - 25-psi Calibration Data	159
103	Senso-Metrics Transducer S/N B384 - 25 psi Calibration Data	159
104	Senso-Metrics Transducer S/N B385 - 25-psi Calibration Data	160
105	Senso-Metrics Transducer S/N B386 - 25-psi Calibration Data	160
106	Senso-Metrics Transducer S/N B387 - 25-psi Calibration Data	161
107	Senso-Metrics Transducer S/N B388 - 25-psi Calibration Data	161
108	Senso-Metrics Transducer S/N B389 - 2,000-psi Calibration Data	162
109	Senso-Metrics Transducer S/N B390 - 25-psi Calibration Data	162
110	Senso-Metrics Transducer S/N B391 - 2,000-psi Calibration Data	163

ILLUSTRATIONS (Continued)

Figure		Page
111	Senso-Metrics Transducer S/N B392 - 25-psi Calibration Data	163
112	Senso-Metrics Transducer S/N B393 - 2,000-psi Calibration Data	164
113	Senso-Metrics Transducer S/N B394 - 2,000-psi Calibration Data	164
114	Senso-Metrics Transducer S/N B395 - 2,000-psi Calibration Data	165
115	Senso-Metrics Transducer S/N B396 25-psi Calibration Data	165
116	Stress Gradients Along Z-Axis Normal to Senso-Metrics Low Profile Stress Transducer Mounted in Tension/ Compression/Shear Device and Subjected to a Pressure Load of 10-psi	168
117	Stress Gradients Along Z-Axis Normal to Senso-Metrics Low Profile Stress Transducer Mounted in Tension/ Compression/Shear Device and Subjected to a Thermal Load of 100-psi	169
118	Stress Gradients Along R-Axis Normal to Senso-Metrics Low Profile Stress Transducer Mounted in TM-1 Subscale Motor and Subjected to a Thermal Load of -100°F	169
119	Test Configuration for Tension/Compression/Shear Device	172
120	Unbond Areas in Shear Fixture with Final Gage Designs	172
121	Test Setup for Tension/Compression/Shear Device Transducer Testing	173
122	Cross Section of TM-1 Motor	188
123	Strain vs Temperature for 25-psi TM-1 Motor	190
124	Maximum Stress vs Temperature for Thermal Testing of TM-1 Motor with 25-psi Gage	190
125	Typical Step Cooldown - Stress vs Temperature for TM-1 Motor (Transducer S/N B396)	191

ILLUSTRATIONS (Continued)

Figure		Page
126	Typical TM-1 Motor Warmup Stress Gage Response (Transducer S/N B396)	191
127	High Rate Pressurization Response in TM-1 Motor (Transducer S/N B393; 2,000 psi)	192
128	High Rate Pressurization Response in TM-1 Motor (Transducer S/N B393; 2,000 psi)	192
129	Maximum Stress vs Temperature for Step-Wise Cooldown Test (Transducer S/N B393 in TM-1 Subscale Motor)	194
130	Cooldown Stress vs Time in TM-1 Motor (Transducer S/N B393; 2,000 psi)	194
131	Comparison of Stress Gage Response With Predicted Linear Viscoelastic and of Corrected Linear Viscoelastic Analysis	198
132	Master Modulus Data for UTP-19,360 to 750/6,452 at 3% Strain	198
133	Simultaneous Straining - Cooling Test With Uniaxial Bars of UTP-19,360 to 750/6,452	199
134	Laboratory Test Simulator Concept	201
135	Typical Grain Simulator Sample Grid With and Without Transducer	202
136	σ_z Stress Disturbance at Bond Line for Square Diaphragm Transducer with 100-psi Tensile Load	205
137	σ_z Stress Disturbance at Bond Line for 45° -0.016-in. Corner Diaphragm Transducer with 100-psi Pressure Load	205
138	σ_z Stress Disturbance at Bond Line for 45° -0.016-in. Corner Diaphragm Transducer with -100°F Thermal Load	206
139	σ_z Stress Disturbance at Bond Line for 0.030-in.-Radius Corner Cantilever Beam Transducer with 100-psi Pressure Load	206
140	σ_z Stress Disturbance at Bond Line for 0.030-in.-Radius Corner Cantilever Beam Transducer with -100°F Thermal Load	207
141	Finite Element Modelling Configurations	209

ILLUSTRATIONS (Continued)

Figure		Page
142	Axial Displacement Values for Transducer in Grain Simulator Sample - Thermal Loading	209
143	Axial Displacement Values for Transducer in Grain Simulator Sample (L/D = 1.1) - Pressure Loading	209
144	Cantilevered Beam Platform Bending Data (p = 100 psi, L/D = 0.3)	210
145	Cantilevered Beam Platform Bending Data (P = 100 psi; L/D = 0.3)	210
146	Cantilevered Beam Platform Bending Data (P = 100 psi; L/D = 0.3)	213
147	Cantilevered Beam Platform Bending Data	213
148	Diaphragm Radial Strain Distribution for Thermal Load Modulus Variation	213
149	End-Burner Test Fixture	214
150	Finite Element Model of Gage in End-Burner Fixture	215
151	Comparison of Preliminary and Final End-Burner Model Stresses Without Transducers	215
152	Transducer Stress Disturbance in End-Burner Test Fixture - Pressure Load	217
153	Pressure Loading of End-Burner Fixture	217
154	Transducer Stress Disturbance in End-Burner Test Fixture - Thermal Load	218
155	Diaphragm Radial Strain vs Radial Distance for Senso-Metrics Transducers (2,000-psi Range, in End-Burner Device)	219
156	Strain Integrating Model for Evaluating Interaction Factor	220
157	Senso-Metrics Prototype Transducer Output vs Propellant Modulus in End-Burner Fixture for Pressure Load	224

ILLUSTRATIONS (Continued)

Figure		Page
158	Senso-Metrics Prototype Transducer Output Ratio vs Propellant Modulus in End-Burner Fixture for Pressure Load	224
159	Senso-Metrics Final Design Ratio vs Modulus	225
160	Effect of End-Burner L/D on Transducer Output Ratio for Thermal Load	225
161	Tension/Compression/Shear Test Device	227
162	Model of Shear Sample	227
163	Stress Distribution Along End Plate of Shear Fixture - Thermal Loading	228
164	Stress Distribution Along End Plate of Shear Fixture	228
165	Stress Distribution Along End Plate of Shear Fixture	229
166	Stress Distribution Along End Plate of Shear Fixture	229
167	Shear Fixture with Gage, Prototype Design	230
168	Thermal Loading in Shear Fixture, Prototype Design	230
169	Uniaxial Displacement of Shear Fixture, Prototype Design	231
170	Pressure Plus Displacement Loading in Shear Fixture, Prototype Design	231
171	Thermal Loading in Shear Fixture, Final Design	232
172	Uniaxial Displacement of Shear Test Fixtures - Final Gage Design	234
173	Circular Port Test Motor (TM-1)	234
174	Finite Element Grid for Circular Port TM-1	235
175	Stresses Along Wall of Circular Port TM-1 Without Gage	235
176	Thermal Stress Analysis of TM-1 Circular Port Motor With and Without Final Gage Design Section at L = 5.0 in.	237

ILLUSTRATIONS (Continued)

Figure		Page
177	Thermal Stress Analysis of TM-1 Circular Port Motor With and Without Final Gage Design Section at L = 2.5 in.	237
178	Effect of Gages on Stress Field Along Line Through Diaphragm Outer Surface (TM-1)	237
179	Typical Stress Disturbance Zone	239
180	Effect of Stress Axiality on Stress Field Disturbance, σ_n - Senso-Metrics Gage	239
181	Effect of Stress Axiality on Stress Field Disturbance, σ_r - Senso-Metrics Gage	240
182	Effect of Gage Size on Stress Field Disturbance, σ_n Uniform Stress Field, $\sigma_r/\sigma_n = 1.10$	240
183	Effect of Gage Size on Stress Field Disturbance, σ_r Uniform Stress Field, $\sigma_r/\sigma_n = 1.10$	241
184	Effect of Gage Aspect Ratio on Stress Field Disturbance	241
185	Transducer Accuracy - S/N B383, NBS-Type Calibration	247
186	Transducer Accuracy - S/N B385, NBS-Type Calibration	247
187	Transducer Accuracy - S/N B388, NBS-Type Calibration	248
188	Stress Transducer No-Load Raw Data Sheet	253
189	No-Load Offset Data Acquisition System	254
190	Stress Transducer Calibration and Data Acquisition System	256
191	Stress Transducer Calibration Data Sheet	257
192	Data Reduction Calculation of Transducer Sensitivity and Uncertainty (Method No. 2)	259
193	11-Point Segmented Sensitivity Curve Fit	260
194	Straight-Line Approximation to Calculate Transducer Sensitivity (Method No. 4)	261
195	Filler Plug Details	262

ILLUSTRATIONS (Continued)

Figure		Page
196	Turnbuckle Details	263
197	Zero Offset for Senso-Metrics, Inc. Production Transducers Bonded in Test Devices	264
198	Zero Offset for Senso-Metrics, Inc. Production Transducers Bonded in Test Devices	265
199	Zero Offset for Senso-Metrics, Inc. Production Transducers Bonded in Test Devices	266
200	Zero Offset for Senso-Metrics, Inc. Production Transducers Bonded in Test Devices	267

TABLES

Table		Page
1	Basic Dimensions of 25-psi Transducers	38
2	Comparison of Precision Elastic Limits	41
3	Stimuli Affecting Semiconductor Gage Results	48
4	Epoxy Creep Sensitivity to Extraneous Stimuli	48
5	Beam Stability Test at 90°F. History of Bonded Tension Gage No. 8	53
6	Beam Stability at 90°F. History of Bonded Compression Gage No. 12	55
7	Beam Stability Test at 90°F. History of Reference Compensation Resistors	57
8	Beam Stability Test at 90°F. History of Reference Compensation Resistors and Unbonded Semiconductor Gage	58
9	Beam Stability Test at 120°F. History of Bonded Tension Gage No. 10	61
10	Beam Stability Test at 120°F. History of Bonded Compression Gage No. 18	63
11	Beam Stability Test at 120°F. History of Reference Compensation Resistors	65
12	Beam Stability Test at 120°F. History of Reference Compensation Resistor and Unbonded Semiconductor Gage	67
13	Beam Stability Test at 160°F. History of Bonded Tension Gage No. 6	69
14	Beam Stability Test at 160°F. History of Bonded Compression Gage No. 17	71
15	Beam Stability Test at 160°F. History of Reference Compensation Resistors	73
16	Beam Stability Test at 160°F. History of Reference Compensation Resistor and Unbonded Semiconductor Gage	75
17	Calibration of Celesco Prototypes (S/N A; 25-psi Flat Diaphragm, Side Exit)	112

TABLES (Continued)

Table		Page
18	Calibration of Celesco Prototypes (S/N B; 25-psi Flat Diaphragm, Side Exit)	114
19	Calibration of Celesco Prototypes (S/N C; 25-psi Flat Diaphragm, Side Exit)	116
20	Calibration of Celesco Prototypes (S/N 1; 25-psi Cantilevered Beam, Rear Exit Leads)	119
21	Calibration of Celesco Prototypes (S/N 2; 25-psi Cantilevered Beam, Rear Exit Leads)	121
22	N_2 Calibration of Celesco Prototype Transducer (S/N 1; 2,000-psig Cantilevered Beam, Rear Exit)	124
23	N_2 Calibration of Celesco Prototype Transducer (S/N A; 2,000-psig Diaphragm, Side Exit)	125
24	Senso-Metrics Prototype Transducer Summary at 70°F and 5-mA Excitation	132
25	High Rate Pressurization Response (Without Propellant) For Senso-Metrics Stress Transducer (S/N 6918; 2,000-psi Diaphragm Gage)	150
26	Compression Test Results For Tension/Compression/ Shear Device	153
27	Tensile Test Results For Tension/Compression/ Shear Device	154
28	Shear Test Results For Tension/Compression/ Shear Device	155
29	Senso-Metrics Production Transducers	157
30	Compression Test Results at 144°F Senso-Metrics, Inc. Production Transducers	175
31	Compression Test Results at 98°F Senso-Metrics, Inc. Production Transducers	176
32	Compression Test Results at Ambient Temperature Senso-Metrics, Inc. Production Transducers	177
33	Compression Test Results at Ambient Temperature Senso-Metrics, Inc. Production Transducers	178

TABLES (Continued)

Table		Page
34	Compression Test Results at 0°F Senso-Metrics, Inc. Production Transducers	179
35	Compression Test Results at -61°F Senso-Metrics, Inc. Production Transducers	180
36	Tensile Test Results at 140°F Senso-Metrics, Inc. Production Transducers	181
37	Tensile Test Results at Ambient Temperature Senso-Metrics, Inc. Production Transducers	182
38	Tensile Test Results at 16°F Senso-Metrics, Inc. Production Transducers	183
39	Tensile Test Results at -63°F Senso-Metrics, Inc. Production Transducers	184
40	Shear Test Results at 136°F Senso-Metrics, Inc. Production Transducers	185
41	Shear Test Results at Ambient Temperature Senso-Metrics, Inc. Production Transducers	186
42	Shear Test Results at -3°F Senso-Metrics, Inc. Production Transducers	187
43	Stress Axiality for Grain Simulator Without Transducer - Thermal Load (E_p = 2,000 psi; ΔT = -100°F)	203
44	Stress Disturbance Data for Normal Stress Transducer in Grain Simulator (E = 100 psi; ΔT = -100°F)	204
45	Summary of Normal Stress Transducer Designs and Analysis	208
46	Partial Summary of Computer Data	211
47	Thermal and Pressure Stress Disturbance for Cantilever Transducer	212

TABLES (Continued)

Table		Page
48	Thermal and Pressure Stress Disturbance for Diaphragm Transducer	212
49	Equipment Measurement Accuracies	252

1.0 INTRODUCTION

Structural analysis is usually conducted on all SRMs to predict anticipated stress levels; however, SRM structural failures have occurred even when large margins of safety have been calculated. Development of an independent direct experimental measurement of bond stress values would bypass the limitations of the numerical stress analysis procedures and the uncertainties in the nonlinear viscoelastic properties of solid propellant and would allow more accurate safety margins to be derived. These direct stress measurements also could be used to calibrate stress analysis techniques.

SRM grains tend to change properties after the motors are manufactured, causing variations in motor stress conditions which can induce failures. If a stable and accurate bond stress transducer were available, it could be used as a gage to determine the useful service life of a rocket motor.

Modified pressure transducers have been used to measure solid propellant stresses since the early 1960s, when they were used to measure the normal bond stresses of motors between the soft propellant and the stiff rocket motor case. Accuracy and stability of the early units were found to be poor. Measured values could not be repeated and were often much higher than predicted by finite element stress analysis.

This report details the program conducted by CSD and subcontractors to provide improved stress transducers which eliminate the difficulties encountered with the previous transducer. The design goals used for this improved transducer are discussed below.

1.1 DESIGN GOALS

Intrinsic Safety

Excitation voltage and current levels must be carefully controlled and circuits protected in case shorts or malfunctions occur after the transducers are embedded in the propellant. These safety limits are not the only major restriction on excitation levels because transducer self heating may cause instability

before the safety imposed power level of 300 mV is reached. Solid propellant is an extremely good insulation material because of its rubber content, so heat generated at the strain gage can cause temperature fluctuations.

Frequency Response

The operating frequency range of dc to 2,000 Hz is no direct problem, but use of static calibrations for higher frequency tests may be questioned.

Operating Range

A 1% accuracy level with the high and low range transducers is considered reasonable for state-of-the-art transducers. The 1,000-psi overpressure requirement for the 25-psi design requires either mechanical stops or very stiff transducer design. Because of structural requirements the stiff transducer design has been selected. The 25-psi design would actually be a 250- to 600-psi transducer, temperature compensated and calibrated for the 25-psi range. As expected, output voltages are reduced significantly by taking this approach.

Semiconductor strain gages are used to increase the electrical output level. Use of the overrange transducer design decreases the signal/noise and signal/age drift ratios which are important for signal resolution and long term service life. The use of stable and accurate digital meters (0.000001 V) now available allows the transducer to operate in a much lower voltage range than gages developed in the 1960s.

Operating Temperature

The operating temperature range of -75° to 160°F is adequate for tactical and ballistic missile applications. This low temperature limit makes compensation more difficult, which generally means that the four semiconductor strain gages must be almost perfectly matched to meet the 1% accuracy requirement over the entire temperature range.

Chemical Protection

Typical solid propellants are highly filled elastomers containing solid oxidizers, powdered metal fuel, and ballistic modifiers. Solid propellants are not corrosive in the normal sense of causing destruction of plastic or metal parts of

a rocket motor; however, solid propellants contain active chemicals which can attack a layer that is a few molecules thick. The chemicals involved are: (1) perchloric acid and hydrochloric acid for propellants containing ammonium perchlorate; (2) oxides of nitrogen and nitric acid for propellants containing nitrocellulose and/or nitroglycerin; (3) hydrofluoric acid for propellants containing high energetic fluoro compounds; (4) solvents (e.g., acetone, toluene, and perchloroethane) used for cleaning parts; and (5) some combustion catalysts like ammonium dichromate.

If the unit being attacked is thin, deterioration of a layer can change the performance of the unit appreciably. Such a change has been demonstrated for wires, solder joints, epoxides, and thin metal diaphragms used in making miniature stress transducers.

Stainless steel 17-4 and 15-5 are among the few metals to survive in this environment; epoxies and other adhesives are attacked and cannot be exposed directly to the propellant. Because of this factor, glass-to-metal feedthroughs are used to bring the wires out, and the transducer is sealed by EB welding. For long-term protection from chemical attack on the internal solder joints and components, the unit is hermetically sealed with vacuum inside. Miniature glass-to-metal hermetic seals are used to minimize transducer size.

To avoid chemical attack on the wire, corrosion resistant materials are used. Rocket motor experience with stainless steel wire has shown large resistance changes in field applications with prolonged exposure to high humidity levels* attributed to solder joint deterioration and contact resistance changes. In early stress transducers, the bridge completion and compensation resistors were external to, and possibly 200 ft from, the transducer. Resistance changes in the critical parts of the transducer circuits caused large output variations, making it difficult, if not impossible, to obtain useful stress data. This

---

* Bills, K., Aerojet Solid Propulsion Company, Verbal Report on ASPC Flexible Case Program, JANNAF Propulsion Conference, Transducer Session, Anaheim, CA, October 1975.

problem was eliminated on the CSD design by having the complete bridge and compensation resistor circuitry inside the hermetically sealed transducer body or a special hermetically sealed compensation package.

All critical parts of the CSD transducer circuit are assembled and sealed at the factory where cleanliness and manufacturing procedures can be carefully controlled. The only field wiring is to attach excitation power and readout devices. The external compensation resistor package is wired in at the manufacturer. Any potential field wire or contact resistance change problems are further eliminated by using constant current excitation.

Stability

Long term stability is critical for embedded solid propellant stress transducers. Once a transducer is embedded in the grain, it cannot be removed nor can zero be reconfirmed. Any electrical drift of the transducer is reflected as a stress change in the motor. Previous motor experience has indicated some measured electrical output changes which could not be related to propellant changes.

In addition to the electrical problems experienced in field applications, any creep of the epoxy used to bond the semiconductor strain gages would contribute to electrical drift. Figure 1 illustrates the relative stiffness of the three materials in the bond system.

If the softer epoxy exhibits longtime creep, sensor strain will decrease with time, which would be measured as a transducer drift. The creep magnitude should be sensitive to epoxy modulus and thickness. Higher epoxy modulus values would reduce the potential creep, so highly filled epoxies are desirable. Rigid and small filler particles also tend to increase the adhesive modulus.

Control of epoxy thickness during bonding of the gages is a critical processing step. Excess epoxy thickness or different thickness layers for each gage could cause apparent drift of the transducer. Agglomeration of filler particles also may cause nonuniform epoxy thickness if not carefully controlled or removed by filtering.

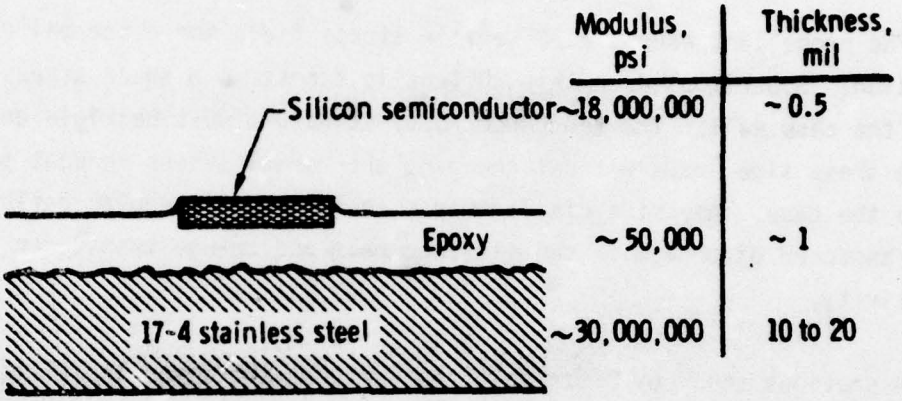


Figure 1. Gage Bond System Modulus and Thickness

18526

One other factor which could affect adhesive effectiveness is the surface texture of the 17-4 stainless steel structural member. Large pits or sandblast holes would tend to increase the epoxy thickness. CSD conducted detailed finite element structural analyses to evaluate the epoxy transfer function for different modulus and thickness values and stainless steel surface textures. Results of this analysis show the optimum design levels and the creep sensitivity of epoxy bonded semiconductor elements. In addition to these numerical analyses, CSD also conducted long term laboratory creep tests to measure the actual epoxy creep behavior for a typical transducer installation process.

Structural Rigidity and Propellant Disturbance

Structural rigidity requirements for embedded SRM transducers are unique because solid propellant is a nonlinear viscoelastic material and typical rocket motor stress conditions are complex because of the near incompressibility of the solid propellant material.

When the rocket motor cools from cure temperatures of approximately 140°F, propellant volume reduction is much greater than rocket motor case shrinkage. If the two materials were not bonded, the propellant would separate from the case, as shown in Figure 2. The bond stress holding the propellant to the case is the major stress contributing to structural failure of rocket motors. When the transducer is mounted on the inside of the case surface as shown in Figure 3, it is placed in a complex stress field.

The propellant exerts a 3D tensile stress field for a thermal cooldown condition. Superimposed on this 3D tensile stress is a shear stress acting along the case wall. The transducer body structure must be rigid enough to absorb these side loads without changing the normal stress readout perpendicular to the case. Any side displacements could cause irregular deflection of the transducer diaphragm or cantilevered beam and change transducer zero and sensitivity.

A previous study by Fitzgerald and Hufferd* confirmed the effect of propellant modulus values on stress transducer response with the older type transducers with very thin diaphragms (~0.0034 in.).

Analysis of a 600-psi diaphragm type transducer showed an output sensitivity decrease of approximately 1% associated with shear modulus values up to 1,000 psi produced by thermal cooling of the propellant (Figure 4). The 25-psi transducer design showed approximately a 50% decrease in sensitivity for the same shear modulus value. An accurate stress determination would be impossible with this 25-psi thin diaphragm model because the solid propellant nonlinear viscoelastic modulus is uncertain for motor conditions.

Two potential diaphragm and cantilevered beam transducer designs were analyzed at CSD to determine rigidity requirements for thermal and pressure loading conditions using finite element computer modelling techniques. The

---

* Fitzgerald, J. E., and W. L. Hufferd, "Interaction of a Diaphragm Pressure Gage with a Viscoelastic Half Space," Experimental Mechanics, July 1970.

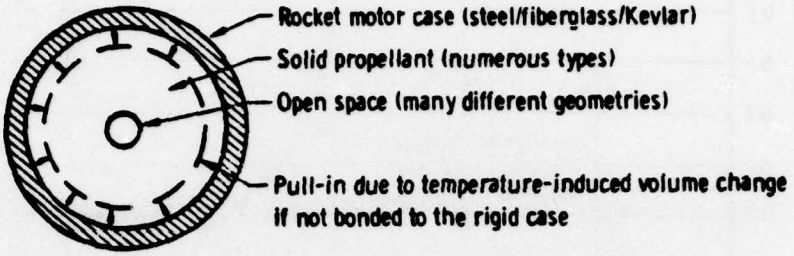


Figure 2. Solid Propellant Thermal Pull-In

18527

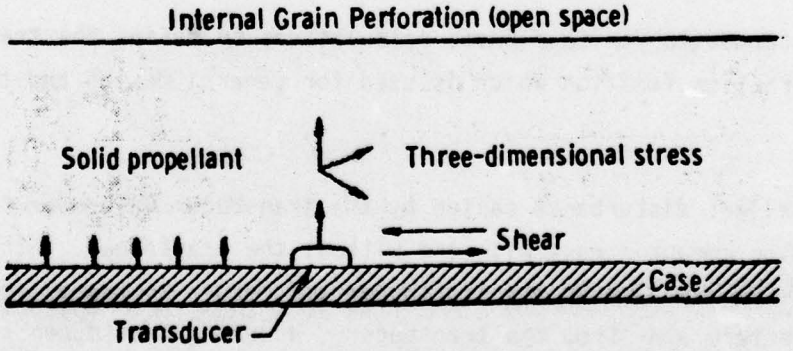


Figure 3. Embedded Transducer Stress Conditions

18528

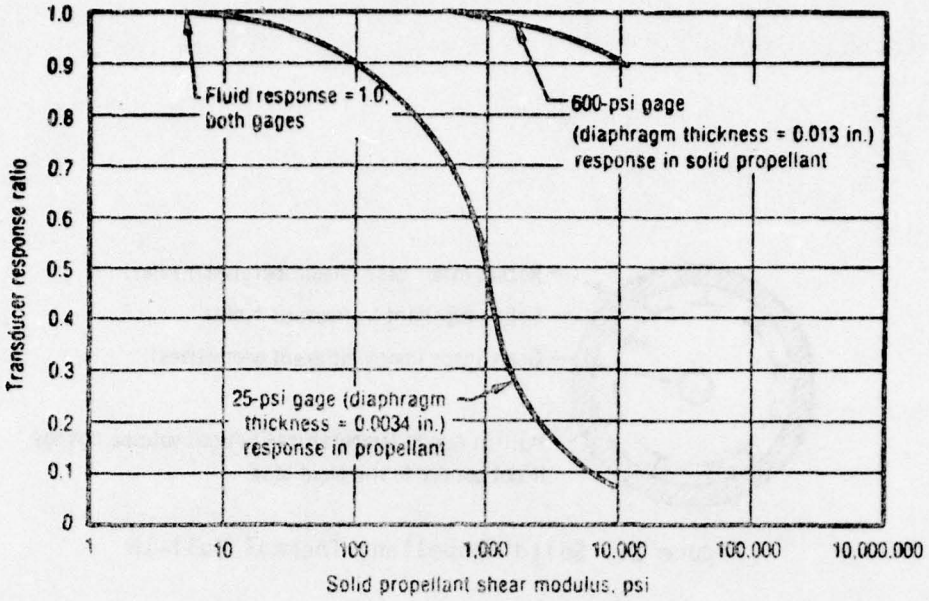


Figure 4. Embedded Stress Response vs Propellant Shear Modulus for Older Type Transducer (by Fitzgerald and Hufferd)

17254

typical transducer designs are shown in a solid propellant end-burner design in Figure 5. This type of rigid steel case fixture exposed to thermal and pressure loads was used for the detailed finite element structural analysis. Propellant stress field and calibration effects were evaluated using finite element analysis with a transducer embedded in the propellant and in a fluid as a reference.

CSD conducted finite element calculations to define the transducer/propellant interaction function which is used for general design and transducer evaluation.

Propellant disturbance caused by the transducer was determined by comparing rocket motor computer runs with and without the transducer. Stresses are disturbed in the area around the transducer and return to normal between two and three diameters away from the transducer. However, transducer side stresses in the propellant were much higher than desired for the early vertical side design models.

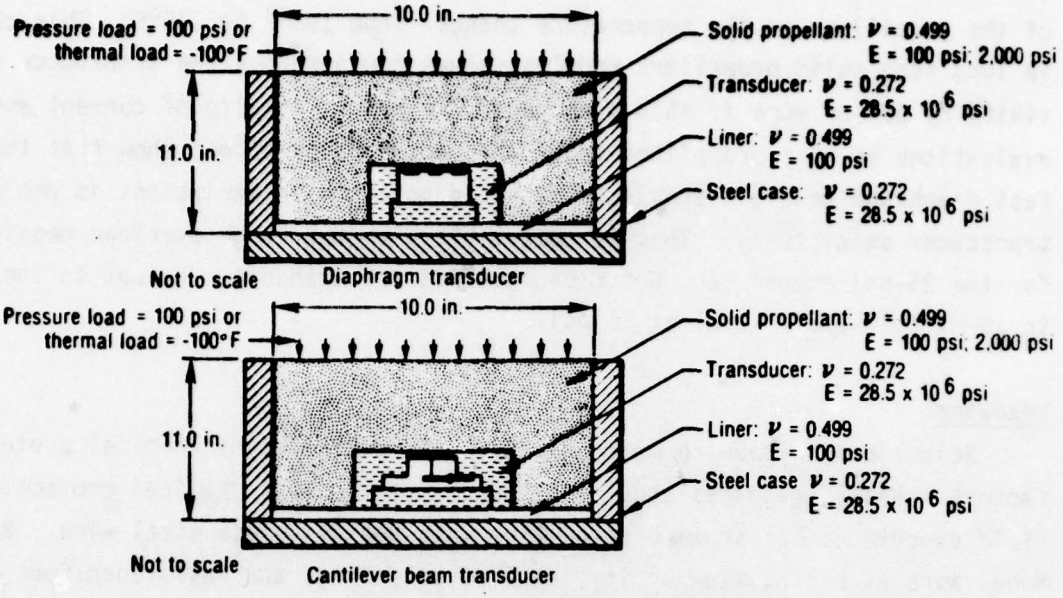


Figure 5. Typical Designs in Rigid End-Burner Fixture

18500

CSD conducted a series of finite element structural analysis runs with different external transducer shapes to select an external design contour which minimizes the propellant stress buildup on the side of the transducer. A 60^{o} side angle was selected as the best compromise for the final transducer shape.

The concern about transducer rigidity centered on propellant/transducer interaction. Pressure transducers are designed to work with gas and fluids which exert a uniform stress across the diaphragm regardless of the diaphragm flexure. When the diaphragm is bonded to a solid propellant, any deflection, however small, causes a change in the propellant stress field, which in turn changes the diaphragm deflection. The resultant impact is to change the sensitivity of the transducer. This final sensitivity is now a function of the rigidity of both the diaphragm and the propellant. If the diaphragm is very stiff compared to the propellant, the transducer will not be sensitive to propellant modulus changes.

However, if the propellant is much stiffer than the diaphragm, the transducer will become very sensitive to the nonlinear viscoelastic modulus changes of the propellant as the temperature changes from 160°F to -75°F. This change in long term solid propellant modulus values could reduce the transducer sensitivity by 50% or more if thin diaphragms are used. Results of current and past evaluations of this propellant transducer interaction effect show that the stiffest diaphragm possible should be selected to minimize variations in embedded transducer sensitivity. This is compatible with the large overload requirement for the 25-psi transducer, but does restrict the transducer output to the 5- to 10-mV full-scale level at 25 psi.

Leadwires

Selection of leadwire materials has been dominated by chemical protection factors. While stainless steel and Monel give the best chemical protection, field experience has shown difficulties with the stainless steel wire. Because Monel wire strength, flexibility, ease of soldering, and resistance/foot are adequate for rocket motor applications, it was selected for the earlier designs, then replaced with copper wires in stainless steel tubes for the final design.

Physical Size

The transducer must be reduced in size to minimum dimensions that allow inclusion of the compensation resistors while maintaining adequate structural rigidity. The two models used for the structural analysis meet the original design requirement, but are still too large for use on some tactical rocket motors. The small diameter rocket motors such as Sidewinder and Maverick have a thin propellant web. The larger the transducer, the greater the area of stress disturbance. If the propellant web is too thin compared to the transducer geometry, the stress measurement reflects only the disturbance, rather than the stress field that occurred before the transducer was installed. The final transducer design decreases the height to 0.130 in. to minimize the stress disturbance. Stress disturbance analysis showed that the stress disturbance was not reduced significantly by further height decreases.

1.2 PROGRAM OUTLINE

The program to accomplish these goals was separated into four phases, described as follows:

Phase I. Initial design and fabrication
Phase II. Developmental testing
Phase III. Calibration procedure development
Phase IV. Final design evaluation.

The first phase included the manufacture of six transducers, three in the 25-psi range and three in the 2,000-psi range. These were to be state-of-the-art designs which would represent the best approximation to meeting the design goals without extensive developmental work. Then, during the second phase, while the initial transducers were being evaluated in the laboratory, mathematical and subscale studies were performed to determine how the designs might be refined to improve performance. Six additional transducers were manufactured during this phase. During phase III a rationale was developed for calibrating these transducers based on their known electrical output, and response under laboratory evaluation, both as pressure transducers and embedded in propellant. During Phase IV, 16 additional transducers were procured of a new design and evaluated in the laboratory. A detailed flow chart of this plan is given in Figure 6.

1.3 TRANSDUCER HISTORY SUMMARY

Several different design concepts were evaluated on this program. Those resulting in a manufactured transducer are briefly described in this section. Three basic configurations were purchased from two different manufacturers.

1.3.1 Early Transducer Design - Celesco

The size and shape of stress transducers have varied greatly. One early type of stress transducer manufactured by Celesco for CSD is shown in Figure 7. Both an internal cantilevered beam and diaphragm design transducer were manufactured. Both transducers included internal temperature compensation resistors. All seals were EB welded, and glass-to-metal headers were used for leadwire exits. Structural analysis of these designs showed that the propellant stress concentrations were large near the gage corners and that an optimum design would include sloping sides.

Fabrication difficulties were encountered at Celesco during prototype fabrication. The Celesco Transducer Division was put up for sale and a significant staff reduction occurred. Because of their indeterminate management situation, their interest in the R&D type transducer field could not be supported. CSD terminated the Celesco subcontract.

1.3.2 Later Transducer Designs - Senso-Metrics

The second generation of stress transducers was manufactured by Senso-Metrics for CSD and had a 64^{o} slope as shown in Figure 8.

Temperature compensation resistors are inside the transducer (Figure 9). The area containing the semiconductor strain gages is under vacuum and separated from the resistor cavity by a glass-to-metal header. Both diaphragm and cantilevered beam transducer models are physically the same size. The leadwires are protected by a 10-ft-long tube, 0.125 in. in diameter, and leadwire tubes can be either side or rear exit.

Evaluation of these transducers showed that the cantilevered beam model exhibited zero offset instability and that the butt welded 10-ft-long leadwire protection tubes were not structurally stable and were difficult to bend. Further structural analyses showed the need for a reduced height transducer to minimize propellant disturbance. This redesign resulted in the model shown in Figures 10 and 11. Transducer height was reduced by removing the temperature compensation resistors from the transducer body and placing them in a remote aluminum box. This box is 10 ft from the body of the transducer and all connections are weatherproof. The transducer body is evacuated and sealed with a glass-to-metal header 10 in. from the body. The leadwire protection tube is 10 ft long, but is a more flexible thin metal tube and is not of a butt-welded design.

The early transducer (Figure 9) had matched semiconductor strain gages 0.080-in. long. Finite element analysis indicates that larger average strains in the outside semiconductor gage are possible if the gages are shortened to 0.060 or 0.040 in. The current Senso-Metrics transducer design uses 0.060-in. gages.

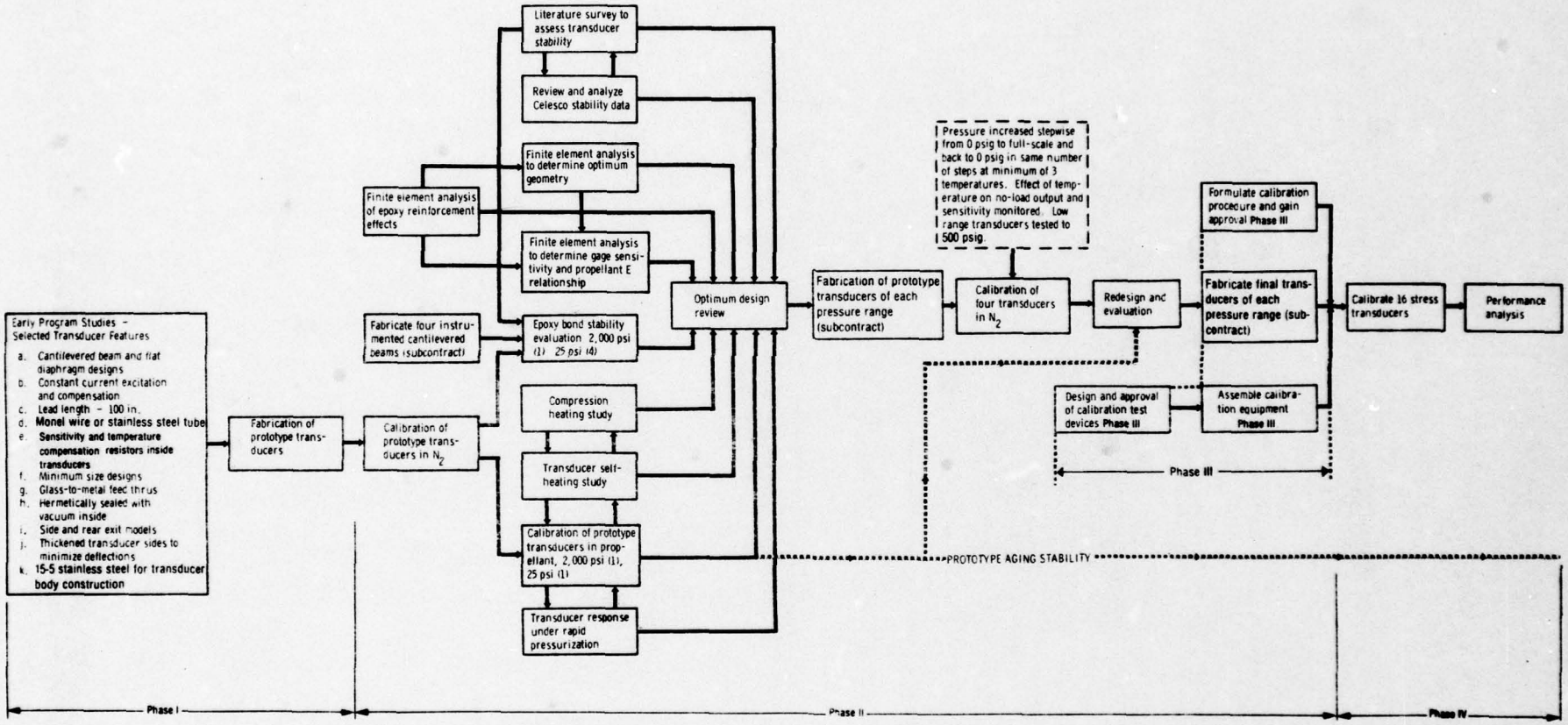


Figure 6. Development of Improved Normal Stress Transducers for Propellant Grains

08120

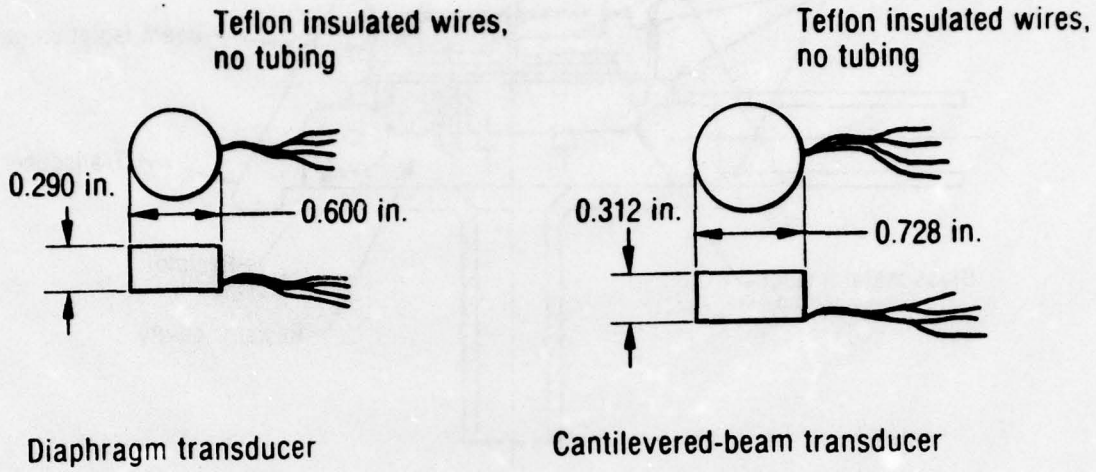


Figure 7. Early in Situ Transducer Designs - Celesco

14020

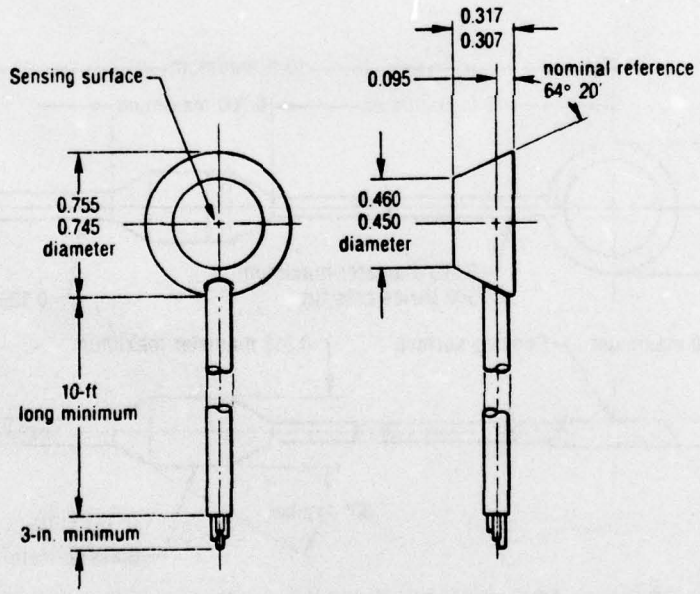


Figure 8. Second Generation Stress Transducer - Senso-Metrics, Inc.

14021

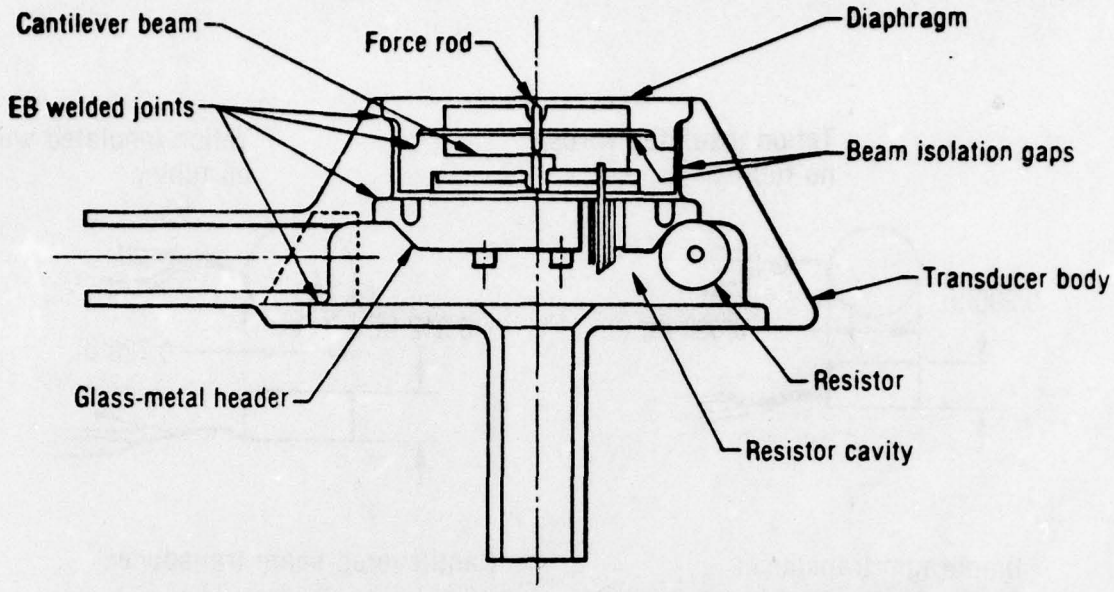


Figure 9. Cross Section of Senso-Metrics Transducer Prototype

14022

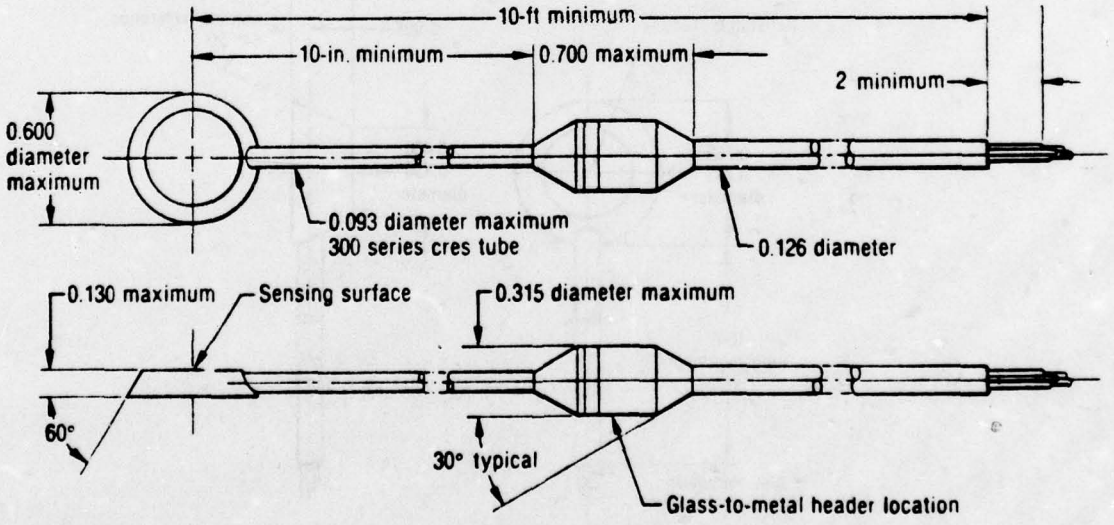


Figure 10. Low Profile Senso-Metrics Stress Transducer

14023

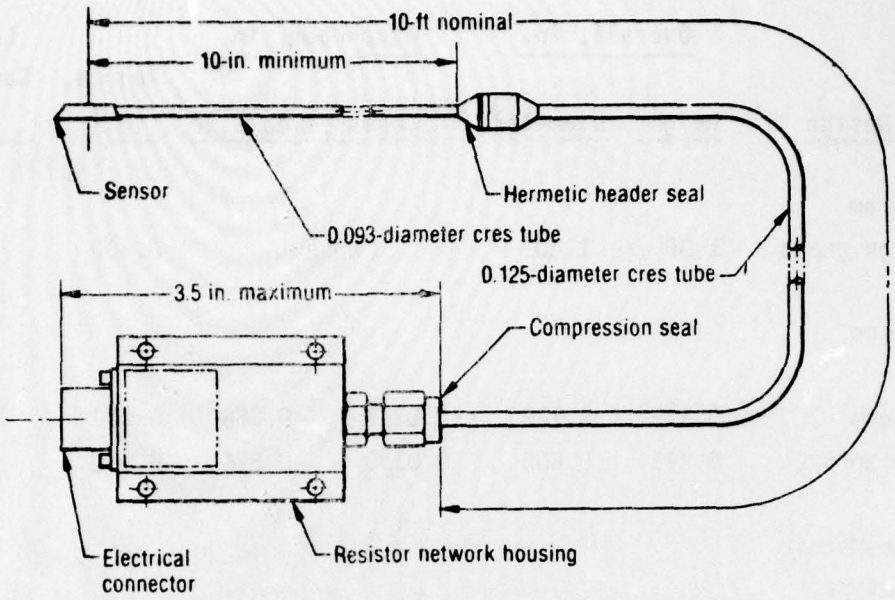


Figure 11. Low Profile Senso-Metrics Stress Transducer Assembly

14024

1.3.3 Discussion

A general summary of the 25-psi gage dimensions for all designs evaluated is given in Table 1. This shows how the design evolved in terms of shape and overall size. Shown also are the design goals which all gages exceed except for the glass-to-metal header casing diameter on the final design.

Both cantilevered beam and diaphragm type transducer data show that the semiconductor strain gage transducers currently manufactured by Senso-Metrics for CSD have the potential capability for 1% or better long time zero offset stability in a solid propellant environment as demonstrated by final design 2,000-psi transducers. Testing of various transducer designs has shown that the chemical seals provided by EB welding and glass-to-metal headers are adequate for the corrosive environment of a typical solid propellant. The heat generated during the final EB welding changes temperature compensation so these resistors are now located in an external box for better stability and can now be a larger size with improved stability and lower temperature correction (1 to 10 ppm/^{o}C). Structural analysis has shown that a reduced height transducer

TABLE 1. BASIC DIMENSIONS OF 25 psi TRANSDUCERS

Design	Overall, in.		Diaphragm, in.		Volume, $in.^3$	Leadwire and Casing Diameter, in.
	Height	Diameter	Thickness	Diameter		
Program design goals	1.00	1.00	none		0.500	0.125
Celesco						
beam	0.312	0.728	0.0115	0.226	0.132	0.11
diaphragm	0.290	0.600	0.0130	0.326	0.082	0.11
Senso-Metric prototype						
beam	0.317	0.750	0.0138	0.250	0.093	0.125
diaphragm	0.317	0.750	0.0132	0.250	0.093	0.125
Senso-Metric final						
diaphragm	0.130	0.600	0.0117	0.250	0.032	0.315

is desirable so the final transducer design was reduced to 0.130 in. high. Transducer analysis indicates that an increased output can be provided by using shorter semiconductor strain gages which was done on the final transducer design.

Many design variations have been considered and improved on before arriving at the latest low profile, remote temperature-compensated transducer. One driver in this activity has been the difficulty in manufacturing small stable transducers with all welded seals and provision for leadwire protection from the corrosive propellant. The latest design meets CSD's original design requirements and has the potential for additional size reductions and fabrication simplification.

2.0 STABILITY STUDIES

2.1 SEMICONDUCTOR STABILITY

A search of the literature by CSD and subcontractors did not yield useful semiconductor stability results. Discussions with the various transducer manufacturers in the United States indicated that the gages appear to be very stable based on internal data, but no definitive measurements have been made. Each transducer company has its own semiconductor manufacturing process which it believes is adequate. Gold lead attachment procedures also vary significantly between corporations with some being much more durable for later leadwire bending and some exhibiting less diode effects than others. The consensus of the project team was that the beam stability tests conducted at CSD would be the first measure of semiconductor strain gage stability.

2.2 EPOXY BOND STABILITY

A suspected critical problem with previous stress transducers is the stability of the epoxy used to bond the semiconductor gages to the metal diaphragm. Most transducers have employed filled or unfilled epoxy to bond the gages. Usually there was little or no control on epoxy thickness, particle size variations, or particle agglomeration. Epoxy often was cured at high temperatures inducing a high zero stress temperature in the epoxy and semiconductor gage system. Thus, when the bonded gages were cooled to 70^{o}F a large thermal stress was induced. This, along with the other epoxy problems, induced more instability in the transducer outputs.

Considerable finite element analysis was performed on this program to study the epoxy bond system. The variables studied were the epoxy modulus, thickness, and contact surface roughness.

Results of the study (section 3.1.1) showed that the epoxy thickness should be kept below 0.001 in. to avoid significant diaphragm stiffening. An epoxy modulus of 500,000 psi or more is desired to transfer at least 98.4% of the metal strain to the silicon gage.

The epoxy on previous transducers often varied in thickness because of variations in the sandblasted metal surface. Any grooves or pits in the metal surface must be filled with epoxy which could result in additional potential epoxy creep. The diaphragms are now sandblasted to a measured surface roughness specification of 22μ in. to avoid this problem.

2.3 METAL STABILITY

The stress-strain curve shown in Figure 12 illustrates typical metal structural behavior. When application stresses exceed the linear range of behavior, the material will not return to its original condition. The metal could have a 2,000-microstrain offset by the material's elastic limit definition. This is adequate for structural applications where long time stability and accuracy are not important. When a transducer has a maximum loaded diaphragm strain of 100 microstrain, a 2,000-microstrain offset is many times greater than full scale of the transducer. Care must be taken to avoid this metal offset and instability problem caused by high stress conditions during machining, fabrication, and later testing. The precision elastic limit (PEL) defines a metal offset of only 1 microstrain (Figure 13). The PEL is usually much less than the proportional elastic limit. The PEL data generally are obtained by slow cyclic loadings in incremental steps (Figure 13) until a 1-microstrain offset is achieved in the metal. This type of evaluation has been conducted on materials for inertial guidance platforms where extreme metal stability is required. A 1-microstrain offset in the transducer metal diaphragm over many years would produce offsets which would be interpreted as a propellant motor stress change. To avoid this metal problem, the metal stress must be completely relieved and transducer overpressure requirements must be reduced to less than the PEL stress value.

Typical differences between ultimate strength and PEL are shown in Table 2. Some metals experience very little difference, but other metals, such as 310 stainless steel, indicate a PEL stress of one-tenth the ultimate strength.*

*Maringer, R. E., W. A. Glaeser, and C. T. Olofson, "Material Properties Pertinent to the ISUS Sensor Block," Battelle Memorial Institute, Columbus Laboratories, April 9, 1968.

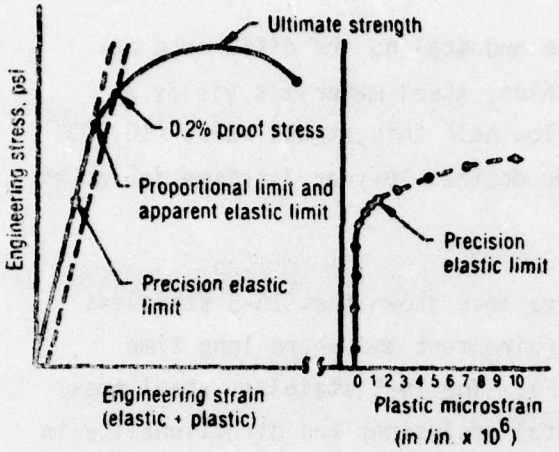


Figure 12. Typical Stress-Strain Curve
18529

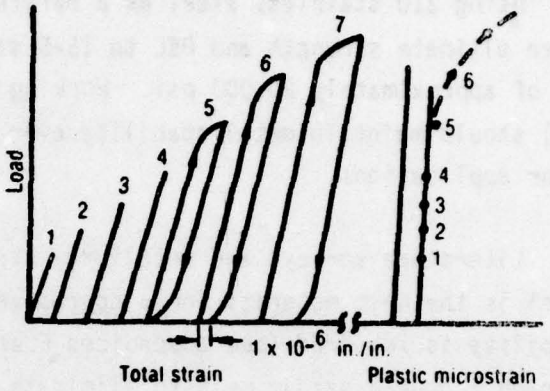


Figure 13. Typical PEL Determination
18530

TABLE 2. COMPARISON OF PRECISION ELASTIC LIMITS

T4573-D

Material	Precision Elastic Limit, psi	Ultimate Strength, psi
High purity alumina	23,000	23,000
High purity beryllia (ceramic)	20,000	20,000
Glass-bonded mica	4,000	9,000
Hot-pressed beryllium	2,000	45,000
AZ-31B magnesium rod	6,000	34,000
A356-T6 aluminum casting	12,000	40,000
2024-T6 aluminum extrusions	25,000	58,000
6AL-4V titanium rod, an	70,000	150,000
310 CRES steel rod, CR and SR	11,000	120,000
Tool steel, high speed	50,000	180,000
Inconel-X	65,000	150,000

Typical creep curves for 310 stainless steel at different temperatures are shown in Figures 14 through 16 to illustrate the degree of microcreep phenomenon that occurs. The creep strains are much greater than full-scale output strains on the current transducer application. It is very important to stay well below the PEL stress.

Using 310 stainless steel as a reference and scaling the difference between ultimate strength and PEL to 15-5 stainless steel materials yields a PEL of approximately 20,000 psi. Working below half this stress value (10,000 psi) should maintain metal stability over the desired 10-year lifetime in rocket motor applications.

Literature surveys and metallurgy studies have shown that 15-5 stainless steel is the best material for a corrosive environment and where long time stability is required (see appendices E and F). The 15-5 stainless steel goes through a double vacuum melt to eliminate metal occlusions and directionality in properties and has chemical corrosion resistance equivalent to or better than 17-4 stainless steel. Since 15-5PH should have fewer and smaller inclusions due to vacuum melting, there is less probability of obtaining a transducer which has a bad inclusion in the thin diaphragm where it could cause trouble. Once the transducer has been machined from the 15-5 stainless steel, it undergoes a precise stress-relief metal conditioning process which consists of the following:

A. Heat treat to $1,900^{\circ} \pm 25^{\circ}F$ in argon atmosphere for 1/2 hr; cool from $1,900^{\circ}$ to $800^{\circ}F$ in 15±10 min (nominal cooling rate of $-75^{\circ}F$/min), and then cool to $70^{\circ}F$ in the same length of time for a nominal coding rate of $-50^{\circ}F$/min.

B. Cold soak samples to $-100^{\circ}F$ for 1 hr within 24 hr after air cooling to $70^{\circ}F$. Place hardware in bucket or other container in $-100^{\circ}F$ environment rather than placing hardware directly into $-100^{\circ}F$ solution; this will prevent excessive thermal stresses exceeding the precision elastic limit during cooldown process. The 15-5 alloy is martensite at $70^{\circ}F$ but may have minute amounts of metastable austenite. Dropping to $-100^{\circ}F$ or lower assures complete transformation to martensite. Air warm samples to $70^{\circ}F$ at a rate of $100^{\circ}F$/hr or less.

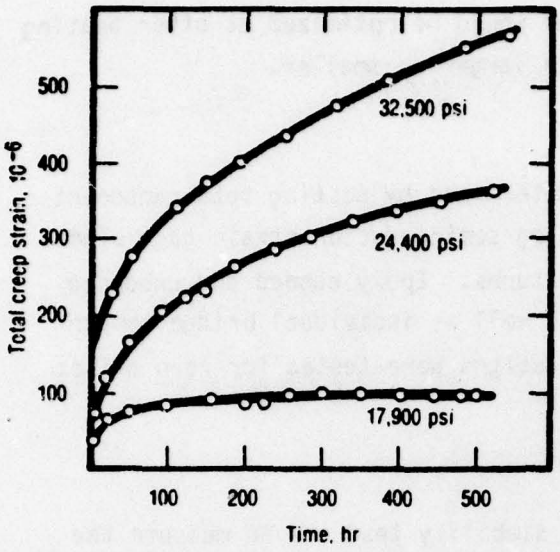


Figure 14. Total Creep Curves of 310 Stainless Steel at 85°F

18531

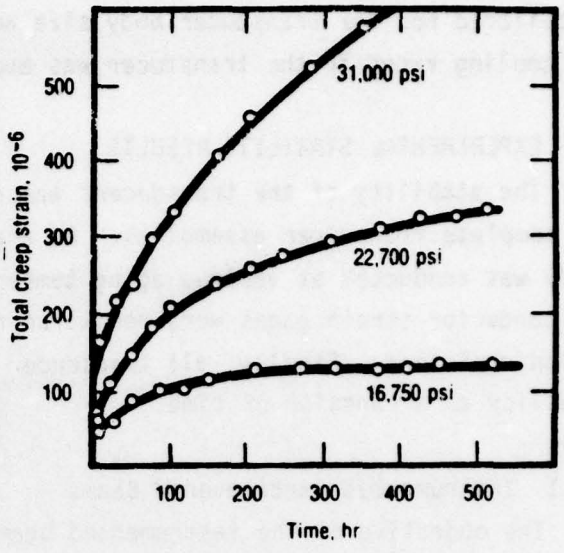


Figure 15. Total Creep Curves of 310 Stainless Steel at 150°F

18532

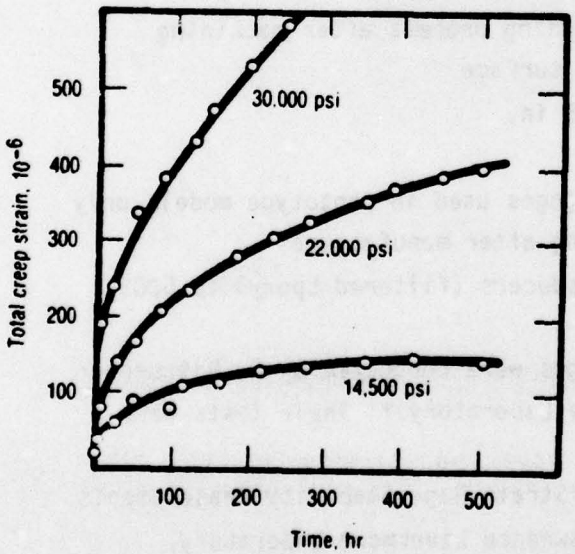


Figure 16. Total Creep Curves of 310 Stainless Steel at 200°F

18533

C. Precipitation harden material at 900°±25°F for 1 hr; air cool to 70°F at a rate of 100°F/hr or less.

D. Descale hardware with grit blast procedure to remove discoloration (oxidation).

This process will relieve the metal stress to below the precision elastic limit which means that less than 1-microstrain offset will remain in the metal. This precision stress relief metal conditioning process was developed by Dr. Wood of the California Institute of Technology

and Dr. Temco of Battelle Memorial Institute. Precision elastic limit data and other metal data in appendices E and F was used with the diaphragm thermal stress data in appendices G and H to arrive at the metal process. This process is tailored for the transducer body size and would be optimized at other heating and cooling rates if the transducer was much larger or smaller.

2.4 EXPERIMENTAL STABILITY RESULTS

The stability of the transducers was determined by testing both components and complete transducer assemblies. An analog semiconductor strain gage/beam study was conducted at various aging temperatures. Epoxy bonded and unbonded semiconductor strain gages were monitored as well as individual bridge compensation resistors. Finally, all transducer designs were tested for zero offset stability as a function of time.

2.4.1 Instrumented Cantilevered Beams

The objective of the instrumented beam stability test was to measure the stability of individual epoxy bonded semiconductor strain gage bond systems as manufactured by Senso-Metrics to specifications for the improved stress transducer program. The following features are common to both the instrumented beams and the prototype and production transducers manufactured by Senso-Metrics:

A. Each undergoes same metal conditioning process after machining
B. Each has same smooth sand-blasted surface
C. Thin filtered epoxy layer $\approx$ 0.0005 in.
D. Step cure of epoxy
E. Same Senso-Metrics semiconductor gages used in prototype models only
F. Same thermal and mechanical cycling after manufacture
G. Same epoxy used on beams and transducers (filtered Epoxylite 6203).

Tests of this type with foil strain gages were conducted by G. Dittbenner and his associates at the Lawrence Livermore Laboratory.* Their tests were

* Dittbenner, G.R., and H.S. Freynik, Jr., "Strain Gage Stability Measurements for Years at 75°F in Air," UCRL-76039, Lawrence Livermore Laboratory, University of California, Livermore, CA, April 1975.

restarted a number of times after equipment improvements were made each time to improve experimental accuracy. Their experience showed the degree of difficulty in conducting an experiment using temperature sensitive gages and maintaining high accuracy over long periods of time.

CSD went to great lengths in setting up this test to use the most accurate equipment possible. The first problem to solve involved measurement of the test temperature to the needed accuracy. Since the semiconductor strain gages are very temperature sensitive, an accuracy of 0.01°F or better was required. After careful analysis, Minco platinum temperature sensors were chosen for this measurement. In order to meet the accuracy requirement these sensors had to be very stable; only Minco had verified special reannealing, heat treatment, and mechanical cycling of their platinum sensors to stabilize them. Even so, a special calibration of these sensors was conducted at the Naval Air Rework Facility in San Diego. The Minco specifications and calibration results from the Naval facility are presented in appendix I. J.F. Berlanga at the Naval Air Rework Facility conducted the calibrations and also ran a 3-month stability check on one of the platinum sensors. The triple point repeatability was 25.54583 ohm, 25.54576 ohm, and 25.54588 ohm. This was a 2-ppm repeatability or 0.0005°C triple point electrical uncertainty. Also, the CSD Fluke 8800A DVM, which was used to record the data, was sent to the Naval facility for their evaluation. The Fluke company specifications say the meter has an accuracy of 8μ V, considering temperature sensitivity and range factors, but evaluation by the Naval facility shows these specifications to be very conservative. The Navy check of this digital meter found the meter had greater accuracy than reported by the manufacturer. It was decided that it would be necessary to measure a minimum strain change in the beam of 1 microstrain. Circuit analysis shows that for 1-$\mu\epsilon$ load on the strain gage and 1-V bridge excitation, the 500Ω bridge output for one active arm is 35μ V. This 35μ V corresponds to a resistance change of 0.70Ω.

To accurately measure the 1-$\mu\epsilon$ variation, all switch resistance and bridge completion resistors must be stable to better than 0.07Ω. The Vishay ultrastable hermetically sealed resistors are quoted as stable to 0.0025Ω/year drift after fabrication; aged resistors are much better. A group of 15 hermetically

sealed resistors (506Ω) was located at the factory; these had been manufactured 2 years ago. The variability of these resistors is estimated to be less than 0.001Ω/year. The L&N switch selected for the stability tests has a contact resistance of 0.0015Ω and a variation after thousands of mechanical cycles of less than 0.005Ω. Both bridge completion resistors and the L&N switches are much more stable than required to accurately measure the desired 1-$\mu\epsilon$ variation of each strain gage.

Appendix J presents stability data on the Vishay resistors purchased by CSD plus 10-year shelf life stability data on other Vishay resistors that attest to their quality.

Before the beam test was started, it was necessary to prepare a detailed test procedure and troubleshooting guide. These items are presented in appendix K.

The beam test uncertainty analysis (appendix L) concludes that the largest source of error (0.11%) is produced by the temperature sensor-readout system. The second largest source of error, 0.06%, is produced by the uncertainty in the beam inclination angle even though the beam is carefully leveled inside an insulated box. The third largest source of error is in measuring the bridge output and is estimated to be 0.02%. All other measurement uncertainties such as barometric pressure, gravity, and tidal effects are at least two orders of magnitude lower.

The semiconductor strain gages are bonded to stainless steel cantilevered beams with Epoxylite 6203. Resistance variations will occur in the semiconductor gages if (1) small variations in some test parameters cause cyclic or random variations in gage resistance; (2) the semiconductor strain gage and metal are unstable; and (3) the epoxy interface between the gage and metal creeps as the gage, epoxy, and metal materials are stressed by mechanical and thermal loads. Some test parameters could cause resistance variations since the bonded semiconductor gage system is sensitive to extraneous stimulation. The bonded semiconductor gage system is defined as the total test network consisting of the gage, epoxy, beam, gage/epoxy/beam environment, and all electrical signals

supplied to the gage circuit. In addition to the intended behavior of the semiconductor strain gage (e.g., resistance of semiconductor material), Table 3 lists the external stimuli to which the gage could respond.

The epoxy interface between the semiconductor gage and metal creeps as the gage, epoxy, and metal materials are stressed by mechanical and thermal loads. The amount of creep is dependent on the thickness of the epoxy layer and the storage temperature of the beam. The items shown in Table 4 are stimuli known to effect epoxy creep.

A typical instrumented beam is shown in Figure 17. Each beam was placed inside an insulated box before being placed in its conditioning oven. The beam test configuration is shown in Figure 18. Each beam had 10 semiconductor gages and one foil strain gage loaded in tension and an equal number in compression. The beams were loaded to approximately 180 microstrain. The typical circuit diagram for this test is shown in Figure 19 and the temperature conditioning ovens in Figure 20. The temperature was measured with precision platinum temperature sensors made by Minco. All data obtained were input to an HP-9825 programmable calculator for complete data reduction. Each gage output was normalized to a constant excitation voltage of exactly 1.0 V by the relationship

$$NOP(t) = E_o/E_{ex} \tag{1}$$

where E_o is the measured gage output, E_{ex} is the measured excitation, and NOP(t) is the excitation normalized gage output at any time (t). The change in aging temperature was calculated as the difference in temperature between the initial test date and the test date at any time, t. Each gage output was zero centered to the initial test date temperature by the relationship

$$NOP'(t) = (E_o - S\Delta T)/E_{ex} \tag{2}$$

where S is the temperature sensitivity of the gage in mV/^oF which was determined before the test, ΔT is the change in aging temperature, and NOP′ is the excitation and temperature normalized gage output. The change in normalized

TABLE 3. STIMULI AFFECTING SEMICONDUCTER GAGE RESULTS

T4574-D

Description	Remarks
Pressure	Barometric pressure affects buoyancy of the beam
Temperature	Semiconductor materials non-linearily dependent on temperature
Shock	Impulse loads on the beam could affect semiconductor gage response
Vibration/sound	Could cause beam to oscillate
Humidity	May degrade semiconductor material and be absorbed by epoxy
Strain	Strains may induce epoxy creep
Light/gamma radiation	Semiconductor materials experience photoelectric behavior
Neutron radiation	Neutron capture will change atomic and molecular construction

TABLE 4. EPOXY CREEP SENSITIVITY TO EXTRANEOUS STIMULI

T4575-D

Description	Remarks
Cure temperature	Gage and metal are cured at elevated temperatures and cooled; materials have different coefficients of thermal expansion
Storage temperature (thermal strain)	Creep behavior accelerated at higher temperatures
Epoxy thickness	Thicker layers generate greater creep
Strain (mechanical)	Creep behavior accelerated at higher strains
Strain history (thermal and mechanical)	Metal hysteresis

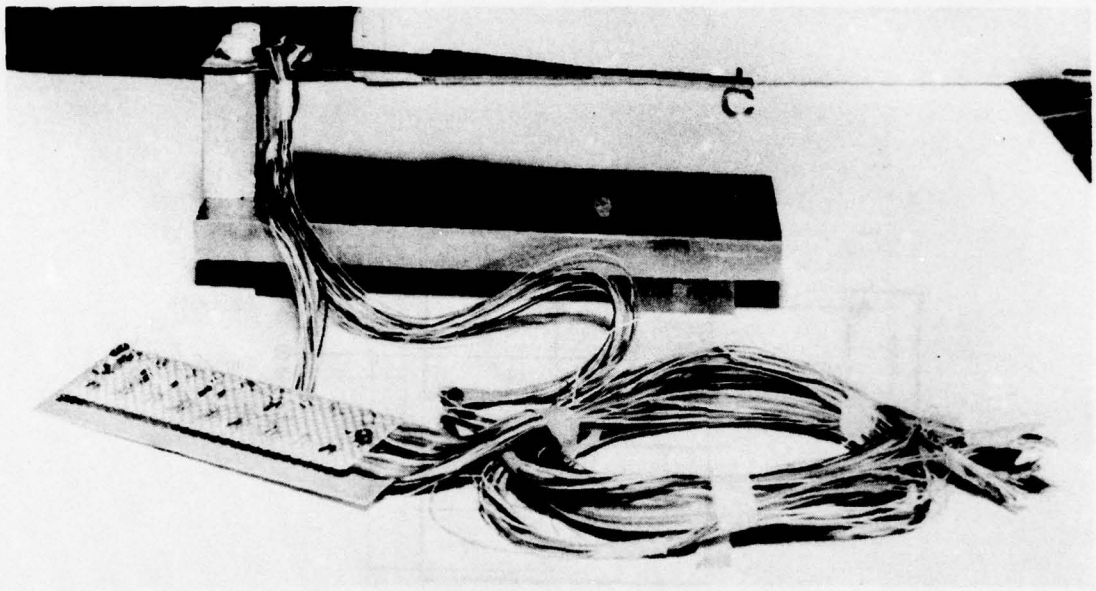


Figure 17. Instrumented Constant-Strain Beam

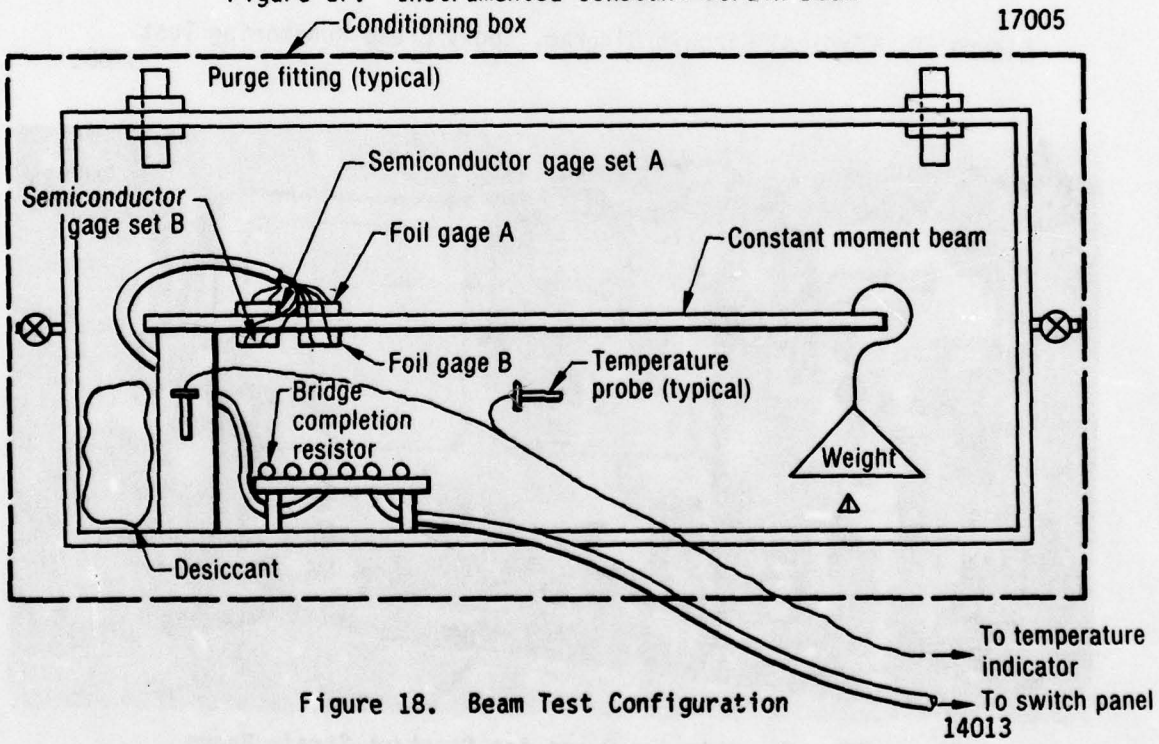


Figure 18. Beam Test Configuration

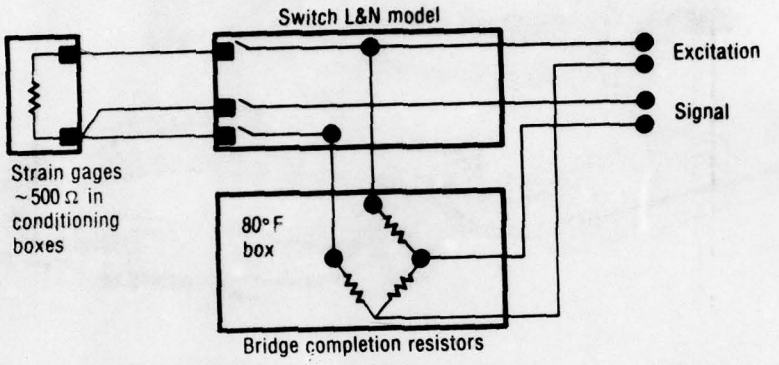


Figure 19. Typical Circuit Diagram, Epoxy Creep Monitoring Test

17001

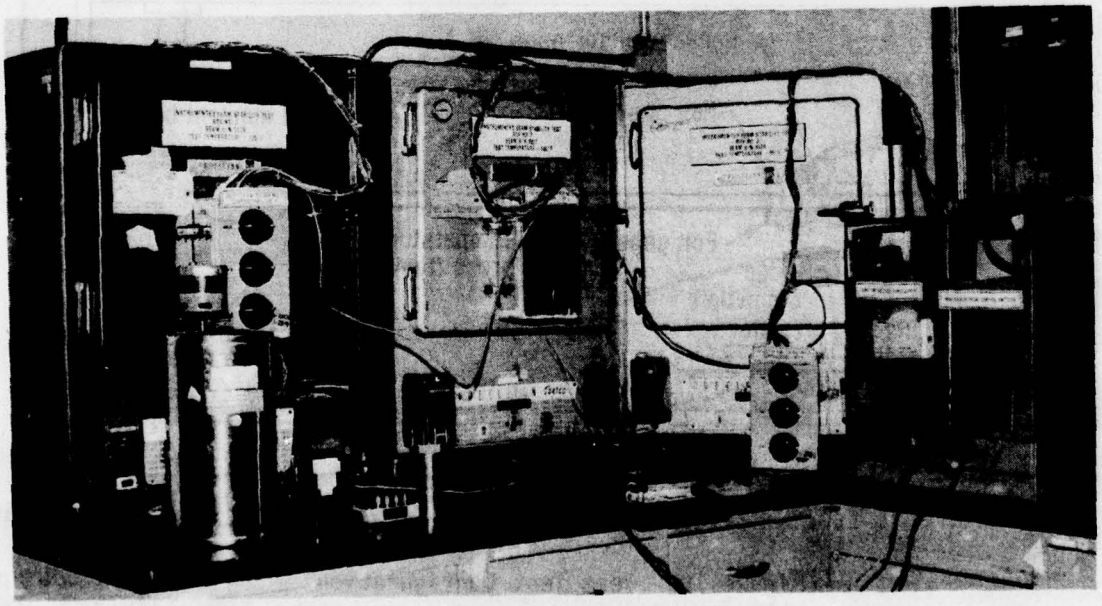


Figure 20. Conditioning Ovens for Constant-Strain Beams

17004

gage output (excitation and temperature corrected) was calculated by the relationship

$$\Delta NOP' = NOP'(t) - NOP'(o) \tag{3}$$

where NOP'(t) is the normalized output at any time, t, and NOP'(o) is the initial normalized output. The initial beam strain was calculated from the output of the bonded foil strain gage and its known gage factor by the relationship

$$\epsilon = \frac{(4)(E_o)}{(GF)(E_{ex})} \tag{4}$$

where ϵ is the initial beam strain at time zero, E_o is the bonded foil gage output, E_{ex} is the excitation voltage at time zero, and GF is the known gage factor. Rearrangement of equation (4) then allowed for the calculation of each semiconductor gage factor based on the initial calculated strain. The beam strain as measured by each semiconductor gage then was calculated by the relationship

$$\epsilon(t) = 4\left[NOP'(t) - NOP(preload)\right]/GF \tag{5}$$

where NOP (preload) is the normalized output at time zero before loading the beam, and GF is the calculated gage factor for the semiconductor gage. The change in beam strain then was calculated as

$$\Delta\epsilon = \epsilon(t) - \epsilon(o) \tag{6}$$

where $\epsilon(t)$ is the strain at time, t, and $\epsilon(o)$ is the initial beam strain at time zero.

Using these equations, the beam test data were analyzed for measurements made from the time of initial beam loading through a period of one year. Tables 5 and 6 show this data for a typical tension and compression semiconductor gage bonded to the beam and stored in the 90°F oven. These gages show no pronounced drift. Also stored in each temperature conditioning oven were

a group of resistors. The purpose of these resistors was to observe if resistors used for stress transducer circuit compensation would drift in value at these elevated temperatures. Included in the test were values of 10 ohms, 1,500 ohms, and 50,000 ohms; in both common carbon resistors and MIL-SPEC RN55C resistors, the latter being used as compensation for the Senso-Metric transducers. Data for these resistors over the one-year test period at 90°F is presented in Tables 7 and 8. Also included in Table 8 are results for an unbonded semiconductor gage identical to those bonded. These results are tabulated as ohms and change in ohms from the start of the test as measured by the Fluke 8800A DVM. Very little resistance change is noted for any of the resistors over the testing period.

Tables 9 and 10 are tabular data for typical tension and compression gages bonded to the 120°F beam. Overall, these data show a slight increase in gage strain over the test period. A much longer period of testing would be required to definitively prove epoxy creep. The compression gage shows a higher strain than the tension gage. This is reasonable because when the gages are bonded to the beam and cured at an elevated temperature, a small compressive strain is introduced into the gage. Then when the beam is loaded, the gages in tension have this thermal strain subtracted from them while it is added to the gages loaded in compression.

Tables 11 and 12 are the aging data for the resistors and unbonded semiconductor gage in the 120°F oven. These changes are very small and do not substantiate an aging trend at 120°F.

Tables 13 and 14 are aging data for typical tension and compression gages bonded to the beam in the 160°F oven. Again, no discernable aging trend is noticeable.

Tables 15 and 16 are the aging data for the 160°F resistors and unbonded semiconductor gage. These data show no aging trends due to 160°F storage.

TABLE 5. BEAM STABILITY TEST AT 90°F. HISTORY OF BONDED TENSION GAGE NO. 8

SYMBOLS:

- t - Elapsed Time from Loading(t=0)
- T(t) - Platinum Resistor Temp @ Time t
- Eo - Bridge Output
- Eex - Bridge Excitation
- NOP(t) - Normalized Output(Excitation Corrected) @ Time t
- NOP'(t) - Normalized Output(Excitation & Temp Corrected) @ Time t
- S - Temperature Sensitivity
- G - Gage Factor
- ϵ - Beam Strain
- ϵ_u - Experimental Strain Uncertainty

RELATIONS:

- ΔT - T(t)-T(0)
- NOP(t) - 10^4(Eo/Eex)
- NOP'(t) - 10^4(Eo-SΔT)/Eex
- ΔNOP - NOP(t)-NOP(0)
- ΔNOP' - NOP'(t)-NOP'(0)
- ϵ(t) - 4[NOP'(t)-NOP(preload)]/G
- $\Delta\epsilon$ - ϵ(t)-ϵ(0)

VALUES:

- S = -.5mV/°F (Preloaded Average Value About 95 ± 15°F)
- ϵ_u = .5$\mu\epsilon$ (see text)
- G = 127 (using ϵ=-211$\mu\epsilon$ From Tension Semiconductor Gage #11 @ t=82min)

HISTORY of GAGE 8

SET	TIME/DATE	t(min)	Eo(mv)	Eex(V)	NOP	ΔNOP	T(°F)	ΔT(°F)	ΔNOP'	ϵ($\mu\epsilon$)	$\Delta\epsilon$($\mu\epsilon$)
1.	10:45/11-15-77	0	21.858	1.0000	21.843	0.000	89.918	0.000	0.000	-211	0
2.	10:49/11-15-77	4	21.858	1.0000	21.853	-0.010	89.904	-0.014	-0.017	-212	-1
3.	10:53/11-15-77	8	21.856	1.0016	21.835	-0.008	89.895	-0.023	-0.019	-212	-1
4.	10:59/11-15-77	14	21.868	1.0039	21.847	0.004	89.904	-0.014	-0.003	-211	0
5.	11:07/11-15-77	22	21.867	1.0057	21.855	0.011	89.909	-0.009	0.007	-211	0
6.	11:13/11-15-77	28	21.852	1.0037	21.848	-0.004	89.904	-0.014	-0.010	-212	0
7.	11:21/11-15-77	36	21.859	1.0073	21.843	-0.000	89.913	-0.005	-0.002	-211	0
8.	11:27/11-15-77	46	21.878	1.0077	21.853	0.010	89.922	0.005	0.012	-211	0
9.	11:37/11-15-77	52	21.848	1.0055	21.836	-0.007	89.900	-0.018	-0.016	-212	-1
10.	11:43/11-15-77	58	21.875	1.0086	21.863	0.020	89.904	-0.014	0.013	-211	0
11.	11:54/11-15-77	69	21.868	1.0065	21.848	0.005	89.904	-0.014	-0.002	-211	0
12.	12:07/11-15-77	82	21.878	1.0056	21.866	0.023	89.918	0.000	0.023	-211	1
13.	12:23/11-15-77	98	21.876	1.0055	21.864	0.021	89.895	-0.023	0.009	-211	0
14.	12:32/11-15-77	107	21.891	1.0097	21.879	0.035	89.891	-0.027	0.022	-211	1
15.	12:47/11-15-77	122	21.889	1.0055	21.877	0.034	89.886	-0.032	0.018	-211	1
16.	13:06/11-15-77	141	21.895	1.0052	21.884	0.048	89.891	-0.027	0.027	-210	1
17.	13:26/11-15-77	161	21.898	1.0055	21.886	0.043	89.891	-0.027	0.029	-210	1
18.	14:06/11-15-77	201	21.875	1.0055	21.863	0.020	89.868	-0.050	-0.005	-211	0
19.	14:38/11-15-77	233	21.888	1.0053	21.876	0.033	89.850	-0.068	-0.001	-211	0
20.	15:25/11-15-77	288	21.893	1.0052	21.882	0.038	89.854	-0.064	0.007	-211	0
21.	16:15/11-15-77	338	21.925	1.0053	21.892	0.058	89.845	-0.073	0.014	-211	0
22.	17:04/11-15-77	379	21.918	1.0053	21.898	0.055	89.836	-0.082	0.014	-211	0
23.	18:35/11-15-77	470	21.928	1.0058	21.917	0.074	89.809	-0.109	0.019	-211	1
24.	8:05/11-16-77	849	21.922	1.0052	21.911	0.067	89.831	-0.086	0.024	-211	1
25.	1:06/11-16-77	981	21.912	1.0052	21.899	-0.044	89.813	-0.105	-0.007	-211	0
26.	4:37/11-16-77	1264	21.915	1.0053	21.903	0.048	89.813	-0.105	0.008	-211	0
27.	9:03/11-16-77	1438	21.855	1.0050	21.842	-0.001	89.911	-0.005	-0.001	-211	0
.	11:10/11-16-77	1445	21.909	1.0058	21.898	0.055	89.854	-0.064	0.023	-211	1
.	7:43/11-17-77	2698	21.878	1.0055	21.856	0.015	89.850	-0.068	-0.019	-212	-1
30.	15:39/11-17-77	3145	21.888	1.0041	21.879	0.036	89.713	-0.205	0.034	-210	1
31.	8:10/11-18-77	4165	21.907	1.0052	21.898	0.054	89.836	-0.082	0.014	-211	0
32.	12:21/11-18-77	4416	21.949	1.0049	21.938	0.095	89.754	-0.164	0.013	-211	0
33.	14:45/11-18-77	4568	21.964	1.0049	21.953	0.110	89.709	-0.209	0.006	-211	0
34.	11:04/11-19-77	5779	21.912	1.0045	21.902	0.059	89.709	-0.209	-0.046	-211	-1
35.	14:51/11-19-77	6026	21.899	1.0053	21.887	0.044	89.781	-0.136	-0.024	-212	-1
36.	8:32/11-21-77	8587	21.768	1.0023	21.746	-0.097	90.102	0.264	0.015	-210	1
37.	8:09/11-22-77	9924	21.796	1.0036	21.783	-0.060	90.113	0.196	0.037	-210	1
38.	16:20/11-22-77	10415	21.955	1.0051	21.944	0.101	90.000	0.118	0.042	-210	1
39.	8:52/11-23-77	11487	21.947	1.0044	21.937	0.094	89.727	-0.191	-0.001	-211	-0
40.	13:36/11-23-77	11691	21.962	1.0047	21.952	0.109	89.722	-0.196	0.011	-211	0
41.	18:40/11-24-77	12955	21.941	1.0049	21.938	0.087	89.802	-0.118	0.029	-210	1
.	18:52/11-25-77	14387	21.875	1.0057	21.863	0.019	90.004	0.086	0.053	-209	2
.	20:46/11-26-77	16441	21.728	1.0050	21.699	-0.134	89.904	-0.014	-0.141	-216	-4
44.	8:29/11-28-77	18584	21.846	1.0036	21.620	-0.215	90.589	0.591	0.001	-209	1
45.	9:19/11-29-77	20074	21.843	1.0059	21.835	-0.008	89.986	0.068	0.026	-210	1
46.	16:06/11-29-77	20481	21.948	1.0059	21.929	0.086	89.909	-0.009	0.031	-210	1
47.	9:30/11-30-77	21513	21.894	1.0035	21.873	0.030	89.909	-0.009	0.009	-210	1
48.	15:32/11-30-77	21897	21.945	1.0049	21.934	0.091	89.818	-0.100	0.041	-210	1
49.	8:28/12- 1-77	22983	21.897	1.0052	21.886	0.042	89.895	-0.023	0.031	-210	1
50.	16:15/12- 1-77	23345	21.948	1.0058	21.831	-0.012	89.804	-0.114	-0.069	-213	-2
51.	16:01/12- 2-77	24798	21.948	1.0058	21.929	0.086	89.754	-0.164	0.004	-211	0
52.	11:05/12- 4-77	27598	21.873	1.0054	21.861	0.018	89.902	-0.064	0.050	-210	2
53.	13:15/12- 5-77	28958	21.878	1.0052	21.867	0.023	90.027	0.189	0.078	-209	2
54.	10:59/12- 6-77	30245	21.936	1.0058	21.925	0.082	89.868	-0.050	0.057	-210	2
55.	15:39/12- 6-77	30534	21.937	1.0047	21.927	0.084	89.809	-0.109	0.039	-210	1
56.	9:31/12- 7-77	31688	21.911	1.0053	21.899	0.056	89.911	-0.014	0.063	-209	2
57.	15:35/12- 7-77	31978	21.995	1.0044	21.985	0.142	89.727	-0.191	0.047	-210	1
58.	8:02/12- 8-77	32957	21.916	1.0049	21.985	0.062	89.798	-0.127	-0.002	-211	-0
59.	9:24/12- 9-77	34479	21.937	1.0043	21.978	0.134	89.722	-0.196	0.037	-210	1
60.	15:37/12- 9-77	34952	21.956	1.0049	21.945	0.102	89.754	-0.164	0.028	-211	1
61.	13:12/12-11-77	37608	21.916	1.0052	21.925	0.081	89.836	-0.082	0.041	-210	1
62.	7:56/12-12-77	38711	21.636	1.0077	21.619	-0.224	90.537	0.619	0.005	-209	3
63.	15:16/12-13-77	40591	21.942	1.0048	21.931	0.088	89.822	-0.096	0.041	-210	1
64.	8:18/12-14-77	41613	21.869	1.0054	21.857	0.014	89.972	0.055	0.041	-210	1
65.	8:03/12-16-77	44478	21.872	1.0053	21.860	0.017	89.922	0.005	0.028	-211	1
66.	9:41/12-16-77	44576	21.867	1.0055	21.858	0.017	89.941	0.023	0.018	-211	1
67.	8:45/12-19-77	48848	21.958	1.0059	21.951	0.108	89.681	-0.237	-0.010	-212	-0
68.	10:49/12-20-77	50484	22.003	1.0062	21.994	0.151	89.699	-0.218	0.041	-210	3
69.	9:43/12-21-77	51778	21.667	1.0083	21.649	-0.194	90.496	0.578	0.095	-208	3
70.	9:52/12-22-77	53227	21.829	1.0074	21.801	-0.042	90.459	0.541	0.108	-208	3
71.	11:02/12-23-77	54737	21.664	1.0078	21.647	-0.196	90.523	0.605	0.106	-208	3
72.	11:32/12-27-77	60527	21.876	1.0053	21.864	0.021	90.041	0.123	0.083	-209	3
73.	12:50/ 1- 1-77	67865	22.008	1.0028	22.002	0.239	89.508	-0.409	0.034	-210	1
74.	9:48/ 1- 3-77	70495	21.894	1.0058	21.894	0.051	89.945	0.027	0.065	-209	2
75.	13:48/ 1- 4-77	72175	21.915	1.0051	21.904	0.061	89.941	0.023	0.072	-209	2
.	11:27/ 1- 5-77	73482	21.848	1.0061	21.827	-0.016	90.141	0.223	0.095	-208	3
.	11:08/ 1- 6-77	75023	21.847	1.0056	21.725	-0.118	90.086	0.168	-0.034	-212	-1
78.	15:41/ 1- 9-77	79498	21.941	1.0057	21.647	-0.197	90.518	0.601	0.101	-208	3
79.	13:34/ 1-10-78	88089	21.781	1.0061	21.647	-0.196	90.168	0.258	-0.072	-214	-2
80.	20:10/ 1-11-78	92653	21.780	1.0076	21.684	-0.168	90.345	0.428	0.054	-210	2
81.	15:39/ 1-12-78	93814	21.870	1.0062	21.806	-0.057	90.141	0.223	0.075	-209	2
82.	15:38/ 1-13-78	95245	21.710	1.0072	21.707	-0.141	90.359	0.441	0.088	-209	3
83.	15:11/ 1-16-78	99148	21.829	1.0061	21.816	-0.027	90.286	0.368	0.107	-208	3
84.	15:34/ 1-17-78	91869	21.876	1.0055	21.864	0.021	90.022	0.105	0.073	-209	2
85.	15:28/ 1-18-78	92435	21.910	1.0058	21.899	0.056	89.872	-0.045	0.033	-210	1
86.	15:22/ 1-19-78	93877	21.885	1.0052	21.874	0.030	89.963	0.045	0.053	-210	2
87.	15:38/ 1-20-78	95328	21.768	1.0069	21.729	-0.114	90.245	0.328	0.058	-210	2
88.	15:32/ 1-24-78	101887	21.950	1.0045	21.948	0.097	89.809	-0.109	0.038	-210	1
89.	20:52/ 1-25-78	102847	21.689	1.0078	21.672	-0.171	90.459	0.541	0.099	-208	3
90.	15:20/ 1-27-78	105399	21.926	1.0050	21.915	0.072	90.111	0.193	0.169	-206	5
91.	8:11/ 1-30-78	109286	21.855	1.0070	21.636	-0.209	90.069	0.151	0.278	-203	6
92.	10:31/ 1-31-78	110871	21.913	1.0060	21.884	-0.039	90.173	0.255	0.088	-209	3
93.	13:38/ 2- 1-78	112493	21.867	1.0056	21.856	0.011	90.236	0.318	0.178	-206	5
94.	8:38/ 2- 3-78	115065	21.777	1.0066	21.763	-0.081	90.473	0.555	0.197	-205	6
95.	8:38/ 2- 4-78	119385	21.102	1.0110	21.158	-0.688	91.502	1.584	0.382	-202	10
96.	15:59/ 2-27-78	128958	21.889	1.0057	21.668	-0.169	90.165	1.247	0.248	-207	8
97.	8:28/ 2- 8-78	122255	21.676	1.0075	21.660	-0.183	90.682	0.764	0.199	-205	6
98.	13:29/ 2- 9-78	124888	21.986	1.0036	21.828	-0.015	90.223	0.305	0.137	-207	4
99.	9:53/ 2-15-78	132428	22.148	1.0027	22.134	0.291	89.031	-0.886	0.248	-204	9
100.	17:31/ 2-16-78	134328	21.936	1.0068	21.926	0.083	89.563	-0.354	0.206	-208	3
101.	15:48/ 2-21-78	141419	21.712	1.0078	21.695	-0.148	90.495	0.487	0.095	-208	3
102.	16:08/ 2-22-78	142975	21.689	1.0090	21.598	-0.254	90.788	0.783	0.137	-207	4
103.	15:25/ 2-23-78	144760	21.830	1.0081	21.600	-0.435	91.019	1.101	0.119	-208	4
104.	15:35/ 2-24-78	146738	21.399	1.0110	21.316	-0.530	91.101	1.183	0.001	-209	2
105.	15:50/ 2- 1-78	150795	21.458	1.0099	21.478	-0.414	91.101	1.183	0.127	-206	7
106.	14:10/ 2-15-78	170495	21.660	1.0090	21.356	-0.489	91.001	1.083	0.047	-210	1
107.	14:05/ 3-23-78	190170	21.386	1.0107	21.361	-0.492	91.365	1.447	0.241	-206	8
108.	14:49/ 3-31-78	201974	21.399	1.0108	21.373	-0.478	91.268	1.342	0.201	-205	6
109.	14:37/ 4-11-78	217750	21.045	1.0094	21.027	-0.809	90.992	1.065	0.240	-202	9
.	12:48/ 4-26-78	236145	20.946	1.0149	20.915	-0.909	92.152	2.414	0.107	-202	10
.	15:58/ 5-16-78	260243	21.010	1.0119	21.011	-0.612	92.091	2.175	0.274	-203	9
112.	15:25/ 5-31-78	289810	21.305	1.0112	21.188	-0.666	91.556	1.738	0.206	-205	6
113.	13:52/ 7-12-78	350197	21.810	1.0077	21.806	-0.059	90.588	0.770	0.115	-205	6
114.	10:27/ 7- 9-78	93113	21.978	1.0060	21.978	0.134	89.979	0.161	0.321	-201	10
115.	9:55/11-27-78	561040	21.974	1.0060	21.965	0.122	89.979	-0.059	0.101	-208	3
116.	10:20/12-11-78	588095	22.169	1.0025	21.167	0.178	89.765	-0.553	0.046	-210	1

THIS PAGE IS BEST QUALITY PRACTICABLE
FROM COPY FURNISHED TO DDC

TABLE 6. BEAM STABILITY AT 90°F. HISTORY OF BONDED COMPRESSION GAGE NO. 12

SYMBOLS:

t	- Elapsed Time from Loading(t=0)
T(t)	- Platinum Resistor Temp @ Time t
Eo	- Bridge Output
Eex	- Bridge Excitation
HOP(t)	- Normalized Output(Excitation Corrected) @ Time t
HOP'(t)	- Normalized Output(Excitation & Temp Corrected) @ Time t
B	- Temperature Sensitivity
G	- Gage Factor
ε	- Beam Strain
εe	- Experimental Strain Uncertainty

RELATIONS:

ΔT	- T(t)-T(0)
HOP(t)	- 10^6(Eo/Eex)
HOP'(t)	- 10^6(Eo-BAT)/Eex
ΔHOP	- HOP(t)-HOP(0)
ΔHOP'	- HOP'(t)-HOP'(0)
σ(t)	- 4[HOP'(t)-HOP(preload)]/G
Δσ	- σ(t)-σ(0)

VALUES:

B = -.3mV/°F (Preloaded Average Value About 90 ± 10°F)
εe = .5με (see text)
G = 115 (using ε= 285με From Compression Semiconductor Gage #22 @ t=82min)

HISTORY of GAGE 12

SET	TIME/DATE	t(min)	Eo(mv)	Eex(V)	HOP	ΔHOP	T(F)	ΔT(F)	ΔHOP'	σ(με)	Δσ(με)
1.	10:45/11-15-77	0	33.563	0.99000	33.936	0.000	89.910	0.000	0.000	286	0
2.	10:49/11-15-77	4	33.545	0.99000	33.910	-0.010	89.904	-0.014	-0.025	285	-1
3.	10:53/11-15-77	8	33.550	0.99000	33.923	-0.013	89.895	-0.023	-0.025	285	-1
4.	10:59/11-15-77	14	33.553	0.98990	33.930	-0.007	89.904	-0.014	-0.014	285	-0
5.	11:07/11-15-77	22	33.551	0.98990	33.928	-0.009	89.909	-0.009	-0.013	285	-0
6.	11:13/11-15-77	28	33.546	0.98989	33.923	-0.013	89.904	-0.014	-0.020	285	-1
7.	11:21/11-15-77	36	33.560	0.98985	33.932	-0.005	89.913	-0.005	-0.007	285	-0
8.	11:31/11-15-77	46	33.550	0.98989	33.920	-0.008	89.922	-0.005	-0.006	285	-0
9.	11:37/11-15-77	52	33.560	0.98989	33.930	-0.006	89.900	-0.018	-0.008	285	-0
10.	11:43/11-15-77	58	33.553	0.98989	33.930	-0.006	89.904	-0.014	-0.013	285	-0
11.	11:54/11-15-77	69	33.555	0.98988	33.932	-0.004	89.904	-0.014	-0.011	285	-0
12.	12:07/11-15-77	82	33.564	0.98988	33.942	0.006	89.918	0.000	0.006	286	0
13.	12:23/11-15-77	98	33.569	0.98986	33.947	0.011	89.895	-0.023	0.001	286	0
14.	12:37/11-15-77	107	33.570	0.98988	33.956	0.019	89.891	-0.027	0.005	286	0
15.	12:47/11-15-77	122	33.560	0.98987	33.938	0.001	89.886	-0.032	-0.015	285	-1
16.	13:06/11-15-77	141	33.586	0.98988	33.964	0.027	89.891	-0.027	-0.014	286	0
17.	13:26/11-15-77	161	33.589	0.98988	33.967	0.030	89.891	-0.027	-0.017	286	1
18.	14:06/11-15-77	201	33.588	0.98985	33.967	0.030	89.868	-0.050	-0.005	286	0
19.	14:38/11-15-77	233	33.582	0.98985	33.961	0.024	89.858	-0.068	-0.010	285	-0
20.	15:25/11-15-77	280	33.595	0.98984	33.974	0.038	89.854	-0.064	0.006	286	0
21.	16:15/11-15-77	330	33.607	0.98982	33.987	0.051	89.845	-0.073	0.014	286	0
22.	17:04/11-15-77	379	33.604	0.98981	33.984	0.047	89.836	-0.082	0.006	286	0
23.	18:35/11-15-77	470	33.625	0.98981	34.006	0.069	89.809	-0.109	0.014	286	0
24.	8:05/11-16-77	800	33.688	0.98985	33.979	0.043	89.831	-0.086	-0.001	286	-0
25.	9:06/11-16-77	901	33.618	0.98983	33.998	0.061	89.813	-0.105	-0.009	286	0
26.	4:29/11-16-77	1064	33.584	0.98985	33.959	0.022	89.813	-0.105	-0.031	285	-1
27.	9:03/11-16-77	1338	33.535	0.98991	33.911	-0.025	89.913	-0.005	-0.028	285	-1
.	11:18/11-16-77	1465	33.597	0.98983	33.977	0.040	89.854	-0.064	0.008	286	0
.	7:43/11-17-77	2698	33.534	0.98989	33.911	-0.026	89.850	-0.068	-0.060	284	-2
28.	15:10/11-17-77	3145	33.688	0.98978	34.078	0.134	89.713	-0.205	0.038	287	1
31.	8:10/11-18-77	4165	33.572	0.98988	33.958	0.013	89.836	-0.082	-0.078	285	-1
32.	12:21/11-18-77	4416	33.637	0.98982	34.012	0.076	89.754	-0.164	-0.007	285	-0
33.	14:45/11-18-77	4568	33.638	0.98979	34.019	0.083	89.709	-0.209	-0.023	285	-1
34.	11:04/11-19-77	5779	33.576	0.98985	33.955	0.018	89.709	-0.209	-0.008	283	-3
35.	14:51/11-19-77	6006	33.555	0.98991	33.931	-0.005	89.781	-0.136	-0.074	283	-3
36.	8:22/11-20-77	8587	33.413	0.99000	33.785	-0.152	90.182	0.264	-0.018	285	-1
37.	8:09/11-22-77	9924	33.456	0.98996	33.829	-0.107	90.113	0.196	-0.008	285	-0
38.	16:20/11-22-77	10415	33.617	0.98985	33.996	0.060	89.888	-0.118	-0.009	286	-0
39.	8:52/11-23-77	11407	33.598	0.98981	33.978	0.034	89.727	-0.191	-0.063	283	-7
40.	13:36/11-23-77	11691	33.622	0.98985	34.001	0.065	89.722	-0.196	-0.034	284	-1
.	10:40/11-24-77	12955	33.582	0.98987	33.968	0.024	89.880	-0.118	-0.036	284	-1
.	10:32/11-25-77	14387	33.521	0.98992	33.897	-0.048	90.004	0.006	0.004	286	0
41.	20:46/11-26-77	16441	33.588	0.98982	33.968	0.023	89.904	-0.014	0.016	286	1
44.	8:29/11-28-77	18584	33.598	0.98917	33.654	-0.282	89.509	-0.391	-0.217	286	1
45.	9:19/11-29-77	20074	33.581	0.98976	33.877	-0.059	89.986	0.068	-0.025	285	-1
46.	16:06/11-29-77	20481	33.587	0.98977	33.905	-0.029	89.809	-0.109	-0.026	285	-1
47.	9:10/11-30-77	21513	33.557	0.98978	33.820	-0.116	89.909	-0.009	-0.021	285	-1
48.	15:12/11-30-77	21987	33.595	0.98985	33.974	0.038	89.818	-0.100	-0.013	285	-0
49.	8:28/12- 1-77	22983	33.528	0.98994	33.904	-0.032	89.895	-0.023	-0.043	284	-2
50.	16:10/12- 1-77	23365	33.586	0.98986	33.964	0.028	89.804	-0.114	-0.029	285	-1
51.	16:03/12- 2-77	24798	33.586	0.98986	33.964	0.028	89.754	-0.164	-0.055	284	-2
52.	13:05/12- 4-77	27508	33.531	0.98990	33.907	-0.029	89.982	0.064	-0.003	286	0
53.	13:15/12- 5-77	28958	33.548	0.98991	33.921	-0.015	90.027	0.109	0.048	287	1
54.	10:50/12- 6-77	30745	33.575	0.98985	33.954	0.017	89.868	-0.050	-0.008	285	-0
55.	15:39/12- 6-77	30534	33.613	0.98982	33.993	0.057	89.889	-0.109	0.002	286	0
56.	9:31/12- 7-77	31686	33.559	0.98990	33.936	-0.001	89.931	-0.014	0.006	286	0
57.	15:35/12- 7-77	31970	33.642	0.98988	34.023	0.087	89.727	-0.191	-0.010	285	-0
58.	8:02/12- 8-77	32957	33.538	0.98987	33.915	-0.021	89.798	-0.127	-0.085	283	-3
59.	9:24/12- 9-77	34479	33.598	0.98984	33.969	0.033	89.722	-0.196	-0.066	283	-2
60.	15:37/12- 9-77	34852	33.587	0.98987	33.965	0.029	89.754	-0.164	-0.054	284	-2
61.	13:33/12-11-77	37600	33.565	0.98990	33.942	0.005	89.836	-0.082	-0.036	284	-1
62.	7:56/12-12-77	38711	33.297	0.98997	33.662	-0.274	89.537	0.619	0.339	287	1
63.	15:16/12-13-77	40591	33.565	0.98987	33.943	0.006	89.822	-0.096	-0.042	284	-1
64.	8:10/12-14-77	41613	33.499	0.98992	33.874	-0.062	89.972	0.055	-0.034	284	-1
65.	9:03/12-16-77	44478	33.588	0.98990	33.976	-0.060	89.922	0.005	-0.058	284	-2
66.	9:41/12-16-77	44578	33.486	0.98994	33.868	-0.074	89.941	-0.023	-0.064	283	-2
67.	9:45/12-19-77	48868	33.565	0.98979	33.946	0.009	89.681	-0.237	-0.118	282	-4
68.	10:49/12-20-77	50404	33.602	0.98982	33.982	0.046	89.699	-0.218	-0.065	283	-2
69.	9:43/12-21-77	51778	33.288	0.98924	33.642	-0.294	90.496	0.578	-0.002	286	-0
70.	9:52/12-22-77	52227	33.329	0.98913	33.695	-0.241	90.459	0.541	0.013	287	1
71.	11:02/12-23-77	54737	33.311	0.98916	33.678	-0.258	90.523	0.605	0.048	287	2
72.	11:12/12-27-77	60527	33.481	0.98894	33.855	-0.081	90.841	0.123	-0.019	285	-1
73.	12:50/ 1- 1-77	67885	33.673	0.98871	34.058	0.121	90.508	-0.409	-0.006	283	-3
74.	9:48/ 1- 3-77	70495	33.517	0.98889	33.894	-0.043	89.945	0.027	-0.029	285	-1
.	13:48/ 1- 4-77	72175	33.536	0.98892	33.912	-0.025	89.941	0.023	-0.013	285	-0
.	11:27/ 1- 5-77	73482	33.458	0.98897	33.830	-0.106	90.141	0.223	0.007	286	0
77.	13:08/ 1- 6-77	75023	33.481	0.98897	33.854	-0.082	90.086	0.168	0.003	286	0
78.	15:43/ 1- 9-77	79498	33.203	0.98916	33.648	-0.289	90.518	0.601	0.015	284	-1
79.	13:34/ 1-10-78	80089	33.399	0.98985	33.769	-0.168	90.169	0.252	-0.041	284	-1
80.	20:10/ 1-11-78	83683	33.316	0.98994	33.681	-0.255	90.345	0.428	-0.039	284	-1
81.	15:39/ 1-12-78	83814	33.445	0.98985	33.816	-0.128	90.141	0.223	-0.080	285	-0
82.	15:30/ 1-23-78	85245	33.325	0.98993	33.691	-0.245	90.359	0.441	-0.022	285	-1
83.	11:53/ 1-16-78	89348	33.450	0.98978	33.822	-0.114	90.186	0.268	-0.021	286	0
84.	15:34/ 1-17-78	91899	33.499	0.98985	33.873	-0.063	89.945	0.027	-0.018	285	-0
85.	15:28/ 1-18-78	92435	33.538	0.98982	33.906	-0.031	89.872	-0.045	-0.054	284	-2
86.	15:22/ 1-19-78	93877	33.508	0.98995	33.874	-0.062	89.963	0.045	-0.039	284	-1
87.	15:30/ 1-20-78	95325	33.353	0.98911	33.708	-0.238	90.245	0.328	-0.071	283	-2
88.	15:32/ 1-24-78	101807	33.494	0.98998	33.878	-0.066	89.808	-0.118	-0.126	281	-4
89.	20:52/ 1-24-78	102847	33.261	0.98921	33.674	-0.312	90.659	0.541	-0.039	284	-1
90.	15:28/ 1-27-78	105395	33.521	0.98993	33.896	-0.048	90.111	0.193	0.050	288	2
91.	8:11/ 1-30-78	109286	33.254	0.98928	33.617	-0.319	90.869	0.951	0.161	211	6
92.	10:36/ 1-31-78	110871	33.506	0.98992	33.881	-0.055	90.173	0.255	0.074	288	3
93.	13:50/ 2- 1-78	112403	33.457	0.98998	33.829	-0.107	90.236	0.318	0.054	287	2
94.	8:38/ 2- 3-78	115045	33.373	0.98987	33.742	-0.195	90.473	0.555	0.006	289	1
95.	9:30/ 2- 6-78	119305	32.798	0.98967	33.149	-0.796	91.982	1.984	0.206	211	7
96.	10:35/ 2- 7-78	120950	33.102	0.98938	33.457	-0.479	91.165	1.247	0.151	212	5
97.	8:20/ 2- 8-78	122255	33.267	0.98918	33.631	-0.305	90.682	0.764	0.041	288	2
98.	13:25/ 2- 9-78	124000	33.473	0.98993	33.846	-0.090	90.223	0.305	0.064	288	2
99.	9:57/ 2-15-78	132428	33.385	0.98982	33.965	0.028	89.831	-0.086	-0.015	285	-1
100.	17:31/ 2-16-78	134326	33.375	0.98911	33.742	-0.196	89.963	0.045	-0.171	280	-6
101.	15:40/ 2-21-78	141419	33.497	0.98935	33.832	-0.093	90.409	0.491	-0.237	197	-8
102.	16:08/ 2-22-78	142875	33.429	0.98943	33.782	-0.093	90.788	0.783	-0.159	200	-6
103.	15:35/ 2-23-78	144288	32.986	0.98953	33.254	-0.682	91.819	1.101	-0.126	201	-4
104.	15:35/ 2-24-78	145730	32.798	0.98967	33.132	-0.806	91.101	1.103	-0.206	198	-7
105.	15:50/ 2- 1-78	150795	32.915	0.98959	33.269	-0.674	91.321	1.203	-0.215	203	-2
106.	14:10/ 2-19-78	170858	32.988	0.98963	33.331	-0.605	91.001	1.003	-0.058	204	-2
107.	14:05/ 2-20-78	170937	32.962	0.98962	33.191	-0.746	91.365	1.447	-0.015	205	-1
108.	16:49/ 3-31-78	201934	32.978	0.98960	33.219	-0.721	91.268	1.342	-0.043	204	-1
.	14:33/ 4-11-78	217758	33.020	0.98945	33.372	-0.564	90.931	1.073	-0.042	206	0
.	12:48/ 4-14-78	220345	32.439	0.99007	32.764	-1.172	93.352	3.434	0.057	208	2
111.	13:58/ 4-18-78	224243	32.489	0.98994	32.819	-1.117	91.893	2.175	-0.019	205	-1
112.	15:25/ 5-31-78	269810	32.647	0.98977	32.984	-0.952	91.656	1.738	-0.074	203	-3
113.	13:52/ 7-12-78	306197	33.211	0.98918	33.574	-0.362	90.368	0.450	-0.135	201	-5
114.	10:27/ 8- 8-78	437912	32.627	0.98983	32.982	-0.974	91.097	1.979	-0.024	199	-1
115.	9:05/11-22-78	861488	33.396	0.98951	33.762	-0.176	89.979	-0.039	-0.194	199	-7
116.	10:30/12-11-78	900869	33.529	0.98951	33.901	-0.035	89.868	-0.553	-0.319	195	-11

THIS PAGE IS BEST QUALITY PRACTICABLE
FROM COPY FURNISHED TO DDC

TABLE 7. BEAM STABILITY TEST AT 90°F. HISTORY OF REFERENCE COMPENSATION RESISTORS

90°F RESISTANCE HISTORY

SET	TIME/DATE	t(min)	T(F)	ΔT(F)	RN55C 1Ω Ohm	RN55C ΔOhm	CARBON 1Ω Ohm	CARBON ΔOhm	RN55C 1500 Ohm	RN55C ΔOhm	CARBON 1500 Ohm	CARBON ΔOhm
1.	10:49/11-15-77	0	89.918	0.000	10.189	0.000	10.375	0.000	1502.43	0.000	1507.63	0.000
2.	11:21/11-15-77	36	89.913	-0.005	10.188	-0.009	10.366	-0.009	1501.31	-1.120	1506.49	-1.140
3.	11:43/11-15-77	58	89.904	-0.014	10.190	0.001	10.377	0.002	1502.43	0.000	1507.66	0.030
4.	12:07/11-15-77	82	89.918	0.000	10.190	0.001	10.377	0.002	1502.49	0.060	1507.66	0.030
5.	12:23/11-15-77	98	89.895	-0.023	10.191	0.002	10.378	0.003	1502.46	0.030	1507.63	0.000
6.	12:47/11-15-77	122	89.886	-0.032	10.190	0.001	10.376	0.001	1502.47	0.040	1507.68	0.050
7.	13:26/11-15-77	161	89.898	-0.020	10.189	0.000	10.376	0.001	1502.41	-0.020	1507.61	-0.020
8.	14:38/11-15-77	233	89.869	-0.049	10.188	-0.001	10.375	0.000	1502.42	-0.010	1507.60	-0.030
9.	15:29/11-15-77	284	89.854	-0.064	10.190	0.001	10.377	0.002	1502.50	0.070	1507.68	0.050
10.	17:06/11-15-77	379	89.835	-0.083	10.189	0.000	10.375	0.000	1502.44	0.010	1507.62	-0.016
11.	18:35/11-15-77	470	89.807	-0.111	10.184	-0.005	10.370	-0.005	1501.56	-0.870	1506.76	-0.870
12.	8:05/11-16-77	900	89.831	-0.087	10.188	-0.001	10.374	-0.001	1502.47	0.040	1506.65	-0.980
13.	9:06/11-16-77	961	89.812	-0.106	10.191	0.002	10.376	0.001	1502.39	-0.040	1507.58	-0.050
14.	9:29/11-16-77	1064	89.813	-0.106	10.190	0.001	10.377	0.002	1502.44	0.010	1507.13	-0.500
15.	9:03/11-16-77	1338	89.913	-0.005	10.190	0.001	10.376	0.001	1502.47	0.040	1507.67	0.040
16.	11:10/11-16-77	1465	89.894	-0.024	10.189	0.000	10.375	0.000	1502.45	0.020	1507.63	0.000
17.	7:43/11-17-77	2638	89.869	-0.049	10.187	-0.002	10.373	-0.002	1502.58	0.070	1507.68	0.050
18.	15:10/11-17-77	3145	89.711	-0.207	10.183	-0.006	10.369	-0.006	1502.07	-0.360	1507.27	-0.360
19.	8:10/11-18-77	4165	89.835	-0.083	10.189	0.000	10.375	0.000	1507.46	5.030	1507.66	0.030
20.	12:21/11-18-77	4416	89.752	-0.166	10.189	0.000	10.375	0.000	1502.36	-0.070	1507.56	-0.070
21.	14:45/11-18-77	4560	89.706	-0.212	10.188	-0.000	10.375	0.000	1502.41	-0.020	1507.60	-0.030
22.	11:06/11-19-77	5779	89.706	-0.212	10.188	-0.001	10.374	-0.001	1502.54	0.110	1507.76	0.130
23.	14:51/11-19-77	6006	89.768	-0.130	10.189	0.000	10.376	0.001	1502.59	0.160	1507.80	0.170
24.	8:32/11-21-77	8587	89.185	0.267	10.188	-0.001	10.373	-0.002	1502.55	0.120	1507.72	0.090
25.	8:09/11-22-77	9924	90.116	0.198	10.178	-0.010	10.364	-0.011	1500.00	-1.550	1506.06	-1.570
26.	16:28/11-22-77	10415	89.798	-0.120	10.190	0.001	10.376	0.001	1502.46	0.030	1507.65	0.020
27.	8:52/11-23-77	11407	89.725	-0.193	10.187	-0.002	10.373	-0.002	1502.47	0.040	1507.66	0.030
28.	15:56/11-23-77	11691	89.726	-0.190	10.186	-0.003	10.372	-0.003	1501.59	-0.840	1506.78	-0.850
29.	18:48/11-24-77	12955	89.798	-0.120	10.192	0.003	10.971	0.596	1503.04	0.610	1508.24	0.610
30.	8:29/11-28-77	16584	90.517	0.599	10.191	0.002	10.376	0.001	1502.46	0.030	1507.63	0.000
31.	9:19/11-29-77	20074	89.987	0.069	10.185	-0.004	10.371	-0.004	1501.95	-0.480	1507.12	-0.510
32.	16:06/11-29-77	20681	89.887	-0.111	10.190	0.001	10.376	0.001	1502.42	-0.010	1507.59	-0.040
33.	9:18/11-30-77	21513	89.989	-0.009	10.190	0.001	10.376	0.001	1502.46	0.030	1507.65	0.020
34.	15:32/11-30-77	21887	89.817	-0.181	10.185	-0.004	10.371	-0.004	1502.39	-0.040	1507.59	-0.040
35.	8:28/12- 1-77	23985	89.895	-0.023	10.189	0.000	10.375	0.000	1502.46	0.030	1507.66	0.030
36.	16:18/12- 1-77	24365	89.883	-0.115	10.186	-0.003	10.371	-0.004	1501.88	-0.630	1506.98	-0.650
37.	16:03/12- 2-77	24798	89.752	-0.166	10.186	-0.003	10.371	-0.004	1501.88	-0.630	1506.98	-0.650
38.	13:05/12- 4-77	27588	89.903	0.065	10.189	0.000	10.376	0.001	1502.43	0.000	1507.63	0.000
39.	18:58/12- 6-77	30245	89.867	-0.051	10.189	0.000	10.375	0.000	1502.45	0.020	1507.63	0.000
40.	15:39/12- 6-77	30534	89.807	-0.111	10.190	0.001	10.377	0.002	1502.43	0.000	1507.61	-0.020
41.	9:31/12- 7-77	31686	89.932	0.014	10.190	0.001	10.377	0.002	1502.41	-0.020	1507.62	-0.010
42.	15:35/12- 7-77	31978	89.725	-0.193	10.187	-0.002	10.375	0.000	1502.48	0.050	1507.68	0.050
43.	8:02/12- 8-77	32957	89.789	-0.129	10.188	-0.001	10.374	-0.001	1502.50	0.070	1507.70	0.070
44.	9:24/12- 9-77	34479	89.726	-0.190	10.191	0.002	10.376	0.001	1502.52	0.090	1507.73	0.100
45.	15:37/12- 9-77	34852	89.752	-0.166	10.191	0.002	10.378	0.003	1502.48	0.050	1507.69	0.060
46.	13:33/12-11-77	37688	89.835	-0.083	10.192	0.003	10.377	0.002	1502.44	0.010	1507.64	0.010
47.	7:56/12-12-77	38711	90.545	0.627	10.178	-0.011	10.365	-0.010	1501.14	-1.290	1506.30	-1.330
48.	15:16/12-13-77	40591	89.821	-0.097	10.190	0.001	10.376	0.001	1502.44	0.010	1507.61	-0.020
49.	8:10/12-14-77	41613	89.973	0.055	10.191	0.002	10.377	0.002	1502.55	0.120	1507.73	0.100
50.	8:03/12-16-77	44478	89.923	0.005	10.190	0.001	10.377	0.002	1502.53	0.100	1507.72	0.090
51.	10:49/12-28-77	58484	89.697	-0.221	10.189	0.000	10.375	0.000	1502.49	0.060	1507.68	0.050
52.	9:43/12-21-77	91778	90.583	0.585	10.194	0.005	10.380	0.005	1502.49	0.060	1507.69	0.060
53.	9:52/12-22-77	93227	90.466	0.548	10.173	-0.016	10.358	-0.017	1499.82	-2.610	1504.99	-2.640
54.	11:02/12-23-77	94737	90.531	0.613	10.192	0.003	10.378	0.003	1502.45	0.020	1507.62	-0.017
55.	11:32/12-27-77	69527	90.062	0.124	10.191	0.002	10.377	0.002	1502.45	0.020	1507.64	0.010
56.	13:58/ 1- 1-78	67885	89.583	-0.415	10.189	0.000	10.376	0.001	1502.43	0.000	1507.65	0.020
57.	9:48/ 1- 3-78	70495	89.946	0.028	10.190	0.001	10.375	0.000	1502.47	0.040	1507.63	0.000
58.	13:08/ 1- 4-78	72175	89.941	0.023	10.192	0.003	10.377	0.002	1502.47	0.040	1507.69	0.060
59.	11:27/ 1- 5-78	73482	90.144	0.226	10.193	0.004	10.380	0.005	1502.49	0.060	1507.67	0.040
60.	11:08/ 1- 6-78	75023	90.089	0.171	10.192	0.003	10.377	0.002	1502.43	0.000	1507.61	-0.020
61.	15:43/ 1- 9-78	79498	90.526	0.608	10.186	-0.003	10.372	-0.003	1502.40	-0.030	1507.55	-0.080
62.	13:34/ 1-10-78	80889	90.172	0.254	10.188	-0.001	10.374	-0.001	1502.49	0.060	1507.66	0.030
63.	20:10/ 1-11-78	82653	90.351	0.433	10.187	-0.002	10.373	-0.002	1502.47	0.040	1507.64	0.010
64.	15:39/ 1-12-78	83814	90.144	0.226	10.189	0.000	10.375	0.000	1502.45	0.020	1507.63	0.000
65.	15:38/ 1-13-78	85265	90.365	0.447	10.190	0.001	10.377	0.002	1502.48	0.050	1507.66	0.030
66.	11:53/ 1-16-78	89348	90.198	0.272	10.191	0.002	10.377	0.002	1502.50	0.070	1507.67	0.040
67.	15:34/ 1-17-78	91089	90.024	0.106	10.189	0.000	10.376	0.001	1502.45	0.020	1507.64	0.010
68.	15:28/ 1-18-78	92435	89.872	-0.046	10.189	0.000	10.376	0.001	1502.45	0.020	1507.64	0.010
69.	15:22/ 1-19-78	93877	89.964	0.046	10.189	0.000	10.376	0.001	1502.44	0.010	1507.62	-0.010
70.	15:38/ 1-20-78	95325	90.258	0.332	10.191	0.002	10.378	0.003	1502.46	0.030	1507.66	0.030
71.	15:32/ 1-24-78	101847	89.798	-0.128	10.189	0.000	10.375	0.000	1502.54	0.110	1507.76	0.130
72.	20:52/ 1-25-78	102847	90.466	0.548	10.188	-0.001	10.374	-0.001	1502.61	0.180	1507.78	0.150
73.	15:28/ 1-27-78	105395	90.114	0.196	10.194	0.005	10.380	0.005	1502.48	0.050	1507.65	0.020
74.	8:11/ 1-30-78	109256	90.881	0.963	10.194	0.005	10.379	0.004	1502.51	0.080	1507.68	0.050
75.	10:36/ 1-31-78	110871	90.176	0.258	10.194	0.005	10.379	0.004	1502.58	0.070	1507.69	0.060
76.	13:38/ 2- 1-78	112491	90.241	0.323	10.194	0.005	10.380	0.005	1502.47	0.040	1507.66	0.030
77.	8:38/ 2- 3-78	115865	90.488	0.562	10.191	0.002	10.378	0.003	1502.52	0.090	1507.70	0.070
78.	8:38/ 2- 6-78	119385	91.928	2.018	10.193	0.004	10.379	0.004	1502.46	0.030	1507.63	0.000
79.	10:15/ 2- 7-78	120958	91.181	1.263	10.196	0.007	10.381	0.006	1502.44	0.010	1507.61	-0.020
80.	8:28/ 2- 8-78	122255	90.692	0.774	10.193	0.004	10.379	0.004	1502.47	0.040	1507.65	0.020
81.	13:25/ 2- 9-78	124888	90.227	0.309	10.191	0.002	10.378	0.003	1502.47	0.040	1507.66	0.030
82.	9:53/ 2-15-78	132428	89.831	-0.087	10.196	0.007	10.382	0.007	1502.53	0.100	1507.73	0.100
83.	17:31/ 2-16-78	134326	89.964	0.046	10.194	0.005	10.379	0.004	1502.48	0.050	1507.71	0.080
84.	16:57/ 2-17-78	135732	91.075	1.157	10.198	0.009	10.377	0.002	1502.59	0.160	1507.75	0.120
85.	15:48/ 2-21-78	141415	90.411	0.493	10.194	0.005	10.378	0.003	1502.51	0.080	1507.68	0.050
86.	16:08/ 2-22-78	142875	90.711	0.793	10.192	0.003	10.379	0.004	1502.48	0.050	1507.64	0.010
87.	15:25/ 2-23-78	144288	91.833	1.115	10.194	0.005	10.380	0.005	1502.51	0.080	1507.66	0.030
88.	15:35/ 2-24-78	145738	91.116	1.198	10.193	0.004	10.378	0.003	1502.54	0.110	1507.69	0.060
89.	14:48/ 2-27-78	149995	91.379	1.461	10.194	0.005	10.380	0.005	1502.63	0.200	1507.79	0.160
90.	15:58/ 3- 1-78	150795	91.218	1.300	10.192	0.003	10.378	0.003	1502.52	0.090	1507.68	0.050
91.	14:18/ 3-15-78	170855	91.015	1.097	10.191	0.002	10.377	0.002	1502.54	0.110	1507.71	0.080
92.	14:05/ 3-23-78	192378	91.384	1.466	10.194	0.005	10.380	0.005	1502.54	0.110	1507.71	0.080
93.	14:49/ 3-31-78	201934	91.278	1.360	10.194	0.005	10.379	0.004	1502.53	0.100	1507.68	0.050
94.	14:33/ 4-11-78	217758	90.964	1.046	10.194	0.005	10.380	0.005	1502.42	-0.010	1507.66	0.030
95.	12:48/ 4-24-78	236365	92.386	2.468	10.193	0.004	10.379	0.004	1502.51	0.080	1507.65	0.020
96.	15:58/ 5-16-78	268243	92.121	2.203	10.195	0.006	10.381	0.006	1502.56	0.130	1507.69	0.060
97.	15:25/ 5-31-78	289818	91.679	1.761	10.194	0.005	10.379	0.004	1502.52	0.090	1507.66	0.030
98.	11:52/ 7-12-78	350197	90.374	0.456	10.193	0.004	10.379	0.004	1502.48	0.050	1507.67	0.040
99.	13:32/ 8- 8-78	389857	92.947	3.029	10.169	-0.020	10.351	-0.024	1502.61	0.180	1507.73	0.100
100.	10:27/ 9- 8-78	433512	91.923	2.005	10.194	0.005	10.381	0.006	1502.47	0.040	1507.50	-0.050
101.	9:55/11-22-78	561488	89.886	-0.032	10.194	0.005	10.380	0.005	1502.66	0.230	1507.86	0.230
102.	10:20/12-11-78	568865	89.365	-0.553	10.200	0.011	10.386	0.011	1502.52	0.090	1507.79	0.160

THIS PAGE IS BEST QUALITY PRACTICABLE
FROM COPY FURNISHED TO DDC

TABLE 8. BEAM STABILITY TEST AT 90°F. HISTORY OF REFERENCE COMPENSATION RESISTORS AND UNBONDED SEMICONDUCTOR GAGE

90° F RESISTANCE HISTORY

SET	TIME/DATE	t(min)	T(F)	ΔT(F)	RN55C 50K Ohm	RN55C ΔOhm	CARBON 50K Ohm	CARBON ΔOhm	SEMICONDUCTOR GAGE UNBONDED Ohm	SEMICONDUCTOR GAGE ΔOhm
1	10:45/11-15-77	0	89.918	0.000	51031.0	0.0	50954.0	0.0	529.14	0.00
2.	11:21/11-15-77	36	89.913	-0.005	51030.0	-1.0	50952.0	-2.0	528.80	-0.34
3.	11:43/11-15-77	58	89.904	-0.014	51033.0	2.0	50955.0	1.0	529.19	0.05
4.	12:07/11-15-77	82	89.918	0.000	51033.0	2.0	50953.0	-1.0	529.18	0.04
5.	12:23/11-15-77	98	89.895	-7.023	51033.0	2.0	50955.0	1.0	529.16	0.02
6.	12:47/11-15-77	122	89.886	-0.032	51033.0	2.0	50955.0	1.0	529.17	0.03
7.	13:26/11-15-77	161	89.890	-0.028	51032.0	1.0	50954.0	0.0	529.15	0.01
8.	14:38/11-15-77	233	89.849	-0.069	51031.0	0.0	50955.0	1.0	529.14	0.00
9.	15:25/11-15-77	280	89.854	-0.064	51032.0	1.0	50953.0	-1.0	529.16	0.02
10.	17:04/11-15-77	379	89.835	-0.083	51029.0	-2.0	50955.0	1.0	529.13	-0.01
11.	18:35/11-15-77	470	89.807	-0.111	51032.0	1.0	50955.0	1.0	528.82	-0.32
12.	8:05/11-16-77	800	89.831	-0.087	51032.0	1.0	50953.0	-1.0	529.14	0.00
13.	3:06/11-16-77	981	89.812	-0.106	51032.0	1.0	50956.0	2.0	529.12	-0.02
14.	4:29/11-16-77	1064	89.812	-0.106	51034.0	3.0	50955.0	1.0	529.16	0.02
15.	9:03/11-16-77	1338	89.913	-0.005	51033.0	2.0	50956.0	2.0	529.26	0.12
16.	11:10/11-16-77	1465	89.854	-0.064	51034.0	3.0	50954.0	0.0	529.10	-0.04
17.	7:43/11-17-77	2698	89.849	-0.069	51031.0	0.0	50956.0	2.0	529.19	0.05
18.	15:10/11-17-77	3145	89.711	-0.207	51033.0	2.0	50954.0	0.0	528.87	-0.27
19.	8:10/11-18-77	4165	89.835	-0.083	51029.0	-2.0	50952.0	-2.0	529.15	0.01
20.	12:21/11-18-77	4416	89.752	-0.166	51033.0	2.0	50953.0	-1.0	529.00	-0.14
21.	14:45/11-18-77	4568	89.706	-0.212	51032.0	1.0	50955.0	1.0	528.99	-0.15
22.	11:04/11-19-77	5779	89.706	-0.212	51033.0	2.0	50957.0	3.0	529.02	-0.12
23.	14:51/11-19-77	6986	89.788	-0.138	51030.0	-1.0	50956.0	2.0	529.04	-0.10
24.	8:32/11-21-77	8507	90.185	0.267	51034.0	3.0	50958.0	4.0	529.23	0.09
25.	8:09/11-22-77	9924	90.116	0.198	51033.0	2.0	50956.0	2.0	528.78	-0.36
26.	16:28/11-22-77	10415	89.798	-0.120	51032.0	1.0	50955.0	1.0	529.15	0.01
27.	8:52/11-23-77	11407	89.725	-0.193	51033.0	2.0	50958.0	4.0	529.09	-0.05
28.	13:36/11-23-77	11691	89.720	-0.198	51032.0	1.0	50955.0	1.0	528.81	-0.33
29.	10:40/11-24-77	12955	89.798	-0.120	51032.0	1.0	50955.0	1.0	529.75	0.61
30.	8:29/11-28-77	18584	90.517	0.599	51034.0	3.0	50955.0	1.0	529.56	0.42
31.	9:19/11-29-77	20074	89.987	0.069	51033.0	2.0	50954.0	0.0	529.02	-0.12
32.	16:06/11-29-77	20401	89.807	-0.111	51030.0	-1.0	50954.0	0.0	529.14	0.00
33.	9:18/11-30-77	21513	89.909	-0.009	51031.0	0.0	50956.0	2.0	529.21	0.07
34.	15:32/11-30-77	21887	89.817	-0.101	51028.0	-3.0	50952.0	-2.0	529.09	-0.05
35.	8:28/12- 1-77	22903	89.895	-0.023	51033.0	2.0	50956.0	2.0	529.18	0.04
36.	16:10/12- 1-77	23365	89.803	-0.115	51033.0	2.0	50953.0	-1.0	528.90	-0.24
37.	16:03/12- 2-77	24798	89.752	-0.166	51033.0	2.0	50953.0	-1.0	528.90	-0.24
38.	13:05/12- 4-77	27500	89.983	0.065	51029.0	-2.0	50951.0	-3.0	529.19	0.05
39.	10:50/12- 6-77	30245	89.867	-0.051	51031.0	0.0	50957.0	3.0	529.15	0.01
40.	15:39/12- 6-77	30534	89.807	-0.111	51030.0	-1.0	50955.0	1.0	529.00	-0.06
41.	9:31/12- 7-77	31686	89.932	0.014	51032.0	1.0	50955.0	1.0	529.21	0.07
42.	15:35/12- 7-77	31970	89.725	-0.193	51033.0	2.0	50953.0	-1.0	529.10	-0.04
43.	8:02/12- 8-77	32957	89.789	-0.129	51033.0	2.0	50954.0	0.0	529.21	0.07
44.	9:24/12- 9-77	34479	89.720	-0.198	51029.0	-2.0	50955.0	1.0	529.01	-0.13
45.	15:37/12- 9-77	34852	89.752	-0.166	51030.0	-1.0	50955.0	1.0	529.00	-0.06
46.	13:33/12-11-77	37688	89.835	-0.083	51034.0	3.0	50954.0	0.0	529.05	-0.09
47.	7:56/12-12-77	38711	90.545	0.627	51033.0	2.0	50953.0	-1.0	528.89	-0.25
48.	15:16/12-13-77	40591	89.821	-0.097	51031.0	0.0	50959.0	5.0	529.08	-0.06
49.	8:18/12-14-77	41613	89.973	0.055	51034.0	3.0	50959.0	5.0	529.16	0.02
50.	8:03/12-16-77	44478	89.923	0.005	51033.0	2.0	50955.0	1.0	529.24	0.10
51.	10:49/12-20-77	50484	89.697	-0.221	51034.0	3.0	50954.0	0.0	528.93	-0.21
52.	9:43/12-21-77	51778	90.583	0.585	51034.0	3.0	50957.0	3.0	529.30	0.16
53.	9:52/12-22-77	53227	90.466	0.548	51032.0	1.0	50955.0	1.0	528.47	-0.67
54.	11:02/12-23-77	54737	90.531	0.613	51037.0	6.0	50954.0	0.0	529.46	0.32
55.	11:32/12-27-77	58527	90.842	0.124	51033.0	2.0	50957.0	3.0	529.23	0.09
56.	12:50/ 1- 1-78	67005	89.503	-0.415	51032.0	1.0	50957.0	3.0	529.03	-0.11
57.	9:40/ 1- 3-78	70495	89.946	0.028	51033.0	2.0	50955.0	1.0	529.26	0.12
58.	13:40/ 1- 4-78	72175	90.171	0.253	51033.0	2.0	50956.0	2.0	529.26	0.12
59.	11:27/ 1- 5-78	73502	90.154	0.226	51032.0	1.0	50956.0	2.0	529.37	0.23
60.	13:08/ 1- 6-78	75023	90.089	0.171	51030.0	-1.0	50953.0	-4.0	529.34	0.20
61.	15:43/ 1- 9-78	79498	90.526	0.608	51031.0	0.0	50955.0	1.0	529.52	0.38
62.	13:34/ 1-10-78	80809	90.172	0.254	51036.0	5.0	50954.0	0.0	529.51	0.37
63.	20:10/ 1-11-78	82653	90.351	0.433	51032.0	1.0	50955.0	1.0	529.58	0.44
64.	15:39/ 1-12-78	83914	90.144	0.226	51029.0	-2.0	50954.0	0.0	529.36	0.22
65.	15:30/ 1-13-78	85245	90.365	0.447	51034.0	3.0	50955.0	1.0	529.51	0.37
66.	11:53/ 1-16-78	89348	90.272	0.272	51030.0	-1.0	50957.0	3.0	529.36	0.22
67.	15:34/ 1-17-78	91009	90.024	0.186	51032.0	1.0	50954.0	0.0	529.25	0.11
68.	15:20/ 1-18-78	92435	89.872	-0.046	51032.0	1.0	50954.0	0.0	529.25	0.11
69.	15:22/ 1-19-78	93877	89.964	0.046	51034.0	3.0	50952.0	-2.0	529.32	0.18
7	15:30/ 1-20-78	95325	90.250	0.332	51032.0	1.0	50960.0	6.0	529.55	0.41
7	15:32/ 1-24-78	101087	89.798	-0.120	51029.0	-2.0	50960.0	6.0	529.00	-0.06
7	20:52/ 1-25-78	102047	90.466	0.548	51033.0	2.0	50958.0	4.0	529.47	0.33
73.	15:20/ 1-27-78	103395	90.114	0.196	51031.0	0.0	50955.0	1.0	529.77	0.63
74.	8:11/ 1-30-78	109206	90.001	0.063	51032.0	1.0	50956.0	2.0	529.09	0.75
75.	10:36/ 1-31-78	110071	90.176	0.258	51032.0	1.0	50959.0	5.0	529.74	0.68
76.	13:30/ 2- 1-78	112493	90.241	0.323	51035.0	4.0	50956.0	2.0	529.83	0.69
77.	8:30/ 2- 3-78	115065	90.488	0.562	51035.0	4.0	50958.0	4.0	529.95	0.81
78.	8:30/ 2- 6-78	119335	91.928	2.002	51033.0	2.0	50959.0	5.0	530.50	1.36
79.	10:35/ 2- 7-78	120850	91.181	1.253	51032.0	1.0	50958.0	4.0	530.31	1.17
80.	8:20/ 2- 8-78	122295	90.692	0.774	51031.0	0.0	50957.0	3.0	530.06	0.92
81.	13:25/ 2- 9-78	124000	90.227	0.309	51031.0	0.0	50957.0	3.0	529.85	0.71
82.	9:53/ 2-15-78	132420	89.991	-0.007	51032.0	1.0	50957.0	3.0	529.63	0.49
83.	17:31/ 2-16-78	134320	89.964	0.046	51031.0	0.0	50958.0	4.0	529.51	0.37
84.	16:57/ 2-17-78	135732	91.075	1.157	51033.0	2.0	50958.0	4.0	530.17	1.03
85.	15:40/ 2-21-78	141415	90.411	0.493	51030.0	-1.0	50957.0	3.0	529.53	0.39
86.	16:00/ 2-22-78	142875	90.711	0.793	51031.0	0.0	50956.0	2.0	529.64	0.50
87.	15:25/ 2-23-78	144280	91.033	1.115	51032.0	1.0	50958.0	4.0	529.75	0.61
88.	15:35/ 2-24-78	145730	91.116	1.198	51031.0	0.0	50957.0	3.0	530.08	0.94
89.	14:40/ 2-27-78	149995	91.379	1.461	51033.0	2.0	50961.0	7.0	530.03	0.89
90	15:50/ 3- 1-78	158795	91.218	1.300	51035.0	4.0	50958.0	4.0	529.92	0.78
9	14:10/ 3-15-78	170855	91.015	1.097	51033.0	2.0	50961.0	7.0	529.75	0.61
9	14:05/ 3-23-78	190370	91.304	1.466	51033.0	2.0	50955.0	1.0	529.91	0.77
9.	14:49/ 3-31-78	201934	91.278	1.360	51030.0	-1.0	50956.0	2.0	530.13	0.99
94.	14:33/ 4-11-78	217758	90.964	1.046	51035.0	4.0	50956.0	2.0	529.74	0.60
95.	12:40/ 4-24-78	236365	92.384	2.466	51034.0	3.0	50961.0	7.0	530.30	1.16
96.	15:50/ 5-16-78	268243	92.121	2.203	51034.0	3.0	50964.0	10.0	531.05	1.91
97.	15:25/ 5-31-78	289810	91.679	1.761	51032.0	1.0	50960.0	6.0	531.35	2.21
98.	13:52/ 7-12-78	350197	90.374	0.456	51033.0	2.0	50957.0	3.0	529.89	0.75
99.	13:32/ 8- 8-78	389357	92.947	3.029	51036.0	5.0	50960.0	6.0	531.30	2.16
100.	10:27/ 9- 8-78	433512	91.923	2.005	51024.0	-7.0	50952.0	-2.0	531.74	2.60
101.	9:55/11-22-78	541480	89.886	-0.032	51037.0	6.0	50969.0	15.0	530.40	1.34
102.	10:20/12-11-78	568865	89.365	-0.553	51030.0	-1.0	50968.0	14.0	529.35	0.21

THIS PAGE IS BEST QUALITY PRACTICABLE
FROM COPY FURNISHED TO DDC

TABLE 9. BEAM STABILITY TEST AT 120°F. HISTORY OF BONDED TENSION GAGE NO. 10

SYMBOLS:

t	- Elapsed Time from Loading(t=0)
T(t)	- Platinum Resistor Temp @ Time t
Eo	- Bridge Output
Eex	- Bridge Excitation
NOP(t)	- Normalized Output(Excitation Corrected) @ Time t
NOP'(t)	- Normalized Output(Excitation & Temp Corrected) @ Time t
S	- Temperature Sensitivity
G	- Gage Factor
e	- Beam Strain
de	- Experimental Strain Uncertainty

RELATIONS:

ΔT	- T(t)-T(0)
NOP(t)	- 10⁴(Eo/Eex)
NOP'(t)	- 10⁴(Eo-SΔT)/Eex
ΔNOP	- NOP(t)-NOP(0)
ΔNOP'	- NOP'(t)-NOP'(0)
e(t)	- 4[NOP'(t)-NOP(preload)]/G
Δe	- e(t)-e(0)

VALUES:

S = -.3mV/°F (Preloaded Average Value About 120 ± 10°F)
e = .5με (see text)
G = 130 (using e=-220με From Tension Semiconductor Gage #11 @ t=99min)

HISTORY OF GAGE 10

SET	TIME/DATE	t(min)	Eo(mv)	Eex(V)	NOP	ΔNOP	T(F)	ΔT(F)	ΔNOP'	e(με)	Δe(με)
1.	9:15/11-11-77	0	-10.659	1.03207	-10.328	0.000	117.240	0.000	0.000	-221	0
2.	9:17/11-11-77	2	-10.671	1.03207	-10.331	-0.012	117.240	0.000	-0.012	-222	-0
3.	9:19/11-11-77	4	-10.672	1.03207	-10.332	-0.013	117.261	0.014	-0.006	-221	-0
4.	9:25/11-11-77	10	-10.667	1.03206	-10.328	-0.008	117.257	0.009	-0.003	-221	-0
5.	9:30/11-11-77	15	-10.658	1.03206	-10.319	0.001	117.252	0.005	0.003	-221	0
6.	9:39/11-11-77	24	-10.655	1.03207	-10.316	0.004	117.240	0.000	0.004	-221	0
7.	9:48/11-11-77	33	-10.652	1.03207	-10.313	0.007	117.252	0.005	0.009	-221	0
8.	10:00/11-11-77	45	-10.644	1.03204	-10.306	0.014	117.240	0.000	0.014	-221	0
9.	10:13/11-11-77	58	-10.640	1.03205	-10.309	0.010	117.234	-0.014	0.004	-221	0
10.	10:26/11-11-77	71	-10.636	1.03205	-10.298	0.022	117.238	-0.009	0.018	-221	1
11.	10:40/11-11-77	85	-10.629	1.03205	-10.291	0.029	117.234	-0.014	0.022	-221	1
12.	10:54/11-11-77	99	-10.622	1.03203	-10.284	0.035	117.229	-0.018	0.027	-220	1
13.	11:16/11-11-77	121	-10.632	1.03203	-10.294	0.026	117.211	-0.037	0.008	-221	0
14.	11:46/11-11-77	151	-10.629	1.03204	-10.291	0.029	117.202	-0.046	0.007	-221	0
15.	12:24/11-11-77	189	-10.637	1.03204	-10.299	0.021	117.206	-0.041	0.001	-221	0
16.	13:22/11-11-77	247	-10.648	1.03205	-10.309	0.010	117.252	0.005	0.013	-221	0
17.	13:52/11-11-77	277	-10.654	1.03205	-10.315	0.005	117.257	0.009	0.009	-221	0
18.	14:42/11-11-77	327	-10.664	1.03208	-10.325	-0.005	117.279	0.032	0.011	-221	0
19.	14:56/11-11-77	341	-10.664	1.03208	-10.323	-0.003	117.264	0.037	0.015	-221	0
20.	15:50/11-11-77	395	-10.671	1.03206	-10.332	-0.012	117.302	0.055	0.025	-221	0
21.	16:54/11-11-77	459	-10.663	1.03206	-10.324	-0.004	117.298	0.050	0.028	-221	1
22.	18:08/11-11-77	533	-10.658	1.03206	-10.319	0.001	117.279	0.032	0.016	-221	1
23.	20:29/11-11-77	674	-10.787	1.03291	-10.366	-0.046	117.388	0.132	0.018	-221	1
24.	9:24/11-12-77	1449	-10.711	1.03291	-10.378	-0.058	117.334	0.087	-0.000	-222	-0
25.	11:11/11-12-77	1576	-10.720	1.03292	-10.378	-0.059	117.385	0.137	0.008	-221	0
26.	12:43/11-12-77	1668	-10.715	1.03292	-10.374	-0.054	117.362	0.114	0.002	-221	0
27.	21:36/11-12-77	2181	-10.561	1.03276	-10.226	0.094	117.035	-0.215	-0.010	-222	-0
28.	22:25/11-12-77	2238	-10.575	1.03278	-10.239	0.080	117.042	-0.206	-0.019	-222	-1
29.	1:18/11-13-77	2395	-10.710	1.03291	-10.377	-0.057	117.343	0.096	-0.010	-221	-0
30.	8:16/11-14-77	4761	-10.720	1.03292	-10.378	-0.059	117.330	0.082	-0.019	-221	-1
31.	8:27/11-15-77	5232	-10.768	1.03296	-10.424	-0.105	117.462	0.215	-0.001	-221	-0
32.	8:24/11-15-77	5709	-10.827	1.03302	-10.481	-0.161	117.512	0.265	-0.033	-221	-1
33.	8:22/11-16-77	6667	-10.826	1.03302	-10.480	-0.160	117.613	0.365	0.017	-221	1
34.	8:49/11-16-77	6813	-10.802	1.03300	-10.457	-0.137	117.548	0.302	0.004	-221	0
35.	8:44/11-16-77	6929	-10.767	1.03297	-10.423	-0.104	117.462	0.215	0.008	-221	0
36.	8:46/11-16-77	7171	-10.865	1.03305	-10.517	-0.198	117.590	0.343	-0.032	-222	-1
37.	11:22/11-16-77	7327	-10.812	1.03300	-10.467	-0.147	117.563	0.315	0.006	-221	0
38.	7:59/11-17-77	8564	-10.842	1.03304	-10.495	-0.175	117.583	0.315	-0.023	-222	-1
39.	14:04/11-17-77	8931	-10.765	1.03295	-10.422	-0.102	117.517	0.269	0.029	-220	1
40.	7:58/ 11-18-77	9995	-10.888	1.03299	-10.455	-0.135	117.517	0.269	-0.005	-221	-0
41.	11:25/11-18-77	10218	-10.783	1.03298	-10.445	-0.125	117.531	0.283	0.012	-221	0
42.	14:22/11-18-77	10387	-10.750	1.03295	-10.407	-0.087	117.458	0.210	0.014	-221	0
43.	11:45/11-19-77	11678	-10.889	1.03308	-10.464	-0.144	117.526	0.279	-0.009	-222	-0
44.	14:33/11-19-77	11838	-10.809	1.03302	-10.474	-0.154	117.567	0.320	0.008	-221	0
45.	8:15/11-21-77	14340	-10.836	1.03302	-10.498	-0.178	117.663	0.416	0.011	-220	1
46.	8:19/11-22-77	15784	-10.831	1.03301	-10.485	-0.165	117.590	0.343	0.001	-221	0
47.	15:49/11-22-77	16231	-10.778	1.03297	-10.426	-0.106	117.467	0.219	-0.000	-221	-0
48.	9:09/11-23-77	17774	-10.888	1.03298	-10.455	-0.135	117.522	0.274	-0.003	-221	-0
49.	11:44/11-23-77	17949	-10.779	1.03299	-10.435	-0.115	117.522	0.274	0.010	-221	1
50.	9:55/11-24-77	18760	-10.786	1.03258	-10.442	-0.122	117.503	0.256	0.002	-221	0
51.	10:20/11-25-77	20235	-10.720	1.03291	-10.378	-0.059	117.416	0.169	0.001	-221	0
52.	10:16/11-26-77	21781	-10.718	1.03291	-10.376	-0.057	117.476	0.228	0.054	-220	2
53.	8:12/11-28-77	24417	-10.755	1.03295	-10.418	-0.098	117.394	0.146	-0.019	-222	-1
54.	9:31/11-29-77	25916	-10.820	1.03307	-10.474	-0.154	117.558	0.311	0.004	-221	0
55.	25:52/11-29-77	26127	-10.796	1.03299	-10.442	-0.122	117.522	0.274	0.011	-221	0
56.	9:06/12- 1-77	27351	-10.781	1.03113	-10.432	-0.112	117.531	0.283	0.075	-221	1
57.	15:46/11-30-77	27751	-10.774	1.03323	-10.427	-0.108	117.503	0.256	0.016	-221	0
58.	8:10/12- 1-77	28735	-10.774	1.03297	-10.438	-0.118	117.485	0.237	0.005	-221	0
59.	14:26/12- 1-77	29111	-10.751	1.03295	-10.408	-0.088	117.458	0.210	0.013	-221	0
60.	15:43/12- 2-77	30620	-10.742	1.03294	-10.399	-0.080	117.458	0.210	0.022	-221	1
61.	12:48/12- 4-77	33333	-10.730	1.03292	-10.388	-0.068	117.440	0.201	0.029	-220	1
62.	13:05/12- 5-77	34798	-10.716	1.03290	-10.375	-0.055	117.412	0.164	0.025	-221	1
63.	11:07/12- 6-77	36112	-10.717	1.03291	-10.376	-0.056	117.426	0.178	0.038	-220	1
64.	15:29/12- 6-77	36374	-10.724	1.03292	-10.382	-0.062	117.426	0.178	0.024	-221	1
65.	9:27/12- 7-77	37447	-10.749	1.03295	-10.406	-0.086	117.494	0.247	0.033	-220	1
66.	15:55/12- 7-77	37844	-10.692	1.03289	-10.352	-0.032	117.343	0.096	0.015	-221	0
67.	7:54/12- 8-77	38799	-10.788	1.03295	-10.436	-0.116	117.476	0.228	-0.006	-221	-0
68.	9:13/12- 9-77	40318	-10.755	1.03291	-10.412	-0.093	117.467	0.219	0.014	-221	0
69.	15:49/12- 9-77	40714	-10.755	1.03296	-10.412	-0.092	117.485	0.237	0.021	-221	1
70.	13:41/12-11-77	43466	-10.670	1.03293	-10.338	-0.018	117.407	0.160	0.068	-219	2
71.	8:14/12-12-77	44579	-10.781	1.03301	-10.359	-0.039	117.348	0.100	0.009	-221	0
72.	15:07/12-13-77	46432	-10.733	1.03294	-10.391	-0.071	117.448	0.201	0.026	-221	1
73.	8:56/12-14-77	47449	-10.754	1.03295	-10.411	-0.091	117.488	0.241	0.022	-221	1
74.	7:49/12-16-77	50314	-10.759	1.03293	-10.416	-0.096	117.451	0.203	0.002	-221	0
75.	8:59/12-16-77	50386	-10.786	1.03297	-10.442	-0.122	117.485	0.237	-0.007	-222	-0
76.	9:15/12-19-77	54728	-10.746	1.03291	-10.404	-0.084	117.435	0.187	0.007	-221	0
77.	10:18/12-20-77	56221	-10.789	1.03289	-10.368	-0.048	117.421	0.174	0.036	-220	1
78.	9:58/12-21-77	57675	-10.776	1.03299	-10.432	-0.112	117.503	0.256	0.040	-220	1
79.	10:07/12-22-78	59892	-10.748	1.03296	-10.405	-0.085	117.498	0.242	0.032	-220	1
80.	10:23/12-23-78	60548	-10.766	1.03207	-10.431	-0.112	117.517	0.269	0.019	-221	1
81.	11:16/12-27-78	66161	-10.563	1.03275	-10.228	0.092	117.129	-0.119	0.034	-220	1
82.	9:35/ 1- 2-78	71648	-10.566	1.03278	-10.231	0.088	117.110	-0.137	0.022	-221	1
83.	9:15/ 1- 3-78	76128	-10.745	1.03291	-10.403	-0.083	117.467	0.219	0.023	-221	1
84.	13:55/ 1- 4-78	78048	-10.678	1.03288	-10.338	-0.018	117.348	0.100	0.030	-220	1
85.	11:17/ 1- 5-78	79318	-10.725	1.03293	-10.383	-0.063	117.448	0.201	0.034	-220	1
86.	13:21/ 1- 6-78	80888	-10.780	1.03291	-10.362	-0.042	117.388	0.151	0.011	-220	0
87.	16:08/ 1- 9-78	85365	-10.728	1.03291	-10.378	-0.059	117.385	0.137	0.008	-221	0
88.	13:21/ 1-10-78	86646	-10.788	1.03298	-10.359	-0.039	117.357	0.110	0.014	-221	0
89.	20:30/ 1-11-78	88515	-10.685	1.03298	-10.345	-0.025	117.321	0.073	0.018	-221	0
90.	16:00/ 1-12-78	89685	-10.679	1.03239	-10.339	-0.019	117.339	0.091	0.025	-221	1
91.	11:11/ 1-13-78	91118	-10.714	1.03293	-10.372	-0.053	117.438	0.183	0.076	-220	1
92.	12:06/ 1-16-78	95211	-10.597	1.03288	-10.262	0.057	117.174	-0.073	0.022	-221	1
93.	15:48/ 1-17-78	96873	-10.788	1.03291	-10.359	-0.039	117.385	0.137	0.017	-229	1
94.	15:33/ 1-18-78	98298	-10.601	1.03287	-10.341	-0.021	117.302	0.055	0.005	-221	0
95.	15:31/ 1-19-78	99716	-10.695	1.03289	-10.345	-0.025	117.415	0.168	0.056	-220	2
96.	15:39/ 1-20-78	101184	-10.689	1.03298	-10.349	-0.029	117.424	0.177	0.057	-220	2
97.	15:44/ 1-24-78	105949	-10.782	1.03288	-10.361	-0.042	117.470	0.222	0.066	-219	2
98.	20:42/ 1-25-78	107607	-10.782	1.03241	-10.366	-0.046	117.557	0.309	0.104	-218	3
99.	15:00/ 1-27-78	111273	-10.685	1.03181	-10.288	0.032	117.348	0.100	0.197	-215	6
100.	8:10/ 1-30-78	115135	-10.521	1.03278	-10.188	0.132	117.365	0.117	0.189	-216	6
101.	10:30/ 1-31-78	116715	-10.674	1.03286	-10.334	-0.015	117.462	0.214	0.186	-216	6
102.	13:35/ 2- 1-78	118348	-10.658	1.03286	-10.311	0.009	117.598	0.350	0.178	-216	5
103.	8:30/ 2- 3-78	122915	-10.724	1.03292	-10.382	-0.062	117.707	0.460	0.160	-216	5
104.	8:20/ 2- 4-78	125215	-10.726	1.03292	-10.384	-0.064	117.698	0.451	0.145	-217	4
105.	10:30/ 2- 7-78	126795	-10.765	1.03300	-10.421	-0.101	117.781	0.533	0.157	-216	5
106.	8:20/ 2- 8-78	128185	-10.825	1.03304	-10.479	-0.159	117.854	0.606	0.134	-217	4
107.	13:35/ 2- 9-78	129868	-10.649	1.03285	-10.306	0.013	117.538	0.291	0.154	-217	5
108.	10:10/ 2-13-78	134239	-10.665	1.03279	-10.249	0.071	117.479	0.232	0.183	-216	6
109.	17:44/ 2-16-78	140189	-10.475	1.03269	-10.143	0.176	117.189	-0.138	0.189	-216	3
110.	17:10/ 2-17-78	141595	-10.518	1.03274	-10.185	0.135	117.187	-0.061	0.106	-218	3
111.	15:45/ 2-21-78	147278	-10.557	1.03275	-10.222	0.098	117.274	0.026	0.110	-218	3
112.	16:10/ 2-22-78	148728	-10.578	1.03278	-10.235	0.085	117.296	0.049	0.109	-218	3
113.	15:35/ 2-23-78	150148	-10.577	1.03280	-10.241	0.079	117.333	0.085	0.128	-218	4
114.	15:45/ 2-26-78	151598	-10.547	1.03275	-10.213	0.107	117.210	-0.038	0.069	-219	3
115.	15:00/ 2-27-78	155065	-10.567	1.03278	-10.232	0.088	117.205	-0.042	0.068	-219	2
116.	16:02/ 3- 1-78	156007	-10.561	1.03277	-10.226	0.094	117.269	0.021	0.104	-218	3
117.	14:30/ 3- 2-78	170875	-10.642	1.03285	-10.304	0.016	117.360	0.113	0.071	-219	2
118.	14:20/ 3-23-78	198305	-10.599	1.03280	-10.262	0.057	117.203	0.035	0.074	-219	2
119.	14:30/ 3-31-78	201915	-10.534	1.03275	-10.200	0.120	117.150	-0.017	0.073	-219	2
120.	15:49/ 4-11-78	217834	-10.705	1.03288	-10.364	-0.044	117.470	0.222	0.063	-219	2
121.	12:48/ 4-24-78	236165	-10.557	1.03278	-10.222	0.098	117.186	-0.052	0.073	-219	2
122.	15:48/ 5-16-78	268225	-10.561	1.03277	-10.226	0.094	117.365	0.117	0.151	-217	5
123.	13:32/ 6- 8-78	309857	-11.000	1.03273	-10.654	-0.334	117.698	0.643	-0.023	-222	-1
124.	10:27/ 9- 8-78	433512	-10.925	1.03315	-10.574	-0.255	117.931	0.686	0.076	-219	2
125.	9:55/11-12-78	561488	-10.758	1.03288	-10.408	-0.088	117.698	0.451	0.138	-217	4
126.	10:20/12-11-78	568805	-10.758	1.03294	-10.415	-0.095	117.644	0.396	0.097	-218	3

THIS PAGE IS BEST QUALITY PRACTICABLE
FROM COPY FURNISHED TO DDC

TABLE 10. BEAM STABILITY TEST AT 120°F. HISTORY OF BONDED COMPRESSION GAGE NO. 18

SYMBOLS:

- t - Elapsed Time from Loading(t-0)
- T(t) - Platinum Resistor Temp @ Time t
- Eo - Bridge Output
- Ex - Bridge Excitation
- NOP(t) - Normalized Output(Excitation Corrected) @ Time t
- NOP'(t) - Normalized Output(Excitation & Temp Corrected) @ Time t
- B - Temperature Sensitivity
- G - Gage Factor
- σ - Beam Strain
- ϵ_u - Experimental Strain Uncertainity

RELATIONS:

- ΔT - T(t)-T(0)
- NOP(t) - 10⁶(Eo/Ex)
- NOP'(t) - 10⁶(Eo-EΔT)/Ex
- ΔNOP - NOP(t)-NOP(0)
- ΔNOP' - NOP'(t)-NOP'(0)
- σ(t) - 4(NOP'(t)-NOP(preload))/G
- Δσ - σ(t)-σ(0)

VALUES:

- B - -.5mV/°F (Preloaded Average Value About 12# ± 1F°F)
- ϵ_u - .5με (see text)
- G - 121 (using σ= 232με From Compression Semiconductor Gage #22 @ t=99min)

HISTORY of GAGE 18

SET	TIME/DATE	t(min)	Eo(mv)	Ex(V)	NOP	ΔNOP	T(F)	ΔT(F)	ΔNOP'	σ(με)	Δσ(με)
1.	9:15/11-11-77	0	-14.275	1.03646	-13.773	0.000	117.248	0.000	0.000	230	0
2.	9:17/11-11-77	2	-14.262	1.03646	-13.760	0.013	117.248	0.000	0.013	230	0
3.	9:18/11-11-77	4	-14.261	1.03646	-13.759	0.014	117.261	0.014	0.001	230	0
4.	9:25/11-11-77	10	-14.261	1.03645	-13.759	0.013	117.257	0.009	0.018	230	
5.	9:30/11-11-77	15	-14.260	1.03647	-13.758	0.015	117.252	0.005	0.017	230	
6.	9:39/11-11-77	24	-14.252	1.03645	-13.749	0.024	117.248	0.000	0.024	230	
7.	9:48/11-11-77	33	-14.243	1.03647	-13.742	0.031	117.252	0.005	0.033	231	
8.	10:00/11-11-77	45	-14.251	1.03644	-13.750	0.023	117.248	0.000	0.023	230	
9.	10:13/11-11-77	58	-14.246	1.03648	-13.745	0.028	117.234	-0.014	0.022	230	
10.	10:26/11-11-77	71	-14.239	1.03646	-13.738	0.035	117.230	-0.009	0.030	231	
11.	10:40/11-11-77	85	-14.232	1.03646	-13.731	0.041	117.234	-0.014	0.035	231	
12.	10:54/11-11-77	99	-14.228	1.03644	-13.728	0.045	117.225	-0.018	0.036	231	
13.	11:16/11-11-77	121	-14.235	1.03645	-13.734	0.038	117.211	-0.037	0.021	230	1
14.	11:46/11-11-77	151	-14.237	1.03645	-13.736	0.037	117.202	-0.046	0.014	230	0
15.	12:24/11-11-77	189	-14.243	1.03646	-13.742	0.031	117.206	-0.041	0.011	230	0
16.	13:22/11-11-77	247	-14.265	1.03647	-13.763	0.010	117.252	0.005	0.012	230	0
17.	13:52/11-11-77	277	-14.268	1.03648	-13.766	0.007	117.257	0.009	0.011	230	0
18.	14:42/11-11-77	327	-14.288	1.03652	-13.777	-0.004	117.279	0.032	0.011	230	0
19.	14:56/11-11-77	341	-14.280	1.03671	-13.782	-0.009	117.284	0.037	0.008	230	0
20.	15:50/11-11-77	395	-14.281	1.03652	-13.778	-0.005	117.302	0.055	0.021	230	1
21.	16:54/11-11-77	459	-14.277	1.03650	-13.774	-0.001	117.298	0.050	0.023	230	1
22.	18:00/11-11-77	533	-14.284	1.03651	-13.781	-0.008	117.279	0.032	0.007	230	0
23.	20:29/11-11-77	674	-14.342	1.03656	-13.836	-0.063	117.388	0.132	0.001	230	0
24.	9:24/11-12-77	1449	-14.342	1.03656	-13.836	-0.063	117.334	0.087	-0.021	229	-1
25.	11:31/12-12-77	1576	-14.359	1.03657	-13.852	-0.078	117.385	0.137	-0.013	229	-0
26.	12:41/11-12-77	1648	-14.351	1.03656	-13.845	-0.072	117.362	0.114	-0.017	229	-1
27.	21:36/11-12-77	2161	-14.214	1.03641	-13.715	0.058	117.033	-0.215	-0.045	228	-1
9.	22:25/11-12-77	2210	-14.210	1.03644	-13.710	0.062	117.042	-0.206	-0.037	228	-1
29.	1:10/11-13-77	2395	-14.367	1.03659	-13.866	-0.087	117.343	0.096	-0.041	228	-1
30.	8:16/11-14-77	4261	-14.382	1.03659	-13.874	-0.101	117.338	0.087	-0.062	228	-2
31.	0:27/11-15-77	5232	-14.431	1.03662	-13.921	-0.148	117.462	0.215	-0.045	228	-1
32.	8:24/11-15-77	5709	-14.403	1.03658	-13.971	-0.198	117.512	0.265	-0.070	227	-2
33.	0:22/11-16-77	6667	-14.500	1.03669	-13.907	-0.214	117.613	0.365	-0.038	228	-1
34.	2:48/11-16-77	6813	-14.461	1.03673	-13.549	-0.176	117.548	0.292	-0.035	229	-1
35.	4:44/11-16-77	6929	-14.427	1.03663	-13.917	-0.144	117.462	0.215	-0.041	228	-1
36.	8:46/11-16-77	7171	-14.525	1.03673	-14.010	-0.238	117.598	0.343	-0.072	227	-2
37.	11:22/11-16-77	7327	-14.478	1.03666	-13.966	-0.193	117.563	0.315	-0.031	228	-1
38.	7:59/11-17-77	8764	-14.513	1.03672	-13.998	-0.225	117.563	0.315	-0.073	227	-2
39.	14:06/11-17-77	8931	-14.437	1.03662	-13.927	-0.154	117.517	0.269	-0.024	229	-1
40.	7:50/11-18-77	9995	-14.466	1.03668	-13.954	-0.181	117.517	0.269	-0.051	228	-2
41.	11:25/11-18-77	10218	-14.459	1.03669	-13.947	-0.174	117.531	0.283	-0.038	228	-1
42.	14:22/11-18-77	10387	-14.419	1.03651	-13.918	-0.137	117.458	0.210	-0.036	228	-1
43.	17:55/11-18-77	11670	-14.480	1.03678	-13.971	-0.198	117.526	0.279	-0.064	228	-2
44.	14:33/11-19-77	11838	-14.533	1.03671	-14.018	-0.246	117.567	0.320	-0.091	227	-3
45.	8:15/11-21-77	14340	-14.531	1.03672	-14.016	-0.243	117.663	0.416	-0.043	228	-1
46.	8:19/11-22-77	15794	-14.501	1.03675	-13.987	-0.214	117.598	0.343	-0.049	228	-2
47.	15:40/11-22-77	16233	-14.448	1.03666	-13.929	-0.157	117.467	0.219	-0.051	228	-2
48.	9:09/11-23-77	17274	-14.491	1.03667	-13.970	-0.205	117.522	0.274	-0.073	227	-2
9.	13:44/11-23-77	17549	-14.452	1.03663	-13.943	-0.168	117.522	0.274	-0.036	228	-1
0.	9:55/11-24-77	18768	-14.463	1.03668	-13.956	-0.183	117.503	0.256	-0.060	228	-2
51.	10:20/11-25-77	20075	-14.472	1.03663	-13.953	-0.180	117.476	0.169	-0.019	228	-1
52.	20:16/11-26-77	22781	-14.398	1.03665	-13.889	-0.116	117.476	0.228	-0.006	229	-0
53.	8:12/11-28-77	24417	-14.448	1.03664	-13.938	-0.157	117.394	0.146	-0.006	227	-1
54.	9:31/11-29-77	25916	-14.513	1.03671	-13.999	-0.226	117.558	0.311	-0.076	227	-1
55.	15:52/11-29-77	26317	-14.475	1.03668	-13.967	-0.194	117.522	0.274	-0.062	228	-2
56.	9:06/11-30-77	27351	-14.477	1.03713	-13.959	-0.186	117.531	0.283	-0.049	228	-2
57.	15:46/11-30-77	27751	-14.463	1.03695	-13.948	-0.175	117.503	0.256	-0.051	228	-2
58.	8:10/12- 1-77	28715	-14.483	1.03668	-13.971	-0.198	117.485	0.237	-0.083	227	-3
59.	14:26/12- 1-77	29111	-14.443	1.03667	-13.937	-0.164	117.458	0.210	-0.063	228	-2
60.	15:43/12- 2-77	30628	-14.444	1.03664	-13.933	-0.161	117.458	0.210	-0.059	228	-2
61.	12:48/12- 4-77	33333	-14.425	1.03663	-13.915	-0.142	117.448	0.201	-0.046	228	-2
62.	13:05/12- 5-77	34798	-14.488	1.03668	-13.899	-0.126	117.412	0.165	-0.047	228	-2
63.	11:07/12- 6-77	36112	-14.428	1.03662	-13.918	-0.145	117.426	0.178	-0.068	228	-2
64.	15:29/12- 6-77	36374	-14.426	1.03662	-13.916	-0.144	117.426	0.178	-0.058	228	-2
65.	9:22/12- 7-77	37447	-14.454	1.03666	-13.943	-0.170	117.494	0.247	-0.051	228	-2
66.	15:55/12- 7-77	37848	-14.414	1.03662	-13.905	-0.132	117.343	0.096	-0.086	227	-3
67.	7:54/12- 8-77	38799	-14.484	1.03669	-13.971	-0.199	117.476	0.228	-0.088	227	-3
68.	9:13/12- 9-77	40318	-14.462	1.03666	-13.951	-0.178	117.467	0.219	-0.072	227	-2
69.	15:49/12- 9-77	40714	-14.461	1.03668	-13.949	-0.176	117.485	0.237	-0.062	228	-2
70.	13:41/12-11-77	43466	-14.388	1.03665	-13.879	-0.106	117.407	0.168	-0.029	229	-1
71.	8:14/12-12-77	44579	-14.487	1.03676	-13.896	-0.123	117.348	0.108	-0.075	227	-2
72.	15:07/12-13-77	46432	-14.439	1.03666	-13.928	-0.156	117.448	0.201	-0.059	228	-2
73.	8:04/12-14-77	47749	-14.463	1.03666	-13.952	-0.179	117.488	0.233	-0.066	227	-3
74.	7:49/12-16-77	50314	-14.466	1.03663	-13.955	-0.182	117.451	0.201	-0.081	227	-3
75.	8:59/12-16-77	50384	-14.499	1.03674	-13.985	-0.212	117.485	0.237	-0.098	226	-3
76.	9:15/12-19-77	54728	-14.472	1.03666	-13.968	-0.187	117.435	0.187	-0.097	226	-3
77.	10:10/12-20-77	56223	-14.429	1.03662	-13.919	-0.146	117.421	0.174	-0.063	228	-2
78.	9:50/12-21-77	57635	-14.501	1.03679	-13.986	-0.214	117.563	0.315	-0.062	228	-2
79.	10:07/12-22-78	59092	-14.517	1.03678	-14.003	-0.230	117.498	0.242	-0.114	226	-4
80.	10:23/12-23-78	60548	-14.504	1.03671	-13.998	-0.218	117.517	0.269	-0.088	227	-3
81.	11:16/12-27-78	66361	-14.321	1.03648	-13.817	-0.044	117.129	-0.119	-0.101	226	-3
82.	1:- 1-78	73744	-14.381	1.03646	-13.798	-0.025	117.118	-0.137	-0.091	227	-3
	9:15/ 1- 3-78	76328	-14.478	1.03669	-13.966	-0.193	117.467	0.219	-0.087	227	-3
...	13:55/ 1- 4-78	78048	-14.415	1.03666	-13.905	-0.132	117.348	0.108	-0.084	227	-3
85.	11:13/ 1- 5-78	79318	-14.485	1.03666	-13.973	-0.200	117.448	0.201	-0.103	226	-3
86.	13:23/ 1- 6-78	80808	-14.463	1.03665	-13.924	-0.151	117.398	0.151	-0.078	227	-3
87.	16:08/ 1- 9-78	85365	-14.482	1.03658	-13.958	-0.177	117.485	0.237	-0.111	226	-4
88.	13:21/ 1-10-78	86646	-14.441	1.03666	-13.938	-0.157	117.357	0.110	-0.105	226	-3
89.	8:38/ 1-11-78	88515	-14.452	1.03669	-13.941	-0.168	117.321	0.073	-0.132	225	-4
90.	16:00/ 1-12-78	89685	-14.443	1.03669	-13.932	-0.159	117.339	0.091	-0.115	226	-4
91.	15:55/ 1-15-78	91318	-14.469	1.03671	-13.956	-0.184	117.458	0.183	-0.095	227	-3
92.	12:06/ 1-16-78	92211	-14.335	1.03655	-13.838	-0.057	117.174	-0.073	-0.092	227	-3
93.	15:48/ 1-17-78	96873	-14.440	1.03667	-13.929	-0.156	117.385	0.137	-0.098	227	-3
94.	15:33/ 1-18-78	98798	-14.452	1.03667	-13.941	-0.168	117.382	0.055	-0.142	225	-5
95.	15:12/ 1-24-78	99736	-14.466	1.03664	-13.955	-0.182	117.435	0.168	-0.104	226	-3
96.	15:39/ 1-28-78	101184	-14.441	1.03667	-13.938	-0.157	117.424	0.177	-0.072	227	-2
97.	15:44/ 1-24-78	106949	-14.468	1.03667	-13.956	-0.183	117.478	0.222	-0.076	227	-3
98.	20:42/ 1-25-78	108687	-14.462	1.03669	-13.950	-0.177	117.557	0.309	-0.028	229	-1
99.	13:00/ 1-27-78	110149	-14.367	1.03668	-13.856	-0.083	117.308	0.060	-0.062	227	2
100.	0:18/ 1-30-78	115135	-14.315	1.03646	-13.811	-0.039	117.305	0.117	-0.018	230	1
101.	10:38/ 1-31-78	116715	-14.438	1.03663	-13.928	-0.155	117.662	0.414	0.045	231	1
102.	13:35/ 2- 1-78	118348	-14.484	1.03663	-13.895	-0.122	117.598	0.350	0.047	231	2
103.	0:18/ 2- 3-78	120915	-14.508	1.03669	-13.987	-0.214	117.707	0.460	0.008	230	0
104.	0:18/ 2- 6-78	125235	-14.473	1.03670	-13.961	-0.188	117.648	0.433	0.028	230	1
105.	10:38/ 2- 7-78	126795	-14.522	1.03676	-14.007	-0.234	117.781	0.533	0.023	230	1
106.	0:28/ 2- 8-78	128185	-14.507	1.03679	-14.069	-0.297	117.854	0.606	-0.006	230	-0
107.	13:35/ 2- 9-78	129860	-14.488	1.03663	-13.899	-0.126	117.538	0.291	0.014	230	0
108.	10:18/ 2-15-78	138295	-14.358	1.03655	-13.844	-0.071	117.432	0.184	-0.013	230	1
109.	17:44/ 2-16-78	140109	-14.244	1.03648	-13.743	0.030	117.109	-0.130	-0.037	228	-1
110.	17:19/ 2-17-78	141595	-14.286	1.03653	-13.783	-0.010	117.187	-0.061	-0.039	228	-1
111.	15:45/ 2-21-78	147278	-14.321	1.03655	-13.816	-0.043	117.274	0.026	-0.031	229	-1
112.	16:18/ 2-22-78	148735	-14.361	1.03655	-13.855	-0.082	117.296	0.049	-0.058	228	-2
113.	15:35/ 2-23-78	150160	-14.339	1.03657	-13.833	-0.060	117.333	0.086	-0.055	229	-1
114.	15:45/ 2-24-78	151598	-14.297	1.03653	-13.793	-0.020	117.218	-0.030	-0.039	228	-1
115.	15:00/ 2-27-78	155065	-14.328	1.03634	-13.823	-0.050	117.205	-0.042	-0.071	227	-2
116.	16:02/ 3- 1-78	158087	-14.338	1.03653	-13.825	-0.052	117.269	0.021	-0.062	228	-1
117.	9:55/11-25-78	170075	-14.413	1.03661	-13.904	-0.131	117.369	0.113	-0.062	227	-3
118.	14:28/ 3-23-78	190305	-14.368	1.03650	-13.861	-0.088	117.285	0.029	-0.071	227	-2
119.	16:38/ 3-31-78	201915	-14.381	1.03654	-13.797	-0.024	117.150	-0.097	-0.071	227	-2
120.	15:49/ 4-11-78	217034	-14.473	1.03666	-13.961	-0.188	117.478	0.222	-0.081	227	-3
121.	12:49/ 4-24-78	236365	-14.322	1.03657	-13.817	-0.044	117.196	-0.052	-0.059	227	-2
122.	19:48/ 5-16-78	262225	-14.344	1.03656	-13.838	-0.065	117.365	0.117	-0.089	229	-0
123.	13:32/ 8- 8-78	389857	-14.881	1.03712	-14.348	-0.576	117.898	0.643	-0.266	221	-9
124.	10:27/ 9- 8-78	433512	-14.885	1.03703	-14.276	-0.504	117.931	0.694	-0.174	226	-6
125.	9:55/11-22-78	561488	-14.662	1.03688	-14.123	-0.350	117.898	0.451	-0.102	225	-4
126.	10:20/12-11-78	580865	-14.667	1.03685	-14.146	-0.373	117.844	0.396	-0.102	224	-4

THIS PAGE IS BEST QUALITY PRACTICABLE
FROM COPY FURNISHED TO DDC

TABLE 11. BEAM STABILITY TEST AT 120°F. HISTORY OF REFERENCE COMPENSATION RESISTORS

					120°F RESISTANCE HISTORY						
					RN55C		CARBON		RN55C		
SET	TIME/DATE	Δ(min)	T(F)	ΔT(F)	1Ω Ohm	ΔOhm	1Ω Ohm	ΔOhm	1500 Ohm	ΔOhm	1500 Ohm	ΔOhm
1.	9:15/11-11-77	0	117.240	0.000	10.220	0.000	10.273	0.000	1498.69	0.000	1504.34	0.000
2.	9:40/11-11-77	33	117.253	0.005	10.233	0.005	10.233	-0.040	1498.95	0.260	1504.59	0.250
3.	10:00/11-11-77	45	117.260	0.000	10.233	0.005	10.277	0.004	1498.96	0.270	1504.66	0.320
4.	10:13/11-11-77	58	117.255	-0.013	10.232	0.004	10.278	0.005	1498.95	0.260	1504.58	0.240
5.	10:26/11-11-77	71	117.239	-0.009	10.234	0.006	10.279	0.006	1498.98	0.290	1504.63	0.290
6.	10:40/11-11-77	85	117.255	-0.013	10.232	0.004	10.277	0.004	1498.93	0.240	1504.56	0.220
7.	10:54/11-11-77	99	117.230	-0.010	10.231	0.005	10.278	0.005	1498.98	0.290	1504.62	0.280
8.	11:16/11-11-77	121	117.212	-0.036	10.233	0.005	10.278	0.005	1498.93	0.240	1504.54	0.200
9.	11:46/11-11-77	151	117.203	-0.045	10.233	0.005	10.278	0.005	1498.98	0.290	1504.64	0.300
10.	12:24/11-11-77	189	117.207	-0.041	10.230	0.002	10.276	0.003	1498.83	0.140	1504.46	0.120
11.	13:22/11-11-77	247	117.253	0.005	10.230	0.002	10.276	0.003	1498.85	0.160	1504.50	0.160
12.	13:52/11-11-77	277	117.257	0.009	10.232	0.004	10.278	0.005	1498.98	0.290	1504.61	0.270
13.	14:42/11-11-77	327	117.280	0.032	10.232	0.004	10.276	0.003	1498.92	0.230	1504.54	0.200
14.	15:58/11-11-77	395	117.303	0.055	10.229	0.001	10.273	0.000	1498.88	0.190	1504.21	-0.130
15.	16:54/11-11-77	459	117.298	0.050	10.232	0.004	10.277	0.004	1498.91	0.220	1504.54	0.200
16.	18:08/11-11-77	533	117.292	0.052	10.229	0.001	10.274	0.001	1498.91	0.220	1504.52	0.180
17.	20:29/11-11-77	674	117.301	0.133	-0.230	0.002	10.276	0.003	1498.89	0.200	1504.51	0.170
18.	9:24/11-12-77	1449	117.335	0.007	10.232	0.004	10.277	0.004	1498.92	0.230	1504.54	0.200
19.	11:31/11-12-77	1576	117.385	0.137	10.232	0.004	10.278	0.005	1498.98	0.210	1504.53	0.190
20.	12:43/11-12-77	1648	117.362	0.114	10.231	0.003	10.276	0.003	1498.93	0.240	1504.54	0.200
21.	21:36/11-12-77	2181	117.034	-0.214	10.231	0.003	10.277	0.004	1498.91	0.220	1504.56	0.220
22.	22:29/11-12-77	2234	117.043	-0.205	10.229	0.001	10.274	0.001	1498.91	0.220	1504.65	0.310
23.	1:10/11-13-77	2395	117.364	0.096	10.232	0.004	10.277	0.004	1498.93	0.240	1504.57	0.230
24.	8:16/11-13-77	2761	117.338	0.092	10.232	0.004	10.277	0.004	1498.95	0.260	1504.59	0.250
25.	8:27/11-15-77	5232	117.463	0.215	10.231	0.003	10.276	0.003	1498.98	0.210	1504.51	0.190
26.	9:24/11-15-77	5289	117.513	0.265	10.232	0.004	10.278	0.005	1498.97	0.288	1504.68	0.260
27.	8:22/11-16-77	6667	117.614	0.366	10.233	0.005	10.277	0.004	1498.95	0.260	1504.56	0.220
28.	2:48/11-16-77	6913	117.561	0.293	10.231	0.003	10.278	0.005	1498.87	0.180	1504.51	0.170
29.	4:44/11-16-77	6929	117.463	0.215	10.231	0.003	10.277	0.004	1498.89	0.200	1504.52	0.180
30.	8:46/11-16-77	7171	117.591	0.343	10.232	0.004	10.277	0.004	1498.94	0.250	1504.54	0.200
*1.	11:22/11-16-77	7327	117.563	0.315	10.232	0.004	10.277	0.004	1498.94	0.250	1504.57	0.230
*.	1:58/11-17-77	7564	117.563	0.315	10.229	0.001	10.275	0.002	1498.95	0.260	1504.55	0.210
33.	14:06/11-17-77	8931	117.518	0.270	10.226	-0.002	10.272	-0.001	1498.56	-0.130	1504.20	-0.140
34.	7:58/11-18-77	9995	117.518	0.270	10.231	0.003	10.276	0.003	1498.85	0.160	1504.46	0.120
35.	11:25/11-18-77	10218	117.531	0.283	10.229	0.001	10.275	0.002	1498.82	0.130	1504.45	0.110
36.	14:21/11-18-77	10387	117.458	0.210	10.231	0.003	10.276	0.003	1498.85	0.160	1504.48	0.140
37.	11:45/11-19-77	11678	117.527	0.279	10.230	0.002	10.275	0.002	1499.88	0.310	1504.64	0.300
38.	14:33/11-19-77	11838	117.568	0.320	10.232	0.004	10.278	0.005	1499.03	0.348	1504.67	0.330
39.	8:15/11-21-77	14348	117.466	0.218	10.230	0.002	10.276	0.003	1498.99	0.308	1504.61	0.270
40.	9:09/11-21-77	17274	117.522	0.274	10.230	0.002	10.275	0.002	1498.95	0.260	1504.58	0.240
41.	13:46/11-23-77	17549	117.522	0.274	10.229	0.001	10.274	0.001	1498.85	-0.640	1503.66	-0.680
42.	8:12/11-28-77	24417	117.394	0.146	10.233	0.005	10.278	0.005	1498.96	0.270	1504.58	0.240
43.	9:31/11-29-77	25936	117.559	0.311	10.229	0.001	10.274	0.001	1498.38	-0.310	1503.99	-0.350
44.	15:52/11-29-77	26317	117.522	0.274	10.232	0.004	10.277	0.004	1498.88	0.190	1504.52	0.180
45.	9:06/11-30-77	27351	117.531	0.283	10.232	0.004	10.277	0.004	1498.93	0.240	1504.55	0.210
46.	15:46/11-30-77	27751	117.584	0.256	10.230	0.002	10.276	0.003	1498.89	0.200	1504.52	0.180
47.	8:18/12- 1-77	28735	117.486	0.238	10.231	0.003	10.276	0.003	1498.89	0.200	1504.52	0.180
48.	14:26/12- 1-77	29111	117.458	0.210	10.227	-0.001	10.273	0.000	1498.21	-0.488	1503.85	-0.490
49.	15:43/12- 2-77	30628	117.458	0.210	10.233	0.005	10.278	0.005	1498.92	0.230	1504.57	0.230
50.	12:48/12- 4-77	33333	117.449	0.201	10.232	0.004	10.278	0.005	1498.92	0.230	1504.28	-0.060
51.	13:09/12- 5-77	34798	117.413	0.165	10.232	0.004	10.278	0.005	1498.97	0.280	1504.68	0.260
52.	11:07/12- 6-77	36112	117.426	0.178	10.231	0.003	10.277	0.004	1498.92	0.230	1504.56	0.220
53.	15:29/12- 6-77	36374	117.426	0.178	10.230	0.002	10.276	0.003	1498.92	0.230	1504.56	0.220
54.	9:22/12- 7-77	37447	117.495	0.247	10.234	0.006	10.280	0.007	1498.96	0.270	1504.57	0.230
55.	15:55/12- 7-77	37868	117.464	0.216	10.232	0.004	10.277	0.004	1498.93	0.240	1504.55	0.210
56.	7:54/12- 8-77	38799	117.477	0.229	10.231	0.003	10.276	0.003	1498.96	0.270	1504.61	0.270
57.	9:13/12- 9-77	40310	117.467	0.219	10.233	0.005	10.279	0.006	1498.97	0.280	1504.68	0.260
58.	15:49/12- 9-77	40714	117.406	0.158	10.233	0.005	10.279	0.006	1498.95	0.260	1504.56	0.220
59.	12:41/12-11-77	43466	117.408	0.160	10.233	0.005	10.276	0.005	1498.95	0.260	1504.68	0.260
60.	15:07/12-13-77	44632	117.469	0.201	10.231	0.003	10.278	0.005	1498.92	0.230	1504.55	0.210
61.	8:04/12-14-77	47449	117.481	0.293	10.233	0.005	10.279	0.006	1498.97	0.280	1504.68	0.260
62.	7:49/12-16-77	50114	117.151	0.283	10.233	0.005	10.278	0.005	1498.98	0.290	1504.68	0.260
63.	9:59/12-16-77	50324	117.486	0.238	10.233	0.005	10.278	0.005	1498.96	0.270	1504.58	0.240
64.	9:15/12-19-77	54720	117.536	0.188	10.234	0.006	10.280	0.007	1498.96	0.270	1505.59	0.250
65.	10:13/12-20-77	56223	117.422	0.174	10.221	-0.007	10.267	-0.006	1497.96	-0.710	1503.58	-0.760
66.	9:50/12-21-77	57635	117.563	0.315	10.236	0.008	10.280	0.007	1498.94	0.250	1504.57	0.230
*.	10:21/12-23-77	60548	117.518	0.270	10.235	0.007	10.280	0.007	1498.96	0.270	1504.57	0.230
68.	11:16/12-27-77	66361	117.129	-0.119	10.232	0.004	10.279	0.006	1498.58	0.198	1504.56	0.220
69.	12:35/ 1- 1-78	73648	117.111	-0.137	10.231	0.003	10.277	0.004	1498.98	0.210	1504.65	0.310
70.	9:15/ 1- 3-78	76320	117.467	0.219	10.232	0.004	10.277	0.004	1498.98	0.290	1504.68	0.260
71.	13:55/ 1- 4-78	78048	117.469	0.181	10.235	0.007	10.281	0.008	1498.97	0.280	1504.68	0.260
72.	11:13/ 1- 5-78	79310	117.449	0.201	10.236	0.008	10.282	0.009	1499.05	0.368	1504.67	0.330
73.	13:21/ 1- 6-78	80888	117.399	0.151	10.235	0.007	10.280	0.007	1498.95	0.268	1504.56	0.220
74.	16:00/ 1- 9-78	85365	117.385	0.137	10.230	0.002	10.276	0.003	1498.89	0.208	1504.56	0.220
75.	14:21/ 1-10-78	86646	117.358	0.110	10.227	-0.001	10.273	0.000	1499.01	0.328	1504.64	0.308
76.	20:38/ 1-11-78	88515	117.321	0.073	10.230	0.002	10.276	0.003	1498.98	0.298	1504.61	0.278
7.	16:00/ 1-12-78	89685	117.348	0.092	10.232	0.004	10.278	0.005	1498.97	0.288	1504.59	0.258
78.	15:45/ 1-13-78	91110	117.431	0.183	10.233	0.005	10.280	0.007	1498.94	0.258	1504.57	0.238
79.	14:06/ 1-14-78	92521	117.175	-0.073	10.233	0.005	10.280	0.007	1498.95	0.268	1504.68	0.268
80.	15:48/ 1-17-78	96073	117.385	0.137	10.233	0.005	10.279	0.006	1498.93	0.248	1504.57	0.238
81.	15:33/ 1-18-78	98298	117.383	0.055	10.233	0.005	10.279	0.006	1498.94	0.258	1504.58	0.248
82.	15:31/ 1-19-78	99736	117.415	0.167	10.233	0.005	10.279	0.006	1498.91	0.228	1504.51	0.190
83.	15:39/ 1-20-78	101394	117.424	0.176	10.234	0.006	10.280	0.007	1498.97	0.288	1504.68	0.268
84.	15:44/ 1-24-78	106949	117.478	0.222	10.232	0.004	10.278	0.005	1499.08	0.318	1504.64	0.320
5.	20:42/ 1-25-78	108607	117.557	0.189	10.230	0.002	10.275	0.002	1499.06	0.370	1504.78	0.360
86.	15:08/ 1-27-78	111233	117.568	0.300	10.235	0.007	10.282	0.009	1498.96	0.278	1504.59	0.258
87.	8:18/ 1-30-78	115115	117.348	0.117	10.235	0.007	10.282	0.009	1498.88	0.318	1504.63	0.298
88.	10:38/ 1-31-78	116715	117.662	0.414	10.235	0.007	10.282	0.009	1498.99	0.308	1504.63	0.298
89.	13:35/ 2- 1-78	118340	117.590	0.350	10.236	0.008	10.288	0.007	1498.98	0.298	1504.68	0.268
90.	8:38/ 2- 3-78	120915	117.787	0.459	10.236	0.008	10.282	0.009	1499.02	0.338	1504.65	0.318
91.	8:38/ 2- 6-78	125215	117.668	0.432	10.234	0.006	10.281	0.008	1498.97	0.288	1504.59	0.258
92.	10:38/ 2- 7-78	126795	117.781	0.533	10.236	0.008	10.282	0.009	1498.96	0.278	1504.59	0.258
93.	8:28/ 2- 8-78	128185	117.854	0.606	10.233	0.005	10.280	0.007	1498.98	0.298	1504.68	0.268
94.	13:35/ 2- 9-78	129868	117.538	0.290	10.234	0.006	10.281	0.008	1498.96	0.278	1504.68	0.268
95.	10:18/ 2-15-78	138189	117.731	0.483	10.239	0.011	10.285	0.012	1499.07	0.372	1504.68	0.328
96.	17:44/ 2-16-78	140109	117.109	-0.139	10.233	0.005	10.279	0.006	1499.07	0.388	1504.76	0.428
97.	17:18/ 2-17-78	141595	117.107	-0.061	10.232	0.004	10.279	0.006	1499.05	0.368	1504.71	0.378
98.	15:45/ 2-21-78	147278	117.274	0.026	10.236	0.008	10.282	0.009	1499.02	0.338	1504.68	0.368
99.	15:18/ 2-22-78	148733	117.274	0.060	10.235	0.007	10.282	0.009	1498.98	0.298	1504.65	0.328
100.	15:35/ 2-23-78	150140	117.333	0.085	10.236	0.008	10.283	0.010	1498.97	0.288	1504.61	0.278
101.	15:45/ 2-24-78	151598	117.218	-0.030	10.234	0.006	10.281	0.008	1498.97	0.288	1504.66	0.328
102.	15:00/ 2-27-78	155865	117.285	-0.043	10.236	0.008	10.283	0.010	1499.06	0.378	1504.72	0.388
103.	14:27/ 3- 1-78	158888	117.251	-0.021	10.235	0.007	10.282	0.009	1498.99	0.308	1504.65	0.318
104.	14:38/ 3-15-78	178875	117.368	0.112	10.234	0.006	10.280	0.007	1498.99	0.308	1504.65	0.318
105.	14:28/ 3-23-78	192385	117.281	0.035	10.235	0.007	10.282	0.009	1499.02	0.338	1504.65	0.318
106.	14:38/ 3-31-78	208915	117.158	-0.098	10.236	0.008	10.283	0.010	1499.02	0.338	1504.67	0.338
107.	15:48/ 4-11-78	217034	117.478	0.222	10.236	0.008	10.283	0.010	1498.98	0.298	1504.62	0.298
108.	12:48/ 4-24-78	236365	117.196	-0.052	10.235	0.007	10.282	0.009	1498.97	0.288	1504.63	0.298
109.	15:48/ 5-16-78	268275	117.365	0.117	10.236	0.008	10.284	0.011	1499.02	0.338	1504.68	0.348
110.	13:32/ 8- 8-78	389057	117.698	0.442	10.353	0.125	10.398	0.125	1499.07	0.388	1504.69	0.358
111.	9:55/11-22-78	541488	117.693	0.458	10.272	0.044	10.318	0.045	1499.17	0.488	1504.84	0.508
112.	10:20/12-11-78	560865	117.644	0.396	10.243	0.015	10.292	0.019	1499.04	0.358	1504.72	0.388

THIS PAGE IS BEST QUALITY PRACTICABLE
FROM COPY FURNISHED TO DDC

TABLE 12. BEAM STABILITY TEST AT 120°F. HISTORY OF REFERENCE COMPENSATION RESISTOR AND UNBONDED SEMICONDUCTOR GAGE

			120° F RESISTANCE HISTORY							
					RN55C		CARBON		SEMICONDUCTOR GAGE	
SET	TIME/DATE	t(min)	T(°F)	ΔT(°F)	50K Ohm	ΔOhm	50K Ohm	ΔOhm	UNBONDED Ohm	ΔOhm
1.	9:15/11-11-77	0	117.248	0.000	51098.0	0.0	50732.0	0.0	0.00	0.00
2.	9:48/11-11-77	33	117.253	0.005	51088.0	-2.0	50730.0	-2.0	0.00	0.00
3	10:00/11-11-77	45	117.248	0.000	51089.0	-1.0	50731.0	-1.0	0.00	0.00
4.	10:13/11-11-77	58	117.235	-0.013	51089.0	-1.0	50731.0	-1.0	0.00	0.00
5.	10:26/11-11-77	71	117.239	-0.009	51089.0	-1.0	50733.0	1.0	0.00	0.00
6.	10:40/11-11-77	85	117.235	-0.013	51089.0	-1.0	50731.0	-1.0	0.00	0.00
7.	10:54/11-11-77	99	117.230	-0.018	51089.0	-1.0	50732.0	0.0	0.00	0.00
8.	11:16/11-11-77	121	117.212	-0.036	51088.0	-2.0	50730.0	-2.0	0.00	0.00
9.	11:46/11-11-77	151	117.203	-0.045	51089.0	-1.0	50731.0	-1.0	0.00	0.00
10.	12:24/11-11-77	189	117.207	-0.041	51088.0	-2.0	50732.0	0.0	0.00	0.00
11.	13:22/11-11-77	247	117.253	0.005	51098.0	0.0	50731.0	-1.0	0.00	0.00
12.	13:52/11-11-77	277	117.257	0.009	51089.0	-1.0	50730.0	-2.0	0.00	0.00
13.	14:42/11-11-77	327	117.280	0.032	51089.0	-1.0	50730.0	-2.0	0.00	0.00
14.	15:50/11-11-77	395	117.303	0.055	51087.0	-3.0	50730.0	-2.0	0.00	0.00
15.	16:54/11-11-77	459	117.298	0.050	51085.0	-5.0	50730.0	-2.0	0.00	0.00
16.	18:00/11-11-77	533	117.280	0.032	51089.0	-1.0	50730.0	-2.0	0.00	0.00
17.	20:29/11-11-77	674	117.381	0.133	51087.0	-3.0	50729.0	-3.0	0.00	0.00
18.	9:24/11-12-77	1449	117.335	0.087	51089.0	-1.0	50731.0	-1.0	0.00	0.00
19.	11:31/11-12-77	1576	117.385	0.137	51089.0	-1.0	50730.0	-2.0	0.00	0.00
20.	12:43/11-12-77	1648	117.362	0.114	51087.0	-3.0	50730.0	-2.0	0.00	0.00
21.	21:36/11-12-77	2181	117.034	-0.214	51087.0	-3.0	50730.0	-2.0	0.00	0.00
22.	22:25/11-12-77	2230	117.043	-0.205	51088.0	-2.0	50730.0	-2.0	0.00	0.00
23.	1:10/11-13-77	2395	117.344	0.096	51098.0	0.0	50732.0	0.0	0.00	0.00
24.	8:16/11-14-77	4261	117.330	0.082	51088.0	-2.0	50731.0	-1.0	0.00	0.00
25.	8:27/11-15-77	5232	117.463	0.215	51098.0	0.0	50730.0	-2.0	0.00	0.00
26.	8:24/11-15-77	5789	117.513	0.265	51089.0	-1.0	50733.0	1.0	0.00	0.00
27.	8:22/11-16-77	6667	117.614	0.366	51098.0	0.0	50732.0	0.0	0.00	0.00
28.	2:48/11-16-77	6813	117.541	0.293	51091.0	1.0	50732.0	0.0	0.00	0.00
29.	4:44/11-16-77	6929	117.463	0.215	51086.0	-4.0	50730.0	-2.0	0.00	0.00
30.	8:46/11-16-77	7171	117.591	0.343	51089.0	-1.0	50732.0	0.0	0.00	0.00
31.	11:22/11-16-77	7327	117.563	0.315	51086.0	-4.0	50730.0	-2.0	0.00	0.00
32.	7:59/11-17-77	8564	117.563	0.315	51089.0	-1.0	50732.0	0.0	0.00	0.00
33.	14:06/11-17-77	8931	117.518	0.270	51089.0	-1.0	50731.0	-1.0	0.00	0.00
34.	7:50/11-18-77	9995	117.518	0.270	51098.0	0.0	50732.0	0.0	0.00	0.00
35.	11:25/11-18-77	10210	117.531	0.283	51089.0	-1.0	50730.0	-2.0	0.00	0.00
36.	14:22/11-18-77	10387	117.458	0.210	51087.0	-3.0	50732.0	0.0	0.00	0.00
37.	11:45/11-19-77	11670	117.527	0.279	51088.0	-2.0	50734.0	2.0	0.00	0.00
38	14:33/11-19-77	11838	117.568	0.320	51089.0	-1.0	50734.0	2.0	0.00	0.00
39	8:15/11-21-77	14348	117.664	0.416	51087.0	-3.0	50733.0	1.0	0.00	0.00
40.	9:09/11-23-77	17274	117.522	0.274	51089.0	-1.0	50733.0	1.0	0.00	0.00
41.	13:44/11-23-77	17549	117.522	0.274	51086.0	-4.0	50731.0	-1.0	0.00	0.00
42.	8:12/11-28-77	24417	117.394	0.146	51088.0	-2.0	50732.0	0.0	0.00	0.00
43.	9:31/11-29-77	25936	117.559	0.311	51098.0	0.0	50732.0	0.0	0.00	0.00
44.	15:52/11-29-77	26317	117.522	0.274	51098.0	0.0	50731.0	-1.0	0.00	0.00
45.	9:06/11-30-77	27351	117.531	0.283	51098.0	0.0	50732.0	0.0	0.00	0.00
46.	15:46/11-30-77	27751	117.504	0.256	51089.0	-1.0	50731.0	-1.0	0.00	0.00
47.	8:10/12- 1-77	28735	117.486	0.238	51089.0	-1.0	50732.0	0.0	0.00	0.00
48.	14:26/12- 1-77	29111	117.458	0.210	51088.0	-2.0	50732.0	0.0	0.00	0.00
49.	15:43/12- 2-77	30628	117.458	0.210	51098.0	0.0	50734.0	2.0	0.00	0.00
50.	12:10/12- 4-77	33313	117.449	0.201	51087.0	-3.0	50731.0	-1.0	0.00	0.00
51.	13:05/12- 5-77	34798	117.413	0.165	51089.0	-1.0	50732.0	0.0	0.00	0.00
52.	11:07/12- 6-77	36112	117.426	0.178	51089.0	-1.0	50732.0	0.0	0.00	0.00
53.	15:29/12- 6-77	36374	117.426	0.178	51098.0	0.0	50730.0	-2.0	0.00	0.00
54.	9:22/12- 7-77	37447	117.495	0.247	51098.0	0.0	50734.0	2.0	0.00	0.00
55.	15:55/12- 7-77	37844	117.344	0.096	51089.0	-1.0	50733.0	1.0	0.00	0.00
56.	7:54/12- 8-77	38799	117.477	0.229	51098.0	0.0	50733.0	1.0	0.00	0.00
57.	9:13/12- 9-77	40318	117.467	0.219	51098.0	0.0	50733.0	1.0	0.00	0.00
58.	15:49/12- 9-77	40714	117.486	0.238	51086.0	-4.0	50733.0	1.0	0.00	0.00
59.	13:41/12-11-77	43466	117.488	0.160	51089.0	-1.0	50735.0	3.0	0.00	0.00
60.	15:07/12-13-77	46432	117.449	0.201	51089.0	-1.0	50733.0	1.0	0.00	0.00
61.	8:04/12-14-77	47449	117.481	0.233	51098.0	0.0	50734.0	2.0	0.00	0.00
62.	7:49/12-15-77	48814	117.451	0.203	51091.0	1.0	50734.0	2.0	0.00	0.00
63.	8:59/12-16-77	50304	117.486	0.238	51098.0	0.0	50734.0	2.0	0.00	0.00
64.	9:15/12-19-77	54729	117.436	0.188	51098.0	0.0	50735.0	3.0	0.00	0.00
65.	10:18/12-20-77	56223	117.422	0.174	51089.0	-1.0	50732.0	0.0	0.00	0.00
66.	9:58/12-21-77	57535	117.563	0.315	51091.0	1.0	50737.0	5.0	0.00	0.00
67.	10:23/12-23-77	60543	117.518	0.270	51091.0	1.0	50735.0	3.0	0.00	0.00
68.	11:16/12-27-77	66361	117.129	-0.119	51089.0	-1.0	50733.0	1.0	0.00	0.00
69.	12:35/ 1- 1-78	73648	117.111	-0.137	51089.0	-1.0	50735.0	3.0	0.00	0.00
70.	9:15/ 1- 3-78	76328	117.467	0.219	51088.0	-2.0	50732.0	0.0	0.00	0.00
71.	13:55/ 1- 4-78	78048	117.349	0.101	51098.0	0.0	50735.0	3.0	0.00	0.00
72.	11:13/ 1- 5-78	79318	117.449	0.201	51089.0	-1.0	50734.0	2.0	0.00	0.00
73.	13:23/ 1- 6-78	80888	117.399	0.151	51087.0	-3.0	50733.0	1.0	0.00	0.00
74.	16:00/ 1- 9-78	85365	117.385	0.137	51088.0	-2.0	50733.0	1.0	0.00	0.00
75.	13:21/ 1-10-78	86646	117.358	0.110	51098.0	0.0	50731.0	-1.0	0.00	0.00
76.	20:30/ 1-11-78	88515	117.321	0.073	51089.0	-1.0	50732.0	0.0	0.00	0.00
77.	16:00/ 1-12-78	89685	117.348	0.092	51088.0	-2.0	50733.0	1.0	0.00	0.00
78.	15:45/ 1-13-78	91110	117.431	0.183	51091.0	1.0	50734.0	2.0	0.00	0.00
79.	12:06/ 1-16-78	95211	117.175	-0.073	51089.0	-1.0	50732.0	0.0	0.00	0.00
80.	15:40/ 1-17-78	96873	117.385	0.137	51089.0	-1.0	50734.0	2.0	0.00	0.00
81.	15:33/ 1-18-78	98298	117.303	0.055	51091.0	1.0	50734.0	2.0	0.00	0.00
82.	15:31/ 1-19-78	99736	117.415	0.167	51098.0	0.0	50732.0	0.0	0.00	0.00
83.	15:39/ 1-20-78	101184	117.424	0.176	51087.0	-3.0	50735.0	3.0	0.00	0.00
84.	15:44/ 1-24-78	106949	117.478	0.222	51089.0	-1.0	50736.0	4.0	0.00	0.00
85.	20:42/ 1-25-78	108607	117.557	0.309	51089.0	-1.0	50737.0	5.0	0.00	0.00
86.	15:00/ 1-27-78	111233	117.548	0.300	51087.0	-3.0	50733.0	1.0	0.00	0.00
87.	8:10/ 1-30-78	115135	117.365	0.117	51098.0	0.0	50735.0	3.0	0.00	0.00
88.	10:30/ 1-31-78	116715	117.662	0.414	51089.0	-1.0	50735.0	3.0	0.00	0.00
89.	13:35/ 2- 1-78	118348	117.598	0.350	51086.0	-4.0	50736.0	4.0	0.00	0.00
90.	8:30/ 2- 3-78	120915	117.787	0.459	51098.0	0.0	50737.0	5.0	0.00	0.00
91.	8:30/ 2- 6-78	125235	117.688	0.432	51098.0	0.0	50734.0	2.0	0.00	0.00
92.	10:30/ 2- 7-78	126795	117.701	0.533	51092.0	2.0	50734.0	2.0	0.00	0.00
93.	8:20/ 2- 8-78	128185	117.854	0.686	51098.0	0.0	50735.0	3.0	0.00	0.00
94.	13:35/ 2- 9-78	129868	117.538	0.290	51088.0	-2.0	50735.0	3.0	0.00	0.00
95.	10:10/ 2-15-78	138295	117.479	0.231	51091.0	1.0	50737.0	5.0	0.00	0.00
96.	17:44/ 2-16-78	140189	117.109	-0.139	51089.0	-1.0	50735.0	3.0	0.00	0.00
97.	17:10/ 2-17-78	141595	117.187	-0.061	51088.0	-2.0	50736.0	4.0	0.00	0.00
98.	15:45/ 2-21-78	147278	117.274	0.026	51098.0	0.0	50736.0	4.0	0.00	0.00
99.	16:10/ 2-22-78	148735	117.296	0.048	51087.0	-3.0	50735.0	3.0	0.00	0.00
100.	15:35/ 2-23-78	150148	117.333	0.085	51089.0	-1.0	50735.0	3.0	0.00	0.00
101.	15:45/ 2-24-78	151598	117.210	-0.038	51098.0	0.0	50735.0	3.0	0.00	0.00
102.	15:00/ 2-27-78	155065	117.205	-0.043	51087.0	-3.0	50738.0	6.0	0.00	0.00
103.	16:02/ 3- 1-78	158007	117.269	0.021	51091.0	1.0	50737.0	5.0	0.00	0.00
104.	14:30/ 3-15-78	178075	117.368	0.112	51094.0	4.0	50741.0	9.0	0.00	0.00
105.	14:20/ 3-23-78	190385	117.283	0.035	51091.0	1.0	50735.0	3.0	0.00	0.00
106.	14:30/ 3-31-78	201915	117.158	-0.090	51089.0	-1.0	50738.0	6.0	0.00	0.00
107.	15:49/ 4-11-78	217034	117.478	0.222	51092.0	2.0	50739.0	7.0	0.00	0.00
108.	12:40/ 4-24-78	236365	117.196	-0.052	51090.0	0.0	50738.0	6.0	0.00	0.00
109.	15:40/ 5-16-78	268225	117.365	0.117	51089.0	-1.0	50738.0	6.0	0.00	0.00
110.	13:32/ 6- 8-78	309857	117.898	0.642	51087.0	-3.0	50731.0	-1.0	0.00	0.00
111.	9:55/11-22-78	541488	117.698	0.450	51092.0	2.0	50745.0	13.0	0.00	0.00
112.	10:20/12-11-78	560865	117.644	0.396	51089.0	-1.0	50744.0	12.0	0.00	0.00

THIS PAGE IS BEST QUALITY PRACTICABLE
FROM COPY FURNISHED TO DDC

TABLE 13. BEAM STABILITY TEST AT 1600°F. HISTORY OF BONDED TENSION GAGE NO. 6

SYMBOLS:

- t - Elapsed Time from Loading(t=0)
- T(t) - Platinum Resistor Temp @ Time t
- Eo - Bridge Output
- Eex - Bridge Excitation
- NDP(t) - Normalized Output(Excitation Corrected) @ Time t
- NDP'(t) - Normalized Output(Excitation & Temp Corrected) @ Time t
- S - Temperature Sensitivity
- G - Gage Factor
- ε - Beam Strain
- $\Delta\varepsilon$ - Experimental Strain Uncertainty

RELATIONS:

- ΔT - T(t)-T(0)
- NDP(t) - 10⁴(Eo/Eex)
- NDP'(t) - 10⁴(Eo-SΔT)/Eex
- ΔNDP - NDP(t)-NDP(0)
- ΔNDP' - NDP'(t)-NDP'(0)
- ε(t) - 4(NDP'(t)-NDP preload)]/G
- $\Delta\varepsilon$ - ε(t)-ε(0)

VALUES:

- S = -.5mV/°F (Preloaded Average Value About 168 ± 18°F)
- $\Delta\varepsilon$ = .5με (see text)
- G = 133 (using ε=-178με From Tension Semiconductor Gage 011 @ t=84min)

HISTORY of GAGE 6

No.	TIME/DATE	t(min)	Eo(mv)	Eex(V)	NDP	ΔNDP	T(°F)	ΔT(°F)	ΔNDP'	ε(με)	Δε(με)
1.	9:44/11-14-77	0	-13.593	1.03633	-13.582	0.000	150.922	0.000	0.000	-179	0
2.	9:45/11-14-77	1	-14.001	1.03633	-13.518	-0.064	150.908	-0.014	-0.014	-179	-0
3.	9:48/11-14-77	4	-13.997	1.03633	-13.586	-0.004	150.908	-0.014	-0.011	-179	-0
4.	9:55/11-14-77	11	-13.988	1.03633	-13.498	0.013	150.909	-0.014	0.006	-179	0
5.	10:01/11-14-77	17	-13.978	1.03631	-13.488	0.014	150.894	-0.028	0.001	-179	0
6.	10:08/11-14-77	24	-13.975	1.03631	-13.485	0.017	150.885	-0.037	-0.001	-179	-0
7.	10:13/11-14-77	29	-13.967	1.03630	-13.478	0.025	150.876	-0.046	0.003	-179	0
8.	10:22/11-14-77	38	-13.959	1.03630	-13.470	0.032	150.876	-0.046	0.010	-179	0
9.	10:32/11-14-77	48	-13.956	1.03628	-13.467	0.035	150.853	-0.069	0.002	-179	0
10.	10:39/11-14-77	55	-13.944	1.03628	-13.456	0.047	150.834	-0.087	0.004	-179	0
11.	10:51/11-14-77	67	-13.941	1.03626	-13.453	0.049	150.838	-0.092	0.005	-179	0
12.	11:00/11-14-77	86	-13.923	1.03626	-13.436	0.067	150.798	-0.124	0.007	-179	0
13.	11:28/11-14-77	96	-13.919	1.03625	-13.432	0.070	150.779	-0.143	0.002	-179	0
14.	11:31/11-14-77	107	-13.905	1.03625	-13.419	0.084	150.766	-0.156	0.006	-179	0
15.	11:43/11-14-77	119	-13.902	1.03623	-13.416	0.087	150.733	-0.188	-0.004	-179	-0
16.	12:02/11-14-77	138	-13.887	1.03622	-13.402	0.101	150.743	-0.179	0.014	-178	0
17.	12:35/11-14-77	171	-13.874	1.03621	-13.389	0.113	150.678	-0.244	-0.004	-179	-0
18.	13:10/11-14-77	212	-13.849	1.03617	-13.366	0.137	150.641	-0.280	0.002	-179	0
19.	13:49/11-14-77	245	-13.836	1.03612	-13.325	0.178	150.637	-0.285	0.048	-178	1
20.	14:28/11-14-77	284	-13.735	1.03606	-13.257	0.246	150.494	-0.428	0.039	-178	1
21.	15:17/11-14-77	333	-13.667	1.03600	-13.192	0.310	150.333	-0.588	0.026	-178	1
22.	16:00/11-14-77	384	-13.602	1.03592	-13.118	0.372	150.228	-0.694	0.017	-178	1
23.	16:58/11-14-77	426	-13.585	1.03590	-13.114	0.388	150.222	-0.699	0.002	-179	0
24.	17:58/11-14-77	494	-13.595	1.03592	-13.124	0.379	150.184	-0.818	-0.016	-179	-0
25.	0:17/11-15-77	873	-13.746	1.03607	-13.267	0.235	150.366	-0.556	-0.033	-188	-1
26.	2:33/11-15-77	1009	-13.866	1.03619	-13.382	0.121	150.595	-0.326	-0.037	-188	-1
27.	4:07/11-15-77	1103	-13.943	1.03624	-13.508	-0.004	150.753	-0.168	0.164	-184	-5
28.	6:56/11-15-77	1272	-13.896	1.03621	-13.418	0.092	150.766	-0.156	0.017	-178	0
29.	8:29/11-15-77	1365	-13.825	1.03614	-13.343	0.168	150.689	-0.313	0.089	-179	0
30.	8:10/11-16-77	2386	-13.711	1.03604	-13.234	0.268	150.379	-0.542	0.087	-179	0
31.	2:53/11-16-77	2469	-13.834	1.03618	-13.351	0.151	150.569	-0.372	-0.028	-188	-1
*.	4:38/11-16-77	2574	-13.919	1.03625	-13.432	0.070	150.738	-0.184	-0.018	-179	-1
J.	8:52/11-16-77	2828	-13.779	1.03609	-13.299	0.203	150.526	-0.395	0.013	-178	0
34.	11:16/11-16-77	2972	-13.655	1.03599	-13.179	0.323	150.343	-0.579	0.044	-178	1
35.	7:49/11-17-77	4285	-13.818	1.03614	-13.336	0.166	150.618	-0.303	0.020	-178	1
36.	14:24/11-17-77	4688	-13.868	1.03567	-12.980	0.603	157.888	-1.122	0.061	-177	2
37.	8:03/11-18-77	5659	-13.742	1.03606	-13.264	0.239	150.485	-0.437	0.028	-178	1
38.	11:56/11-18-77	5892	-13.788	1.03603	-13.231	0.271	150.375	-0.547	0.007	-179	0
39.	14:33/11-18-77	6049	-13.694	1.03602	-13.218	0.285	150.352	-0.570	0.009	-179	0
40.	11:24/11-19-77	7388	-13.622	1.03594	-13.149	0.353	150.228	-0.694	0.018	-178	1
41.	14:45/11-19-77	7581	-13.785	1.03603	-13.228	0.274	150.379	-0.542	0.012	-179	0
42.	8:25/11-21-77	10881	-13.895	1.03622	-13.409	0.093	150.694	-0.228	0.068	-176	2
43.	8:09/11-22-77	11819	-13.874	1.03619	-13.389	0.113	150.798	-0.124	0.053	-177	2
44.	15:53/11-22-77	12889	-13.796	1.03613	-13.315	0.188	150.572	-0.349	0.019	-178	1
45.	9:04/11-23-77	12928	-13.658	1.03596	-13.176	0.326	150.287	-0.634	0.028	-178	1
46.	13:30/11-23-77	13166	-13.769	1.03622	-13.289	0.223	150.583	-0.438	0.033	-179	0
47.	10:34/11-24-77	14450	-13.765	1.03589	-13.286	0.217	150.494	-0.428	0.011	-179	0
48.	10:26/11-25-77	15883	-13.902	1.03623	-13.416	0.087	150.682	-0.128	0.029	-178	1
49.	20:41/11-26-77	17937	-13.898	1.03621	-13.405	0.098	150.728	-0.202	0.008	-179	0
50.	8:10/11-28-77	20874	-14.056	1.03648	-13.562	-0.068	159.874	9.152	0.013	-178	0
51.	9:24/11-29-77	21588	-13.764	1.03689	-13.285	0.218	150.536	-0.386	0.032	-178	1
52.	16:01/11-29-77	21977	-13.646	1.03597	-13.172	0.338	150.274	-0.648	0.017	-178	1
*3.	15:12/11-30-77	23898	-13.668	1.03651	-13.188	0.322	150.733	-0.188	0.031	-178	1
.	15:51/11-30-77	23987	-13.637	1.03597	-13.164	0.339	150.268	-0.662	0.019	-178	1
55.	8:23/12- 1-77	24399	-13.756	1.03687	-13.277	0.225	150.580	-0.414	0.026	-178	1
56.	16:17/12- 1-77	24873	-13.659	1.03599	-13.184	0.318	150.381	-0.621	0.018	-178	1
57.	15:54/12- 2-77	26298	-13.535	1.03588	-13.065	0.417	150.898	-0.812	0.015	-178	0
58.	12:59/12- 4-77	28895	-13.822	1.03615	-13.348	0.163	150.674	-0.248	0.043	-178	1
59.	13:18/12- 5-77	30446	-13.773	1.03612	-13.293	0.218	150.688	-0.322	0.054	-177	2
60.	11:08/12- 6-77	31756	-13.756	1.03609	-13.277	0.226	150.959	-0.363	0.050	-177	2
61.	15:34/12- 6-77	32838	-13.698	1.03588	-13.224	0.279	150.882	-0.919	0.035	-178	1
62.	9:27/12- 7-77	33183	-13.734	1.03606	-13.256	0.246	150.685	-0.437	0.036	-178	1
63.	15:47/12- 7-77	33483	-13.711	1.03605	-13.234	0.269	150.379	-0.542	0.007	-179	0
64.	7:55/12- 8-77	34451	-13.644	1.03596	-13.178	0.332	150.333	-0.588	0.040	-177	1
65.	9:19/12- 9-77	35973	-13.326	1.03562	-12.868	0.635	157.713	-1.289	0.051	-177	2
66.	15:44/12- 9-77	36368	-13.649	1.03599	-13.175	0.328	150.237	-0.695	-0.003	-179	-0
67.	13:34/12-11-77	39116	-13.883	1.03616	-13.321	0.181	150.591	-0.331	0.022	-178	1
68.	9:02/12-12-77	40218	-13.923	1.03626	-13.436	0.067	150.878	-0.044	0.046	-178	1
69.	15:13/12-13-77	42089	-13.794	1.03613	-13.313	0.189	150.959	-0.363	0.014	-178	0
70.	8:18/12-14-77	43186	-13.825	1.03613	-13.343	0.168	150.687	-0.234	0.046	-177	1
71.	7:54/12-15-77	45978	-13.748	1.03605	-13.262	0.241	150.931	-0.391	0.052	-177	1
72.	9:22/12-16-77	46858	-13.683	1.03600	-13.208	0.295	150.379	-0.542	0.033	-178	1
73.	20:58/12-19-77	51874	-13.305	1.03559	-12.848	0.655	157.639	-1.283	0.035	-178	1
74.	10:48/12-20-77	51896	-13.584	1.03581	-13.037	0.465	157.998	-0.924	0.019	-178	1
75.	9:18/12-21-77	53246	-14.022	1.03648	-13.538	-0.037	159.846	0.124	0.033	-178	1
76.	10:02/12-22-77	54730	-13.951	1.03629	-13.462	0.048	158.936	0.014	0.047	-177	1
77.	10:40/12-23-77	56216	-13.961	1.03931	-13.453	0.058	158.931	0.009	0.074	-177	2
78.	11:05/12-27-77	62891	-14.031	1.03634	-13.539	-0.037	159.846	0.124	0.023	-178	1
79.	12:48/ 1- 1-78	69296	-13.582	1.03587	-13.112	0.391	158.154	-0.768	0.028	-178	1
80.	9:24/ 1- 3-78	71988	-13.668	1.03598	-13.194	0.309	158.324	-0.598	0.028	-178	1
81.	13:48/ 1- 4-78	73684	-13.731	1.03605	-13.253	0.249	158.439	-0.483	0.016	-178	0
82.	11:28/ 1- 5-78	74976	-13.928	1.03626	-13.433	0.078	158.816	-0.186	0.019	-178	1
83.	13:15/ 1- 6-78	76531	-13.821	1.03613	-13.339	0.163	158.586	-0.336	0.001	-179	0
84.	19:52/ 1- 9-78	81889	-13.922	1.03625	-13.435	0.068	158.819	-0.133	0.007	-179	0
85.	13:20/ 1-10-78	82384	-13.888	1.03620	-13.395	0.107	158.678	-0.244	-0.018	-179	-0
86.	20:25/ 1-11-78	84199	-13.976	1.03632	-13.490	0.016	158.909	-0.014	0.010	-179	0
.	15:45/ 1-12-78	85321	-13.888	1.03623	-13.402	0.108	158.747	-0.175	0.016	-178	0
.	15:39/ 1-16-78	88758	-13.923	1.03625	-13.436	0.067	158.812	-0.119	0.013	-178	0
89.	12:00/ 1-16-78	90856	-13.712	1.03605	-13.235	0.267	158.956	-0.365	-0.006	-179	-0
90.	15:41/ 1-17-78	92517	-13.805	1.03614	-13.323	0.179	158.536	-0.386	-0.007	-179	-0
91.	13:27/ 1-18-78	93943	-13.732	1.03605	-13.254	0.248	158.378	-0.592	-0.018	-179	-0
92.	19:16/ 1-19-78	95892	-13.789	1.03624	-13.294	0.208	158.479	-0.479	-0.013	-179	-0
93.	13:32/ 1-20-78	96878	-13.875	1.03628	-13.398	0.113	158.655	-0.267	-0.016	-179	-0
94.	15:36/ 1-24-78	101893	-13.634	1.03596	-13.168	0.323	158.255	-0.667	0.000	-179	0
95.	20:46/ 1-25-78	104342	-14.008	1.03638	-13.527	-0.036	159.893	0.133	0.030	-177	2
96.	15:14/ 1-27-78	106898	-13.884	1.03613	-13.323	0.180	158.788	-0.236	0.116	-178	1
97.	8:18/ 1-28-78	111786	-13.923	1.03625	-13.436	0.067	158.966	-0.244	0.155	-178	0
98.	18:36/ 1-31-78	113373	-13.595	1.03587	-13.806	0.417	158.363	-0.599	0.147	-176	4
99.	13:38/ 2- 1-78	113994	-13.836	1.03616	-13.353	0.169	158.816	-0.186	0.098	-176	3
100.	8:28/ 2- 3-78	116564	-13.763	1.03618	-13.281	0.219	158.887	-0.115	0.164	-176	5
101.	8:38/ 2- 6-78	120886	-14.071	1.03637	-13.577	-0.074	159.471	0.558	0.193	-176	6
102.	18:38/ 2- 7-78	122446	-14.012	1.03636	-13.528	-0.010	159.288	0.366	0.159	-176	5
103.	8:28/ 2- 8-78	123756	-13.916	1.03626	-13.429	0.073	159.148	0.219	0.179	-173	5
104.	13:38/ 2- 9-78	125506	-13.930	1.03626	-13.443	0.058	159.098	0.168	0.141	-175	4
105.	18:04/ 2-19-78	133848	-14.771	1.03699	-14.142	-2.648	164.881	5.950	0.189	-178	3
106.	11:38/ 2-16-78	133834	-17.892	1.03944	-16.444	-5.962	165.232	6.300	0.099	-178	3
107.	17:06/ 2-17-78	137242	-17.269	1.03961	-16.611	-3.189	165.567	6.645	0.087	-176	3
108.	15:42/ 2-21-78	142918	-17.878	1.03948	-16.423	-2.928	165.189	6.277	0.099	-176	3
109.	16:05/ 2-22-78	144701	-17.807	1.03942	-16.439	-2.917	165.239	6.327	0.112	-176	3
110.	15:38/ 2-23-78	145786	-17.134	1.03948	-16.403	-2.501	165.389	6.447	0.155	-176	4
111.	19:48/ 2-24-78	147258	-17.115	1.03955	-16.568	-3.058	165.438	6.516	0.077	-177	3
112.	14:45/ 2-27-78	151581	-17.106	1.03931	-16.514	-3.011	165.388	6.466	0.099	-176	3
113.	16:00/ 3- 1-78	154696	-17.107	1.03944	-16.498	-2.955	165.177	6.256	0.084	-177	3
114.	14:20/ 3-18-78	174016	-16.319	1.03908	-15.712	-2.209	151.686	6.683	0.043	-178	1
115.	14:18/ 3-23-78	184076	-16.319	1.03872	-15.772	-2.270	167.737	4.807	0.041	-178	1
116.	14:52/ 3-31-78	197588	-16.415	1.03875	-15.887	-2.388	163.779	4.857	0.038	-178	1
117.	14:42/ 4-11-78	213618	-16.248	1.03859	-15.837	-2.136	163.452	4.530	0.047	-177	1
118.	13:13/ 4-24-78	232849	-16.513	1.03887	-15.989	-2.993	163.981	5.059	0.042	-178	1
119.	19:58/ 5-16-78	263896	-16.589	1.03905	-15.986	-2.383	164.114	5.193	0.116	-178	3
120.	15:33/ 5-31-78	285469	-16.457	1.03877	-15.843	-2.348	163.935	5.013	0.073	-177	2
1.	13:58/ 7-12-78	349054	-15.859	1.03815	-15.257	-1.754	162.932	3.618	-0.016	-179	-0
2.	13:31/ 8- 8-78	384787	-14.638	1.03696	-14.109	-0.602	160.893	1.131	-0.057	-181	-2
123.	18:27/ 8- 9-78	386163	-15.079	1.03752	-14.588	0.394	161.972	-0.030	0.167	-173	6
124.	9:59/11-22-78	937131	-15.804	1.03836	-15.637	0.065	167.518	-1.484	0.187	-173	6
125.	10:30/12-11-78	966916	-11.993	1.03392	-11.213	2.390	154.434	-4.488	0.119	-175	4

THIS PAGE IS BEST QUALITY PRACTICABLE
FROM COPY FURNISHED TO DDC

TABLE 14. BEAM STABILITY TEST AT 160°F. HISTORY OF BONDED COMPRESSION GAGE NO. 17

SYMBOLS:

t	-	Elapsed Time from Loading(t=0)
T(t)	-	Platinum Resistor Temp @ Time t
Bo	-	Bridge Output
Bex	-	Bridge Excitation
NOP(t)	-	Normalized Output(Excitation Corrected) @ Time t
NOP'(t)	-	Normalized Output(Excitation & Temp Corrected) @ Time t
S	-	Temperature Sensitivity
G	-	Gage Factor
e	-	Beam Strain
e_u	-	Experimental Strain Uncertainty

RELATIONS:

ΔT	-	T(t)-T(0)
NOP(t)	-	1P*(Bo/Bex)
NOP'(t)	-	1P*(Bo-SΔT)/Bex
ΔNOP	-	NOP(t)-NOP(0)
ΔNOP'	-	NOP'(t)-NOP'(0)
e(t)	-	4([NOP'(t)-NOP(preload)])/G
Δe	-	e(t)-e(0)

VALUES:

S = -.5mV/°F (Preloaded Average Value About 160 ± 10°F)
e_u = .5με (see text)
G = 130 (using e= 177με From Compression Semiconductor Gage 022 @ t=84min)

HISTORY of GAGE 17

#	TIME/DATE	t(min)	Bo(mv)	Bex(V)	NOP	ΔNOP	T(°F)	ΔT(°F)	ΔNOP'	e(με)	Δe(με)
1.	9:44/11-14-77	0	-3.688	1.02682	-3.594	0.000	158.922	0.000	0.000	177	0
2.	9:45/11-14-77	1	-3.692	1.02682	-3.598	-0.004	158.908	-0.014	-0.011	177	-0
3.	9:48/11-14-77	4	-3.695	1.02682	-3.601	-0.007	158.908	-0.014	-0.014	177	-0
4.	9:55/11-14-77	11	-3.696	1.02682	-3.602	-0.008	158.908	-0.014	-0.015	177	-0
5.	10:01/11-14-77	17	-3.689	1.02682	-3.595	-0.001	158.894	-0.028	-0.014	177	-0
6.	10:08/11-14-77	24	-3.688	1.02688	-3.595	-0.000	158.885	-0.037	-0.018	177	-1
7.	10:13/11-14-77	29	-3.682	1.02688	-3.589	0.006	158.876	-0.046	-0.017	177	-0
8.	10:22/11-14-77	38	-3.677	1.02681	-3.584	0.011	158.876	-0.046	-0.012	177	-0
9.	10:32/11-14-77	48	-3.668	1.02688	-3.567	0.027	158.853	-0.069	-0.006	177	-0
10.	10:39/11-14-77	55	-3.666	1.02599	-3.573	0.021	158.834	-0.087	-0.021	177	-1
11.	10:51/11-14-77	67	-3.655	1.02598	-3.562	0.032	158.838	-0.092	-0.013	177	-0
12.	11:00/11-14-77	84	-3.647	1.02598	-3.555	0.040	158.798	-0.124	-0.021	177	-1
13.	11:28/11-14-77	96	-3.637	1.02598	-3.545	0.050	158.779	-0.143	-0.020	177	-1
14.	11:31/11-14-77	107	-3.633	1.02596	-3.541	0.053	158.766	-0.156	-0.023	177	-1
15.	11:43/11-14-77	119	-3.622	1.02595	-3.530	0.064	158.733	-0.188	-0.028	176	-1
16.	12:02/11-14-77	138	-3.608	1.02594	-3.517	0.078	158.742	-0.179	-0.018	177	-0
17.	12:55/11-14-77	171	-3.588	1.02593	-3.589	0.085	158.678	-0.244	-0.033	176	-1
18.	13:16/11-14-77	212	-3.567	1.02598	-3.477	0.118	158.641	-0.280	-0.019	177	-1
19.	13:49/11-14-77	245	-3.551	1.02584	-3.442	0.152	158.637	-0.285	0.013	178	0
20.	14:28/11-14-77	284	-3.462	1.02578	-3.375	0.219	158.494	-0.428	0.011	178	0
21.	15:17/11-14-77	333	-3.385	1.02571	-3.300	0.294	158.333	-0.588	0.007	177	0
22.	16:08/11-14-77	384	-3.324	1.02565	-3.241	0.354	158.228	-0.694	0.015	178	0
23.	16:58/11-14-77	426	-3.283	1.02562	-3.220	0.374	158.122	-0.800	-0.016	177	-0
24.	17:58/11-14-77	494	-3.319	1.02563	-3.236	0.358	158.184	-0.818	-0.041	176	-1
25.	0:17/11-15-77	873	-3.495	1.02588	-3.407	0.187	158.166	-0.756	-0.064	175	-2
26.	2:33/11-15-77	1809	-3.616	1.02594	-3.525	0.070	158.595	-0.326	-0.089	175	-3
27.	4:07/11-15-77	1103	-3.698	1.02681	-3.604	-0.010	158.756	-0.166	-0.098	175	-3
28.	6:56/11-15-77	1272	-3.648	1.02596	-3.556	0.039	158.766	-0.156	-0.057	176	-1
29.	8:29/11-15-77	1365	-3.588	1.02588	-3.490	0.103	158.609	-0.313	-0.048	176	-1
30.	0:18/11-16-77	2386	-3.475	1.02579	-3.388	0.207	158.379	-0.542	-0.058	176	-2
31.	2:53/11-16-77	2469	-3.688	1.02592	-3.589	0.005	158.549	-0.372	-0.096	174	-3
32.	4:38/11-16-77	2574	-3.689	1.02688	-3.596	-0.001	158.738	-0.184	-0.091	175	-3
3.	8:52/11-16-77	2828	-3.586	1.02585	-3.457	0.138	158.526	-0.395	-0.055	176	-2
4.	11:10/11-16-77	2972	-3.414	1.02565	-3.378	0.266	158.343	-0.579	-0.016	177	-0
35.	7:49/11-17-77	4285	-3.598	1.02598	-3.499	0.095	158.618	-0.303	-0.053	176	-2
36.	14:24/11-17-77	4688	-3.117	1.02543	-3.042	0.553	157.808	-1.122	0.006	177	0
37.	0:03/11-18-77	5659	-3.516	1.02533	-3.427	0.167	158.405	-0.437	-0.046	176	-1
38.	11:56/11-18-77	5892	-3.401	1.02548	-3.303	0.291	158.375	-0.547	-0.066	175	-2
39.	14:33/11-18-77	6849	-3.469	1.02579	-3.382	0.215	158.352	-0.570	-0.065	175	-2
40.	11:24/11-19-77	7388	-3.396	1.02571	-3.311	0.284	158.228	-0.694	-0.055	176	-2
41.	14:45/11-19-77	7581	-3.478	1.02559	-3.391	0.204	158.379	-0.543	-0.060	176	-2
42.	0:25/11-21-77	10661	-3.688	1.02681	-3.595	-0.000	158.894	-0.028	-0.013	177	-0
43.	8:03/11-22-77	11419	-3.676	1.02599	-3.583	0.012	158.798	-0.124	-0.049	176	-1
44.	15:53/11-22-77	11889	-3.599	1.02591	-3.508	0.086	158.572	-0.349	-0.004	175	-2
45.	9:04/11-23-77	12928	-3.444	1.02573	-3.358	0.237	158.287	-0.634	-0.072	175	-2
46.	13:30/11-23-77	13186	-3.570	1.02539	-3.488	0.115	158.503	-0.418	-0.009	175	-3
47.	9:34/11-24-77	14488	-3.562	1.02539	-3.472	0.122	158.494	-0.428	-0.005	175	-2
48.	10:26/11-25-77	15882	-3.718	1.02683	-3.624	-0.029	158.882	-0.120	-0.067	175	-3
49.	20:41/11-26-77	17937	-3.788	1.02653	-3.614	-0.019	158.720	-0.282	-0.118	174	-3
50.	8:18/11-28-77	20874	-3.889	1.02623	-3.798	-0.195	159.074	0.152	-0.121	174	-4
51.	9:24/11-29-77	21588	-3.577	1.02558	-3.487	0.106	158.536	-0.386	-0.000	175	-2
52.	10:01/11-29-77	21977	-3.456	1.02569	-3.369	0.225	158.274	-0.648	-0.091	175	-3
53.	9:12/11-30-77	23888	-3.684	1.02642	-3.589	0.005	158.733	-0.188	-0.087	175	-3
.	15:51/11-30-77	23487	-3.451	1.02577	-3.364	0.230	158.260	-0.662	-0.093	175	-3
.	8:23/12- 1-77	24399	-3.577	1.02599	-3.487	0.108	158.508	-0.414	-0.094	175	-3
54.	10:17/12- 1-77	24873	-3.470	1.02589	-3.791	0.284	158.391	-0.621	-0.099	174	-3
57.	15:54/12- 2-77	26298	-3.363	1.02569	-3.279	0.316	158.098	-0.832	-0.098	175	-3
58.	12:59/12- 4-77	28995	-3.653	1.02597	-3.561	0.034	158.674	-0.248	-0.087	175	-3
59.	13:10/12- 5-77	30446	-3.616	1.02594	-3.525	0.070	158.600	-0.322	-0.087	175	-3
60.	11:00/12- 6-77	31756	-3.578	1.02591	-3.488	0.107	158.559	-0.363	-0.078	175	-2
61.	15:36/12- 6-77	32038	-3.512	1.02583	-3.229	0.365	158.092	-0.919	-0.093	175	-2
62.	9:27/12- 7-77	33183	-3.572	1.02589	-3.482	0.113	158.485	-0.437	-0.100	174	-3
63.	15:47/12- 7-77	33483	-3.542	1.02587	-3.453	0.142	158.379	-0.542	-0.123	174	-4
64.	7:55/12- 8-77	34451	-3.474	1.02578	-3.387	0.208	158.333	-0.588	-0.079	175	-2
65.	9:19/12- 9-77	35975	-3.139	1.02542	-3.061	0.533	157.713	-1.209	-0.076	176	-2
66.	15:44/12- 9-77	36368	-3.481	1.02588	-3.393	0.201	158.237	-0.685	-0.133	173	-4
67.	13:36/12-11-77	39118	-3.639	1.02688	-3.547	0.048	158.591	-0.331	-0.114	174	-3
68.	8:02/12-12-77	40218	-3.738	1.02603	-3.635	-0.041	158.878	-0.044	-0.062	175	-2
69.	15:13/12-12-77	42888	-3.634	1.02596	-3.542	0.052	158.559	-0.363	-0.125	174	-4
70.	8:10/12-14-77	43186	-3.661	1.02597	-3.568	0.026	158.687	-0.234	-0.008	175	-3
71.	7:54/12-16-77	45978	-3.583	1.02588	-3.493	0.102	158.531	-0.391	-0.069	175	-3
72.	9:22/12-16-77	46858	-3.914	1.02583	-3.426	0.169	158.379	-0.542	-0.095	174	-3
73.	20:58/12-16-77	51877	-3.137	1.02542	-3.059	0.535	157.629	-1.292	-0.098	175	-3
74.	10:48/12-28-77	51096	-3.339	1.02564	-3.256	0.339	157.998	-0.924	-0.111	174	-3
75.	9:10/12-21-77	53246	-3.880	1.02627	-3.781	-0.186	159.046	0.124	-0.126	174	-4
76.	10:07/12-22-77	54738	-3.885	1.02614	-3.711	-0.117	158.936	0.014	-0.118	174	-3
77.	10:40/12-23-77	56218	-3.818	1.02618	-3.723	-0.126	158.931	0.009	-0.122	174	-4
78.	11:05/12-27-77	62091	-3.981	1.02628	-3.881	-0.287	159.046	0.124	-0.146	173	-4
79.	12:48/ 1- 1-78	69296	-3.435	1.02572	-3.349	0.246	158.154	-0.768	-0.129	174	-4
80.	9:24/ 1- 3-78	71988	-3.328	1.02582	-3.439	0.155	158.324	-0.598	-0.136	173	-4
81.	13:48/ 1- 4-78	73684	-3.594	1.02591	-3.503	0.091	158.439	-0.483	-0.144	173	-4
82.	11:28/ 1- 6-78	74976	-3.789	1.02613	-3.693	-0.098	158.816	-0.106	-0.158	173	-5
83.	13:15/ 1- 6-78	76531	-3.685	1.02601	-3.592	0.003	158.586	-0.336	-0.161	173	-5
84.	15:52/ 1- 9-78	81888	-3.888	1.02612	-3.793	-0.199	158.789	-0.133	-0.174	172	-5
85.	13:28/ 1-10-78	82384	-3.768	1.02689	-3.664	-0.070	158.678	-0.244	-0.189	172	-5
86.	20:23/ 1-11-78	86158	-3.894	1.02628	-3.796	-0.161	158.988	-0.014	-0.168	172	-5
87.	15:45/ 1-12-78	85321	-3.767	1.02616	-3.671	-0.077	158.747	-0.255	-0.182	173	-5
.	15:39/ 1-13-78	86755	-3.884	1.02613	-3.787	-0.113	158.812	-0.110	-0.166	172	-5
88.	12:00/ 1-16-78	90856	-3.998	1.02598	-3.499	0.095	158.356	-0.565	-0.180	172	-5
89.	13:41/ 1-17-78	92517	-3.888	1.02681	-3.595	-0.000	158.536	-0.186	-0.168	172	-5
91.	15:27/ 1-18-78	93943	-3.695	1.02592	-3.514	0.081	158.378	-0.552	-0.168	172	-5
92.	15:26/ 1-19-78	95382	-3.665	1.02599	-3.572	0.022	158.494	-0.428	-0.186	172	-5
93.	15:32/ 1-20-78	96828	-3.757	1.02689	-3.661	-0.067	158.655	-0.267	-0.197	172	-6
94.	15:36/ 1-26-78	102592	-3.527	1.02588	-3.438	0.156	158.255	-0.667	-0.169	172	-5
95.	20:46/ 1-26-78	106143	-3.899	1.02621	-3.799	-0.205	159.055	0.133	-0.148	173	-4
96.	10:14/ 1-27-78	105898	-3.895	1.02642	-3.792	-0.003	158.786	-0.136	-0.063	175	-2
97.	9:10/ 1-30-78	110706	-3.816	1.02614	-3.719	-0.124	158.166	0.244	-0.006	177	-0
98.	10:36/ 1-31-78	112372	-3.633	1.02574	-3.547	0.048	158.363	-0.559	-0.025	177	-1
99.	13:30/ 1- 1-78	113994	-3.713	1.02686	-3.619	-0.026	158.016	-0.186	-0.076	175	-2
100.	9:30/ 1- 2-78	115364	-3.668	1.02697	-3.568	0.026	158.087	-0.115	-0.089	176	-2
101.	9:30/ 1- 4-78	120006	-3.901	1.02633	-3.879	-0.286	159.671	0.950	-0.067	177	-0
102.	10:30/ 1- 7-78	122446	-3.988	1.02626	-3.888	-0.214	159.288	0.366	-0.035	176	-1
103.	9:20/ 1- 8-78	123730	-3.817	1.02619	-3.720	-0.125	159.148	0.219	-0.019	177	-1
104.	13:30/ 1- 8-78	125506	-3.829	1.02616	-3.731	-0.137	159.098	0.168	-0.055	176	-1
105.	10:04/ 1-19-78	133948	-3.801	1.02711	-3.716	-0.122	164.981	5.959	-0.211	169	-8
106.	17:30/ 2-16-78	195834	-7.137	1.02945	-6.933	-3.338	165.222	6.388	-0.278	169	-8
107.	17:00/ 2-17-78	197242	-7.325	1.02966	-7.114	-3.520	165.367	6.645	-0.291	169	-8
108.	15:12/ 2-21-78	142910	-7.116	1.02946	-6.912	-3.318	165.199	6.277	-0.269	169	-8
109.	11:05/ 2-22-78	144301	-7.117	1.02947	-6.913	-3.318	165.259	6.337	-0.261	169	-8
110.	15:30/ 2-23-78	145708	-7.193	1.02953	-6.987	-3.392	165.369	6.447	-0.261	170	-8
111.	15:40/ 2-26-78	147236	-7.277	1.02961	-7.069	-3.474	165.438	6.516	-0.310	169	-9
112.	14:45/ 2-27-78	151501	-7.225	1.02957	-7.017	-3.423	165.388	6.466	-0.283	169	-8
113.	6:00/ 3- 1-78	154498	-7.159	1.02950	-6.954	-3.358	165.177	6.256	-0.321	169	-9
114.	14:20/ 3-19-78	174316	-6.913	1.02909	-6.170	-2.581	163.684	4.682	-0.306	168	-9
115.	14:10/ 3-23-78	186820	-6.414	1.02876	-6.235	-2.048	163.723	4.681	-0.307	168	-9
116.	14:52/ 3-31-78	197588	-6.679	1.02890	-6.297	-2.702	163.779	4.857	-0.342	167	-10
117.	14:47/ 4-11-78	213618	-6.294	1.02881	-6.119	-2.524	163.452	4.530	-0.322	168	-10
118.	13:13/ 4-24-78	232749	-6.598	1.02892	-6.405	-2.810	163.981	4.859	-0.343	167	-10
119.	15:50/ 5-16-78	261886	-6.575	1.02898	-6.398	-2.796	164.114	5.193	-0.272	169	-8
120.	19:33/ 5-31-78	285469	-6.533	1.02883	-6.359	-2.755	163.935	5.013	-0.319	169	-9
.	13:58/ 7-12-78	145054	-5.893	1.02621	-5.731	-2.127	162.532	1.618	-0.381	166	-11
.	13:31/ 8- 8-78	196787	-6.043	1.02647	-5.871	-0.927	160.853	1.131	-0.376	166	-11
122.	10:27/ 9- 8-78	429163	-3.588	1.02592	-3.498	0.105	158.492	-0.436	-0.104	174	-3
126.	9:55/11-22-78	537131	-3.675	1.02604	-3.583	0.592	157.518	-1.404	-0.091	175	-3
129.	10:20/12-11-78	564910	-1.919	1.02595	-1.404	2.111	154.434	-4.488	-0.081	175	-2

THIS PAGE IS BEST QUALITY PRACTICABLE
FROM COPY FURNISHED TO DDC

TABLE 15. BEAM STABILITY TEST AT 160°F. HISTORY OF REFERENCE COMPENSATION RESISTORS

					160°F RESISTANCE HISTORY							
					RN55C		Carbon		RN55C		Carbon	
SET	TIME/DATE	t (min)	T (°F)	ΔT (°F)	1Ω Ohm	ΔOhm	1Ω Ohm	ΔOhm	1500 Ohm	ΔOhm	1500 Ohm	ΔOhm
1.	9:46/11-14-77	0	158.922	0.092	1Ω.209	0.000	1Ω.175	0.000	1501.38	0.000	1500.20	0.000
2.	10:13/11-14-77	29	158.876	0.046	1Ω.209	0.000	1Ω.175	0.000	1501.38	-0.000	1500.18	-0.100
3.	10:22/11-14-77	38	158.876	0.046	1Ω.211	0.002	1Ω.176	0.001	1501.37	-0.010	1500.18	-0.020
4.	10:32/11-14-77	48	158.853	0.023	1Ω.211	0.002	1Ω.176	0.001	1501.48	0.020	1500.21	0.010
5.	10:39/11-14-77	55	158.834	0.004	1Ω.212	0.003	1Ω.177	0.002	1501.38	0.000	1500.18	-0.020
6.	10:51/11-14-77	67	158.830	-0.000	1Ω.212	0.003	1Ω.177	0.002	1501.39	0.010	1500.19	-0.010
7.	11:21/11-14-77	107	158.766	-0.064	1Ω.211	0.002	1Ω.176	0.001	1501.35	-0.030	1500.16	-0.040
8.	12:02/11-14-77	138	158.743	-0.087	1Ω.210	0.001	1Ω.175	0.000	1501.09	-0.290	1507.98	-0.300
9.	12:35/11-14-77	171	158.678	-0.152	1Ω.211	0.002	1Ω.177	0.002	1501.42	0.040	1500.20	0.000
10.	13:49/11-14-77	245	158.637	-0.193	1Ω.207	-0.002	1Ω.171	-0.004	1500.87	-0.510	1507.67	-0.530
11.	14:20/11-14-77	284	158.494	-0.336	1Ω.206	-0.003	1Ω.170	-0.005	1500.95	-0.430	1507.74	-0.460
12.	13:17/11-14-77	333	158.333	-0.497	1Ω.209	0.000	1Ω.174	-0.001	1501.37	-0.010	1500.17	-0.030
13.	15:46/11-14-77	364	158.220	-0.610	1Ω.210	0.001	1Ω.175	0.000	1501.42	0.040	1500.21	0.010
14.	16:50/11-14-77	426	158.122	-0.708	1Ω.211	0.002	1Ω.176	0.001	1501.39	0.010	1500.19	-0.010
15.	17:50/11-14-77	486	158.104	-0.726	1Ω.211	0.002	1Ω.176	0.001	1501.34	-0.040	1500.15	-0.050
16.	9:17/11-15-77	873	158.966	-0.464	1Ω.212	0.003	1Ω.177	0.002	1501.33	-0.050	1500.13	-0.070
17.	4:07/11-15-77	1183	158.874	-0.074	1Ω.202	-0.007	1Ω.168	-0.007	1500.25	-1.130	1507.06	-1.140
18.	4:56/11-15-77	1272	158.766	-0.064	1Ω.195	-0.014	1Ω.160	-0.015	1494.42	-6.960	1506.21	-1.990
19.	8:29/11-15-77	1365	158.689	-0.221	1Ω.212	0.003	1Ω.178	0.003	1501.41	0.030	1500.20	0.000
20.	9:10/11-16-77	2306	158.379	-0.451	1Ω.211	0.002	1Ω.177	0.002	1501.33	-0.050	1500.16	-0.040
21.	3:53/11-16-77	2469	158.213	-0.481	1Ω.211	0.002	1Ω.176	0.001	1501.33	-0.050	1500.14	-0.060
22.	4:38/11-16-77	2574	158.738	-0.092	1Ω.212	0.003	1Ω.178	0.003	1501.33	-0.050	1500.16	-0.040
23.	8:52/11-16-77	2828	158.526	-0.304	1Ω.212	0.003	1Ω.177	0.002	1501.48	0.020	1500.19	-0.010
24.	11:10/11-16-77	2972	158.343	-0.487	1Ω.211	0.002	1Ω.177	0.002	1501.41	0.030	1500.20	0.000
25.	7:49/11-17-77	4285	158.756	-0.212	1Ω.210	0.001	1Ω.174	-0.001	1501.36	-0.020	1500.16	-0.040
26.	14:24/11-17-77	4680	157.800	-1.030	1Ω.205	-0.004	1Ω.170	-0.005	1501.03	-0.350	1507.01	-0.390
27.	8:03/11-18-77	5659	158.405	-0.345	1Ω.211	0.002	1Ω.176	0.001	1500.16	6.780	1500.16	-0.040
28.	11:36/11-18-77	5892	158.375	-0.495	1Ω.210	0.001	1Ω.176	0.001	1501.28	-0.100	1500.07	-0.130
29.	14:53/11-18-77	6049	158.352	-0.478	1Ω.211	0.002	1Ω.176	0.001	1501.29	-0.090	1500.10	-0.100
30.	11:24/11-19-77	7380	158.228	-0.602	1Ω.209	0.000	1Ω.174	-0.001	1501.42	0.040	1500.23	0.030
31.	14:45/11-19-77	7581	158.179	-0.651	1Ω.212	0.003	1Ω.178	0.003	1501.42	0.040	1500.25	0.050
32.	9:29/11-21-77	10001	158.894	0.064	1Ω.210	0.001	1Ω.175	0.000	1501.43	0.050	1500.22	0.020
33.	4:03/11-22-77	11419	158.798	-0.032	1Ω.201	-0.008	1Ω.166	-0.009	1499.56	-1.820	1506.45	-1.550
34.	15:53/11-22-77	11989	158.572	-0.258	1Ω.212	0.003	1Ω.177	0.002	1501.48	0.020	1500.18	-0.020
35.	9:04/11-23-77	12928	158.287	-0.543	1Ω.209	0.000	1Ω.175	0.000	1501.39	0.010	1500.20	0.000
36.	13:38/11-23-77	13166	158.503	-0.327	1Ω.200	-0.009	1Ω.173	-0.002	1500.51	-0.870	1507.31	-0.890
37.	10:54/11-24-77	14458	158.494	-0.336	1Ω.787	0.578	1Ω.760	0.585	1501.92	0.540	1500.73	0.530
38.	10:26/11-25-77	15802	158.802	-0.028	1Ω.894	0.685	1Ω.854	0.679	1502.87	0.490	1500.87	0.670
39.	20:41/11-26-77	17937	158.730	-0.110	1Ω.888	0.671	1Ω.848	0.665	1502.14	0.760	1500.92	0.720
40.	9:10/11-28-77	20874	159.874	0.044	1Ω.213	0.004	1Ω.178	0.003	1501.43	0.050	1500.23	0.030
41.	9:54/11-29-77	21388	158.836	-0.294	1Ω.208	-0.001	1Ω.173	-0.002	1500.86	-0.520	1507.67	-0.470
42.	14:01/11-29-77	21977	158.274	-0.556	1Ω.212	0.003	1Ω.177	0.002	1501.33	-0.050	1500.14	-0.060
43.	9:12/11-30-77	23888	158.733	-0.097	1Ω.212	0.003	1Ω.178	0.003	1501.48	0.020	1500.20	0.000
44.	15:51/11-30-77	23487	158.268	-0.570	1Ω.209	0.000	1Ω.175	0.000	1501.33	-0.050	1500.14	-0.060
45.	8:23/12- 1-77	24399	158.588	-0.323	1Ω.211	0.002	1Ω.176	0.001	1501.37	-0.010	1500.17	-0.030
46.	16:17/12- 1-77	24873	158.381	-0.529	1Ω.208	-0.001	1Ω.172	-0.003	1500.78	-0.600	1507.49	-0.710
47.	15:54/12- 2-77	26298	158.898	-0.748	1Ω.212	0.003	1Ω.178	0.003	1501.48	0.020	1500.19	-0.010
48.	12:59/12- 4-77	28995	158.674	-0.156	1Ω.212	0.003	1Ω.177	0.002	1501.41	0.030	1500.21	0.010
49.	13:18/12- 5-77	30446	158.680	-0.238	1Ω.213	0.004	1Ω.178	0.003	1501.43	0.050	1500.22	0.020
50.	11:00/12- 6-77	31756	158.559	-0.271	1Ω.211	0.002	1Ω.177	0.002	1501.48	0.020	1500.21	0.010
51.	15:34/12- 6-77	32038	158.802	-0.028	1Ω.211	0.002	1Ω.177	0.002	1501.39	0.010	1500.20	0.000
52.	9:27/12- 7-77	33103	158.405	-0.345	1Ω.213	0.004	1Ω.179	0.004	1501.48	0.020	1500.20	0.000
53.	15:47/12- 7-77	33483	158.379	-0.451	1Ω.211	0.002	1Ω.177	0.002	1501.42	0.040	1500.23	0.030
54.	7:55/12- 8-77	34451	158.333	-0.497	1Ω.211	0.002	1Ω.176	0.001	1501.43	0.050	1500.25	0.050
55.	9:19/12- 9-77	35975	157.713	-1.117	1Ω.212	0.003	1Ω.178	0.003	1501.44	0.060	1500.23	0.030
56.	15:44/12- 9-77	36348	158.237	-0.593	1Ω.212	0.003	1Ω.178	0.003	1501.39	0.010	1500.18	-0.020
57.	13:34/12-11-77	39118	158.591	-0.239	1Ω.213	0.004	1Ω.179	0.004	1501.42	0.040	1500.23	0.030
58.	8:02/12-12-77	40210	158.878	0.048	1Ω.208	-0.009	1Ω.166	-0.009	1500.09	-1.290	1506.88	-1.320
59.	15:13/12-13-77	42089	158.559	-0.271	1Ω.212	0.003	1Ω.178	0.003	1501.37	-0.010	1500.19	-0.010
60.	8:18/12-14-77	41106	159.687	-0.143	1Ω.213	0.004	1Ω.179	0.004	1501.44	0.060	1500.26	0.060
61.	7:54/12-16-77	45978	158.531	-0.299	1Ω.212	0.003	1Ω.178	0.003	1501.45	0.070	1500.26	0.060
62.	10:48/12-20-77	51096	157.998	-0.832	1Ω.211	0.002	1Ω.176	0.001	1501.41	0.030	1500.23	0.030
63.	9:10/12-21-77	52046	159.746	0.216	1Ω.216	0.007	1Ω.182	0.007 F	1501.42	0.040	1500.24	0.040
64.	10:02/12-22-77	54730	158.926	0.196	1Ω.196	-0.013	1Ω.161	-0.014	1498.88	-2.500	1505.60	-2.600
65.	10:40/12-23-77	56216	158.931	0.101	1Ω.215	0.006	1Ω.181	0.006	1501.45	0.070	1500.25	0.050
66.	11:05/12-27-77	62001	159.046	0.216	1Ω.213	0.004	1Ω.179	0.004	1501.43	0.050	1500.23	0.030
67.	12:48/ 1- 1-78	69796	158.134	-0.676	1Ω.211	0.002	1Ω.177	0.002	1501.47	0.090	1500.25	0.050
68.	9:24/ 1- 1-78	71909	158.324	-0.586	1Ω.212	0.003	1Ω.178	0.003	1501.48	0.100	1500.28	0.080
69.	13:48/ 1- 4-78	73684	158.439	-0.391	1Ω.215	0.006	1Ω.181	0.006	1501.43	0.050	1500.26	0.060
70.	11:28/ 1- 5-78	74976	158.816	-0.014	1Ω.216	0.007	1Ω.182	0.007	1501.58	0.120	1500.32	0.120
71.	13:15/ 1- 6-78	76931	158.586	-0.244	1Ω.214	0.005	1Ω.180	0.005	1501.44	0.060	1500.27	0.070
72.	15:52/ 1- 7-78	78769	158.797	-0.033	1Ω.210	0.001	1Ω.176	0.001	1501.39	0.010	1500.21	0.010
73.	13:28/ 1-10-78	82384	158.670	-0.152	1Ω.209	0.000	1Ω.176	0.001	1501.49	0.110	1500.38	0.100
74.	20:23/ 1-11-78	84159	158.988	0.078	1Ω.210	0.001	1Ω.176	0.001	1501.58	0.120	1500.29	0.090
75.	19:45/ 1-12-78	85321	158.747	-0.163	1Ω.212	0.003	1Ω.177	0.002	1501.45	0.070	1500.28	0.080
76.	14:39/ 1-13-78	86755	158.818	-0.018	1Ω.213	0.004	1Ω.179	0.004	1501.41	0.030	1500.22	0.020
77.	12:08/ 1-16-78	90856	158.356	-0.474	1Ω.214	0.005	1Ω.179	0.004	1501.45	0.070	1500.26	0.060
78.	15:41/ 1-17-78	92517	158.536	-0.294	1Ω.213	0.004	1Ω.179	0.004	1501.38	0.000	1500.22	0.020
79.	15:27/ 1-18-78	93943	158.378	-0.468	1Ω.212	0.003	1Ω.177	0.002	1501.41	0.030	1500.19	-0.010
80.	15:26/ 1-19-78	95382	158.494	-0.336	1Ω.212	0.003	1Ω.179	0.004	1501.48	0.020	1500.22	0.020
81.	15:32/ 1-20-78	96828	158.655	-0.175	1Ω.214	0.005	1Ω.180	0.005	1501.42	0.040	1500.24	0.040
82.	15:36/ 1-24-78	101752	158.255	-0.575	1Ω.212	0.003	1Ω.178	0.003	1501.45	0.070	1500.28	0.080
83.	20:46/ 1-25-78	104142	159.935	0.225	1Ω.209	0.000	1Ω.175	0.000	1501.52	0.140	1500.36	0.160
84.	15:14/ 1-27-78	106497	158.786	-0.044	1Ω.216	0.007	1Ω.182	0.007	1501.44	0.060	1500.27	0.070
85.	0:10/ 1-30-78	110705	159.166	0.336	1Ω.216	0.007	1Ω.182	0.007	1501.47	0.090	1500.31	0.110
86.	10:36/ 1-31-78	113372	159.363	0.467	1Ω.216	0.007	1Ω.182	0.007	1501.46	0.080	1500.30	0.100
87.	13:30/ 2- 1-78	114994	158.016	-0.814	1Ω.216	0.007	1Ω.182	0.007	1501.96	0.580	1500.28	0.080
88.	9:20/ 2- 3-78	118564	159.087	0.023	1Ω.217	0.008	1Ω.183	0.008	1501.50	0.120	1500.31	0.110
89.	9:30/ 2- 6-78	120886	159.471	0.641	1Ω.215	0.006	1Ω.182	0.007	1501.46	0.080	1500.28	0.080
90.	10:30/ 2- 7-78	122446	159.287	0.457	1Ω.217	0.008	1Ω.184	0.009	1501.46	0.080	1500.28	0.080
91.	8:20/ 2- 8-78	123756	159.148	0.318	1Ω.215	0.006	1Ω.181	0.006	1501.43	0.050	1500.27	0.070
92.	15:10/ 2- 9-78	125506	159.098	0.268	1Ω.214	0.005	1Ω.180	0.005	1501.46	0.080	1500.28	0.080
93.	10:04/ 2-15-78	133948	164.881	6.051	1Ω.219	0.010	1Ω.187	0.012	1501.49	0.110	1500.41	0.210
94.	17:30/ 2-16-78	135834	165.221	6.391	1Ω.213	0.004	1Ω.182	0.007	1501.57	0.190	1500.50	0.300
95.	17:06/ 2-17-78	137242	165.566	6.736	1Ω.216	0.007	1Ω.182	0.007	1501.58	0.120	1500.47	0.270
96.	15:42/ 2-21-78	142918	165.198	6.368	1Ω.217	0.008	1Ω.183	0.008	1501.49	0.110	1500.43	0.230
97.	16:05/ 2-22-78	144381	165.258	6.428	1Ω.215	0.006	1Ω.184	0.009	1501.45	0.070	1500.41	0.210
98.	15:38/ 2-23-78	145786	165.368	6.538	1Ω.217	0.008	1Ω.185	0.010	1501.44	0.060	1500.38	0.180
99.	15:48/ 2-24-78	147236	165.437	6.607	1Ω.216	0.007	1Ω.183	0.008	1501.45	0.070	1500.40	0.200
100.	14:45/ 2-27-78	151501	165.387	6.557	1Ω.217	0.008	1Ω.183	0.010	1501.52	0.140	1500.46	0.260
101.	16:00/ 3- 1-78	154456	165.253	6.423	1Ω.215	0.006	1Ω.113	-0.062	1501.48	0.100	1500.43	0.230
102.	14:20/ 3-15-78	174516	163.688	4.858	1Ω.216	0.007	1Ω.183	0.008	1501.52	0.140	1500.42	0.220
103.	14:10/ 3-23-78	186876	163.799	4.969	1Ω.216	0.007	1Ω.184	0.009	1501.51	0.130	1500.41	0.210
104.	14:52/ 3-24-78	197588	163.852	5.022	1Ω.217	0.008	1Ω.185	0.010	1501.57	0.190	1500.46	0.260
105.	14:42/ 4-11-78	713418	163.528	4.698	1Ω.216	0.007	1Ω.185	0.010	1501.49	0.110	1500.39	0.190
106.	13:13/ 4-24-78	230049	164.857	5.227	1Ω.215	0.006	1Ω.184	0.009	1501.58	0.120	1500.43	0.230
107.	15:50/ 5-16-78	263026	164.198	5.368	1Ω.217	0.008	1Ω.186	0.011	1501.53	0.150	1500.46	0.260
108.	15:33/ 5-31-78	285469	164.911	5.191	1Ω.216	0.007	1Ω.184	0.009	1501.52	0.140	1500.46	0.260
109.	15:50/ 7-12-78	345054	162.608	3.778	1Ω.217	0.008	1Ω.186	0.011	1501.58	0.200	1500.58	0.380
110.	13:31/ 8- 8-78	384787	159.129	1.299	1Ω.352	0.143	1Ω.318	0.143	1501.73	0.350	1500.59	0.390
111.	9:55/12-22-78	537131	157.518	-1.312	1Ω.217	0.008	1Ω.186	0.011	1501.88	0.420	1500.62	0.420
112.	10:20/12-11-78	964516	154.434	-4.396	1Ω.221	0.012	1Ω.188	0.013	1501.64	0.260	1500.45	0.250

THIS PAGE IS BEST QUALITY PRACTICABLE
FROM COPY FURNISHED TO DDC

TABLE 16. BEAM STABILITY TEST AT 160°F. HISTORY OF REFERENCE COMPENSATION RESISTOR AND UNBONDED SEMICONDUCTOR GAGE

160° F RESISTANCE HISTORY

SET	TIME/DATE	t(min)	T(F)	ΔT(F)	50K Ohm	ΔOhm	50K Ohm	ΔOhm	UNBONDED Ohm	ΔOhm
1.	9:44/11-14-77	0	158.922	0.092	51596.0	400.0	50967.0	0.0	554.62	0.00
2.	10:13/11-14-77	29	158.876	0.046	51199.0	3.0	50968.0	1.0	553.67	-0.35
3.	10:22/11-14-77	38	158.876	0.046	51197.0	1.0	50969.0	2.0	553.70	-0.32
4.	10:32/11-14-77	48	158.853	0.023	51199.0	3.0	50969.0	2.0	553.70	-0.32
5.	10:39/11-14-77	55	158.834	0.004	51198.0	2.0	50969.0	2.0	553.68	-0.34
6.	10:51/11-14-77	67	158.830	-0.000	51199.0	3.0	50969.0	2.0	553.68	-0.34
7.	11:31/11-14-77	107	158.766	-0.064	51196.0	0.0	50969.0	2.0	553.63	-0.39
8.	12:02/11-14-77	138	158.743	-0.087	51199.0	3.0	50970.0	3.0	553.52	-0.50
9.	12:35/11-14-77	171	158.678	-0.152	51199.0	3.0	50970.0	3.0	553.63	-0.39
10.	13:49/11-14-77	245	158.637	-0.193	51199.0	3.0	50971.0	4.0	553.21	-0.81
11.	14:28/11-14-77	284	158.494	-0.336	51199.0	3.0	50971.0	4.0	553.16	-0.86
12.	15:17/11-14-77	333	158.333	-0.497	51195.0	-1.0	50969.0	2.0	553.16	-0.86
13.	16:00/11-14-77	384	158.228	-0.602	51199.0	3.0	50970.0	3.0	553.15	-0.87
14.	16:50/11-14-77	426	158.122	-0.708	51198.0	2.0	50969.0	2.0	553.14	-0.88
15.	17:50/11-14-77	494	158.104	-0.726	51198.0	2.0	50970.0	3.0	553.24	-0.78
16.	0:17/11-15-77	873	158.366	-0.464	51199.0	3.0	50970.0	3.0	553.53	-0.49
17.	4:07/11-15-77	1103	158.756	-0.074	51196.0	0.0	50969.0	2.0	553.38	-0.64
18.	6:56/11-15-77	1272	158.766	-0.064	51197.0	1.0	50968.0	-7.0	552.82	-1.20
19.	8:29/11-15-77	1365	158.689	-0.221	51200.0	4.0	50970.0	3.0	553.51	-0.51
20.	8:18/11-16-77	2386	158.379	-0.451	51202.0	6.0	50970.0	3.0	553.44	-0.58
21.	2:53/11-16-77	2469	158.549	-0.281	51198.0	2.0	50970.0	3.0	553.65	-0.37
22.	4:38/11-16-77	2574	158.738	-0.092	51199.0	3.0	50968.0	1.0	553.78	-0.24
23.	8:52/11-16-77	2828	158.526	-0.304	51199.0	3.0	50970.0	3.0	553.48	-0.54
24.	11:16/11-16-77	2972	158.343	-0.487	51197.0	1.0	50971.0	4.0	553.22	-0.80
25.	7:49/11-17-77	4285	158.618	-0.212	51200.0	4.0	50969.0	2.0	553.52	-0.50
26.	14:24/11-17-77	4688	157.808	-1.030	51198.0	2.0	50972.0	5.0	552.68	-1.42
27.	8:03/11-18-77	5659	158.485	-0.345	51198.0	2.0	50970.0	3.0	553.27	-0.75
28.	11:56/11-18-77	5892	158.375	-0.455	51200.0	4.0	50971.0	4.0	553.36	-0.66
29.	14:33/11-18-77	6049	158.352	-0.478	51199.0	3.0	50970.0	3.0	553.33	-0.69
30.	11:24/11-19-77	7308	158.228	-0.602	51200.0	4.0	50973.0	6.0	553.22	-0.80
31.	14:45/11-19-77	7501	158.379	-0.451	51199.0	3.0	50972.0	5.0	553.39	-0.63
32.	8:25/11-21-77	10081	158.894	0.064	51199.0	3.0	50972.0	5.0	553.55	-0.47
33.	8:03/11-22-77	11419	158.798	-0.032	51199.0	3.0	50970.0	3.0	553.03	-0.99
34.	15:53/11-22-77	11889	158.572	-0.258	51199.0	3.0	50971.0	4.0	553.60	-0.42
35.	9:04/11-23-77	12928	158.287	-0.543	51199.0	3.0	50973.0	6.0	553.28	-0.74
36.	13:30/11-23-77	13186	158.583	-0.327	51197.0	1.0	50971.0	4.0	553.27	-0.75
37.	10:34/11-24-77	14458	158.494	-0.336	51200.0	4.0	50972.0	5.0	554.06	0.04
38.	10:26/11-25-77	15882	158.802	-0.028	51200.0	4.0	50972.0	5.0	554.33	0.31
39.	20:41/11-26-77	17937	158.728	-0.110	51200.0	4.0	50972.0	5.0	554.46	0.44
40.	8:18/11-28-77	20874	159.074	0.244	51200.0	4.0	50970.0	3.0	553.99	-0.03
41.	9:24/11-29-77	21588	158.536	-0.294	51199.0	3.0	50972.0	5.0	553.21	-0.81
42.	16:01/11-29-77	21977	158.274	-0.556	51199.0	3.0	50972.0	5.0	553.28	-0.74
43.	9:12/11-30-77	23000	158.733	-0.097	51199.0	3.0	50972.0	5.0	553.64	-0.38
44.	15:51/11-30-77	23467	158.268	-0.570	51199.0	3.0	50970.0	3.0	553.19	-0.83
45.	8:23/12- 1-77	24399	158.588	-0.322	51199.0	3.0	50973.0	6.0	553.48	-0.62
46.	16:17/12- 1-77	24873	158.381	-0.529	51199.0	3.0	50970.0	3.0	553.02	-1.08
47.	15:54/12- 2-77	26298	158.098	-0.748	51200.0	4.0	50973.0	6.0	552.97	-1.05
48.	12:59/12- 4-77	28995	158.674	-0.156	51198.0	2.0	50969.0	2.0	553.47	-0.55
49.	13:10/12- 5-77	30446	158.688	-0.238	51199.0	3.0	50973.0	6.0	553.39	-0.63
50.	11:00/12- 6-77	31756	158.559	-0.271	51199.0	3.0	50973.0	6.0	553.38	-0.64
51.	15:34/12- 6-77	32030	158.002	-0.828	51199.0	3.0	50972.0	5.0	552.95	-1.07
52.	9:27/12- 7-77	33103	158.485	-0.345	51200.0	4.0	50972.0	5.0	553.35	-0.67
53.	15:47/12- 7-77	33483	158.379	-0.451	51200.0	4.0	50970.0	3.0	553.36	-0.66
54.	7:55/12- 8-77	34451	158.333	-0.497	51202.0	6.0	50974.0	7.0	553.13	-0.89
55.	9:19/12- 9-77	35975	157.713	-1.117	51200.0	4.0	50976.0	9.0	552.64	-1.38
56.	15:44/12- 9-77	36360	158.237	-0.593	51197.0	1.0	50975.0	8.0	553.15	-0.87
57.	13:34/12-11-77	39110	158.591	-0.239	51199.0	3.0	50971.0	4.0	553.39	-0.63
58.	8:02/12-12-77	40218	158.078	0.648	51198.0	2.0	50970.0	3.0	552.97	-1.05
59.	15:13/12-13-77	42089	158.559	-0.271	51199.0	3.0	50973.0	6.0	553.39	-0.63
60.	8:10/12-14-77	43106	158.687	-0.143	51203.0	7.0	50975.0	8.0	553.27	-0.75
61.	7:54/12-16-77	45978	158.531	-0.299	51202.0	6.0	50975.0	8.0	553.19	-0.83
62.	10:48/12-20-77	51896	157.998	-0.832	51196.0	0.0	50976.0	9.0	552.92	-1.10
63.	9:10/12-21-77	53216	159.046	0.216	51200.0	4.0	50973.0	6.0	553.53	-0.49
64	10:02/12-22-77	54738	158.936	0.106	51200.0	4.0	50971.0	4.0	552.58	-1.44
6	10:48/12-23-77	56216	158.931	0.101	51200.0	4.0	50972.0	5.0	553.59	-0.43
66.	11:05/12-27-77	62201	159.046	0.216	51202.0	6.0	50973.0	6.0	553.73	-0.29
67.	12:48/ 1- 1-78	69296	158.154	-0.676	51200.0	4.0	50974.0	7.0	553.09	-0.93
68.	9:24/ 1- 3-78	71985	158.324	-0.506	51200.0	4.0	50970.0	3.0	553.22	-0.80
69.	13:48/ 1- 4-78	73684	158.439	-0.391	51200.0	4.0	50974.0	7.0	553.34	-0.68
70.	11:28/ 1- 5-78	74976	158.816	-0.014	51200.0	4.0	50975.0	8.0	553.59	-0.43
71.	13:15/ 1- 6-78	76531	158.586	-0.244	51197.0	1.0	50973.0	6.0	553.45	-0.57
72.	15:52/ 1- 9-78	81008	158.789	-0.041	51200.0	4.0	50971.0	4.0	553.58	-0.44
73.	13:28/ 1-10-78	82384	158.678	-0.152	51200.0	4.0	50970.0	3.0	553.60	-0.42
74.	20:23/ 1-11-78	84159	158.980	0.070	51199.0	3.0	50972.0	5.0	553.69	-0.33
75.	15:45/ 1-12-78	85321	158.747	-0.003	51199.0	3.0	50970.0	3.0	553.55	-0.47
76.	15:39/ 1-13-78	86755	158.812	-0.018	51200.0	4.0	50970.0	3.0	553.62	-0.40
77.	12:00/ 1-16-78	90056	158.356	-0.474	51201.0	5.0	50974.0	7.0	553.37	-0.65
78.	19:41/ 1-17-78	92517	158.536	-0.294	51199.0	3.0	50970.0	3.0	553.46	-0.56
79.	19:27/ 1-18-78	93943	158.378	-0.468	51200.0	4.0	50972.0	5.0	553.32	-0.70
80.	15:26/ 1-19-78	95382	158.494	-0.336	51198.0	2.0	50972.0	5.0	553.40	-0.62
81.	15:32/ 1-20-78	96820	158.655	-0.175	51200.0	4.0	50974.0	7.0	553.60	-0.42
82.	15:36/ 1-24-78	102592	158.255	-0.575	51198.0	2.0	50974.0	7.0	553.17	-0.85
83.	20:16/ 1-25-78	104142	158.005	0.225	51197.0	1.0	50974.0	7.0	553.65	-0.37
84.	15:14/ 1-27-78	106098	158.786	-0.044	51197.0	1.0	50975.0	8.0	554.38	0.36
8	8:10/ 1-30-78	110736	159.166	0.336	51198.0	2.0	50977.0	10.0	554.33	0.31
8.	10:36/ 1-31-78	112372	158.363	-0.467	51200.0	4.0	50977.0	10.0	553.96	-0.06
87.	13:38/ 2- 1-78	113994	158.816	-0.014	51201.0	5.0	50973.0	6.0	554.41	0.39
88.	8:28/ 2- 3-78	116564	158.087	-0.823	51202.0	6.0	50976.0	9.0	554.18	0.16
89.	8:38/ 2- 6-78	120886	159.471	0.641	51198.0	2.0	50974.0	7.0	554.64	0.62
90.	10:38/ 2- 7-78	122446	159.287	0.457	51202.0	6.0	50973.0	6.0	554.74	0.72
91.	8:28/ 2- 8-78	123756	159.148	0.318	51199.0	3.0	50975.0	8.0	554.41	0.39
92.	13:38/ 2- 9-78	125586	159.090	0.260	51200.0	4.0	50975.0	8.0	554.54	0.52
93.	10:04/ 2-15-78	133948	164.881	6.051	51200.0	4.0	50969.0	2.0	558.72	4.70
94.	17:38/ 2-16-78	135834	165.221	6.391	51200.0	4.0	50967.0	0.0	558.27	4.25
95.	17:06/ 2-17-78	137242	165.566	6.736	51199.0	3.0	50963.0	-4.0	558.58	4.48
96.	15:42/ 2-21-78	142918	165.198	6.368	51201.0	5.0	50967.0	0.0	558.18	4.08
97.	16:05/ 2-22-78	144381	165.258	6.428	51201.0	5.0	50965.0	-2.0	558.11	4.09
98.	15:38/ 2-23-78	145786	165.368	6.538	51200.0	4.0	50968.0	1.0	558.14	4.12
99.	15:48/ 2-24-78	147236	165.437	6.607	51198.0	2.0	50964.0	-3.0	558.36	4.34
100.	14:45/ 2-27-78	151501	165.387	6.557	51201.0	5.0	50968.0	1.0	558.24	4.22
101.	16:00/ 3- 1-78	154456	165.293	6.423	51200.0	4.0	50968.0	1.0	558.17	4.15
102.	14:28/ 3-18-78	174516	163.688	4.818	51200.0	4.0	50970.0	3.0	556.94	2.92
103.	14:10/ 3-23-78	188826	163.799	4.969	51204.0	8.0	50970.0	3.0	557.03	3.01
104.	14:52/ 3-31-78	197588	163.885	5.025	51203.0	7.0	50968.0	1.0	557.17	3.15
105.	14:42/ 4-11-78	213418	163.820	4.698	51202.0	6.0	50972.0	5.0	556.80	2.78
106.	13:13/ 4-24-78	232849	164.057	5.227	51201.0	5.0	50965.0	-2.0	557.14	3.12
107.	15:58/ 5-16-78	263066	164.198	5.368	51202.0	6.0	50974.0	7.0	558.19	4.17
108.	15:33/ 5-30-78	285469	164.011	5.181	51200.0	4.0	50972.0	5.0	558.43	4.41
109.	23:58/ 7-12-78	345854	162.688	3.778	51202.0	6.0	50973.0	6.0	556.16	2.14
110.	13:31/ 8- 8-78	384707	160.129	1.299	51203.0	7.0	50974.0	7.0	554.54	0.52
111.	9:55/11-22-78	537131	157.518	-1.312	51208.0	12.0	50994.0	27.0	552.60	-1.42
112.	10:28/12-11-78	564516	154.434	-4.396	51201.0	5.0	50996.0	29.0	549.13	-4.89

THIS PAGE IS BEST QUALITY PRACTICABLE
FROM COPY FURNISHED TO DDC

2.4.2 Celesco P-95 Transducer 500-Hr Stability Data

Celesco provided documentation on the stability of their P-95 transducer manufactured for Lockheed. This P-95 transducer is a rectangular cantilevered beam semiconductor strain gage transducer with integral electronics. The sensor yields 100 mV for a 500-μ strain load at full-scale pressure.

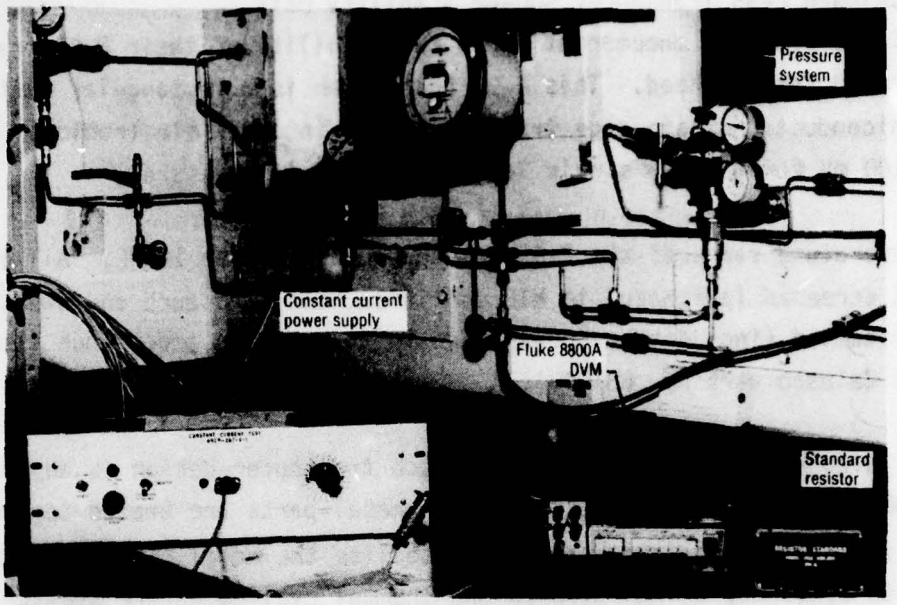
Temperature range of the P-95 transducer is -10° to 140°F. All components are 100% screened (purchased to MIL specifications) and each end item is functionally tested (including a 500-hr burn-in test to the acceptance test procedure for Celesco part No. 631093).

The diaphragm thickness of the Celesco transducer design is adjusted to yield 500-$\mu\varepsilon$ at full-scale pressure. All metal parts are brazed together at 1,700°F and hardened before gaging to stabilize the metal. All transducers were exposed to 1,000 mechanical strokes and thermal cycling before static calibration was initiated at zero time.

The total transducer zero shift through the 500-hr burn-in was generally less than 0.5% of full scale and the average for the 51 transducers was 0.19%. Average transducer shift at full-scale pressure during the 500-hr burn-in was 0.27%. These shifts in electrical output include both the contribution from the transducer and the integral electronics. A complete data report for these Celesco transducers is presented in appendix D.

2.4.3 Stability Data for Celesco Prototype Transducers

Six Celesco prototype transducers were tested. The stability tests were performed at 70°F on bare transducers and consisted of measuring zero offset. The stability test data acquisition system is shown in Figure 21. The data were monitored on a Fluke 8800A DVM. Various system checks were run on the DVM to ensure its accuracy before each data point was measured. Ambient barometric pressure was measured with a Wallace-Tiernan absolute pressure meter. All data were normalized to exactly 5.0 mA excitation and 14.7 psi ambient pressure. The initial data point measured at CSD was used as the baseline reading. All subsequent data points measured were referenced to the initial data point as a change



11617-6

Figure 21. Stress Transducer No-Load Output Data Acquisition System
17002

in output (if any). Figures 22 and 23 show plots of change in output as a percentage of full-scale output of 100 mV versus time for all the Celesco prototype transducers. Shown on the right-hand side of these figures are scales based on a full-scale output for the rated gage pressure. The cantilevered beam transducers were considerably more unstable than the diaphragm transducers. The 2,000-psi diaphragm transducer showed a change of 0.2% of full-scale output at 100 mV after 1,100 days in test; the 2,000-psi cantilevered beam transducer had changed more than 2.0%. One of the 25-psi diaphragm transducers showed a change of less than 0.1% after 1,100 days and another 25-psi diaphragm transducer had changed 0.4%. The two worst 25-psi transducers (one a diaphragm gage and the other a cantilevered beam gage) had changed approximately 1.1%. The stability of these 25-psi transducers may also be referenced to their full-scale output at 25 psi (right-hand scales in the figures). When this is done, the changes are increased substantially to 12% and 33% from 1.1%. The large electrical offset of the cantilevered beam designs was considered unacceptable and the drift of these designs further confirmed their design limitation.

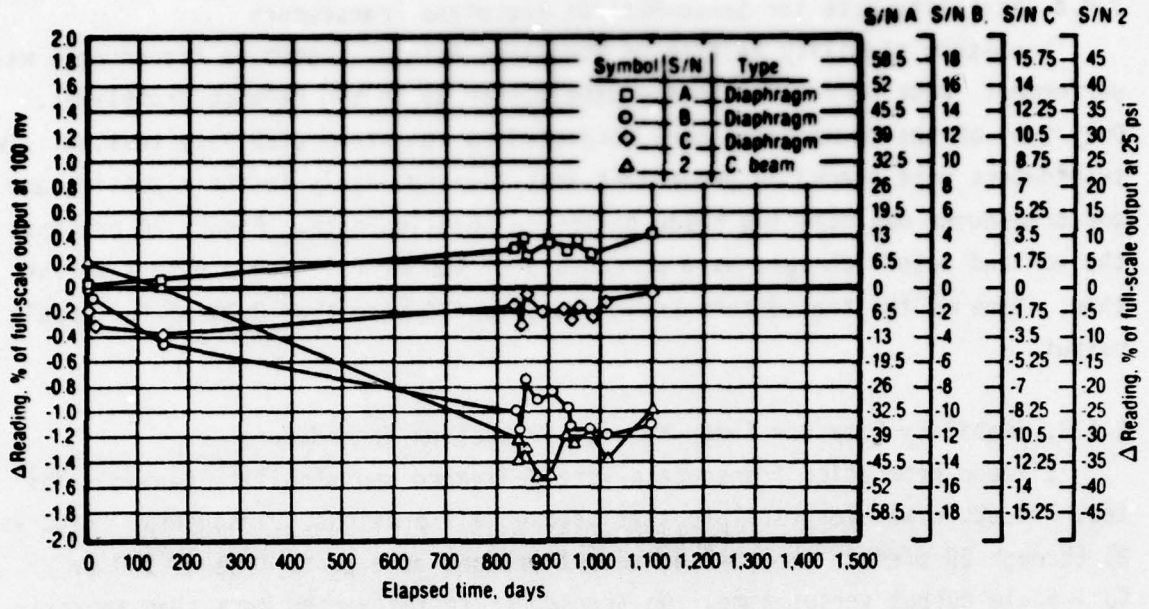


Figure 22. Celesco Prototype Transducer Zero Offset History (25-psi Gages)

16515

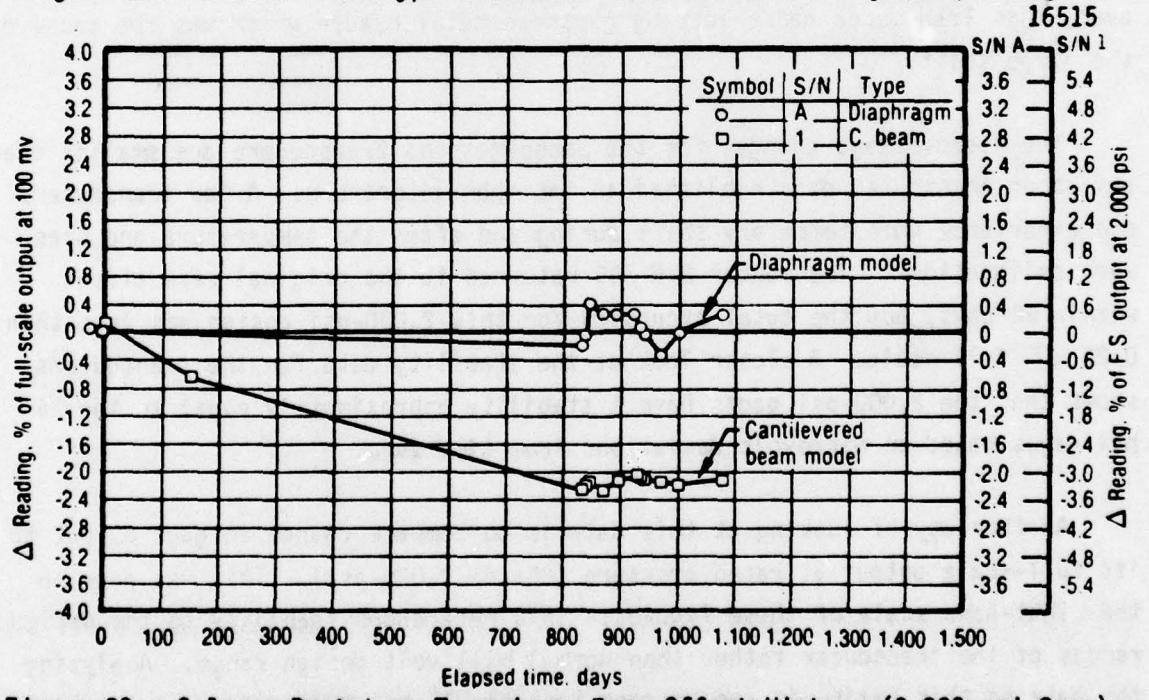


Figure 23. Celesco Prototype Transducer Zero Offset History (2,000-psi Gage)

16514

2.4.4 Stability Data for Senso-Metrics Prototype Transducers

Long-term stability testing on the Senso-Metrics prototype transducers was performed. Data were taken in the same manner as on the Celesco prototypes. Only four of the transducers were subjected to long-term stability testing. Two transducers were placed in propellant test fixtures early in their testing and one transducer was rejected based on the calibration data. Figure 24 presents the no-load output changes as a percentage of 100 mV full-scale output versus time. None of the transducers tested have varied more than 0.3% of full-scale output.

2.4.5. Stability Data for Senso-Metrics Production Transducers

Sixteen production transducers were delivered and stability tested. The test procedure was identical to that used on all previous transducers. Figures 25 through 29 present the no-load output changes as a percentage of 100 mV full-scale output versus time. No transducer tested varied more than approximately 0.3% of full scale except for transducer B385 which changed 0.6%. However, this transducer had a leaking glass-to-metal header which was the cause of the large shift.

The microvoltage changes for the Senso-Metrics transducers are smaller than any other transducer data published in the open literature. A few transducers did experience some temporary shift during and after the temperature and pressure calibrations. Transducer S/N 389 returned to the original zero offset within 60 days, but the total excursion for this 2,000-psi design was less than 0.2% of full scale. A closer look at the stability data for the transducers shows that the 2,000-psi gages have a stability approximately equal to the 25-psi gages based on microvolt deviations from time zero.

Another way of looking at this data is to compare change in gage output to its full-scale output at rated pressure (25- or 2,000-psi). This was done on the right-hand scale of these figures. This references stability to the design ranges of the transducer rather than normal millivolt design range. Analyzing the data on this basis, it can be seen that the 25-psi transducers have a zero offset stability of about ±2% and the 2,000 psi transducers are stable to within

±0.15%. The major perturbations in the zero offset measurements were those obtained after full-range pressure calibrations. This implied some recovery time after each pressurization response. These transducers generally returned near the original zero offset with sufficient recovery time.

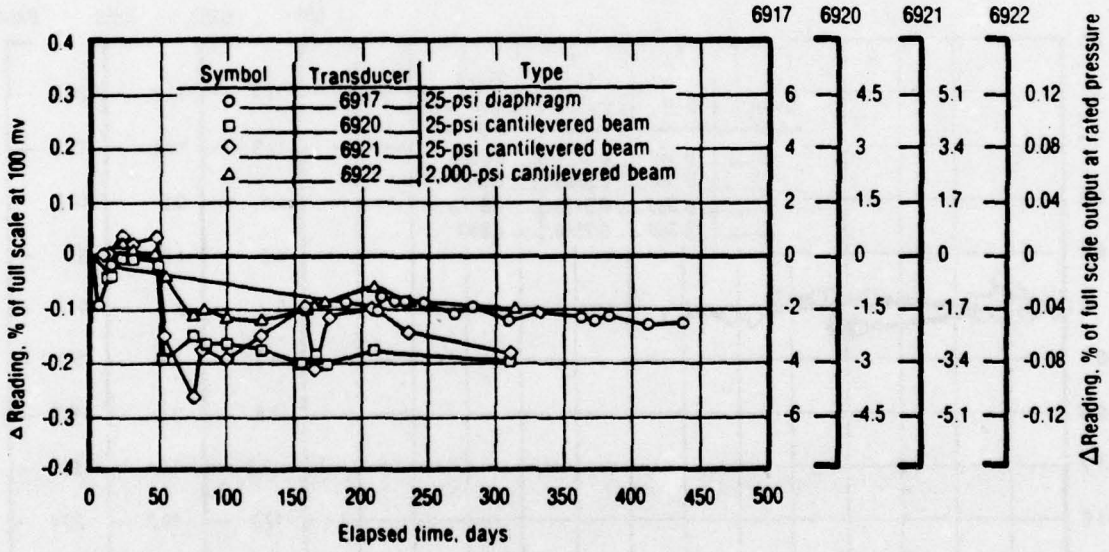


Figure 24. Zero Offset Histories for Senso-Metrics Prototype Transducers
16516

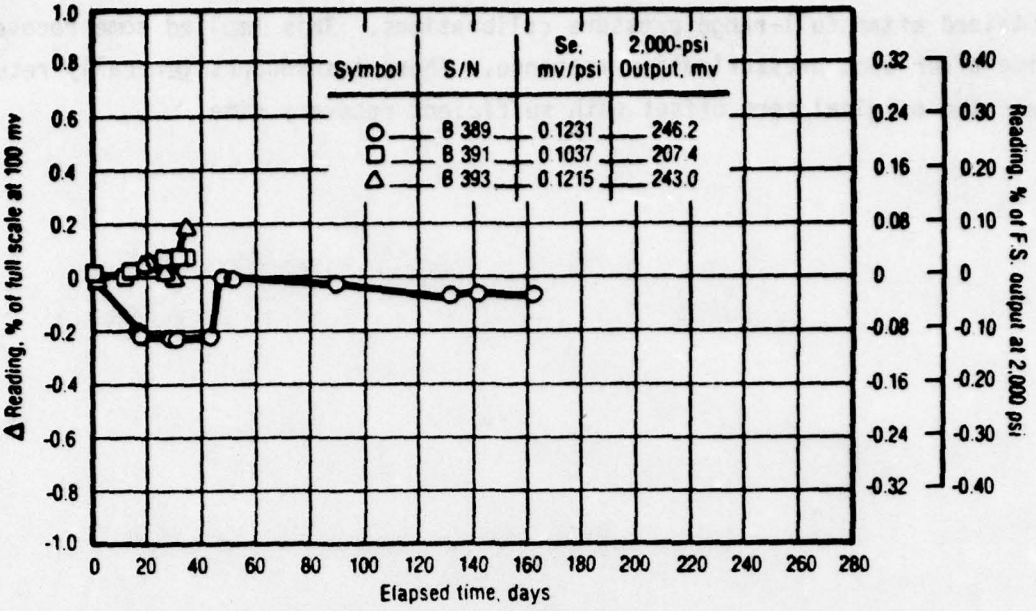


Figure 25. Zero Offset Histories for Senso-Metrics Stress Transducer (Model No. 601156; 2,000-psi, Low Profile Models)

16517

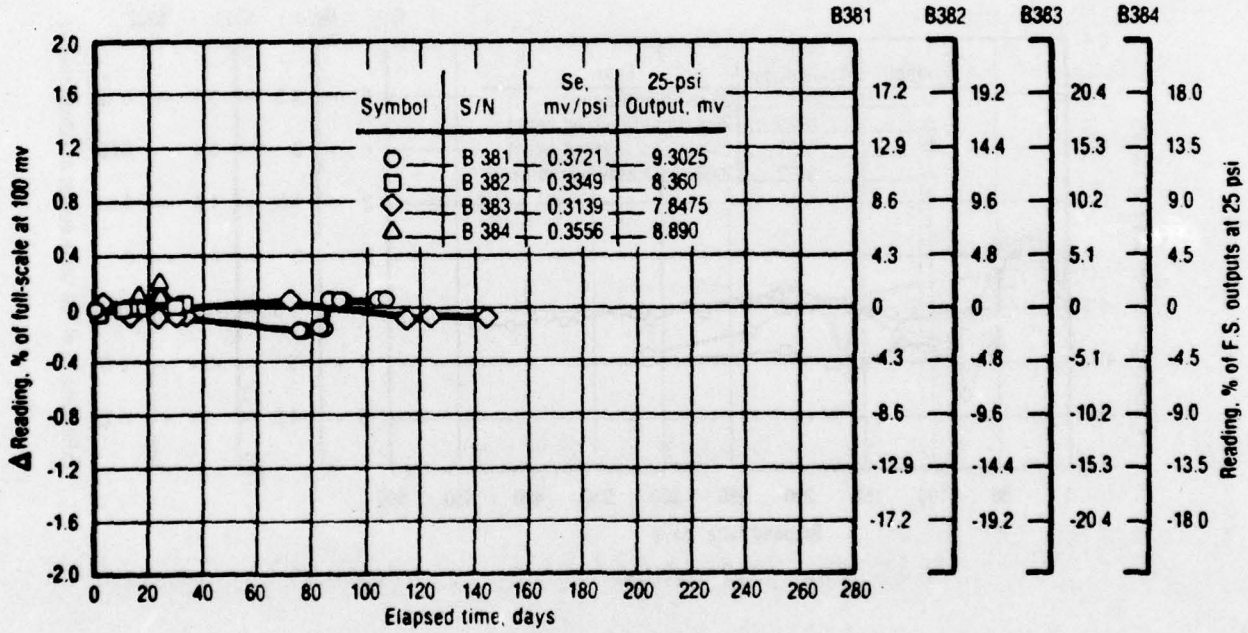


Figure 26. Zero Offset History for Senso-Metrics Stress Transducer (Model No. 601156; 25-psi, Low Profile Models)

17143

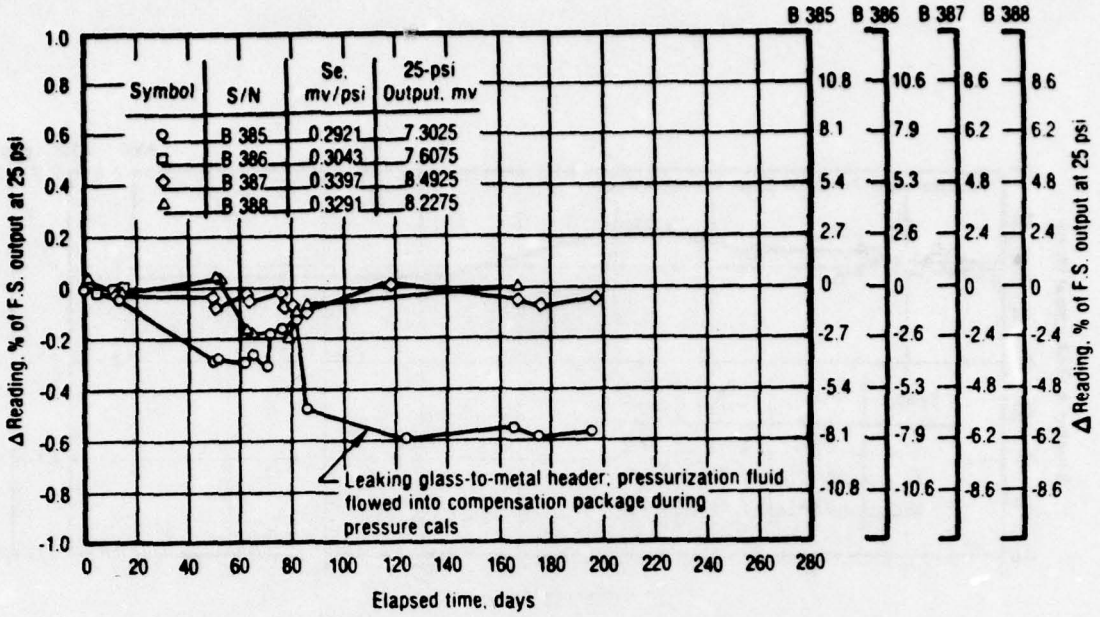


Figure 27. Zero Offset History for Senso-Metrics Stress Transducer (Model No. 601156; 25-psi, Low Profile Model)

17144

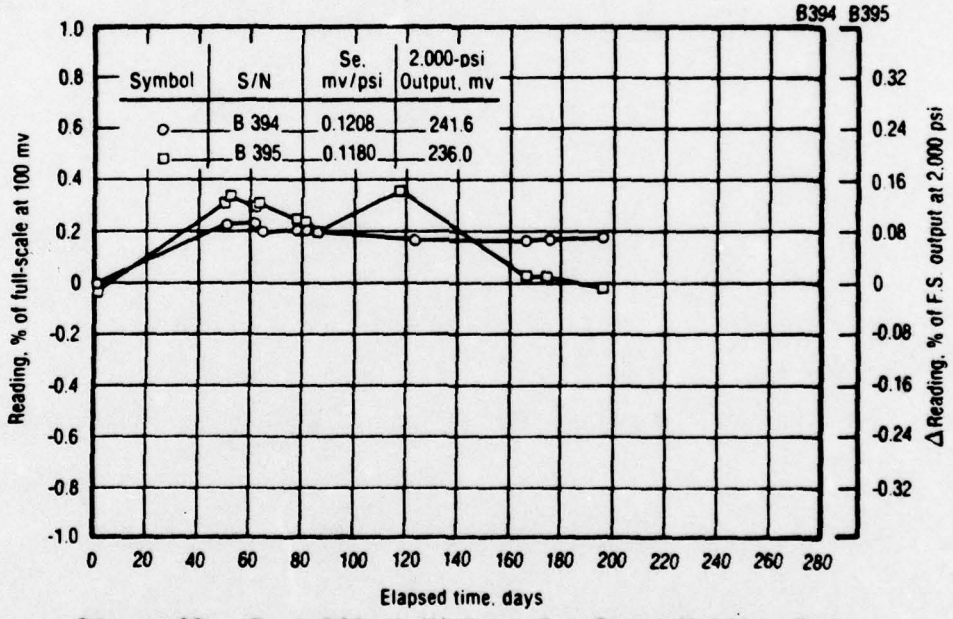


Figure 28. Zero Offset History for Senso-Metrics Stress Transducer Model No. 601156 (2,000-psi, Low Profile Models)

17145

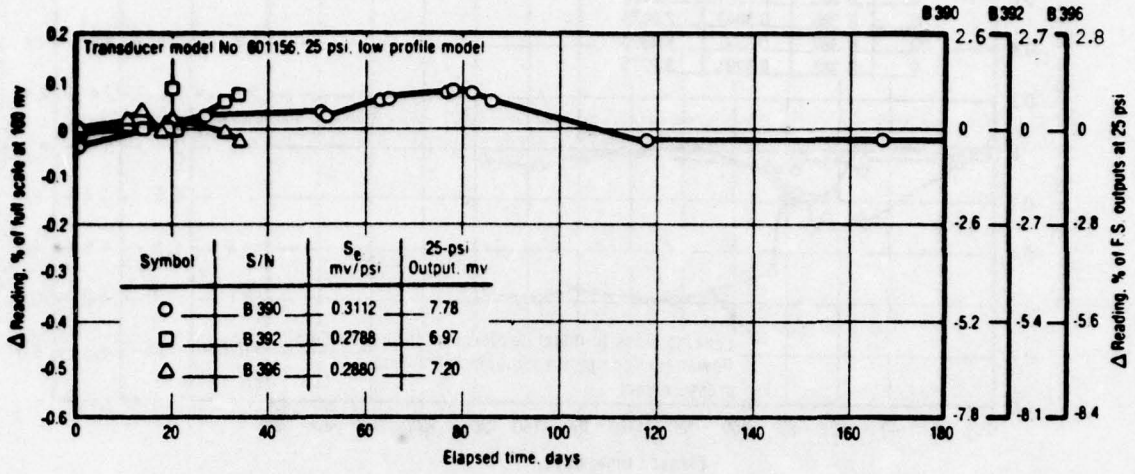


Figure 29. Zero Offset History for Senso-Metrics Stress Transducers

16453

3.0 FINITE ELEMENT GAGE DESIGN ANALYSIS

Effective design of a normal stress transducer requires not only the design, experimental, and literature survey tasks described in the previous sections, but some mathematical analyses of the design parameters. On this program, TEXGAP finite element techniques were used to evaluate the design parameters considered important for transducer optimization.

3.1 EPOXY REINFORCEMENT STUDY

Epoxy bonded semiconductor strain gages are the basic system for measuring diaphragm or beam strain with present gage designs. Structural analyses were performed to gain insight into the important parameters for this system (Figure 30). The significant variables considered included epoxy thickness, epoxy modulus, and contact surface roughness.

3.1.1 Epoxy Thickness

An epoxy layer was modelled over the entire diaphragm as shown in Figure 31.

Reduction in metal diaphragm strain for various epoxy thicknesses was determined assuming good bond contact across the entire surface. The results for an epoxy modulus of 500,000 and 100 psi pressure are listed below.

Epoxy Thickness, in.	Mid-Diaphragm Strain, μ in./in.	Strain Reduction, %
0.0	188.20	--
0.0005	187.85	0.19
0.0010	187.37	0.43
0.0020	186.18	1.07

The above shows that an epoxy thickness of 1 mil or less is desirous if the epoxy reinforcement effects are to be less than 0.5%. This analysis is for a 25-psi transducer with a diaphragm thickness of 0.0100 in. Of course, the effect would be less for a thicker diaphragm transducer such as the final 25-psi design (0.012 in.) or the 2,000-psi transducer (0.020 in.). Sample gages with semiconductor strain gages bonded to their surface were provided

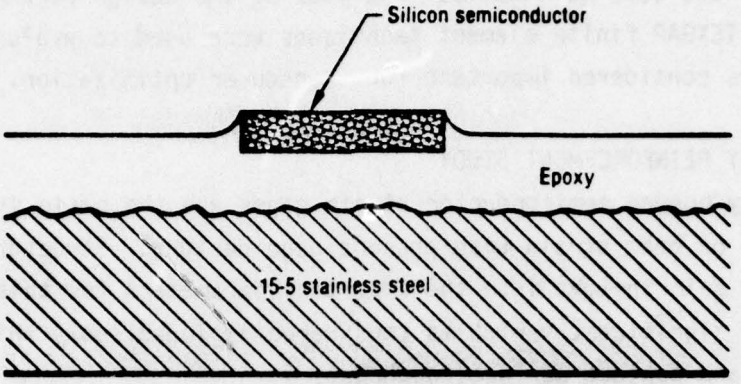


Figure 30. Gage Bond System

18499

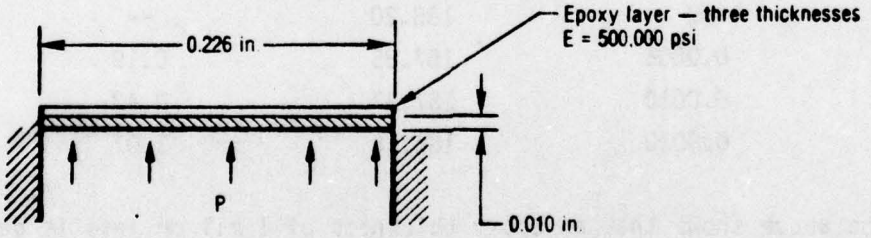


Figure 31. Epoxy Coated Diaphragm Model

18498

to AFRPL for electron microscope inspection, sectioning, and bondline thickness determination. Results of the Air Force evaluation are presented in AFRPL-TR-77-39*; the pertinent measured parameters are the following:

A. Epoxy layer thickness = 0.000498 ± 0.000067 in.

B. Gage thickness = 0.000449 ± 0.000053 in.

C. Gage width - 0.00471 ± 0.00012 in.

The final transducer manufactured by Senso-Metrics has the desired epoxy thickness which is obtained by epoxy filtering and special processing techniques.

3.1.2 Epoxy Modulus

Strain transfer from the metal diaphragm to the silicon semiconductor strain gage through the epoxy was analyzed next. Finite element analyses were made with a fixed epoxy thickness of 0.0006 in. and varying epoxy modulus from 100,000 to 1,000,000 psi. With the addition of the strain gage, the geometry loses its axisymmetry so plane stress calculations were used as being more closely analogous to the real model. The model of the loading condition is shown in Figure 32.

Various epoxy moduli, at an epoxy thickness of 0.0006 in., were used for this study. Figure 33 shows the strain gradient through the epoxy thickness. The beneficial effects of using an epoxy of high modulus, at least 500,000 psi, are shown. The high modulus epoxy transfers 98.4% of the metal strain to the semiconductor, compared to a 100,000-psi modulus epoxy which transfers only 92.6% of the strain.

Epoxylite 6203 which is used by Senso-Metrics is a filled epoxy and has a flexural modulus of 400,000 psi according to the manufacturer (Epoxylite).

---

*Chew, T. J. C., and D. H., Banasiak, "A Microphotographic Study of an Epoxy Bond System for Semiconductor Stress Transducers," AFRPL-TR-77-39, Air Force Rocket Propulsion Laboratory, Edwards AFB, CA, August 1977.

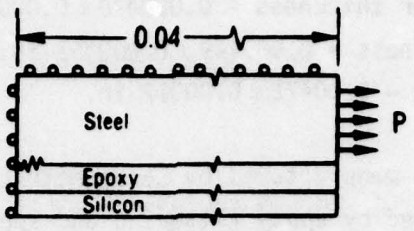


Figure 32. Epoxy Transfer Function Model

18520

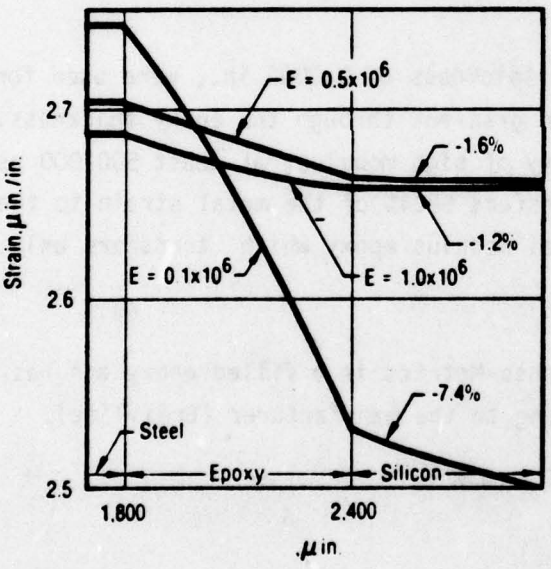


Figure 33. Strain Gradient Through Steel/Epoxy/Silicon for Three Epoxy Moduli

18496

3.1.3 Surface Roughness

Surface roughness was included in the model to encompass the most complete representation of the strain gage/diaphragm system. Actual surface roughness was used based on digital profilometer measurements made on the strain gage beams which measured 22μ in. The model and calculated stresses are provided in Figure 34. Stresses were computed at the center and end of the silicon element for three different values of epoxy modulus.

The stresses increased with epoxy modulus and peaked out at 840 psi for a 500,000-psi modulus and the rough bond area near the load application end of the model. Under no conditions do the stress concentrations appear to be great enough to cause a structural problem.

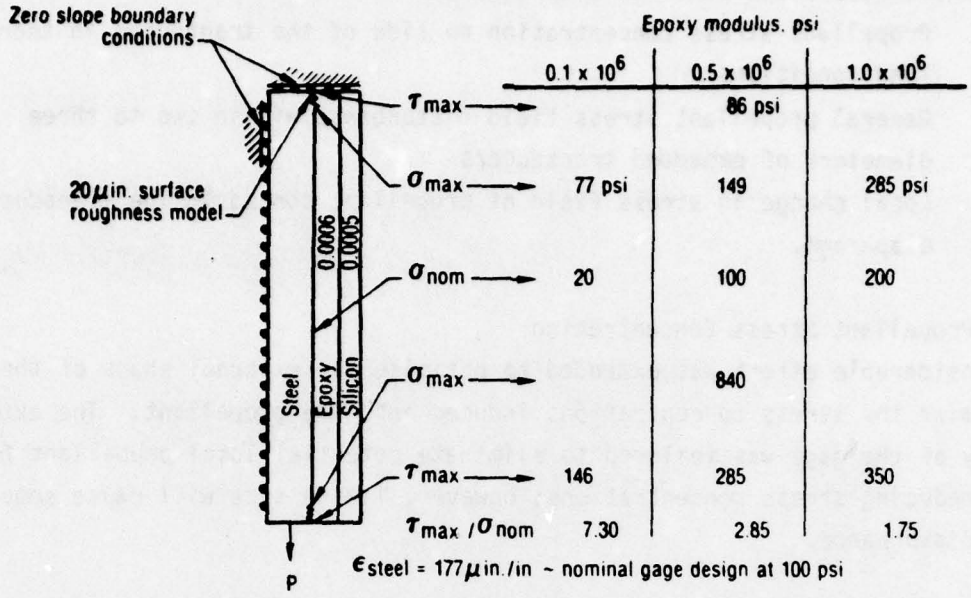


Figure 34. Surface Roughness Model and Calculated Stresses

18521

Using the plane stress model in Figure 32, which includes the steel/epoxy and semiconductor strain gage, a series of epoxy thickness and modulus study computer runs were conducted. The reduction in strain transferred from steel to the silicon for various epoxy moduli and bondline thickness combinations are shown below.

Percentage Strain Reduction

Epoxy Thickness,	Epoxy Modulus, psi 100,000	500,000	1,000,000
0.0005 in.		-1.3%	
0.0006 in.	-7.4%	-1.6%	-1.2%
0.0010 in.		-2.9%	
0.0020 in.		-5.6%	

3.2 OPTIMAL EXTERNAL GEOMETRY

A detailed finite element analysis of the propellant/transducer interaction was conducted to determine the optimum external geometry which will cause

minimum propellant stress disturbance. The following three major zones of propellant stress disturbance were considered:

A. Propellant stress concentration on side of the tranaducer in thermal load conditions
B. General propellant stress field disturbance within two to three diameters of embedded transducers
C. Local change in stress field of propellant bonded to the transducer diaphragm.

3.2.1 Propellant Stress Concentration

Considerable effort was extended to optimize the external shape of the gage to minimize the stress concentrations induced into the propellant. The external geometry of the gage was tailored to eliminate potential local propellant failure by reducing stress concentrations; however, finite size will cause some stress disturbance.

The shape studies on gage geometries were analyzed in the end-burner test vehicle. It is a propellant-filled stiff steel case of axisymmetric geometry with the gage located at the centerline. Typical thermal stresses are given in Figure 35. Analysis of this vehicle included case wall (1.0-in. thick), liner, insulation and propellant properties. The finite element structural analyses were conducted with the TEXGAP 2D program because of its highly accurate determination of stress and deformation fields in solid propellant rocket motors, especially in the critical areas near the interfaces of the case, insulation, liner, and propellant.*

The transducer geometries analyzed are shown in Figure 36. The gage external shape evolved through preliminary designs of 60^{o} and 90^{o} side angles to the 45^{o} side angle. The radius between the diaphragm and side was increased at a side angle of 75^{o}. The height was reduced at a 60^{o} side angle and further modified with a bottom 45^{o} flare. A bridge completion resistor (to scale) is shown in Figure 36. Four may be included in a gage package.

---

*E. E. Francis et al., "Case Liner Bond Analysis," AFRPL-TR-74-23, Air Force Rocket Propulsion Laboratory, Edwards, CA, June 1974.

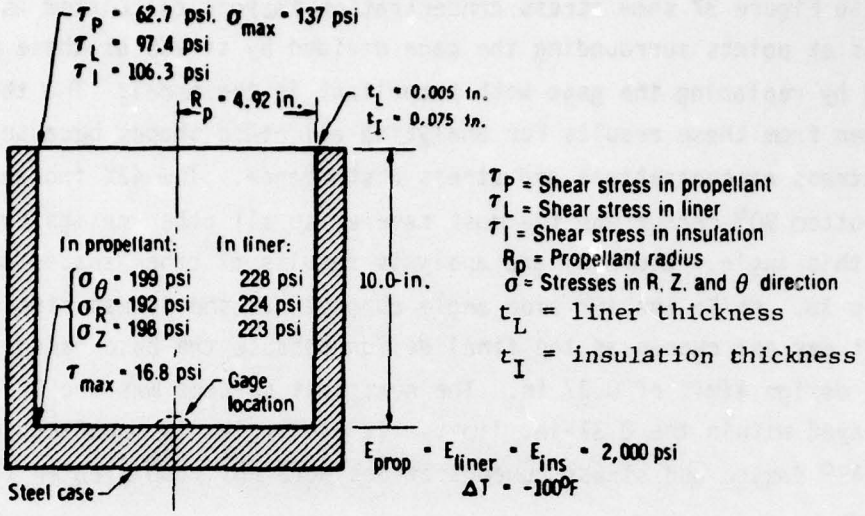
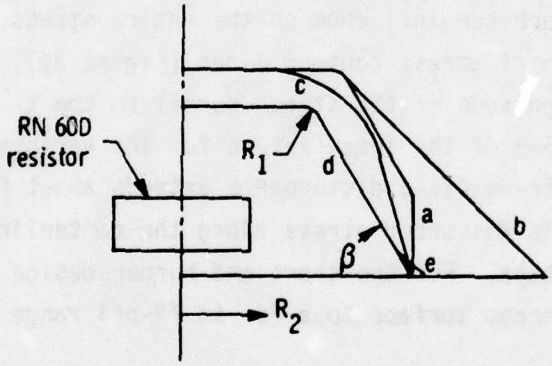


Figure 35. End-Burner Test Vehicle Used for Gage External Geometry Analyses

17259



	Height, in.	Angle, β, °	R_1, in.	R_2, in.
a. Preliminary April 1976 Senso concept	0.34	60/90	0.025	0.37
b. 45° modification	0.34	45	0.025	0.59
c. Large radius design	0.34	75	0.200	0.37
d. Reduced height design	0.28	60	0.050	0.37
e. Bottom flare	0.28	60/45	0.050	0.39

Figure 36. External Geometry Analysis Models

17264

The preliminary 60°/90° design was first analyzed for a uniform hydrostatic pressure load on the propellant surface and then for a 100°F thermal load. Results in Figure 37 show stress concentration factors calculated as the ratio of stress at points surrounding the gage divided by stress at these points analyzed by replacing the gage with propellant in the model. The thermal load was chosen from these results for analyzing all other shapes because it gave higher stress concentrations and stress disturbance. The 42% increase in stress at the bottom 90° corner was the most severe, so all other design concepts reduced this angle. Geometry and analysis results of other shapes are shown in Figure 38. While the 45° side angle concept had the lowest stress concentrations, it was not chosen as the final design because the base radius was larger than the design limit of 0.37 in. The next best concept was the 60° gage, which stayed within the 0.37-in. limit. It was easier to manufacture than the 60°/45° design and stress concentrations were not much greater than the 45° design.

3.2.2 Thermal Stress Field Disturbance and Local Stress Change

Since these finite element analyses include the entire transducer propellant system, gage disturbance influence on the entire stress field can be reviewed. A comparison of stress contour lines (Figure 39), with and without the gage, shows the magnitude of the stress normal to the transducer surface (σ_z) along the centerline of the test fixture for the various transducer shapes. The general stress field disturbance extends about five times the transducer height. This disturbed stress along the centerline is irrespective of the gage external shape. For the short end-burner design the gages reduce the stress at the diaphragm surface to a 76- to 79-psi range compared to 109 psi without the gage.

The normal stress distribution parallel to the fixture base at the transducer diaphragm surface height is shown in figure 40. These analyses were run with the thermal load at 100°F for a propellant modulus of 2,000 psi. The normal stress disturbance is limited to about 0.5 in. above the diaphragm surface.

Cross plots of stress disturbance at other angles for propellant depth from the gage are shown in Figure 41. The 60° gage with a reduced height shows

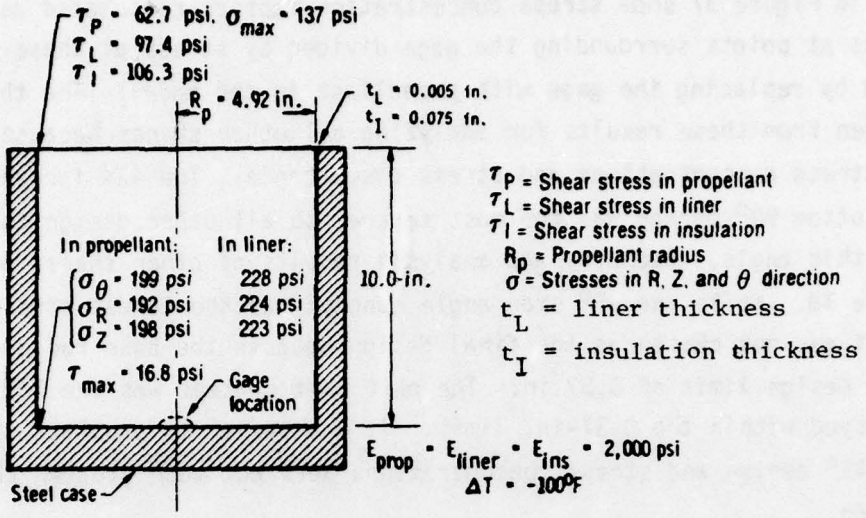
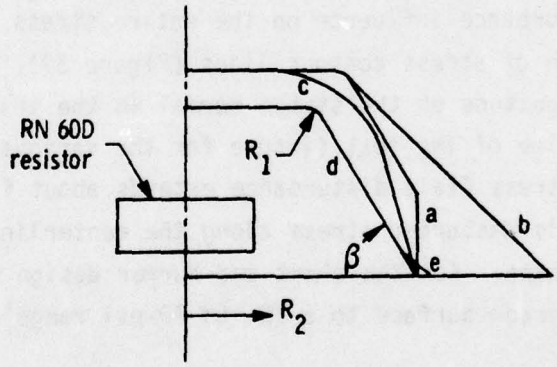


Figure 35. End-Burner Test Vehicle Used for Gage External Geometry Analyses

17259



	Height, in.	Angle, β, °	R_1, in.	R_2, in.
a. Preliminary April 1976 Senso concept	0.34	60/90	0.025	0.37
b. 45° modification	0.34	45	0.025	0.59
c. Large radius design	0.34	75	0.200	0.37
d. Reduced height design	0.28	60	0.050	0.37
e. Bottom flare	0.28	60/45	0.050	0.39

Figure 36. External Geometry Analysis Models

17264

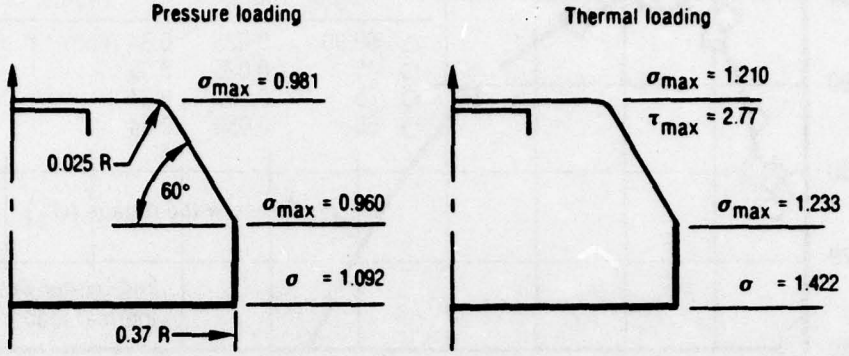


Figure 37. Stress Concentration Factors - $60^{0}/90^{0}$ Design

18497

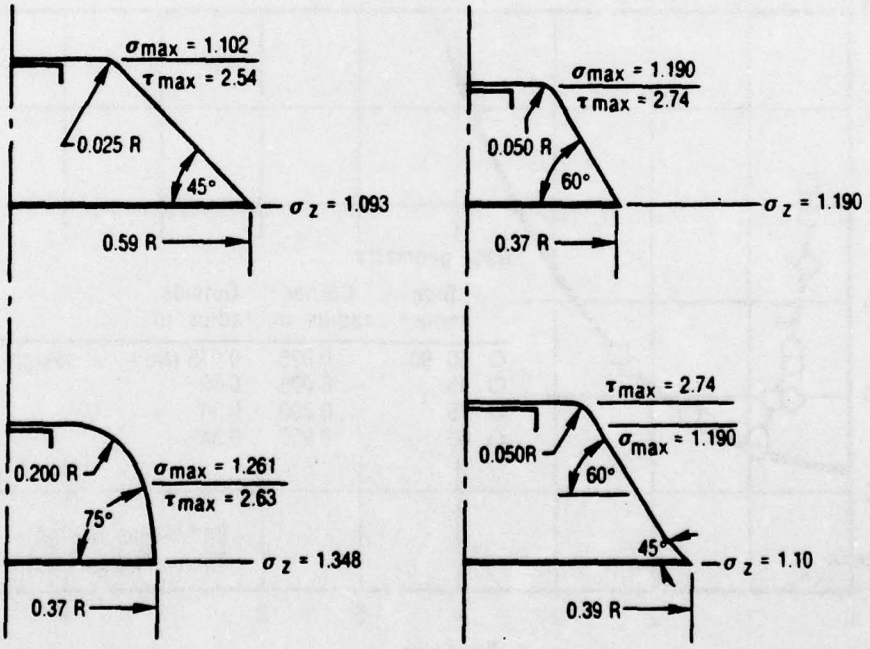


Figure 38. Stress Concentrations in Propellant Surrounding Gage and Design Variations for Thermal Loading

18496

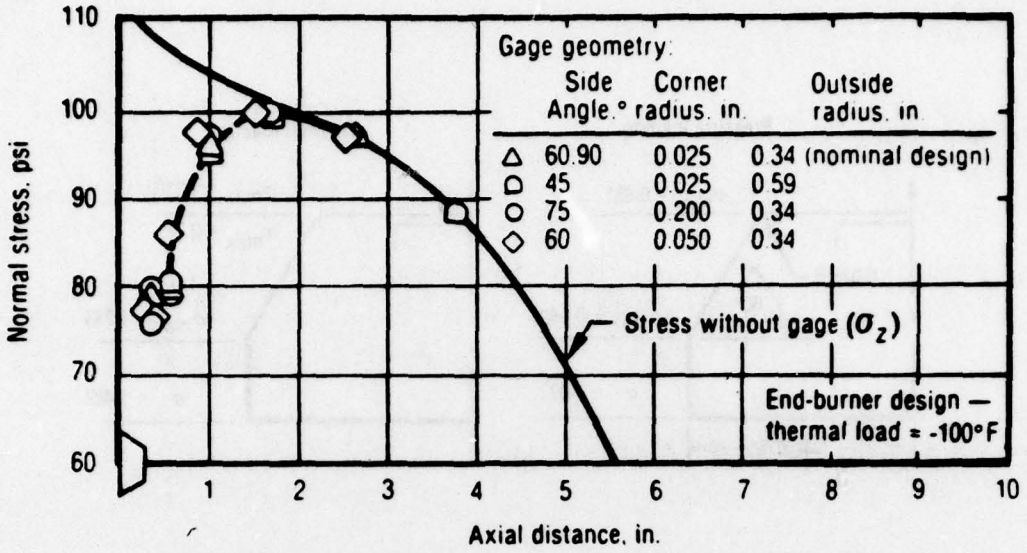


Figure 39. Axial Stress Distribution With and Without Gage

17263

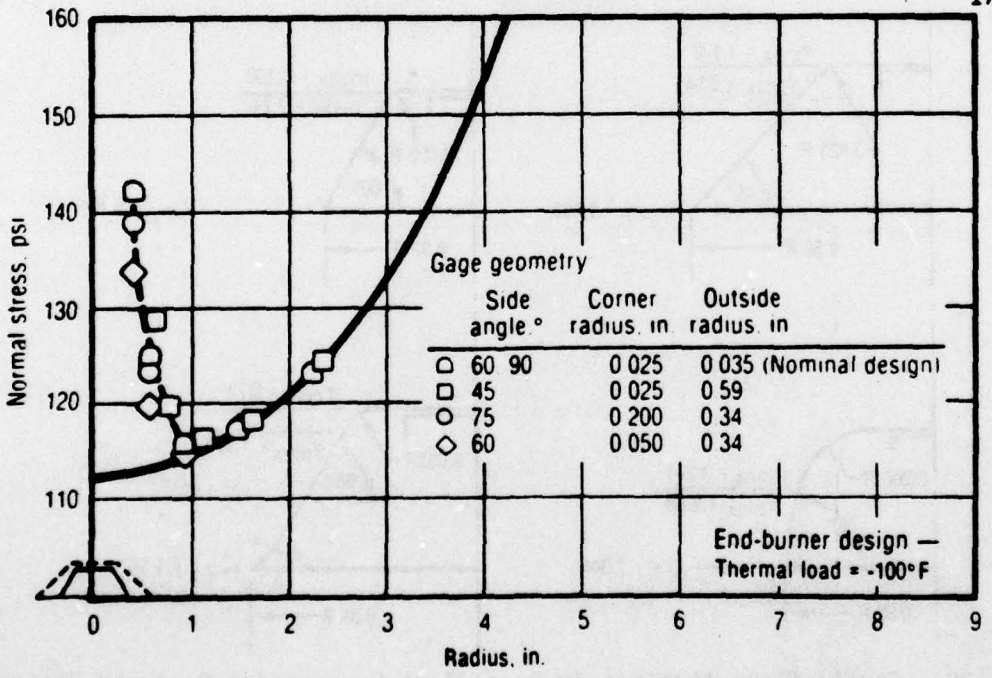


Figure 40. Normal Stress Distribution With and Without Gage 17267

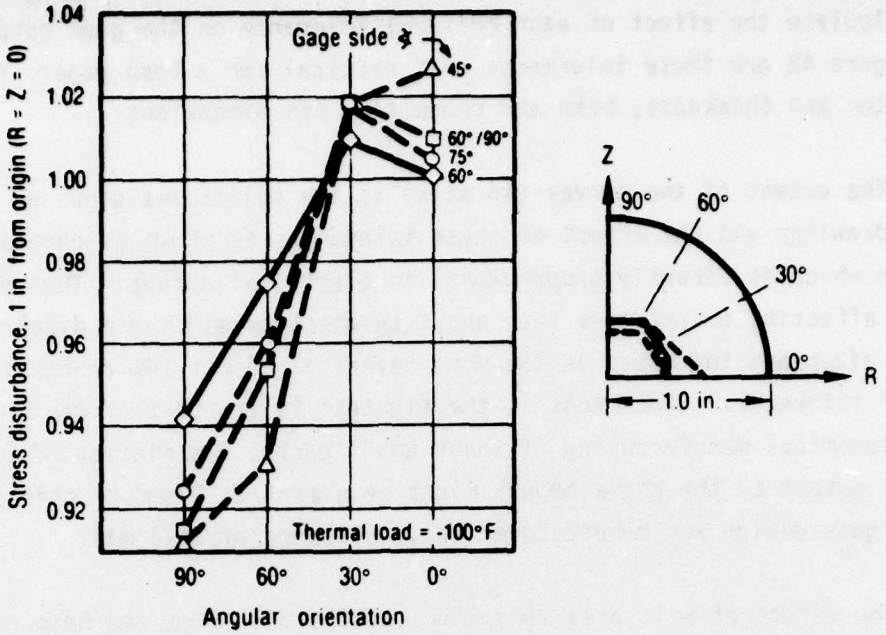


Figure 41. Effect of Gage Geometry on Propellant Stress Disturbance at 1 in.

17268

the least stress disturbance in the direction normal to its diaphragm and the 45° gage, with an increased outer radius, indicates the largest stress disturbance parallel to its base (0° on Figure 41).

These studies resulted in the Senso-Metrics prototype external shape of a 60° side angle and 0.31-in. height. This was a compromise between the best analytical concept and gage manufacture practicality.

3.3 MANUFACTURING TOLERANCE STUDY, PRELIMINARY GAGE DESIGN

Gage manufacturing tolerances were analyzed to determine their effect on performance. All of the metal parts of a transducer have tolerances associated with their dimensions. Some are more critical to gage performance than others. The tolerances that are most important from a gage performance standpoint are those most physically close to and including the diaphragm and/or beam.

Dimensional tolerance extremes from the final detail drawings were used to calculate the effect of each critical tolerance on the gage output. Shown in Figure 42 are those tolerances most critical for a beam gage: the diaphragm diameter and thickness, beam and connecting pin dimensions.

The extent of the curves (in mils) is the tolerances given on the gage part drawings and the effect of these tolerances is shown as change in beam strain which is directly proportional to electrical output. The only tolerances affecting output more than about 1% are beam width and diaphragm thickness; diaphragm thickness is the more severe at almost 14% change for ±1/2 mil of thickness. Since this is the tightest tolerance that can be expected for economical manufacturing of these small parts, a variation of gage electrical output by the above amount might be expected. Based on this study, the final gage design was manufactured to a tolerance of ±1/4 mil.

The effect of weld area variations at the diaphragm and beam ring joint was also analyzed. These weld areas can vary because of manufacturing tolerances in the chamfer and inside radius of their mating surfaces as well as the amount of weld penetration.

Figure 43 shows how the chamfer tolerance or weld penetration would effect gage output. The row labeled "diaphragm gage" shows a worst case of 0.2%. Consequently, only dimensions associated most closely with the diaphragm are important.

Lastly, the question is how these tolerances affect interaction. This may be most easily discussed by referring to Figure 44. The worst case is clearly for a 25-psi transducer which has the least diaphragm thickness (0.0135 ±0.0005 in. for the prototype) as shown below.

Diaphragm Thickness, in.	Output Ratio for Various Propellant Modulii		
	1,000 psi	2,000 psi	5,000 psi
0.0130	0.990	0.980	0.951
0.0135 (nominal)	0.991	0.982	0.956
0.0140	0.992	0.984	0.961

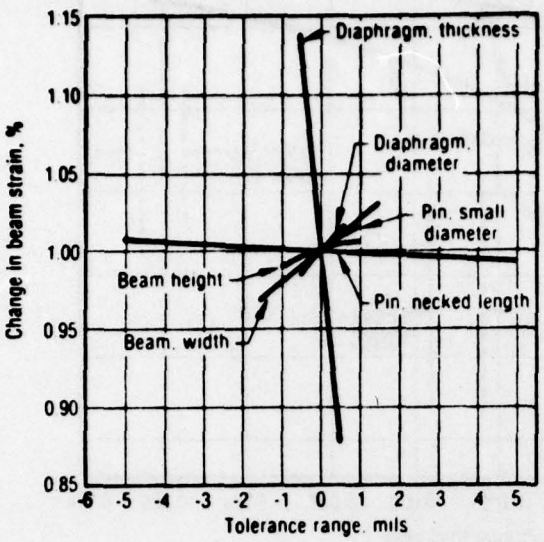
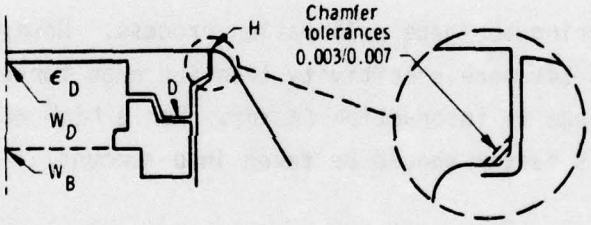


Figure 42. Effect of Critical Component Tolerances on Beam Gage Output 17266

The above shows that the change in interaction is greatest for the high propellant modulus (5,000 psi) and represents a variation of ±0.5% in interaction over the diaphragm thickness tolerance range. This is only applicable to the preliminary gage design since other designs on this program used different thicknesses and tolerances.

In summary, the importance of these tolerances on gage use should be considered. The 14% change in electrical output with diaphragm thickness is of little consequence since it is taken



Weld depth \ Run	0	1	2	3	4
Diameter, in.	0.025	0.028	0.022	0.025	0.025
Height, in.	0.025	0.025	0.025	0.028	0.022
Diaphragm gage					
ϵ_D, μin./in.	167.72	168.05	167.34	167.85	167.71
Ratio	-	1.002	0.998	1.001	1.000
Beam gage					
$(W_D - W_B)$, in.	-190.8	-188.9	-193.0	-189.7	-191.9
Ratio	-	0.990	1.011	0.994	1.006

Figure 43. Effect of Weld Joint Tolerances

17265

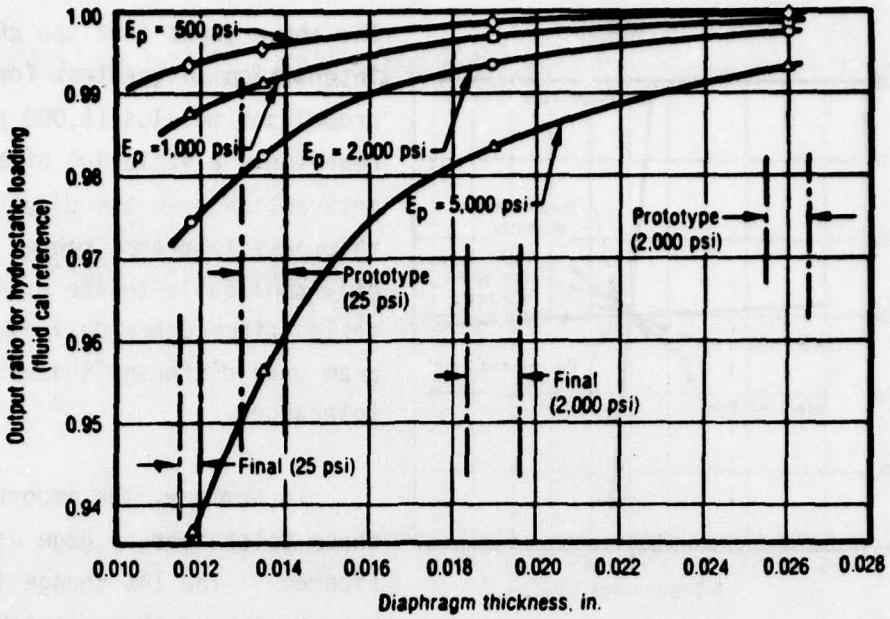


Figure 44. Propellant Modulus Interaction vs Diaphragm Thickness - Senso-Metrics Gages (Diaphragm Diameter = 0.125)

17242

into account during the gage calibration process. However a gage that calibrates with 14% more sensitivity than the mean for a batch of gages would have a 0.5% change in interaction factor. For a high accuracy stress gage application this factor should be taken into account.

3.4 DIAPHRAGM THICKNESS STUDY - DESIGN CONSIDERATIONS

Previous considerations of the basic transducer design include the housing shape and manufacturing tolerances. One factor not analyzed was actual diaphragm thickness. This choice was left open for a complete stress analysis of the gage design as a function of diaphragm thickness. This was necessitated by the following tradeoff factors which entered into this selection process.

The tradeoffs that must be considered to choose a diaphragm thickness are shown in Figure 45.

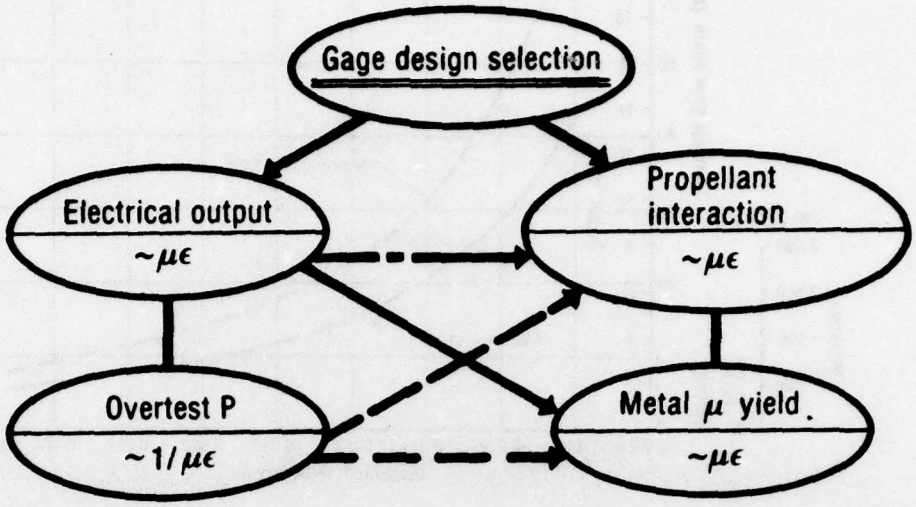


Figure 45. Gage Design Selection Tradeoffs

18495

It is desirable to maximize the electrical output and overtest pressure, and minimize the propellant interaction and metal stress condition. The basic dilemma comes from the fact that some quantities that are directly proportional to diaphragm strain conditions should be either minimized or maximized (e.g., electrical output versus propellant interaction). Likewise, parameters that must be maximized (electrical output and overtest pressure) are directly and inversely proportional to metal stress. Hence, the selection of a diaphragm thickness involves some compromises which can most easily be assessed from a series of design curves.

The electrical output was considered first. Using conventional relationships, diaphragm strain was converted into transducer output voltage. Diaphragm strains and output voltage versus load and thickness were determined in a series of finite element runs as shown in Figure 46. The use of a computer for this study may seem unneccessary since the closed form mathematical solutions for a pressurized circular plate are well known, but it was found that the transducer designs studied deviated greatly from these solutions. The explanation

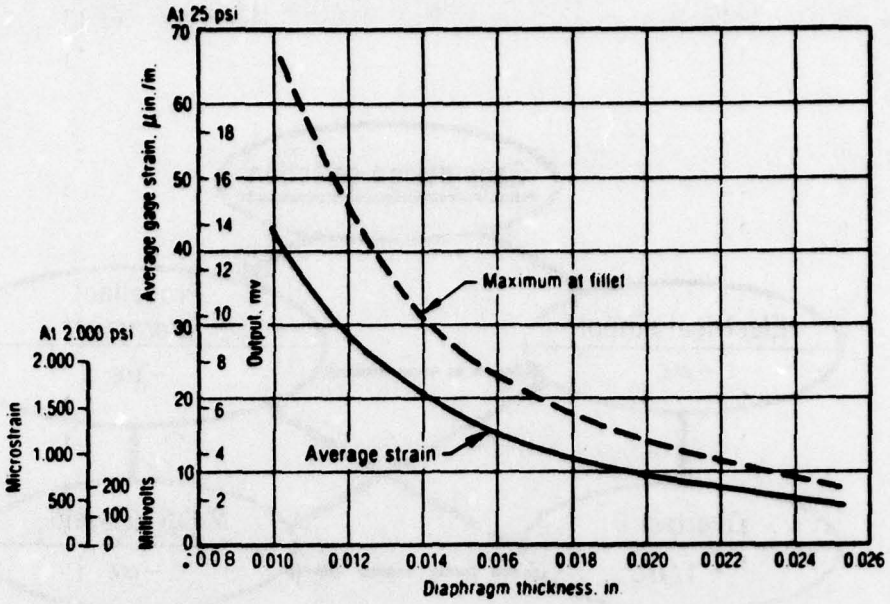


Figure 46. Diaphragm Gage Design Curve (0.005-in. Fillet Radius)

17265

lies in the fact that these transducer designs have nothing like a fixed edge for a boundary condition. The complexity of internal design, when taken into account by finite element analysis, allows considerable rotation and translation of the diaphragm edge. Consequently it was seen that some stress and strain values in the diaphragm deviated by from 12% to 25% from closed form solutions.

The solid line in Figure 46 is for average conditions seen by a strain gage of 0.090-in. length; the dashed line is for maximum strain at the diaphragm outer radius. All output is related to a gage acting at the two different design requirements of 25 or 2,000 psi.

Another curve is constructed for the beam gage design including the variables of beam dimensions which also affect output (Figure 47). Some gain in output is shown which is achieved by increasing beam thickness. However, a diaphragm deflection limit is reached as the beam becomes stiffer (e.g., enlarged section). These two curves are the design control for electrical output.

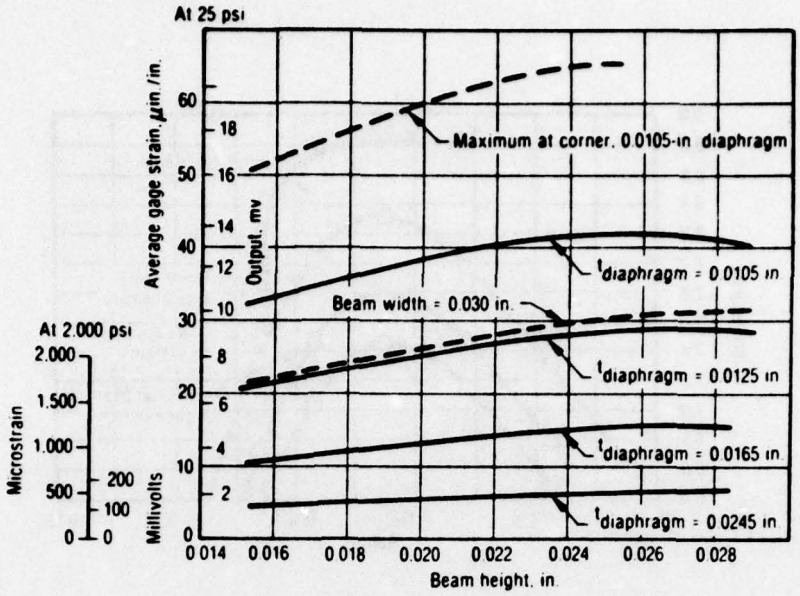


Figure 47. Beam Gage Design Curve (Beam Width = 0.042 in. Except Where Noted)

Overtest pressure and metal microyield are both related to the maximum stress in the diaphragm which occurs at the outer radius (see appendix H). This area was analyzed using the rezone capability of TEXGAP to give detailed solutions. Figure 48 shows the effect of diaphragm support condition on stress at this corner. As a measure of the refinement of this grid, note that the figure shows only the outer 0.012 in. of the diaphragm radius (10%). When the whole gage structure is considered (denoted on Figure 48 as "normal beam gage design"), maximum stress is significantly reduced as compared to the edge of the diaphragm fixed (a handbook solution). An alternate design also was considered for the diaphragm gage where the gage sidewall was considerably stiffened by eliminating the beam isolation groove while retaining the same internal shape. This curve fell between the other two, as would be expected for the stiffer sidewall.

Another area contributing to diaphragm stress was the fillet radius at the junction of the diaphragm with the transducer shell (although this radius would be hard to control and inspect). Figure 49 shows the diaphragm stress

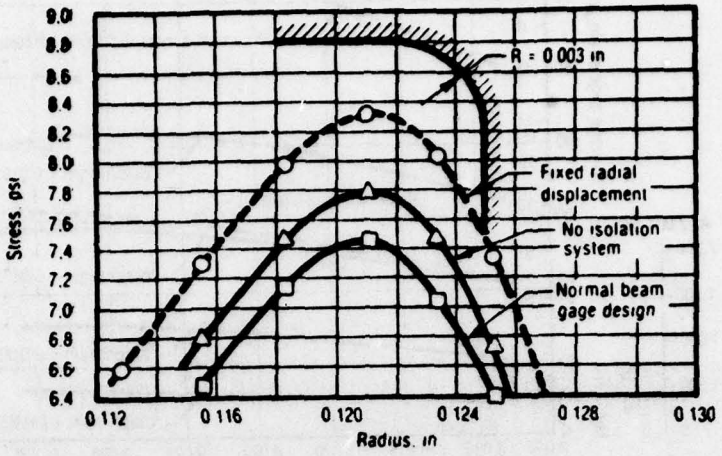


Figure 48. Effect of Support Condition on Maximum Diaphragm Stress (Hydrostatic Loading: P = 100 psi; Diaphragm t = 0.0105)

18534

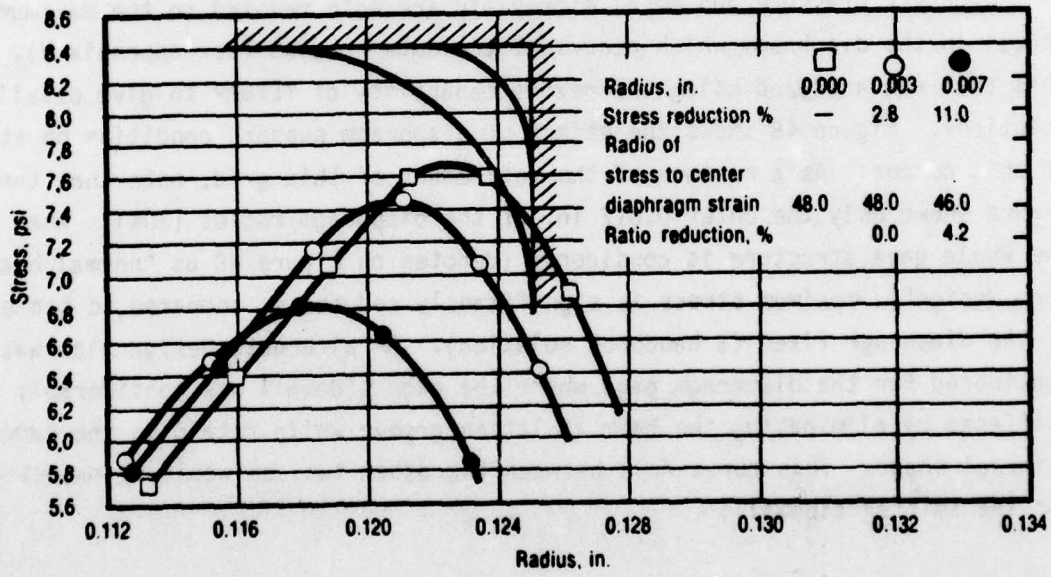


Figure 49. Effect of Corner Fillet Radius on Diaphragm Stress (Hydrostatic Loading: P = 100 psi; Diaphragm t = 0.0105)

18494

effect caused by varying this radius from zero to 0.007 in. An 11% reduction in stress was obtained with the 0.007-in. radius, but the radius has a stiffening effect which reduces diaphragm strain. The net stress reduction is only 4.2% at a 0.007-in. radius and there is no net reduction at the 0.003-in. radius. A nominal radius of 0.005 in. was selected from these analyses for computing the overpressure/yield stress design curve in Figure 50. This gives the overpressure versus thickness for the specified yield stresses of 10,000 and 20,000 psi. Details of microyield stress, as applied to this gage, are presented in section 2.0.

Another design curve computed was for propellant interaction as a function of diaphragm thickness (Figure 51). This shows the obvious trend of a reduction in interaction with increasing thickness. This interaction is defined as the reduction in gage output caused by a propellant modulus increase from zero to 2,000 psi (e.g., the normal range of expected gage operation). The 2,000-psi gage has about one half the interaction of a 25-psi gage. This curve indicates that pressure interaction can be ignored with an error of ±1% for the 25-psi gage and ±0.5% for the 2,000-psi model.

The data from the electrical output and overpressure/yield stress design curves were combined in Figure 52, which gives the best overall picture of the design selection process. Two gages were to be designed: a 25-psi and a 2,000-psi model. Based on considerations of sensitivity of currently available readout devices, 6-mV output was considered a desired minimum for the 25-psi gage with a 1% accuracy. This establishes a nominal diaphragm thickness of 0.0135 ± 0.0005 in. and an overpressure limit of 250 psi, conservatively. Electrical output is not a limiting factor for the 2,000-psi gage, so a diaphragm thickness of 0.0260 in. would be selected to provide an overpressure limit of just over 2,000 psi with considerably less propellant interaction.

The many parametric design curves giving gage geometry as a function of various design goals are of particular importance to the gage designer. These include propellant interaction, diaphragm microyield, overtest pressure, operating pressure, and electrical output. Curves are given for evaluating the

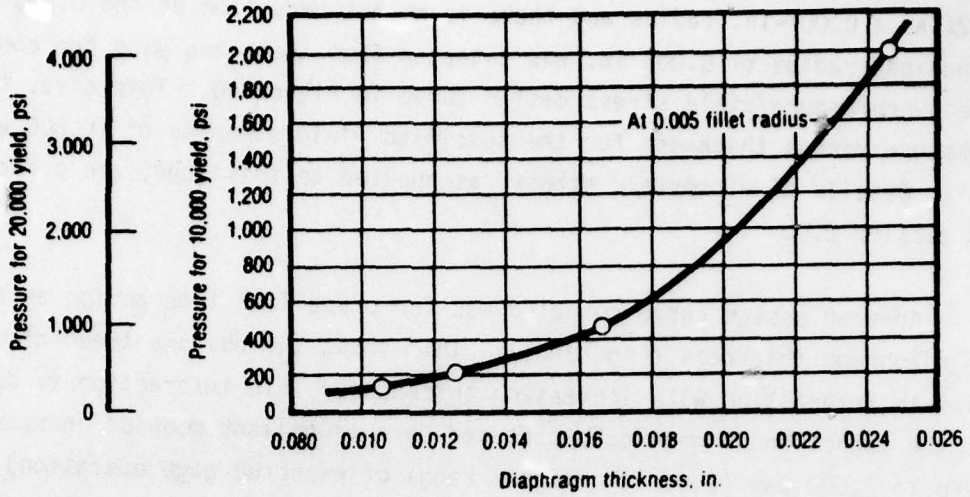


Figure 50. Overpressure and Yield Stress Design Curve

18493

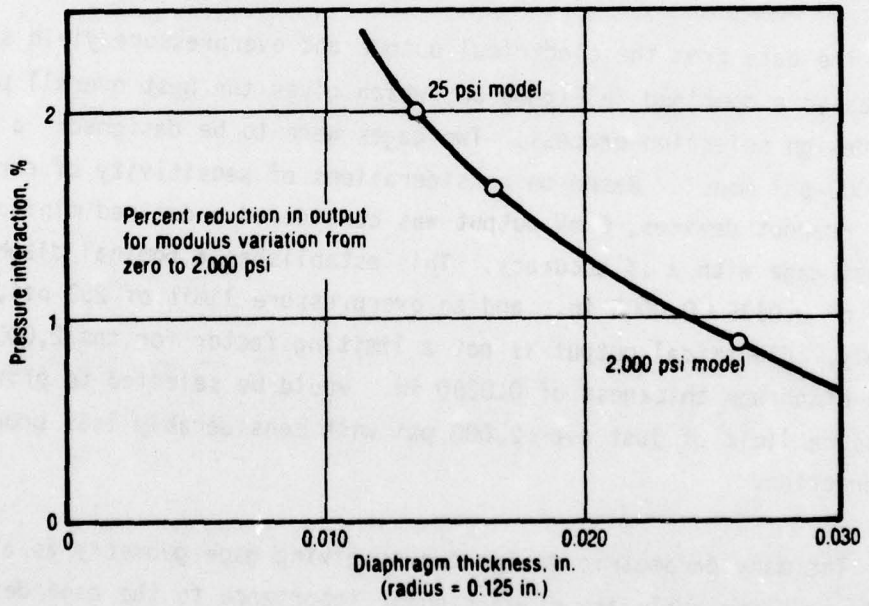


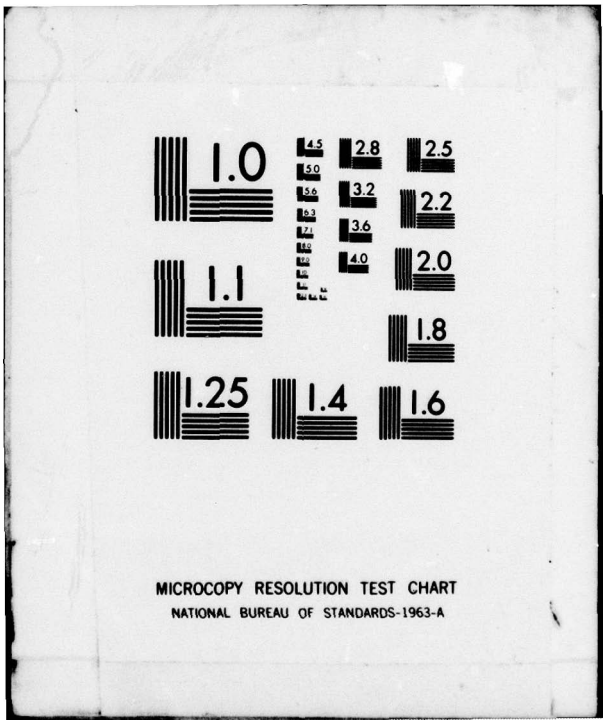
Figure 51. Propellant Interaction vs Diaphragm Thickness

18492

AD-A073 659 UNITED TECHNOLOGIES CORP SUNNYVALE CALIF CHEMICAL SY--ETC F/G 9/1
THE DEVELOPMENT OF IMPROVED NORMAL STRESS TRANSDUCERS FOR PROPE--ETC(U)
JUN 79 E C FRANCIS, R E THOMPSON, W E BRIGGS F04611-75-C-0042
UNCLASSIFIED CSD-2548-FR-VOL-1 AFRPL-TR-79-34-VOL-1 NL

2 OF 3
AD
A073659




1.0
1.1
1.25
1.4
1.6
1.8
2.0
2.2
2.5
2.8
3.2
3.6
4.0
4.5
5.0
5.6
6.3
7.1
MICROCOPY RESOLUTION TEST CHART
NATIONAL BUREAU OF STANDARDS-1963-A

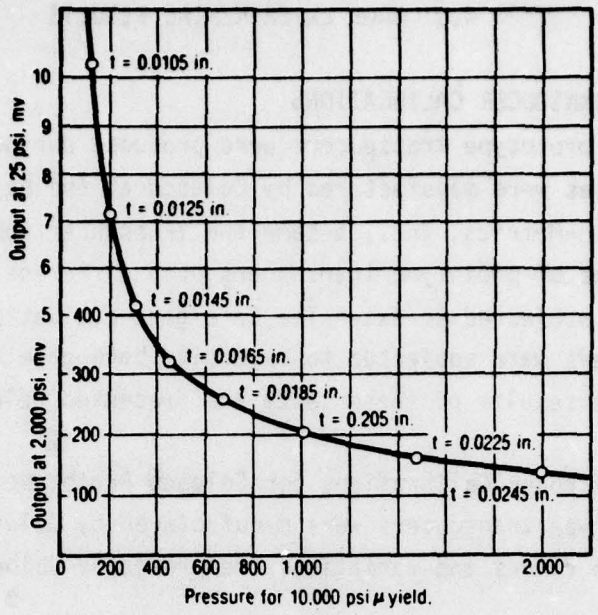


Figure 52. Diaphragm Thickness Design Curve for Output vs Pressure-to-Yield Limit

18535

transducer in propellant that relate stress concentration in the propellant to gage shape as well as diaphragm deflection effect on propellant.

From these data and other considerations, a diaphragm thickness of 0.0135 in. was chosen for the Senso-Metrics prototype designs. This gage would have an interaction for pressure loading of less than 2% for a propellant modulus between 0 and 2,000 psi. Diaphragm thickness was reduced for the final designs to increase the electrical outputs. These changes were within the other constraint limits and caused only minor adjustments in the transducer interaction factor.

4.0 GAGE EXPERIMENTAL RESULTS

4.1 PROTOTYPE TRANSDUCER CALIBRATIONS

Two sets of prototype transducers were produced during the program. The original prototypes were manufactured by Celesco at the beginning of the program. Later, after Senso-Metrics, Inc., became the transducer subcontractor, they produced a second set of prototype transducers of a different design. The Celesco transducers were subjected to extensive bare gage evaluation and the Senso-Metrics transdurers were subjected to extensive bare gage and embedded evaluations. The results of these tests are presented below.

4.1.1 Gaseous Nitrogen Calibrations for Celesco Prototype Transducers

Seven prototype transducers were manufactured by Celesco. These seven transducers with their ranges and variations are presented below.

Transducer S/N	Range, psi	Characteristics
A	25	Diaphragm, side exit leads
B	25	Diaphragm, side exit leads
C	25	Diaphragm, side exit leads
1	25	Cantilevered beam, rear exit leads
2	25	Cantilevered beam, rear exit leads
1	2,000	Cantilevered beam, rear exit leads
A	2,000	Diaphragm, side exit leads

These seven transducers were subjected to gaseous nitrogen pressure calibrations. Testing was conducted with the 25-psi transducers in one pressure vessel and the 2,000-psi transducers in a second pressure vessel. A special calibrated Taber pressure transducer supplied by CSD's instrumentation department was used to accurately measure the test pressure. A constant current excitation of approximately 5 mA was used. The test tempeature was measured by a copper-constantan thermocouple located in each pressure vessel. The total calibration and data acquisition system is presented in Figure 53.

Data for these early prototypes were recorded on a Digitrend 210 data logger rather than the Fluke 8800A DVM. Also, the pressure vessels were filled with

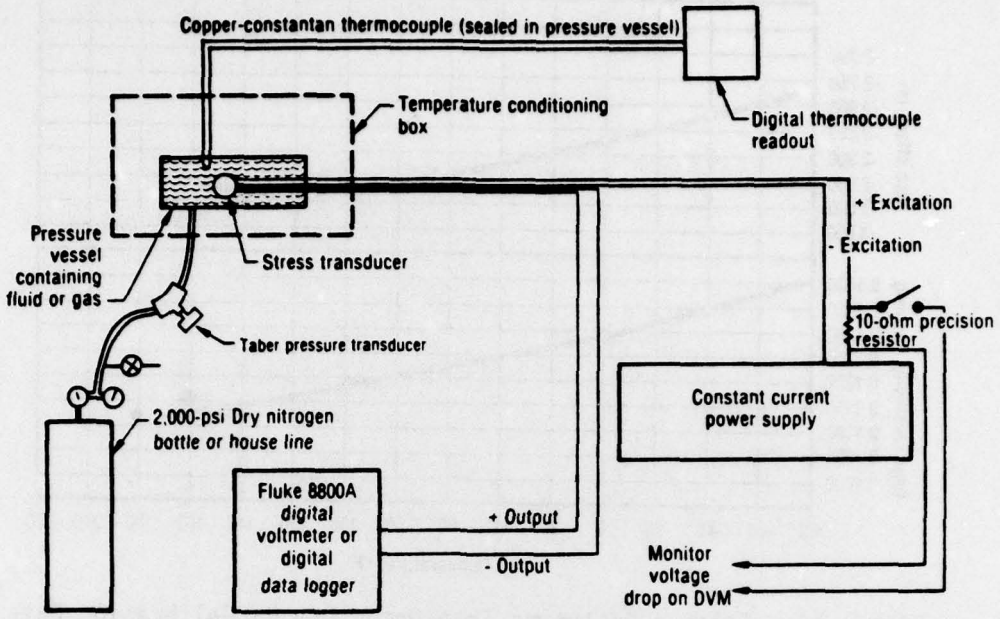


Figure 53. Stress Transducer Calibration and Data Acquisition System
14011

nitrogen rather than a fluid which was used later during pressurization. During each pressure step sufficient time was allowed for the temperature to stabilize. The pressure was applied in incremental steps from 0 psig to nearly full scale and back to 0 psig. Nine data points were taken at each test temperature. Test temperature, Taber output, transducer output, and transducer excitation were recorded at each pressure increment. A nominal excitation current of 5 mA was used for all the calibrations. Figures 54 through 60 present the sensitivity and zero offset versus temperature for each of the seven transducers; the tabular data for all calibrations are presented in Tables 17 through 23. Fluctuations in temperature for these gaseous calibrations can be seen in the tables, particularly for the 2,000-psi transducers. Data reduction was performed with a least squares curve-fit analysis.

Sensitivity at each temperature was the slope of the least squares curve fit and zero offset was the slope intercept. These calculated values for each temperature, along with correlation coefficients and standard deviations, are tabulated in Tables 17 through 23.

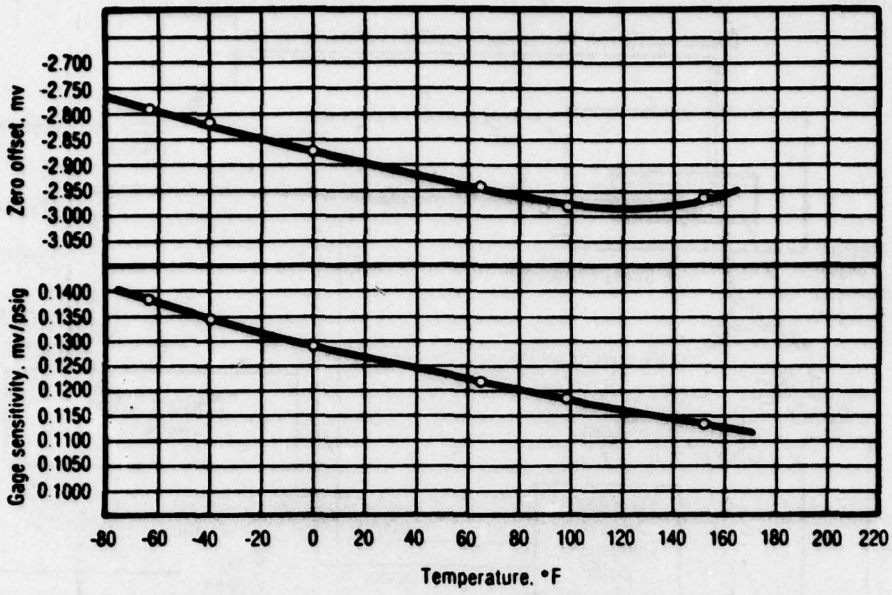


Figure 54. Celesco Prototype Transducer Dry N_2 Calibration Data (S/N A; 25-psi Flat Diaphragm; Side Exit Leads)

17157

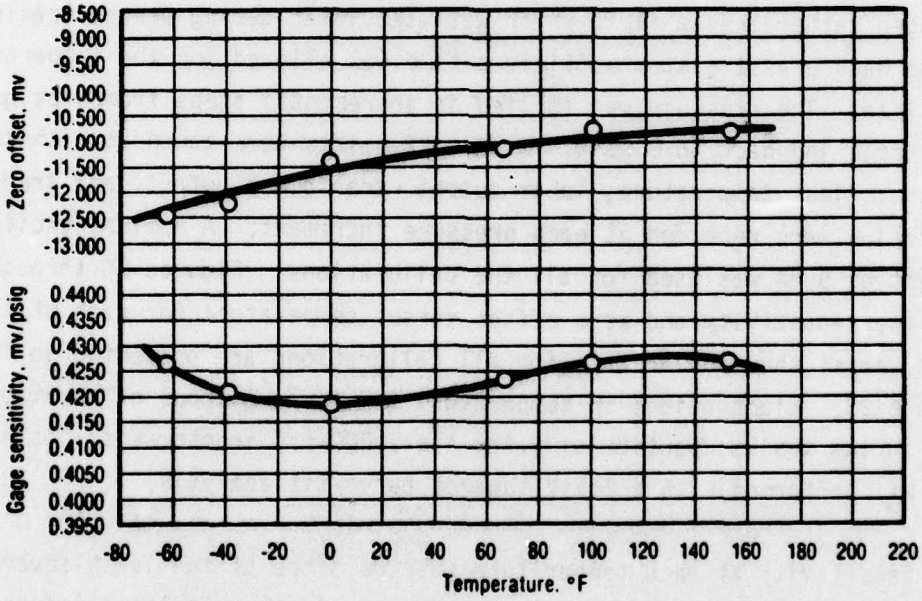


Figure 55. Celesco Prototype Transducer Dry N_2 Calibration Data (S/N B; 25-psi Flat Diaphragm; Side Exit Leads)

17158

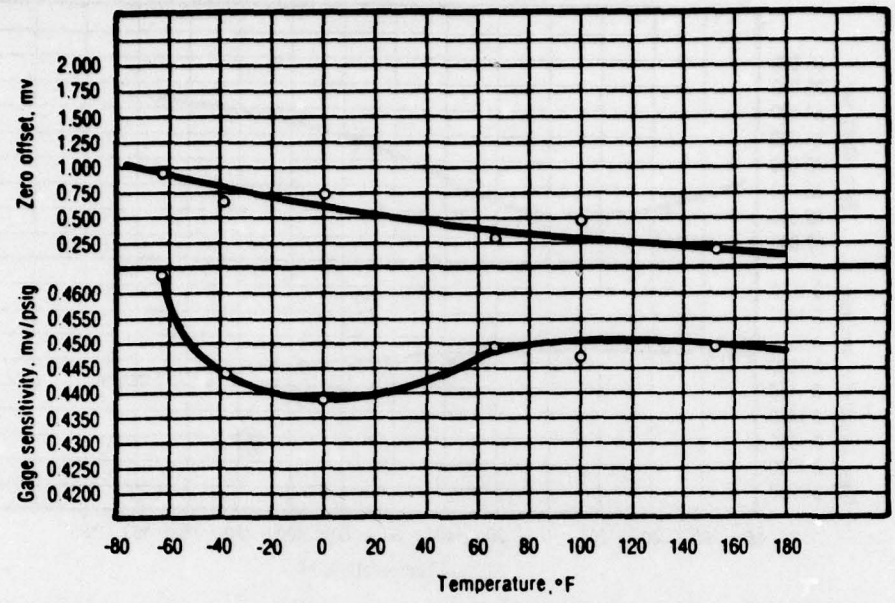


Figure 56. Celesco Prototype Transducer Dry N_2 Calibration Data (S/N C; 25-psi Flat Diaphragm; Side Exit Leads)

17159

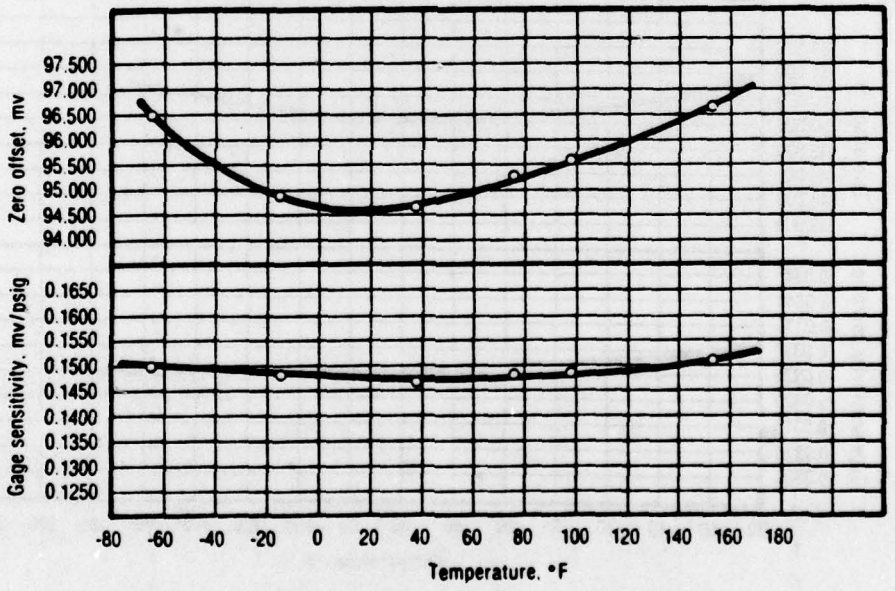


Figure 57. Celesco Prototype Transducer Dry N_2 Calibration Data (S/N 1; 25-psi Cantilevered Beam; Rear Exit Leads)

17160

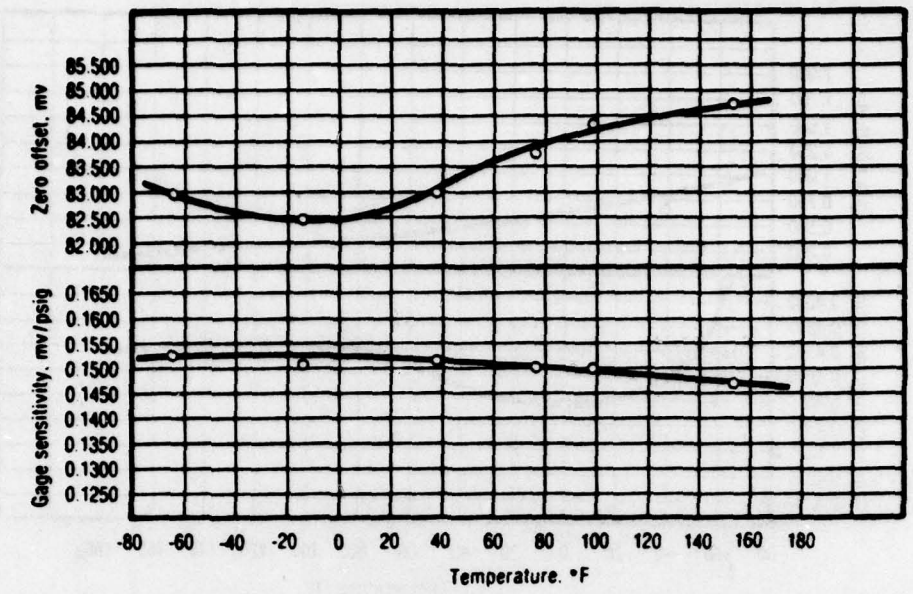


Figure 58. Celesco Prototype Transducer Dry N_2 Calibration Data (S/N 2; 25-psi Cantilevered Beam; Rear Exit Leads)

17161

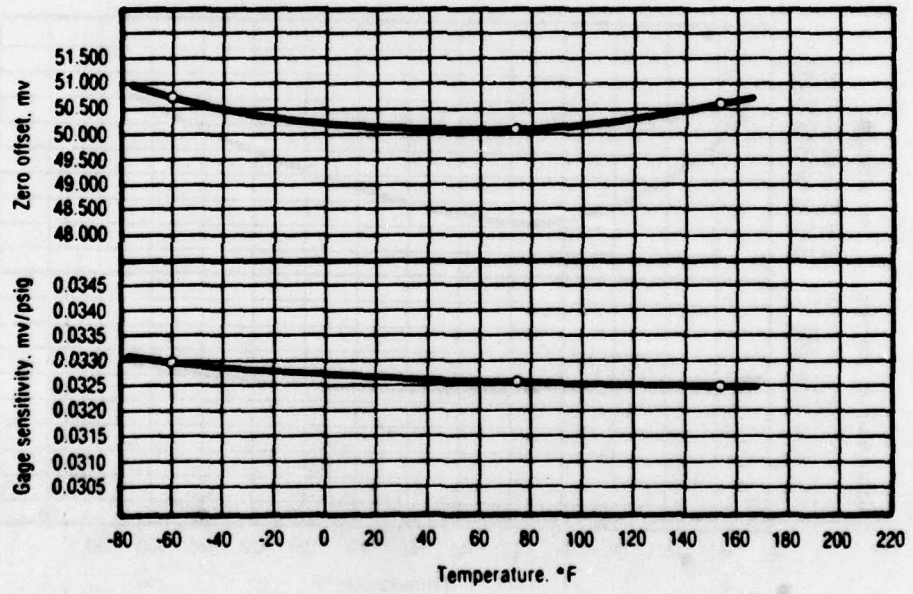


Figure 59. Celesco Prototype Transducer Dry N_2 Calibration Data (S/N 1; 2,000-psi Cantilevered Beam; Rear Exit Leads)

17162

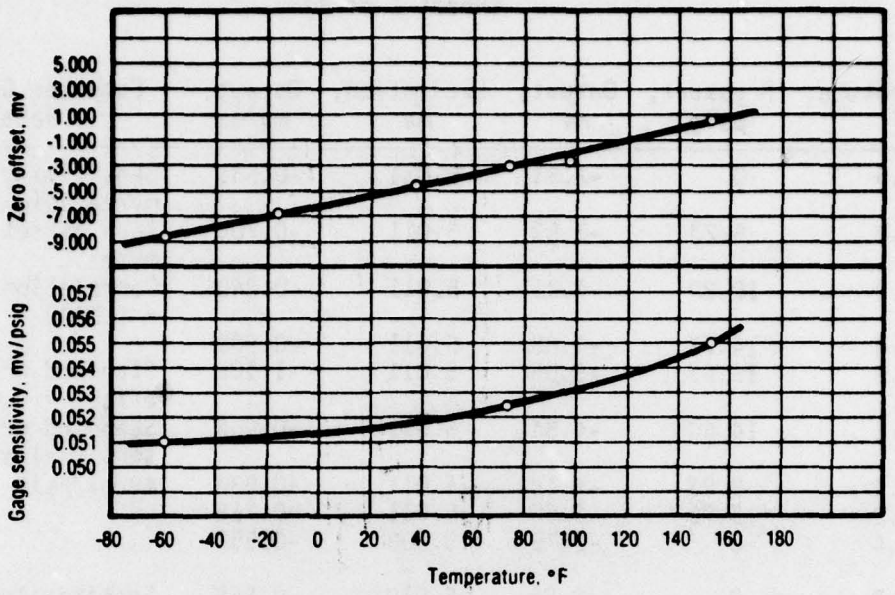


Figure 60. Celesco Prototype Transducer Dry N_2 Calibration Data (S/N A; 2,000-psi Flat Diaphragm; Side Exit Leads)

17163

It was clear after calibrating these Celesco prototypes that greater care had to be taken in manufacturing cantilevered beam transducers. As shown in Figures 57 through 59, the zero offsets for these cantilevered beam transducers varied from 50 to 100 mV which is several times the full-scale output of the transducers. The cantilevered beam transducers also were physically much larger than the diaphragm transducers, although they were still within the prescribed limits. The magnitude of sensitivity for gages S/N A, S/N 1, and S/N 2 (25 psi) were low, being in the range of 0.11- to 0.15-mV/psi. Also, two of the transducers, S/N A and S/N C (25 psi) show a large change in sensitivity as a function of temperature which is undesirable when trying to interpret stress for a transient temperature experiment. All cantilevered beam gages had unacceptably high zero offset values. The compensation resistors housed within the transducer body seemed to be acceptable but better protection for the leadwires was desirable. As a result of these tests several changes were incorporated into the Senso-Metrics prototype transducers manufactured for the next phase of the program.

TABLE 17. CALIBRATION OF CELESCO PROTOTYPES
(S/N A; 25-PSI FLAT DIAPHRAGM, SIDE EXIT)
(Sheet 1 of 3)

T4583-D

Temperature, °F	Pressure, psig	Output, mv	Excitation, ma	Output, mv/ma	Computer Curve-Fit Data
-64.5	0	-2.81	5.011	-0.561	Sensitivity = -0.0276 mv/ma/psig
-63.0	5.23	-3.53	5.011	-0.704	Zero offset = -0.5591 mv/ma
-63.0	10.20	-4.21	5.011	-0.840	Correlation coefficient = 1.0000
-62.6	14.77	-4.85	5.011	-0.968	
-62.8	19.93	-5.55	5.011	-1.108	Standard error of zero offset = 0.0011 mv/ma
-63.1	14.60	-4.84	5.011	-0.966	Standard error of sensitivity = 9.752 E-05
-63.4	9.93	-4.18	5.011	-0.834	mv/ma/psig
-63.2	5.76	-3.60	5.011	-0.718	
-63.4	0	-2.79	5.008	-0.557	
0.0	0	-2.85	5.010	-0.569	Sensitivity = -0.0257 mv/ma/psig
0.0	4.24	-3.58	5.008	-0.715	Zero offset = -0.5760 mv/ma
-0.3	10.00	-4.15	5.011	-0.828	Correlation coefficient = 0.9977
0.0	14.70	-4.81	5.011	-0.960	
0.2	19.93	-5.45	5.009	-1.088	Standard error of zero offset = 0.0071 mv/ma
0.1	14.57	-4.74	5.009	-0.946	Standard error of sensitivity = 0.0007
0.0	10.07	-4.16	5.011	-0.830	mv/ma/psig
0.0	5.23	-3.53	5.011	-0.704	
-0.2	0	-2.85	5.012	-0.569	
98.6	0	-2.99	5.010	-0.597	Sensitivity = -0.0237 mv/ma/psig
98.6	5.36	-3.63	5.010	-0.725	Zero offset = -0.5969 mv/ma
99.1	10.13	-4.20	5.010	-0.838	Correlation coefficient = 1.0000
99.1	15.10	-4.79	5.008	-0.956	
99.2	19.80	-5.35	5.010	-1.068	Standard error of zero offset = 0.0004 mv/ma
99.0	14.60	-4.73	5.010	-0.944	Standard error of sensitivity = 3.5741 E-05 mv/ma/psig

TABLE 17. CALIBRATION OF CELESCO PROTOTYPES
(S/N A; 25-PSI FLAT DIAPHRAGM, SIDE EXIT)
(Sheet 2 of 3)

T4583-D

Temperature, °F	Pressure, psig	Output, mv	Excitation, ma	Output, mv/ma	Computer Curve-Fit Data
99.2	10.00	-4.17	5.008	-0.833	
99.0	4.97	-3.58	5.010	-0.715	
99.2	0	-2.99	5.010	-0.597	
152.2	0	-2.97	5.010	-0.593	Sensitivity = -0.0226 mv/ma/psig
152.4	5.50	-3.60	5.010	-0.719	Zero offset = -0.5932 mv/ma
152.3	10.00	-4.10	5.010	-0.818	Correlation coefficient = 1.0000
152.5	14.83	-4.65	5.010	-0.928	
152.6	19.93	-5.23	5.010	-1.044	Standard error of zero offset = 0.0006 mv/ma
152.4	15.03	-4.68	5.010	-0.934	Standard error of sensitivity = 5.0454 E-05 mv/ma/psig
152.4	10.79	-4.19	5.010	-0.836	
152.3	6.16	-3.67	5.010	-0.733	
152.0	0	-2.97	5.010	-0.593	
66.3	0	-2.95	5.010	-0.589	Sensitivity = -0.0243 mv/ma/psig
66.1	5.50	-3.62	5.010	-0.723	Zero offset = -0.5884 mv/ma
66.4	10.07	-4.17	5.010	-0.832	Correlation coefficient = 1.0000
66.4	14.83	-4.76	5.010	-0.950	
66.6	20.00	-5.39	5.010	-1.076	Standard error of zero offset = 0.0005 mv/ma
66.4	15.10	-4.79	5.010	-0.956	Standard error of sensitivity = 4.4980 E-05 mv/ma/psig
66.4	9.87	-4.15	5.010	-0.828	
66.3	5.23	-3.58	5.009	-0.715	
66.3	0	-2.95	5.011	-0.589	
-38.9	0	-2.82	5.010	-0.563	Sensitivity = -0.0268 mv/ma/psig
-38.7	10.86	-4.29	5.009	-0.856	Zero offset = -0.5638 mv/ma
-38.7	15.17	-4.86	5.010	-0.970	Correlation coefficient = 1.0000
-38.7	18.87	-5.36	5.006	-1.071	

TABLE 17. CALIBRATION OF CELESCO PROTOTYPES
(S/N A; 25-PSI FLAT DIAPHRAGM, SIDE EXIT)
(Sheet 3 of 3)

T4583-D

Temperature, °F	Pressure, psig	Output, mv	Excitation, ma	Output, mv/ma	Computer Curve-Fit Data
-38.8	24.37	-6.10	5.010	-1.216	Standard error of zero offset = 0.0007 mv/ma
-38.8	20.26	-5.55	5.010	-1.108	Standard error of sensitivity = 4.4947 E-05 mv/ma/psig
-38.8	16.09	-4.98	5.009	-0.994	
-38.9	10.60	-4.25	5.010	-0.848	
-38.8	5.83	-3.60	5.010	-0.719	
-38.8	0	-2.83	5.010	-0.565	

TABLE 18. CALIBRATION OF CELESCO PROTOTYPES
(S/N B; 25-PSI FLAT DIAPHRAGM, SIDE EXIT)
(Sheet 1 of 3)

T4584-D

Temperature, °F	Pressure, psig	Output, mv	Excitation, ma	Output, mv/ma	Computer Curve-Fit Data
-64.5	0	-12.50	5.017	-2.492	Sensitivity = -0.0853 mv/ma/psig
-63.0	5.23	-14.76	5.017	-2.942	Zero offset = -2.495 mv/ma
-63.0	10.20	-16.88	5.017	-3.365	Correlation coefficient = 1.0000
-62.6	14.77	-18.83	5.017	-3.753	
-62.8	19.93	-21.01	5.017	-4.188	Standard error of zero offset = 0.0030 mv/ma
-63.1	14.60	-18.82	5.017	-3.751	Standard error of sensitivity = 0.0003 mv/ma/psig
-63.4	9.93	-16.79	5.017	-3.347	
-63.2	5.76	-14.98	5.017	-2.986	
-63.4	0	-12.51	5.016	-2.494	
0.0	0	-11.35	5.016	-2.263	Sensitivity = -0.0836 mv/ma/psig
0.0	4.24	-13.63	5.015	-2.718	Zero offset = -2.282 mv/ma
-0.3	10.00	-15.64	5.017	-3.117	Correlation coefficient = 0.9984
0.0	14.70	-17.70	5.017	-3.528	
0.2	19.93	-19.77	5.017	-3.941	Standard error of zero offset = 0.0198 mv/ma

TABLE 18. CALIBRATION OF CELESCO PROTOTYPES
(S/N B; 25-PSI FLAT DIAPHRAGM, SIDE EXIT)
(Sheet 2 of 3)

T4584-D

Temperature, °F	Pressure, psig	Output, mv	Excitation, ma	Output, mv/ma	Computer Curve-Fit Data
0.1	14.57	-17.50	5.017	-3.488	Standard error of sensitivity = 0.0018 mv/ma/psig
0.0	10.07	-15.59	5.017	-3.107	
0.0	5.23	-13.52	5.017	-2.695	
-0.2	0	-11.34	5.017	-2.260	
98.6	0	-10.84	5.017	-2.161	Sensitivity = -0.0852 mv/ma/psig
98.6	5.36	-13.14	5.107	-2.619	Zero offset = -2.162 mv/ma
99.1	10.13	-15.19	5.017	-3.028	Correlation coefficient = 1.0000
99.1	15.10	-17.33	5.017	-3.454	
99.2	19.80	-19.31	5.017	-3.849	Standard error of zero offset = 0.0019 mv/ma
99.0	14.60	-17.07	5.018	-3.402	Standard error of sensitivity = 0.0002 mv/ma/psig
99.2	10.00	-15.10	5.018	-3.009	
99.0	4.97	-12.98	5.017	-2.587	
99.2	0	-10.85	5.018	-2.162	
152.2	0	-10.90	5.018	-2.172	Sensitivity = -0.0854 mv/ma/psig
152.4	5.50	-13.26	5.019	-2.640	Zero offset = -2.172 mv/ma
152.3	10.00	-15.18	5.019	-3.025	Correlation coefficient = 1.0000
152.5	14.83	-17.27	5.019	-3.441	
152.6	19.93	-19.45	5.019	-3.875	Standard error of zero offset = 0.0008 mv/ma
152.4	15.03	-17.35	5.019	-3.457	Standard error of sensitivity = 7.2548 E-05 mv/ma/psig
152.4	10.79	-15.53	5.019	-3.094	
152.3	6.16	-13.54	5.019	-2.698	
152.0	0	-10.91	5.019	-2.174	
66.3	0	-11.22	5.017	-2.236	Sensitivity = -0.0847 mv/ma/psig

TABLE 18. CALIBRATION OF CELESCO PROTOTYPES
(S/N B; 25-PSI FLAT DIAPHRAGM, SIDE EXIT)
(Sheet 3 of 3)

T4584-D

Temperature, °F	Pressure, psig	Output, mv	Excitation, ma	Output, mv/ma	Computer Curve-Fit Data
66.1	5.50	-13.53	5.017	-2.697	Zero offset = -2.233 mv/ma
66.4	10.07	-15.48	5.017	-3.086	Correlation coefficient = 1.0000
66.4	14.83	-17.53	5.017	-3.494	
66.6	20.00	-19.71	5.016	-3.929	Standard error of zero offset = 0.0020 mv/ma
66.4	15.10	-17.61	5.017	-3.510	Standard error of sensitivity = 0.0002 mv/ma/psig
66.4	9.87	-15.38	5.017	-3.066	
66.3	5.23	-13.40	5.017	-2.671	
66.3	0	-11.22	5.017	-2.236	
-38.9	0	-12.24	5.016	-2.440	Sensitivity = -0.0843 mv/ma/psig
-38.7	10.86	-16.84	5.016	-3.357	Zero offset = -2.442 mv/ma
-38.7	15.17	-18.65	5.014	-3.720	Correlation coefficient = 1.0000
-38.7	18.87	-20.22	5.003	-4.042	
-38.8	24.37	-22.56	5.015	-4.499	Standard error of zero offset = 0.0033 mv/ma
-38.8	20.26	-20.81	5.016	-4.149	Standard error of sensitivity = 0.0002 mv/ma/psig
-38.8	16.09	-19.03	5.016	-3.794	
-38.9	10.60	-16.73	5.016	-3.335	
-38.8	5.83	-14.68	5.016	-2.927	
-38.8	0	-12.30	5.016	-2.452	

TABLE 19. CALIBRATION OF CELESCO PROTOTYPES
(S/N C; 25-PSI FLAT DIAPHRAGM, SIDE EXIT)
(Sheet 1 of 4)

T4585-D

Temperature, °F	Pressure, psig	Output, mv	Excitation, ma	Output, mv/ma	Computer Curve-Fit Data
-64.5	0	0.94	5.005	0.188	Sensitivity = -0.0927 mv/ma/psig
-63.0	5.23	-1.42	5.006	-0.284	Zero offset = 0.1915 mv/ma

TABLE 19. CALIBRATION OF CELESCO PROTOTYPES
(S/N C; 25-PSI FLAT DIAPHRAGM, SIDE EXIT)
(Sheet 2 of 4)

T4585-D

Temperature, °F	Pressure, psig	Output, mv	Excitation, ma	Output, mv/ma	Computer Curve-Fit Data
-63.0	10.20	-3.64	5.006	-0.727	Correlation coefficient = 0.9949
-62.6	14.77	-5.70	5.006	-1.139	
-62.8	19.93	-7.99	5.006	-1.596	Standard error of zero offset = 0.0390 mv/ma
-63.1	14.60	-5.69	5.006	-1.324	Standard error of sensitivity = 0.0035 mv/ma/psig
-63.4	9.93	-3.56	5.006	-0.711	
-63.2	5.76	-1.65	5.006	-0.330	
-63.4	0	0.95	5.004	0.190	
0.0	0	0.82	5.007	0.164	Sensitivity = -0.0878 mv/ma/psig
0.0	4.24	-1.56	5.006	-0.312	Zero offset = 0.1457 mv/ma
-0.3	10.00	-3.60	5.007	-0.719	Correlation coefficient = 0.9984
0.0	14.70	-5.83	5.007	-1.164	
0.2	19.93	-8.02	5.006	-1.602	Standard error of zero offset = 0.0203 mv/ma
0.1	14.57	-5.64	5.007	-1.126	Standard error of sensitivity = 0.0019 mv/ma/psig
0.0	10.07	-3.63	5.007	-0.724	
0.0	5.23	-1.46	5.006	-0.292	
-0.2	0	0.83	5.007	0.166	
98.6	0	0.48	5.007	0.096	Sensitivity = -0.0895 mv/ma/psig
98.6	5.36	-1.93	5.007	-0.385	Zero offset = 0.0962 mv/ma
99.1	10.13	-4.08	5.007	-0.815	Correlation coefficient = 1.0000
99.1	15.10	-6.28	5.007	-1.254	
99.2	19.80	-8.41	5.007	-1.680	Standard error of zero offset = 0.0013 mv/ma
99.0	14.60	-6.06	5.007	-1.210	Standard error of sensitivity = 0.0001 mv/ma/psig
99.2	10.00	-3.99	5.007	-0.797	
99.0	4.97	-1.74	5.007	-0.348	

TABLE 19. CALIBRATION OF CELESCO PROTOTYPES
(S/N C; 25-PSI FLAT DIAPHRAGM, SIDE EXIT)
(Sheet 3 of 4)

T4585-D

Temperature, °F	Pressure, psig	Output, mv	Excitation, ma	Output, mv/ma	Computer Curve-Fit Data
99.2	0	0.48	5.007	0.096	
152.2	0	0.19	5.009	0.038	Sensitivity = -0.0899 mv/ma/psig
152.4	5.50	-2.29	5.008	-0.457	Zero offset = 0.0375 mv/ma
152.3	10.00	-4.30	5.008	-0.859	Correlation coefficient = 1.0000
152.5	14.83	-6.50	5.008	-1.298	
152.6	19.93	-8.80	5.008	-1.757	Standard error of zero offset = 0.0012 mv/ma
152.4	15.03	-6.59	5.008	-1.316	Standard error of sensitivity = 0.0001 mv/ma/psig
152.4	10.79	-4.67	5.009	-0.932	
152.3	6.16	-2.58	5.009	-0.515	
152.0	0	0.17	5.008	0.034	
66.3	0	0.28	5.006	0.056	Sensitivity = -0.0900 mv/ma/psig
66.1	5.50	-2.15	5.006	-0.429	Zero offset = 0.0614 mv/ma
66.4	10.07	-4.18	5.006	-0.835	Correlation coefficient = 0.9996
66.4	14.83	-6.34	5.006	-1.266	
66.6	20.00	-8.64	5.006	-1.726	Standard error of zero offset = 0.0107 mv/ma
66.4	15.10	-6.44	5.006	-1.342	Standard error of sensitivity = 0.0010 mv/ma/psig
66.4	9.87	-4.09	5.006	-0.817	
66.3	5.23	-2.01	5.006	-0.402	
66.3	0	0.28	5.006	0.056	
-38.9	0	0.66	5.005	0.132	Sensitivity = -0.0888 mv/ma/psig
-38.7	10.86	-4.17	5.005	-0.833	Zero offset = 0.1349 mv/ma
-38.7	15.17	-6.07	5.005	-1.213	Correlation coefficient = 1.0000
-38.7	18.87	-7.72	5.005	-1.542	
-38.8	24.37	-10.18	5.005	-2.034	Standard error of zero offset = 0.0016 mv/ma

TABLE 19. CALIBRATION OF CELESCO PROTOTYPES
(S/N C; 25-PSI FLAT DIAPHRAGM, SIDE EXIT)
(Sheet 4 of 4)

T4585-D

Temperature, °F	Pressure, psig	Output, mv	Excitation, ma	Output, mv/ma	Computer Curve-Fit Data
-38.8	20.26	-8.34	5.006	-1.666	Standard error of sensitivity = 0.0001 mv/ma/psig
-38.8	16.09	-6.47	5.006	-1.292	
-38.9	10.60	-4.04	5.006	-0.807	
-38.8	5.83	-1.89	5.005	-0.378	
-38.8	0	0.67	5.005	0.134	

TABLE 20. CALIBRATION OF CELESCO PROTOTYPES
(S/N 1; 25-PSI CANTILEVERED BEAM, REAR EXIT LEADS)
(Sheet 1 of 3)

T4586-D

Temperature, °F	Pressure, psig	Output, mv	Excitation, ma	Output, mv/ma	Computer Curve-Fit Data
75.9	0	95.88	5.033	19.050	Sensitivity = -0.0297 mv/ma/psig
76.4	5.23	95.11	5.034	18.894	Zero offset = 19.051 mv/ma
76.4	10.13	94.38	5.034	18.749	Correlation coefficient = 1.0000
76.7	14.90	93.68	5.034	18.609	
76.7	20.26	92.87	5.034	18.449	Standard error of zero offset = 0.0009 mv/ma
77.2	14.70	93.72	5.035	18.614	Standard error of sensitivity = 8.5171 E-05 mv/ma/psig
77.4	9.67	94.49	5.035	18.767	
77.6	5.23	95.16	5.036	18.896	
77.7	0	95.93	5.035	19.053	
98.6	0	96.49	5.048	19.115	Sensitivity = -0.0297 mv/ma/psig
98.1	5.89	95.61	5.048	18.940	Zero offset = 19.116 mv/ma
98.0	10.07	94.97	5.048	18.813	Correlation coefficient = 1.0000
98.2	14.70	94.29	5.048	18.679	
98.2	20.00	93.49	5.048	18.520	Standard error of zero offset = 0.0009 mv/ma

TABLE 20. CALIBRATION OF CELESCO PROTOTYPES
(S/N 1; 25-PSI CANTILEVERED BEAM, REAR EXIT LEADS)
(Sheet 2 of 3)

T4586-D

Temperature, °F	Pressure, psig	Output, mv	Excitation, ma	Output, mv/ma	Computer Curve-Fit Data
98.3	15.36	94.18	5.048	18.657	Standard error of sensitivity = 7.7765 E-05 mv/ma/psig
98.2	10.73	94.89	5.048	18.798	
98.2	5.17	95.72	4.048	18.962	
98.3	0	96.50	5.048	19.116	
152.7	0	97.57	5.049	19.325	Sensitivity = -0.0301 mv/ma/psig
152.8	5.36	96.75	5.049	19.162	Zero offset = 19.324 mv/ma
152.7	9.93	96.06	5.049	19.026	Correlation coefficient = 1.0000
152.8	14.70	95.32	5.049	18.879	
152.8	20.07	94.51	5.049	18.719	Standard error of zero offset = 0.0006 mv/ma
152.7	14.57	95.35	5.049	18.885	Standard error of sensitivity = 5.3630 E-05 mv/ma/psig
152.7	10.60	95.95	5.049	19.004	
152.8	6.09	96.64	5.049	19.140	
152.7	0	97.56	5.049	19.323	
-63.8	0	97.06	5.034	19.281	Sensitivity = -0.0299 mv/ma/psig
-64.3	4.97	96.32	5.034	19.134	Zero offset = 19.289 mv/ma
-64.3	10.00	95.57	5.034	18.985	Correlation coefficient = 0.9996
-64.6	15.03	94.82	5.034	18.836	
-64.7	19.34	94.15	5.034	18.703	Standard error of zero offset = 0.0034 mv/ma
-64.7	15.17	94.83	5.034	18.838	Standard error of sensitivity = 0.0003 mv/ma/psig
-65.1	10.00	95.62	5.034	18.995	
-65.4	5.03	96.38	5.034	19.146	
-65.3	0	97.15	5.035	19.295	
37.7	0	95.21	5.031	18.925	Sensitivity = -0.0293 mv/ma/psig
38.0	5.23	94.44	5.031	18.772	Zero offset = 18.926 mv/ma

TABLE 20. CALIBRATION OF CELESCO PROTOTYPES
(S/N 1; 25-PSI CANTILEVERED BEAM, REAR EXIT LEADS)
(Sheet 3 of 3)

T4586-D

Temperature, °F	Pressure, psig	Output, mv	Excitation, ma	Output, mv/ma	Computer Curve-Fit Data
38.1	10.07	93.71	5.030	18.630	Correlation coefficient = 1.0000
38.1	14.70	93.02	5.030	18.493	
38.2	19.54	92.30	5.029	18.354	Standard error of zero offset = 0.0007 mv/ma
38.1	15.10	92.97	5.030	18.483	Standard error of sensitivity = 6.6994 E-05 mv/ma/psig
38.1	10.13	93.71	5.030	18.630	
38.1	5.17	94.45	5.031	18.774	
38.1	0	95.21	5.030	18.928	
-14.8	0	94.91	5.002	18.974	Sensitivity = -0.0296 mv/ma/psig
-14.7	5.23	94.15	5.002	18.822	Zero offset = 18.974 mv/ma
-14.7	10.07	93.43	5.003	18.675	Correlation coefficient = 0.9999
-14.7	14.97	92.73	5.004	18.531	
-14.5	19.54	92.05	5.004	18.395	Standard error of zero offset = 0.0013 mv/ma
-14.5	15.17	92.73	5.006	18.524	Standard error of sensitivity = 0.0001 mv/ma/psig
-14.5	10.00	93.51	5.007	18.676	
-14.4	5.30	94.23	5.007	18.820	
-14.4	0	95.02	5.009	18.970	

TABLE 21. CALIBRATION OF CELESCO PROTOTYPES
(S/N 2; 25-PSI CANTILEVERED BEAM, REAR EXIT LEADS)
(Sheet 1 of 4)

T4587-D

Temperature, °F	Pressure, psig	Output, mv	Excitation, ma	Output, mv/ma	Computer Curve-Fit Data
75.9	0	84.18	5.027	16.746	Sensitivity = -0.0301 mv/ma/psig
76.4	5.23	83.39	5.027	16.588	Zero offset = 16.749 mv/ma
76.4	10.13	82.66	5.027	16.443	Correlation coefficient = 0.9999

TABLE 21. CALIBRATION OF CELESCO PROTOTYPES
(S/N 2; 25-PSI CANTILEVERED BEAM, REAR EXIT LEADS)
(Sheet 2 of 4)

T4587-D

Temperature, °F	Pressure, psig	Output, mv	Excitation, ma	Output, mv/ma	Computer Curve-Fit Data
76.7	14.90	81.94	5.027	16.300	
76.7	20.26	81.12	5.027	16.137	Standard error of zero offset = 0.0017 mv/ma
77.2	14.70	81.99	5.028	16.307	Standard error of sensitivity = 0.0002 mv/ma/psig
77.4	9.67	82.76	5.028	16.460	
77.6	5.23	83.45	5.028	16.597	
77.7	0	84.22	5.028	16.750	
98.0	0	84.91	5.037	16.857	Sensitivity = -0.0300 mv/ma/psig
98.1	5.89	84.01	5.037	16.679	Zero offset = 16.856 mv/ma
98.0	10.07	83.38	5.037	16.554	Correlation coefficient = 0.9999
98.2	14.70	82.69	5.037	16.417	
98.2	20.00	81.87	5.037	16.254	Standard error of zero offset = 0.0021 mv/ma
98.3	15.36	82.58	5.038	16.391	Standard error of sensitivity = 0.0002 mv/ma/psig
98.2	10.73	83.29	5.037	16.536	
98.2	5.17	84.13	5.036	16.706	
98.3	0	84.92	5.037	16.859	
152.7	0	85.34	5.038	16.939	Sensitivity = -0.0293 mv/ma/psig
152.8	5.36	84.53	5.038	16.778	Zero offset = 16.939 mv/ma
152.7	9.93	83.84	5.038	16.642	Correlation coefficient = 0.9972
152.8	14.70	83.10	5.038	16.495	
152.8	20.07	82.29	5.038	16.334	Standard error of zero offset = 0.0092 mv/ma
152.7	14.57	83.13	5.024	16.547	Standard error of sensitivity = 0.0008 mv/ma/psig
152.7	10.60	83.74	5.038	16.635	
152.8	6.09	84.41	5.038	16.755	
152.7	0	85.34	5.038	16.939	

TABLE 21. CALIBRATION OF CELESCO PROTOTYPES
(S/N 2; 25-PSI CANTILEVERED BEAM, REAR EXIT LEADS)
(Sheet 3 of 4)

T4587-D

Temperature, °F	Pressure, psig	Output, mv	Excitation, ma	Output, mv/ma	Computer Curve-Fit Data
-63.8	0	83.34	5.026	16.582	Sensitivity = -0.0305 mv/ma/psig
-64.3	4.97	82.57	5.026	16.429	Zero offset = 16.587 mv/ma
-64.3	10.00	81.83	5.026	16.281	Correlation coefficient = 0.9998
-64.6	15.03	81.05	5.026	16.126	
-64.7	19.54	80.36	5.026	15.989	Standard error of zero offset = 0.0024 mv/ma
-64.7	15.17	81.05	5.026	16.126	Standard error of sensitivity = 0.0002 mv/ma/psig
-65.1	10.00	81.85	5.026	16.285	
-65.4	5.03	82.61	5.026	16.437	
-65.3	0	83.39	5.026	16.592	
37.7	0	83.34	5.024	16.588	Sensitivity = -0.0302 mv/ma/psig
38.0	5.23	82.55	5.024	16.431	Zero offset = 16.589 mv/ma
38.1	10.07	81.81	5.022	16.290	Correlation coefficient = 0.9999
38.1	14.70	81.10	5.024	16.143	
38.2	19.54	80.36	5.024	15.995	Standard error of zero offset = 0.0014 mv/ma
38.1	15.10	81.05	5.024	16.133	Standard error of sensitivity = 0.0001 mv/ma/psig
38.1	10.13	81.80	5.024	16.282	
38.1	5.17	82.56	5.024	16.433	
38.1	0	83.34	5.024	16.588	
-14.8	0	82.50	5.003	16.490	Sensitivity = -0.0302 mv/ma/psig
-14.7	5.23	81.72	5.004	16.331	Zero offset = 16.489 mv/ma
-14.7	10.07	80.99	5.004	16.185	Correlation coefficient = 1.0000
-14.7	14.97	80.26	5.005	16.036	
-14.5	19.54	79.57	5.005	15.898	Standard error of zero offset = 0.0006 mv/ma

TABLE 21. CALIBRATION OF CELESCO PROTOTYPES
(S/N 2; 25-PSI CANTILEVERED BEAM, REAR EXIT LEADS)
(Sheet 4 of 4)

T4587-D

Temperature, °F	Pressure, psig	Output, mv	Excitation, ma	Output, mv/ma	Computer Curve-Fit Data
-14.5	15.17	80.26	5.006	16.033	Standard error of sensitivity = 5.8430 E-05 mv/ma/psig
-14.5	10.00	81.05	5.007	16.187	
-14.4	5.30	81.78	5.008	16.330	
-14.4	0	82.59	5.009	16.488	

TABLE 22. N_2 CALIBRATION OF CELESCO PROTOTYPE TRANSDUCER
(S/N 1; 2,000-PSIG CANTILEVERED BEAM, REAR EXIT)
(Sheet 1 of 2)

T4588-D

Test Temperature, °F	Pressure, psig	Excitation, ma	Output, mv	Output, mv/ma	Computer Curve-Fit Data
152.5	0	5.001	50.07	10.012	Zero offset = 10.129 mv/ma
153.1	496.27	5.000	34.01	6.802	Sensitivity = 0.00650 mv/ma/psig
153.5	1,036.02	5.000	16.47	3.294	Correlation coefficient = 0.9997
153.7	1,414.91	4.998	4.40	0.880	
154.0	1,704.35	4.998	-4.86	-0.972	Standard error of zero offset = 0.0579 mv/ma
153.2	1,329.19	4.998	7.75	1.551	Standard error of sensitivity = 5.7336 E-05 mv/ma/psig
152.5	962.73	4.999	19.82	3.965	
151.7	493.79	4.999	35.07	7.015	
151.9	0	4.999	51.15	10.232	
73.1	0	4.983	49.68	9.970	Zero offset = 10.017 mv/ma
74.7	511.80	4.990	33.21	6.655	Sensitivity = 0.00653 mv/ma/psig
75.7	1,045.34	4.993	15.87	3.178	Correlation coefficient = 1.0000

TABLE 22. N_2 CALIBRATION OF CELESCO PROTOTYPE TRANSDUCER
(S/N 1; 2,000-PSIG CANTILEVERED BEAM, REAR EXIT)
(Sheet 2 of 2)

T4588-D

Test Temperature, °F	Pressure, psig	Excitation, ma	Output, mv	Output, mv/ma	Computer Curve-Fit Data
76.1	1,426.09	4.992	3.43	0.687	
76.2	1,616.15	4.992	-2.78	-0.557	Standard error of zero offset = 0.0194 mv/ma
75.8	1,251.55	4.993	9.35	1.873	Standard error of sensitivity = 1.9823 E-05 mv/ma/psig
75.3	896.89	4.993	20.98	4.202	
75.3	502.48	4.993	33.81	6.771	
75.2	0	4.992	50.10	10.036	
-62.0	0	4.994	50.33	10.078	Zero offset = 10.147 mv/ma
-60.0	570.19	4.998	31.81	6.365	Sensitivity = 0.00660 mv/ma/psig
-60.3	1,045.34	4.994	16.15	3.234	Correlation coefficient = 0.9999
-59.6	1,289.44	4.994	8.07	1.616	
-61.0	806.21	4.994	24.15	4.836	Standard error of zero offset = 0.0308 mv/ma
-60.9	0	4.995	50.53	10.116	Standard error of sensitivity = 3.5137 E-05 mv/ma/psig
-57.0	1,549.69	4.997	-0.32	-0.064	
-61.6	0	4.997	51.27	10.260	

TABLE 23. N_2 CALIBRATION OF CELESCO PROTOTYPE TRANSDUCER
(S/N A; 2,000-PSIG DIAPHRAGM, SIDE EXIT)
(Sheet 1 of 3)

T4589-D

Test Temperature, °F	Pressure, psig	Excitation, ma	Output, mv	Output, mv/ma	Computer Curve-Fit Data
152.5	0	5.001	0.51	0.102	Zero offset = 0.0790 mv/ma
153.1	496.27	4.999	-26.83	-5.367	Sensitivity = 0.00110 mv/ma/psig

TABLE 23. N_2 CALIBRATION OF CELESCO PROTOTYPE TRANSDUCER
(S/N A; 2,000-PSIG DIAPHRAGM, SIDE EXIT)
(Sheet 2 of 3)

T4589-D

Test Temperature °F	Pressure, psig	Excitation, ma	Output, mv	Output, mv/ma	Computer Curve-Fit Data
153.5	1,036.02	4.999	-56.70	-11.342	Correlation coefficient = 1.0000
153.7	1,414.91	4.998	-77.78	-15.562	
154.0	1,704.35	4.998	-93.93	-18.794	Standard error of zero offset = 0.0214 mv/ma
153.2	1,329.19	4.998	-72.91	-14.588	Standard error of sensitivity = 2.1245 E-05 mv/ma/psig
152.5	962.73	4.998	-52.66	-10.536	
151.7	493.79	4.999	-26.92	-5.385	
151.9	0	4.999	0.07	0.014	
73.1	0	4.987	-3.24	-0.650	Zero offset = -0.637 mv/ma
74.7	511.80	4.992	-29.95	-6.000	Sensitivity = 0.0105 mv/ma/psig
75.7	1,045.34	4.994	-58.00	-11.614	Correlation coefficient = 1.0000
76.1	1,426.09	4.993	-78.12	-15.646	
76.2	1,616.15	4.994	-88.22	-17.665	Standard error of zero offset = 0.0131 mv/ma
75.8	1,251.55	4.994	-68.82	-13.781	Standard error of sensitivity = 1.3333 E-05 mv/ma/psig
75.3	896.89	4.994	-50.19	-10.050	
75.3	502.48	4.994	-29.51	-5.909	
75.2	0	4.994	-3.31	-0.663	
-62.0	0	4.995	-8.65	-1.732	Zero offset = 1.776 mv/ma
-60.0	570.19	4.998	-37.13	-7.429	Sensitivity = 0.00999 mv/ma/psig
-60.3	1,045.34	4.996	-61.03	-12.216	Correlation coefficient = 1.0000

TABLE 23. N_2 CALIBRATION OF CELESCO PROTOTYPE TRANSDUCER
(S/N A; 2,000-PSIG DIAPHRAGM, SIDE EXIT)
(Sheet 3 of 3)

T4589-D

Test Temperature °F	Pressure, psig	Excitation, ma	Output, mv	Output, mv/ma	Computer Curve-Fit Data
-59.6	1,289.44	4.995	-73.29	-14.673	
-61.0	806.21	4.995	-49.04	-9.818	Standard error of zero offset = 0.0265 mv/ma
-60.9	0	4.996	-8.75	-1.751	Standard error of sensitivity = 3.0271 E-05 mv/ma/psig
-57.0	1,549.69	4.997	-86.28	-17.266	
-61.6	0	4.997	-9.37	-1.875	

4.1.2 Gaseous Nitrogen Calibrations for Senso-Metrics Prototype Transducers

Seven prototype transducers were manufactured by Senso-Metrics, Inc. The seven transducers with their ranges and variations are presented below.

Transducer S/N	Range, psi	Characteristics
6916	25	Diaphragm, side exit leads
6917	25	Diaphragm, side exit leads
6920	25	Cantilevered beam, side exit leads
6921	25	Cantilevered beam, side exit leads
6918	2,000	Diaphragm, side exit leads
6919	2,000	Diaphragm, side exit leads
6922	2,000	Cantilevered beam, side exit leads

The seven transducers were subjected to gaseous nitrogen pressure calibrations. During these calibrations the pressure vessels were filled with Shell Diala oil to minimize temperature fluctuation during pressurization; the data were recorded on a Fluke 8800A digital multimeter.

Pressure calibrations were performed at several temperatures. At each temperature pressure was applied stepwise in increments of 20% of full-scale range of the transducer to full scale and back to 0 psig in the same number of

increments. This is the standard 11-point calibration. In addition, a 33-point NBS-type* calibration was performed at ambient temperature. The 33-point calibration is the same as the 11-point calibration except it is performed three times in succession. The test temperature, Taber pressure transducer output, transducer excitation, and output were recorded at each pressure increment. An excitation of approximately 5 mA was used and the data were normalized to 5 mA for plotting. The sensitivity and zero offset data versus temperature for each transducer are presented in Figures 61 through 66. Calibration data for transducer S/N 6919 (2,000-psi diaphragm gage) are not shown because the transducer was found to have a leaky glass-to-metal header. A summary of the 33-point calibration at 70°F is presented in Table 24. In a 33-point calibration, data at each 20% increment of full scale, and 0% of full scale, are recorded six times. This table shows the repeatability (in psi) at each increment of full scale for each of the transducers. In addition, the repeatability in percentage of full scale is tabulated.

Results of the Senso-Metrics prototype transducer testing pointed out certain changes that would be desirable in the production model. The lengthy steel tube containing the leadwires was fine in principle. However, the weld joint near the tube was weak and failures occured when the tube was bent causing leadwires to short. Also, the tube itself was not flexible enough. The physical size of the transducers, while within design limits, was fairly large and the cantilevered beam transducers again had large offsets and were not as stable as diaphragm gages. Based on these tests, it was decided to remove the compensation resistors from within the transducer bodies and place them in a weatherproof container external to the transducer for the production gages. The hermetic seal also would be external. The leadwire tube would be made of a more flexible steel. The transducer would be physically smaller and the cantilevered beam models would be eliminated entirely.

---

*Natrella, M. G., "Experimental Statistics," National Bureau of Standards Handbook 91, August 1963.

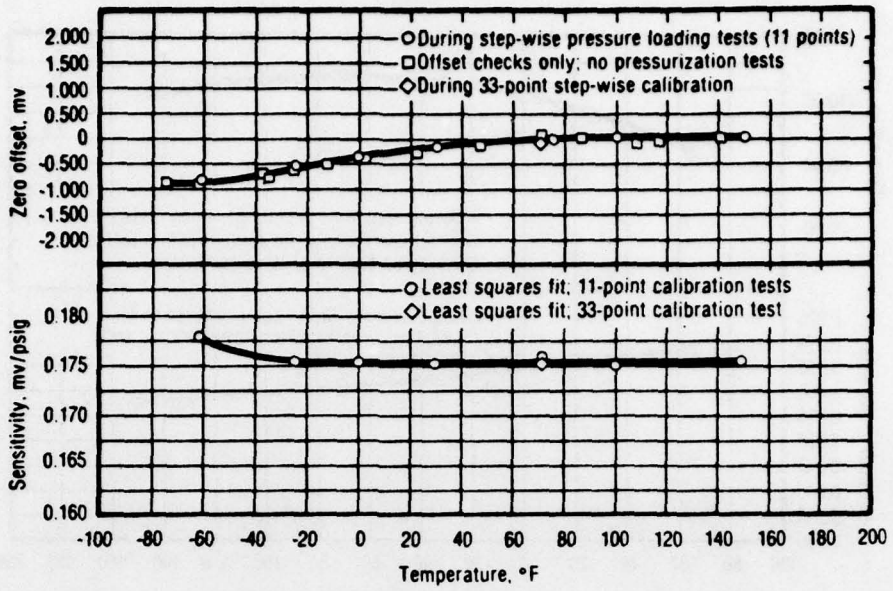


Figure 61. Senso-Metrics Prototype Stress Transducer Calibration Data at 5-mA Excitation (S/N 6916; 25-psi Diaphragm Transducer)

17151

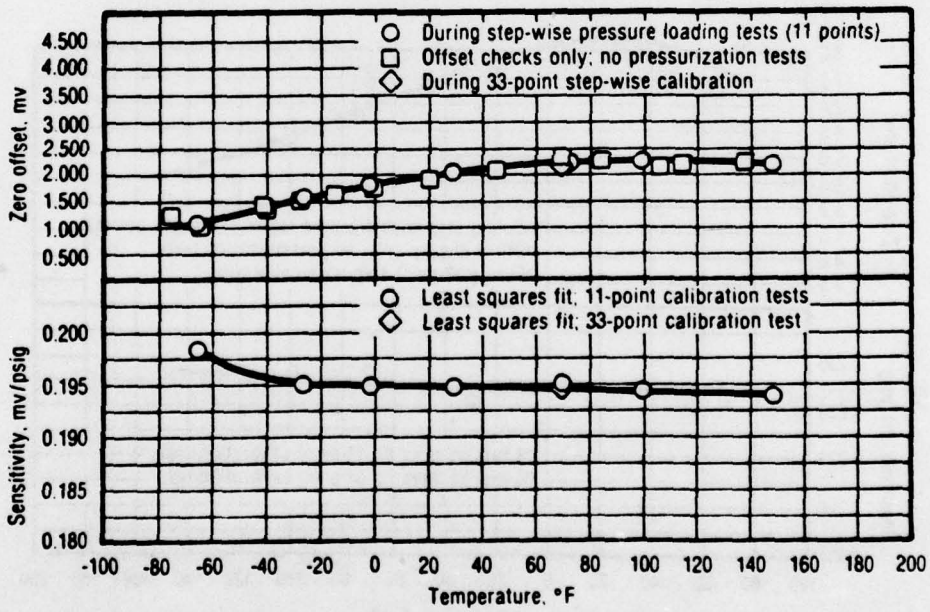


Figure 62. Senso-Metrics Prototype Stress Transducer Calibration Data at 5-mA Excitation (S/N 6917; 25-psi Diaphragm Transducer)

17152

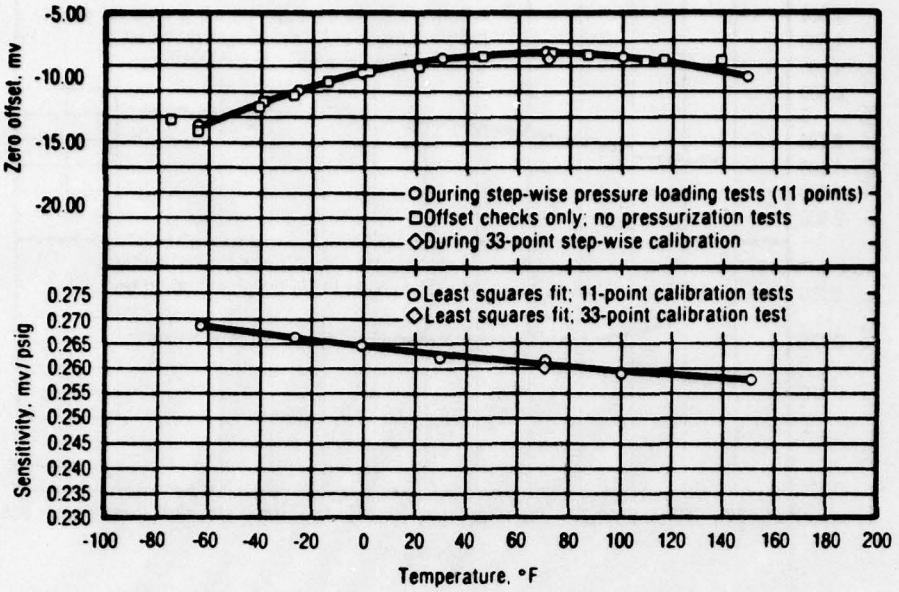


Figure 63. Senso-Metrics Prototype Stress Transducer Calibration Data at 5-mA Excitation (S/N 6920; 25-psi Cantilevered Beam Transducer)

17153

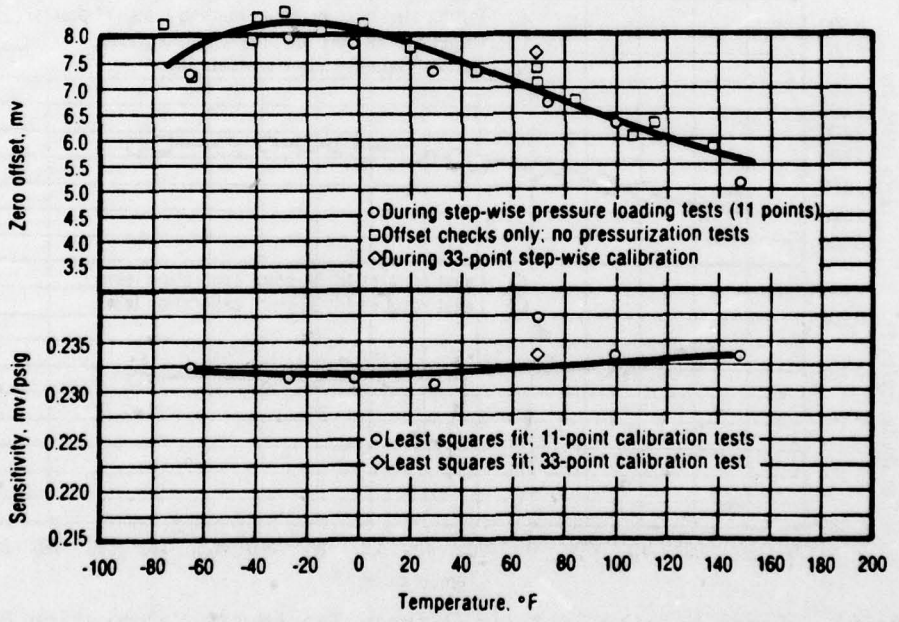


Figure 64. Senso-Metrics Prototype Stress Transducer Calibration Data at 5-mA Excitation (S/N 6921; 25-psi Cantilevered Beam Transducer)

17154

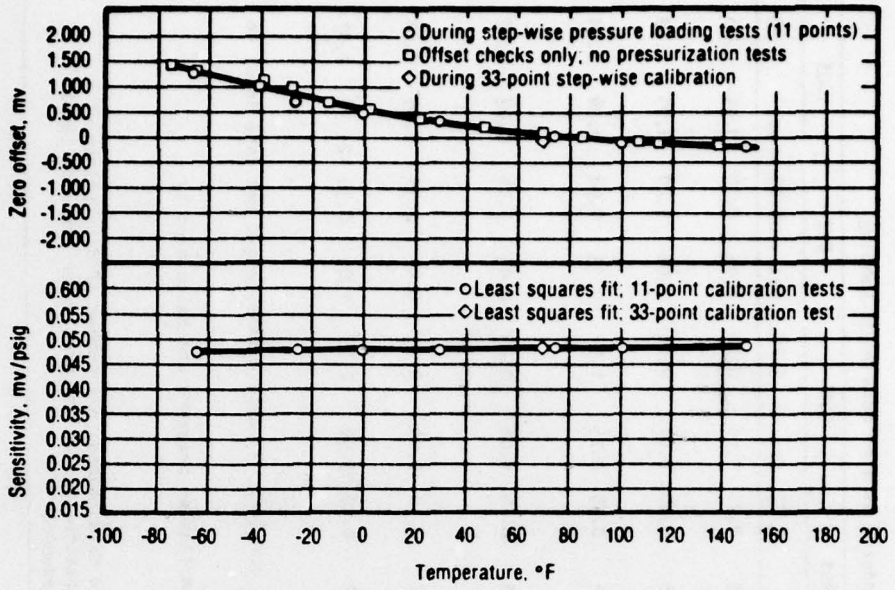


Figure 65. Senso-Metrics Prototype Stress Transducer Calibration Data at 5-mA Excitation (S/N 6918; 2,000-psi Diaphragm Transducer)

17155

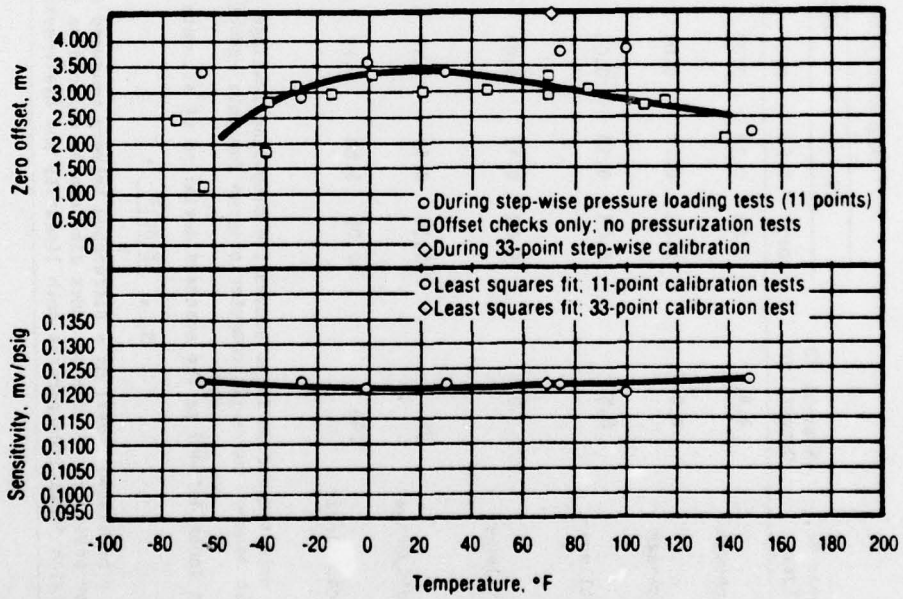


Figure 66. Senso-Metrics Prototype Stress Transducer Calibration Data at 5-mA Excitation (S/N 6922; 2,000-psi Cantilevered Beam Transducer)

17156

TABLE 24. SENSO-METRICS PROTOTYPE TRANSDUCER SUMMARY AT 70°F AND 5-mA EXCITATION

T4582-D

Transducer No. and Type	Nominal FS Output, mv	Repeatability (Precision Index*) at % of Full-Scale Loading											
		0%		20%		40%		60%		80%		100%	
		psi	% FS	psi	% FS	psi	% FS	psi	% FS	psi	% FS	psi	% FS
S/N 6916 25-psi diaphragm	4.4	0.03	0.12	0.04	0.16	0.05	0.20	0.06	0.24	0.05	0.20	0.04	0.16
S/N 6917 25-psi diaphragm	4.8	0.03	0.12	0.04	0.16	0.05	0.20	0.07	0.29	0.05	0.20	0.03	0.12
S/N 6920 25-psi cantilever beam	6.5	0.03	0.12	0.05	0.20	0.04	0.16	0.25	1.0	0.13	0.53	0.08	0.34
S/N 6921 25-psi cantilever beam	5.8	0.03	0.12	0.04	0.16	0.04	0.16	0.06	0.25	0.03	0.14	0.03	0.12
S/N 6918 2,000-psi diaphragm	96	2.38	0.12	1.10	0.06	2.02	0.10	0.94	0.05	6.94	0.35	5.55	0.28
S/N 6922 2,000-psi cantilever beam	240	12.06	0.60	5.78	0.29	11.97	0.60	12.59	0.63	7.05	0.35	21.38	1.07

NOTE: All data taken from three successive step-wise loadings to full scale and back, 33 data points total; raw data input to least squares curve-fit computer program for data reduction

* Precision index defined as the standard deviation of all data ponts at a particular pressure and calculated by

$$S_i = \frac{\Sigma(\Delta Y)^2}{n - 1} ,$$

where S_i = precision index; Δy = difference between measured and calculated data points; n = number of data points at a particular pressure. Precision index also can be defined as transducer repeatability at the particular pressure level. The precision index incorporates both linearity and hysteresis of the transducer.

Overpressure Test for Low Range Transducer

An overpressure test was conducted on Senso-Metrics transducer S/N 6916 (25-psi diaphragm transducer). The purpose of the overpressure test was to determine if the transducer's sensitivity or zero offset changed when the transducer was subjected to a gross overpressure, and to determine if the transducer would ever survive the overpressure. The overpressure test data are tabulated below (test temperature = 70°F).

Output at 0 psig, mV	Output at 25 psig, mV	Output at 500 psig, mV
-0.02 (before test)	4.33	87.78
-0.02 (after test)		

Low range (25 psi) sensitivity = 0.1740 mV/psi

High range (500 psi) sensitivity = 0.1756 mV/psi

From the above data, it is clear that the 500-psi overtest did not significantly affect the zero offset or sensitivity of the 25-psi transducer. This transducer was later tested in the tension compression shear device (bare gage and embedded in propellant) and performed normally, which demonstrated the durability of the low range transducer to measure gross overpressures without degrading its performance.

4.1.3 Celesco Prototype Transducers, Self-Heating Studies

Transducer Self-Heating Tests and Diode Effects

Two Celesco transducers were chosen for self-heating evaluation. Transducer S/Ns 1 (25-psi cantilevered beam) and A (2,000-psi diaphragm) were subjected to self-heating tests at five temperatures each. The objective of the self-heating test was to determine the highest excitation level the transducer could be subjected to without heating the silicon semiconductor strain gages to a point where transducer performance would be altered. In addition, diode effect studies were conducted at two of the test temperatures. Diode effect was studied by reversing excitation leadwire polarity and measuring the resulting output.

Excitation levels between 1 and 10 mA approximately were applied to each transducer; transducer output over a period of time was measured. Graphs of

transducer output versus time for various temperatures and excitation levels for the 25-psi cantilevered beam transducer are presented in Figures 67 through 71. These figures show that an excitation level of up to 5 mA does not produce electrical change as a function of time (except at -63°F) while higher levels of excitation do change transducer electrical readings indicating self heating. The zero offset did change by 20μ V at 5-mA excitation at the -63°F test during the 15-min test.

Figures 72 and 73 show transducer output versus time at ambient temperature for two excitation levels with excitation leadwires reversed. The significance of these two graphs is the demonstration of the diode effect. Comparison of Figures 69 and 72 at 5-mA excitation and 0 min in time shows an absolute difference in transducer output of 0.246 mV at ambient temperature. This numerical change is equivalent to a 1.29% change in transducer output. At -63°F, the change is 0.241 mV or 1.25% change in transducer output. These figures demonstrate the necessity of monitoring transducer leadwire polarity with semiconductor strain gage transducers.

Figures 74 through 79 show the self-heating studies for the 2,000-psi diaphragm transducer S/N A. Again, 5-mA excitation current appears to be the optimum level. Figures 80 and 81 demonstrate the diode effect for this 2,000-psi transducer. Comparison of Figures 76 and 80 shows that at 5-mA excitation, the difference in transducer output at 0 time is 0.40% (0.002 mV) at ambient temperature. At -63°F, the diode effect amounts to 0.043 mV or 2.63% of the output. The diode effect is significant for both the 25- and 2,000-psi transducers manufactured by Celesco.

4.1.4 Self-Heating Studies for Senso-Metrics Prototype Transducers

Two Senso-Metrics transducers were chosen for self-heating testing. Testing was the same as that done on the Celesco prototypes. Transducer S/N 6916 (25-psi diaphragm) was subjected to both bare gage and embedded self-heating tests at several temperatures and excitation levels. Figures 82 through 85 show the self-heating effects on the bare gage; Figures 86 through 89 show the self-heating effects on the tranaducer embedded in propellant. An excitation

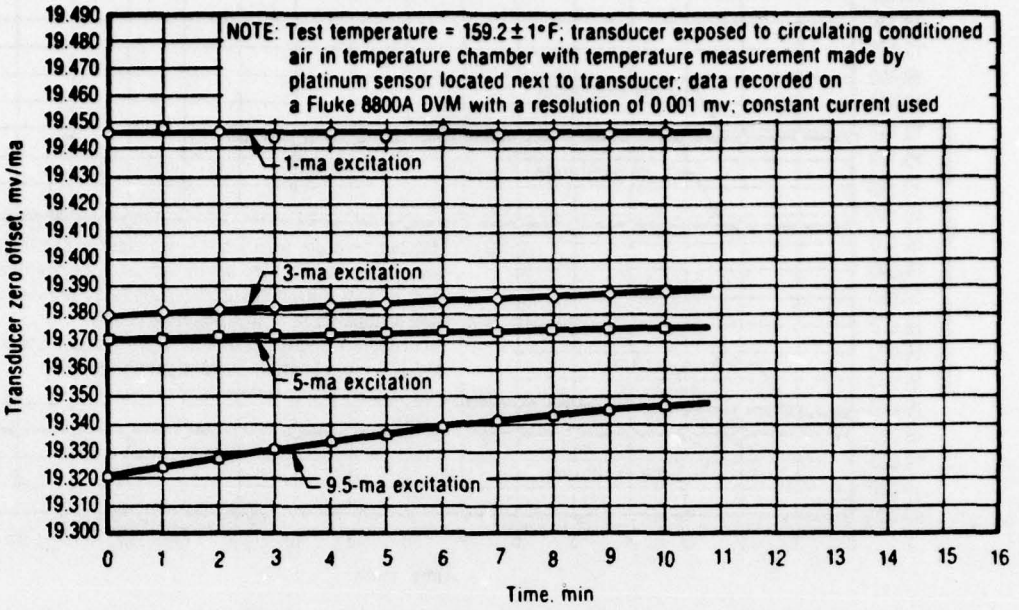


Figure 67. Celesco Prototype Transducer S/N 1 - 25-psi Cantilevered Beam (Self-Heating Stability Test Without Propellant; Excitation Leadwires Connected Normally)

17228

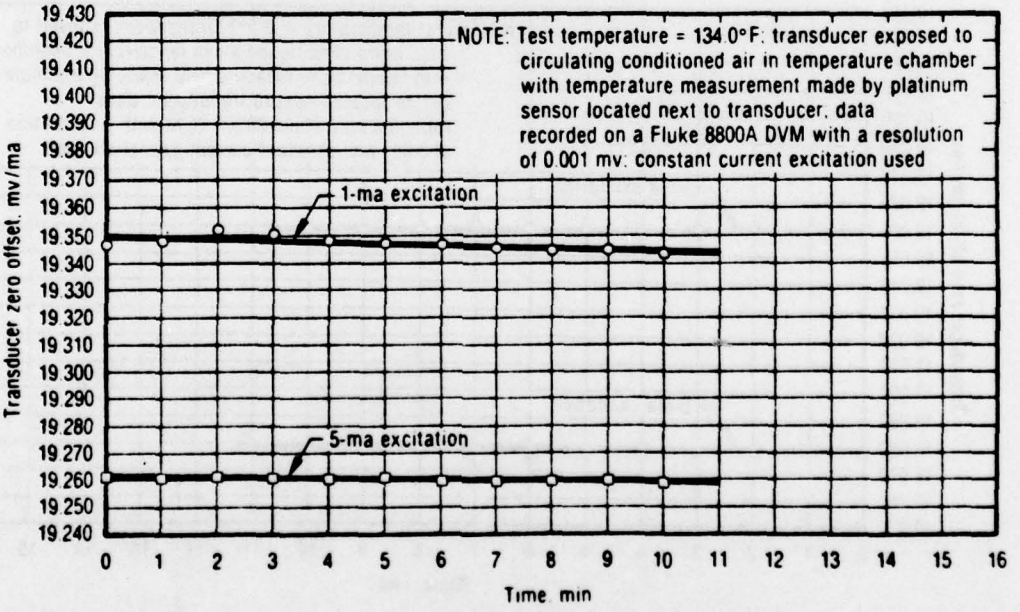


Figure 68. Celesco Prototype Transducer S/N 1 - 25-psi Cantilevered Beam (Self-Heating/Stability Test Without Propellant; Excitation Leadwires Connected Normally)

17229

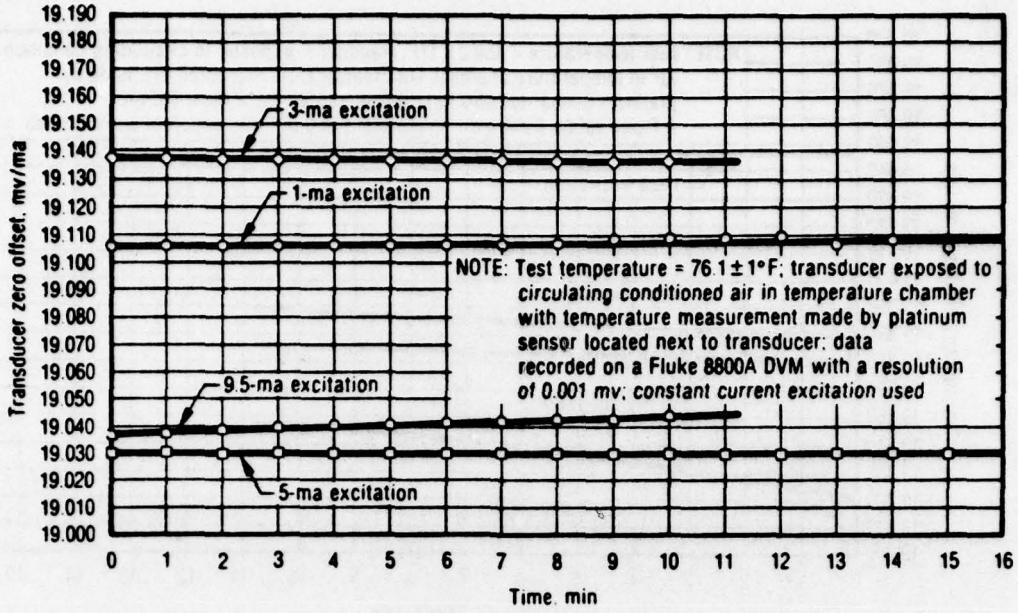


Figure 69. Celesco Prototype Transducer S/N 1 - 25-psi Cantilevered Beam (Self-Heating/Stability Test Without Propellant; Excitation Leadwires Connected Normally)

17230

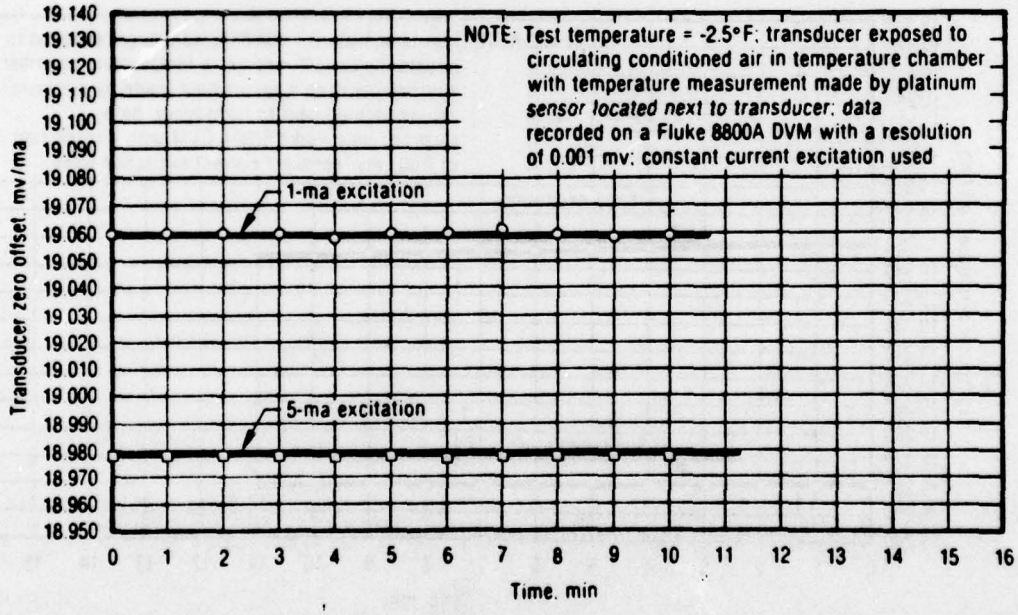


Figure 70. Celesco Prototype Transducer S/N 1 - 25-psi Cantilevered Beam (Self-Heating/Stability Test Without Propellant; Excitation Leadwires Connected Normally)

17231

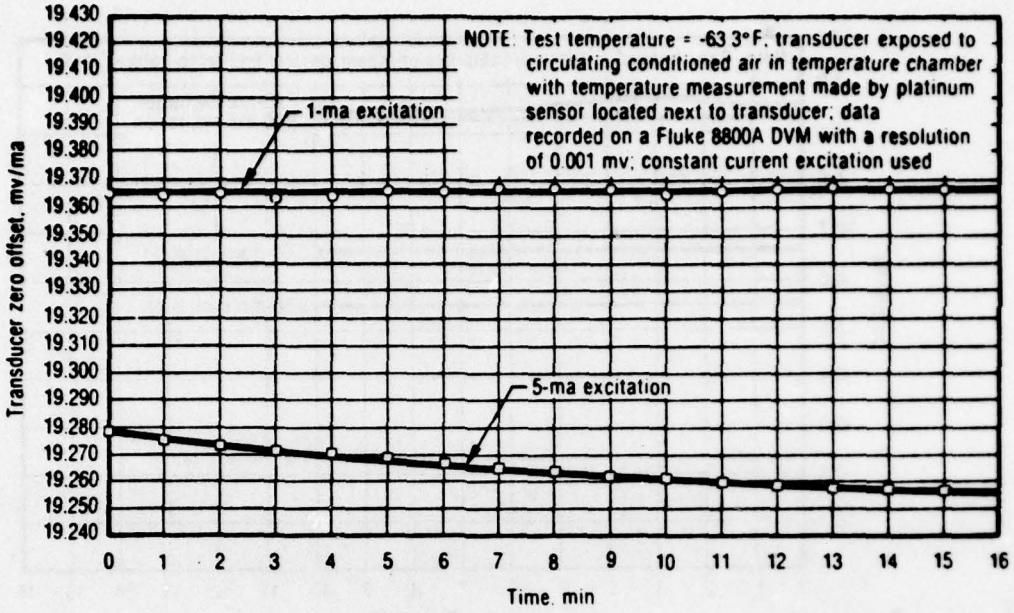


Figure 71. Celesco Prototype Transducer S/N 1 - 25-psi Cantilevered Beam (Self-Heating/Stability Test Without Propellant; Excitation Leadwires Connected Normally)

17232

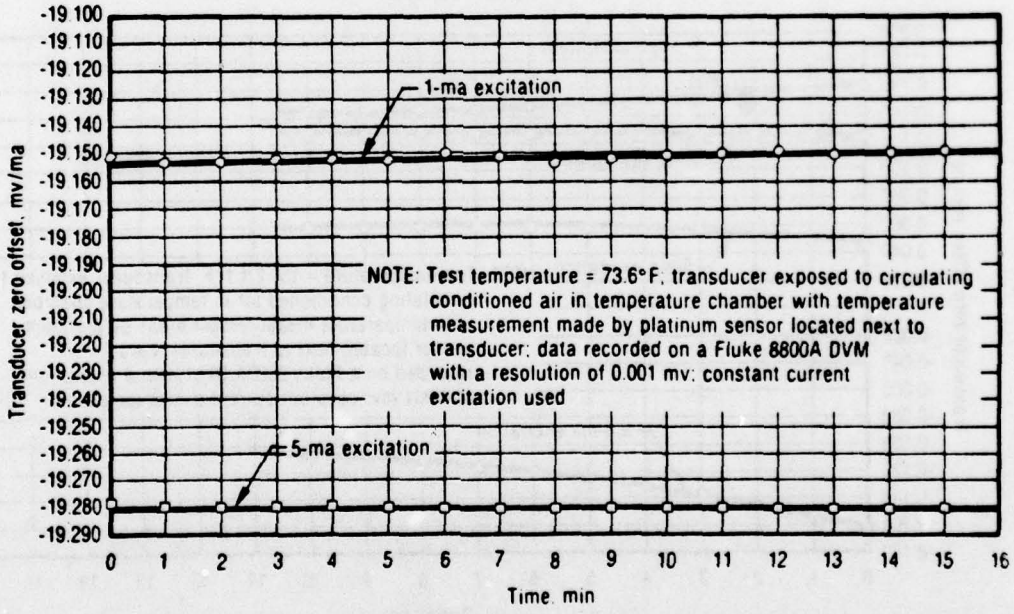


Figure 72. Celesco Prototype Transducer S/N 1 - 25-psi Cantilevered Beam (Self-Heating/Stability Test Without Propellant; Excitation Leadwires Reversed)

17227

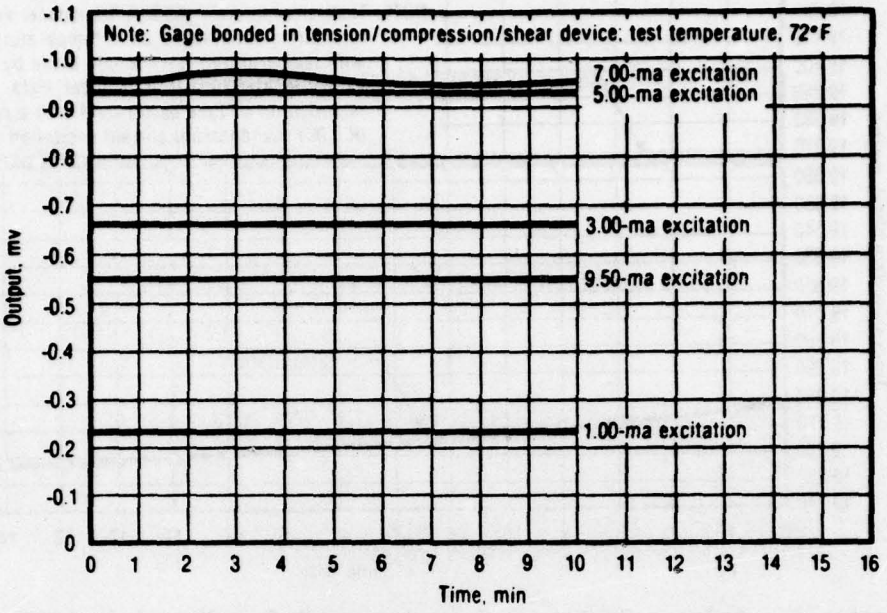


Figure 73. Celesco Prototype Transducer S/N 1 - 25-psi Cantilevered Beam (Self-Heating/Stability Test Without Propellant; Excitation Leadwires Reversed)

17170

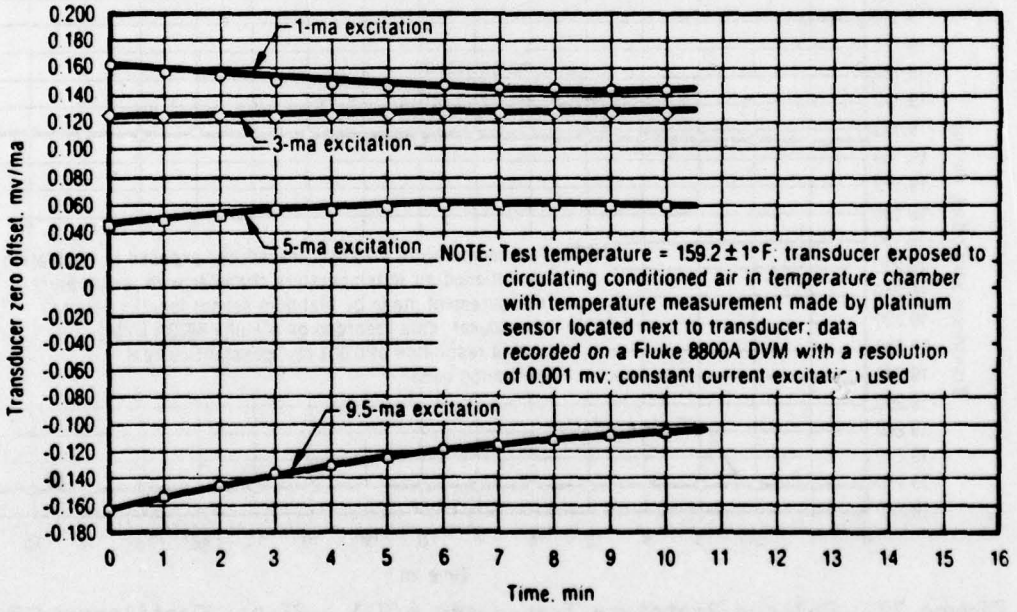


Figure 74. Celesco Prototype Transducer S/N A - 2,000-psi Flat Diaphragm (Self-Heating/Stability Test Without Propellant; Excitation Leadwires Connected Normally)

17235

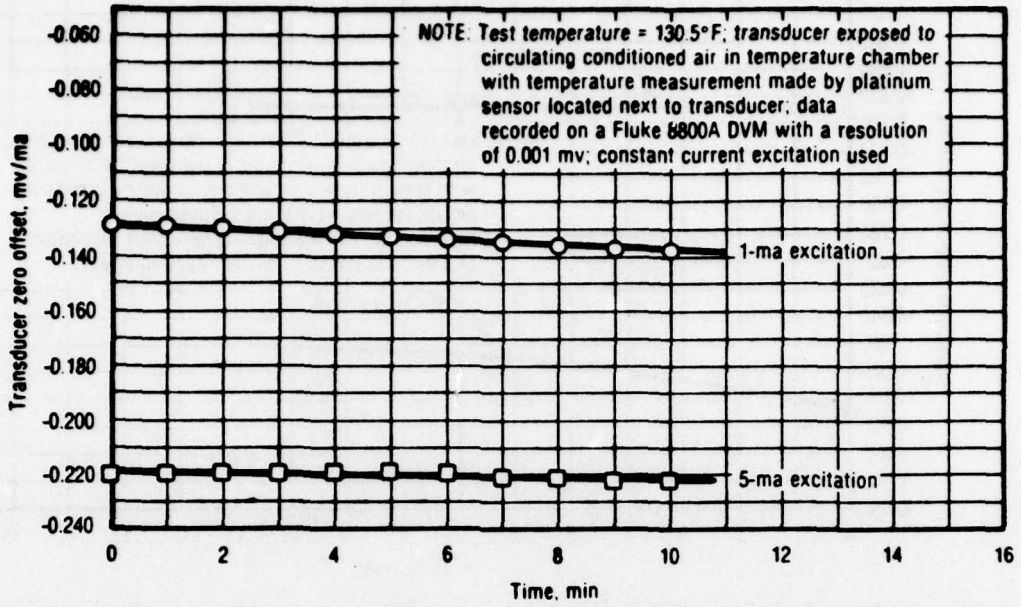


Figure 75. Celesco Prototype Transducer S/N A - 2,000-psi Flat Diaphragm (Self-Heating/Stability Test Without Propellant; Excitation Leadwires Connected Normally)

17236

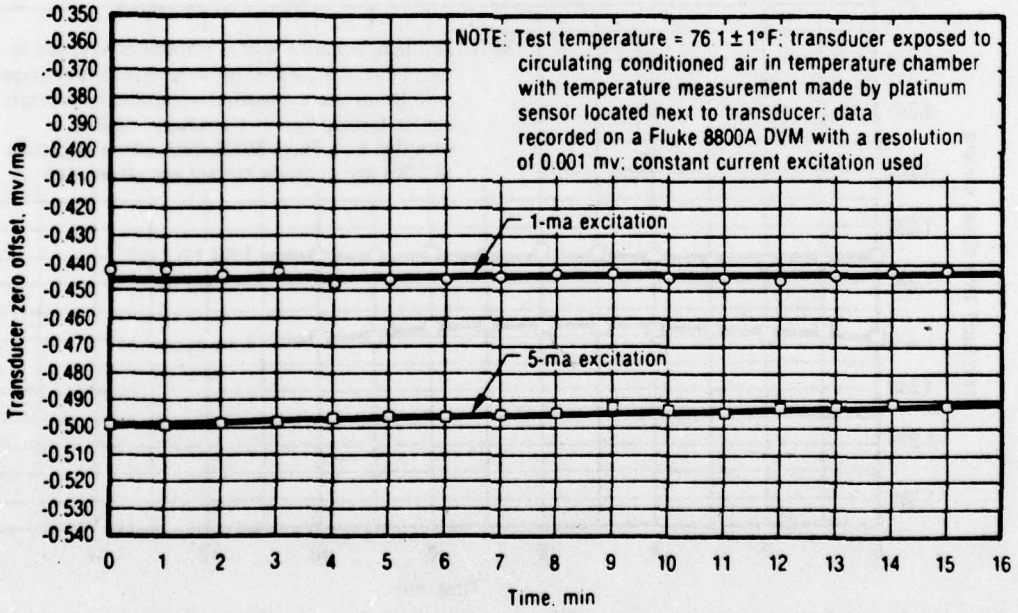


Figure 76. Celesco Prototype Transducer S/N A - 2,000-psi Flat Diaphragm (Self-Heating/Stability Test Without Propellant; Excitation Leadwires Connected Normally)

17237

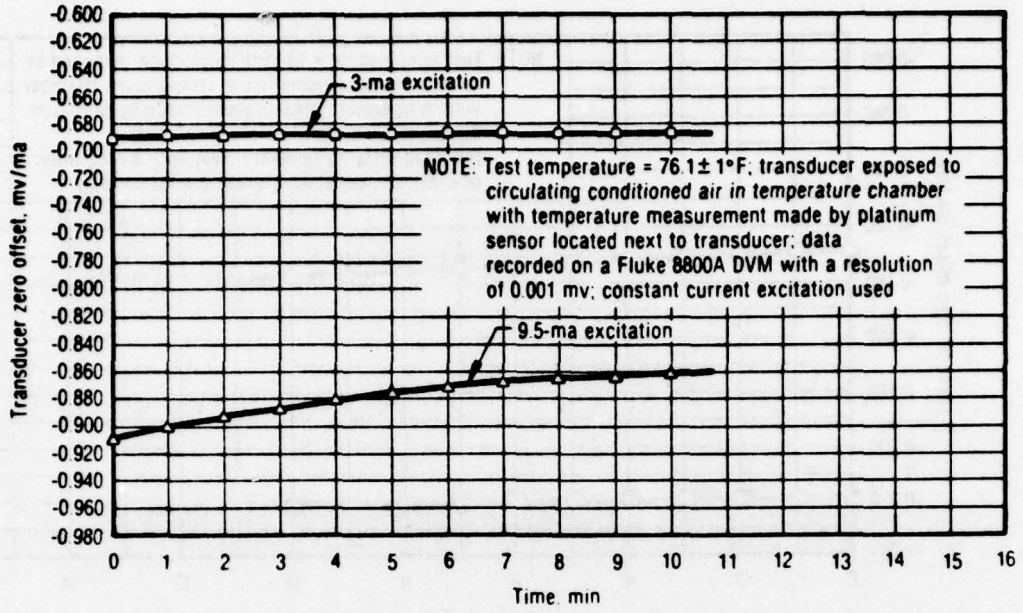


Figure 77. Celesco Prototype Transducer S/N A - 2,000-psi Flat Diaphragm (Self-Heating/Stability Test Without Propellant; Excitation Leadwires Connected Normally)

17238

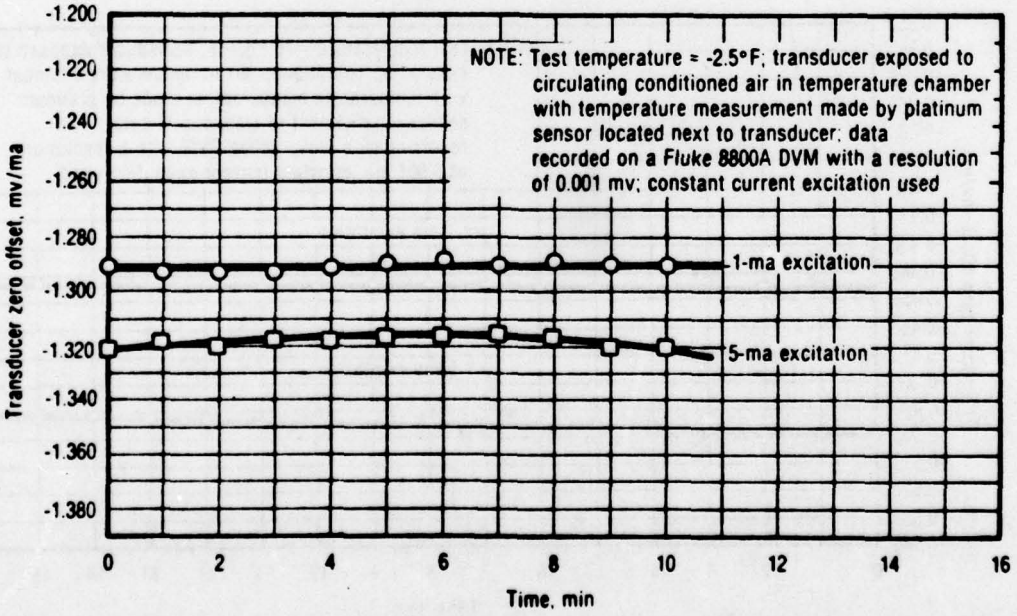


Figure 78. Celesco Prototype Transducer S/N A - 2,000-psi Flat Diaphragm (Self-Heating/Stability Test Without Propellant; Excitation Leadwires Connected Normally)

17239

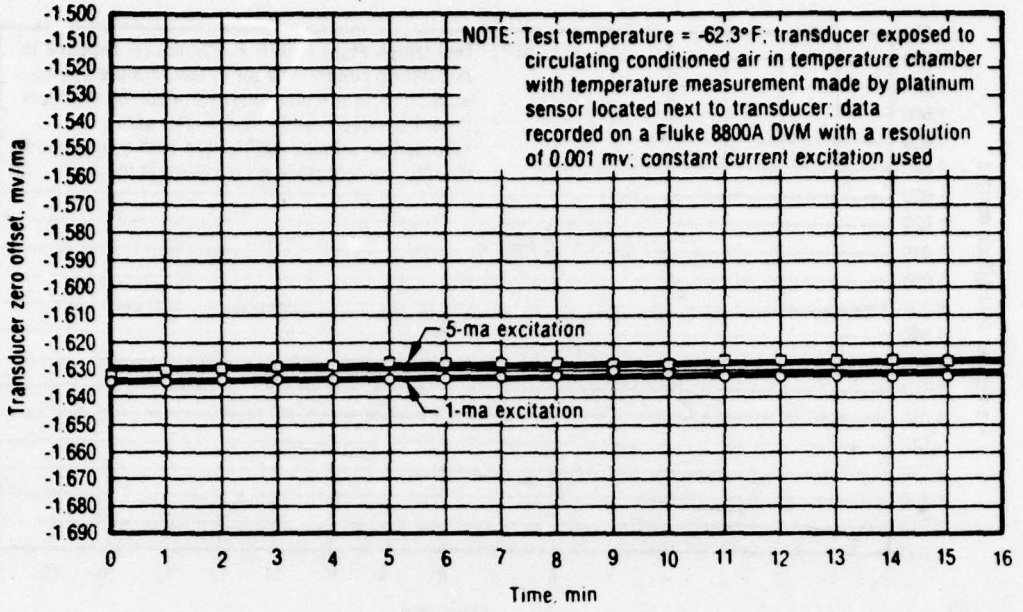


Figure 79. Celesco Prototype Transducer S/N A - 2,000-psi Flat Diaphragm (Self-Heating/Stability Test Without Propellant; Excitation Leadwires Connected Normally)

17240

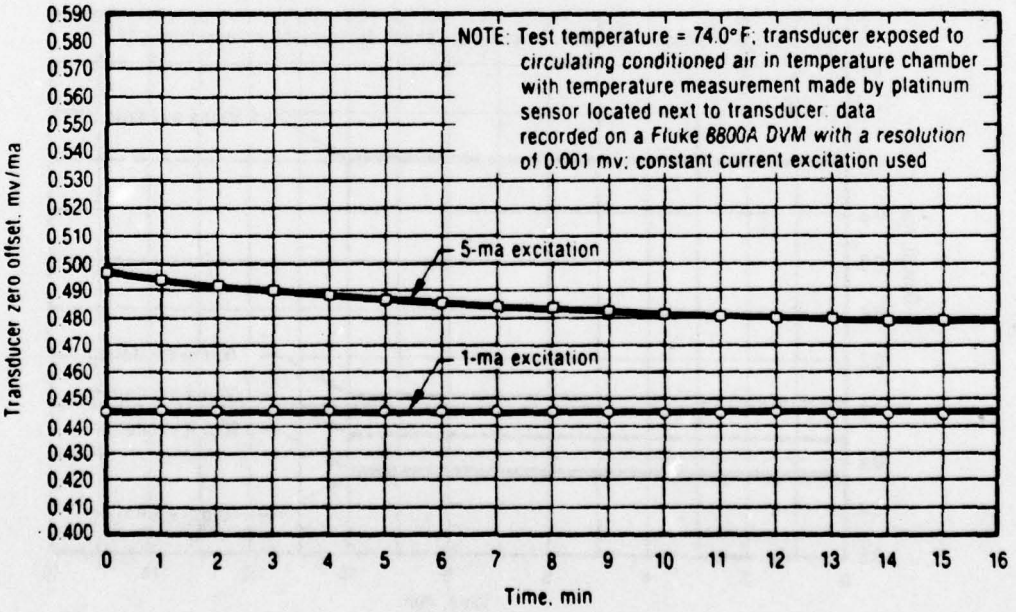


Figure 80. Celesco Prototype Transducer S/N A - 2,000-psi Flat Diaphragm (Self-Heating/Stability Test Without Propellant; Excitation Leadwires Reversed)

17234

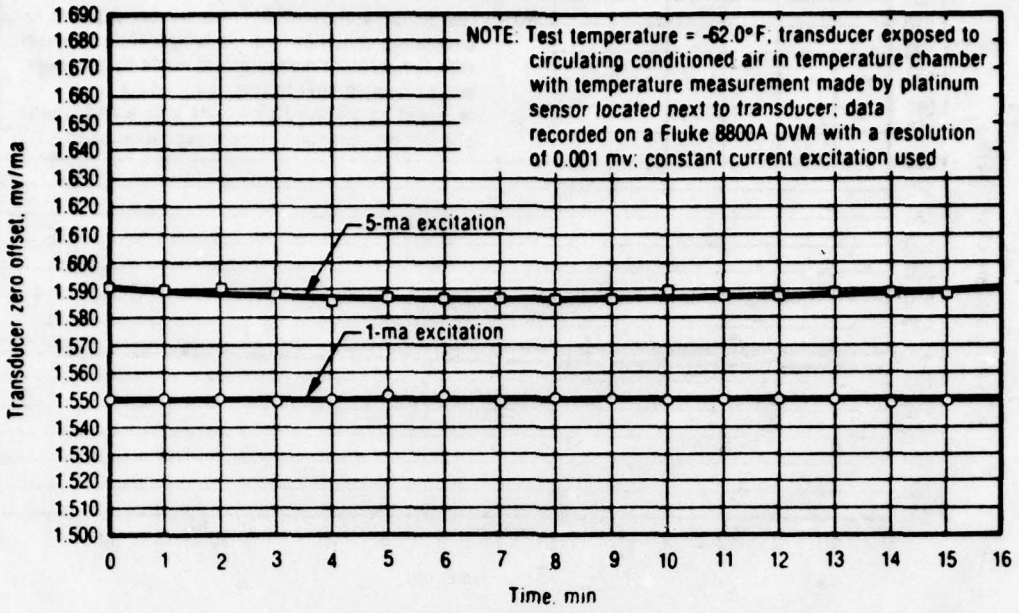


Figure 81. Celesco Prototype Transducer S/N A - 2,000-psi Flat Diaphragm (Self-Heating/Stability Test Without Propellant; Excitation Leadwires Reversed)

17233

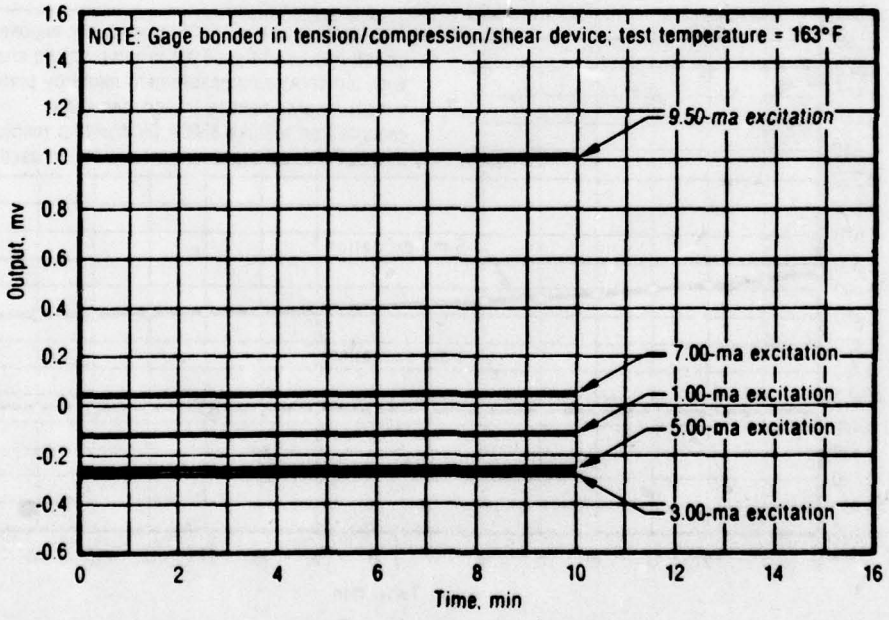


Figure 82. Senso-Metrics Transducer S/N 6916 - 25-psi Range (Self-Heating Effects on Bare Gage Bonded in Tension/Compression/Shear Device; Test Temperature = 163°F)

17169

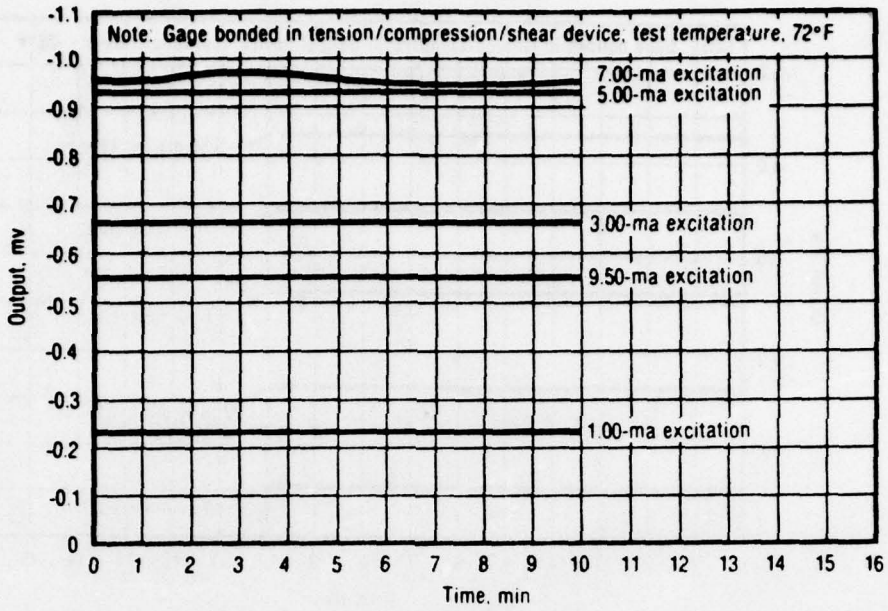


Figure 83. Senso-Metrics Transducer S/N 6916 - 25-psi Range (Self-Heating Effects on Bare Gage Bonded in Tension/Compression/Shear Device; Test Temperature = 72°F) 17170

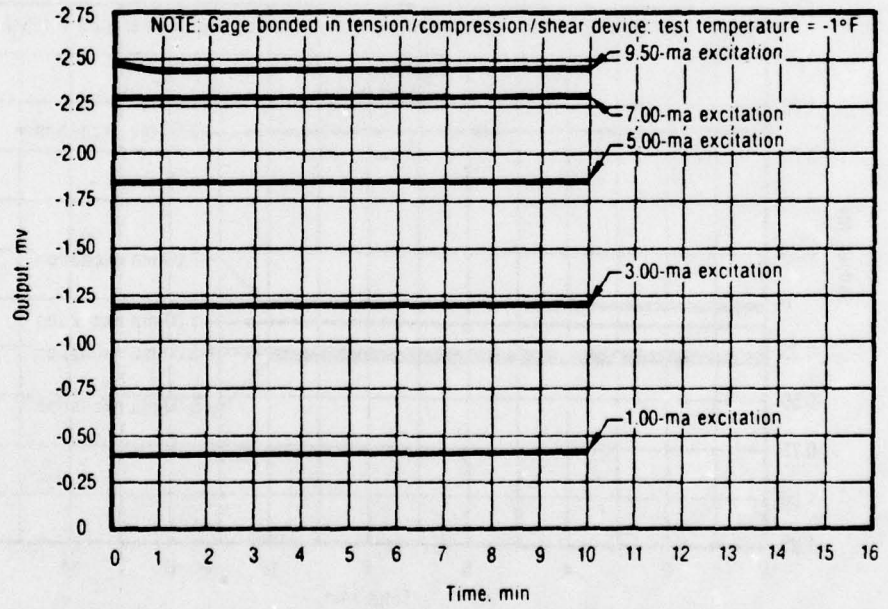


Figure 84. Senso-Metrics Transducer S/N 6916 - 25-psi Range (Self-Heating Effects on Bare Gage with Gage Bonded in Tension/Compression/Shear Device; Test Temperature = -1°F) 17171

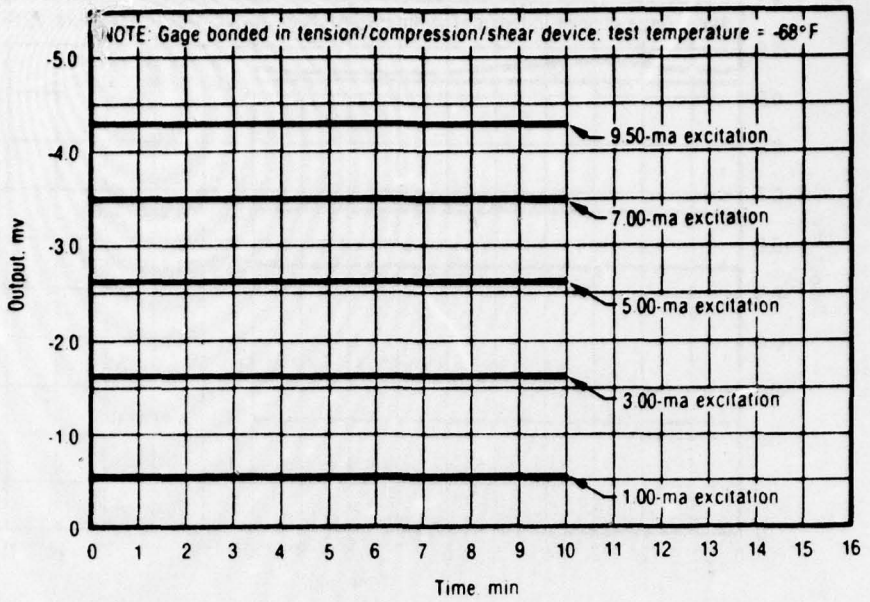


Figure 85. Senso-Metrics Transducer S/N 6916 - 25-psi Range (Self-Heating Effects on Bare Gage Bonded in Tension/Compression/Shear Device; Test Temperature = -68°F) 17172

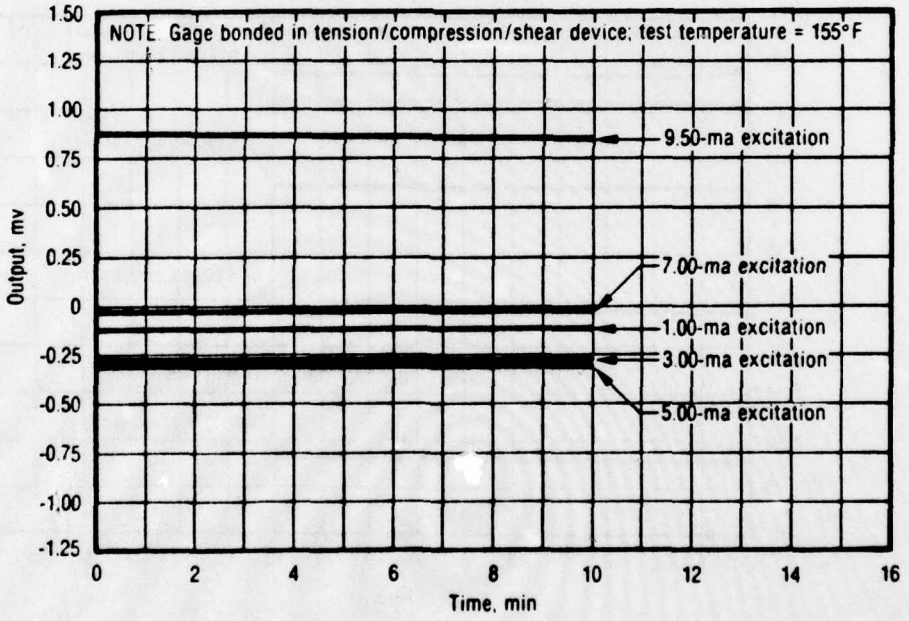


Figure 86. Senso-Metrics Transducer S/N 6916 - 25-psi Range (Self-Heating Effects While Embedded in Propellant with Gage Bonded in Tension/Compression/Shear Device; Test Temperature = 155°F) 17173

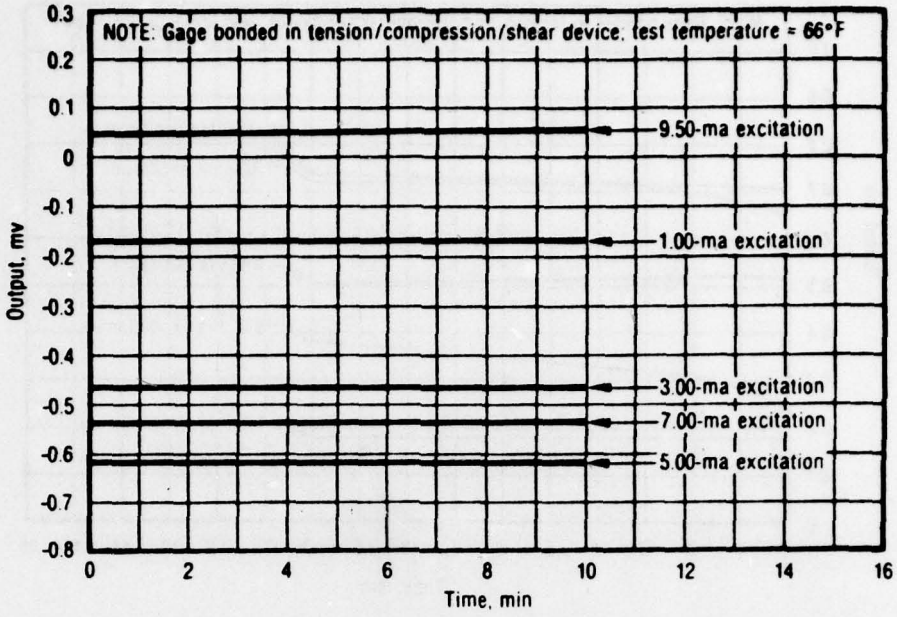


Figure 87. Senso-Metrics Transducer S/N 6916 - 25-psi Range (Self-Heating Effects While Embedded in Propellant with Gage Bonded in Tension/Compression/ Shear Device; Test Temperature = 66°F) 17174

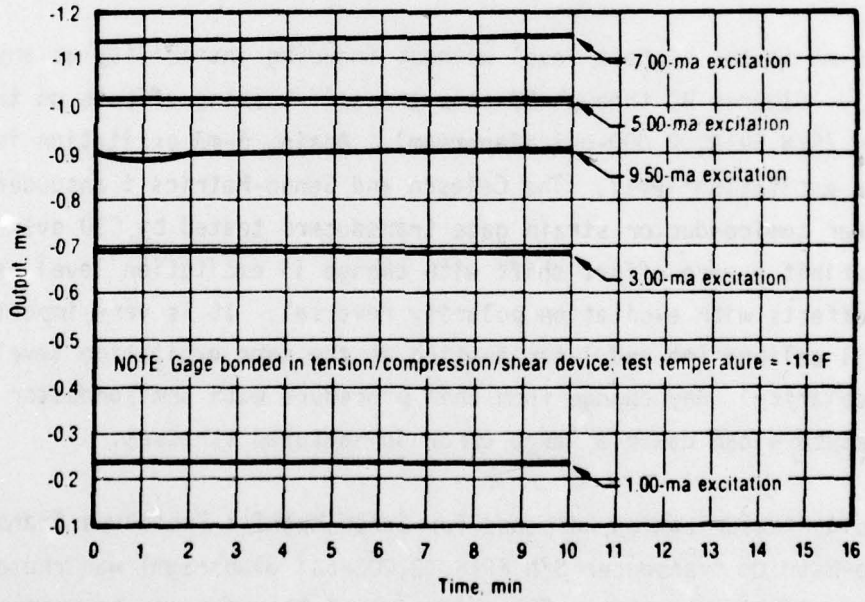


Figure 88. Senso-Metrics Transducer S/N 6916 - 25-psi Range (Self-Heating Effects While Embedded in Propellant with Gage Bonded in Tension/Compression/ Shear Device; Test Temperature = -11°F) 17175

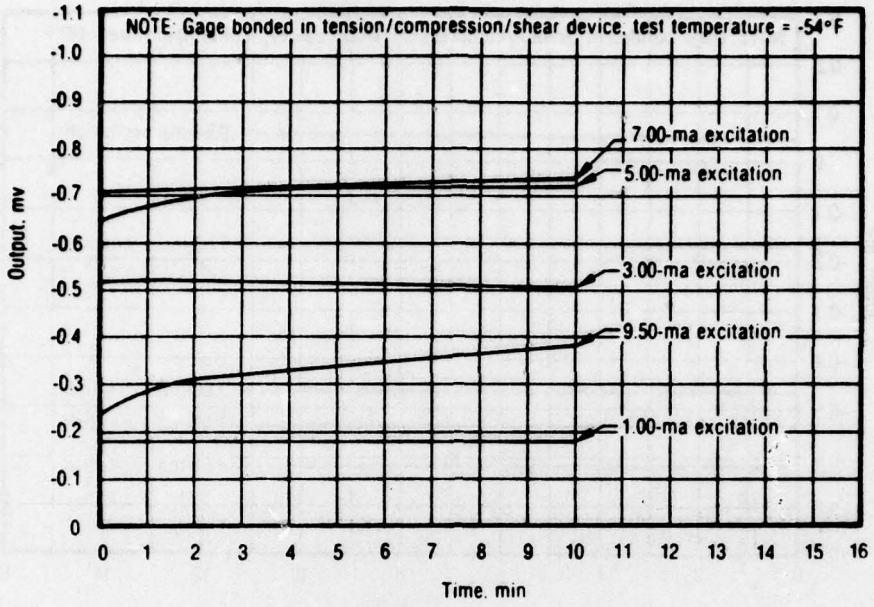


Figure 89. Senso-Metrics Transducer S/N 6916 - 25-psi Range (Self-Heating Effects While Embedded in Propellant with Gage Bonded in Tension/Compression/Shear Device; Test Temperature = -54°F) 17176

level of 5 mA is the highest level without inducing instability at any temperature level. Figures 90 through 93 show the self-heating effects on the bare transducer (S/N 6918, 2,000-psi diaphragm). Again, 5-mA excitation is the highest stable excitation level. The Celesco and Senso-Metrics transducers as well as all other semiconductor strain gage transducers tested by CSD over the last 3 years exhibit a zero offset shift with change in excitation level as well as diode effects with excitation polarity reversal. It is very important to conduct all calibration and later testing at the same excitation level and with the same polarity. Any change from this procedure with semiconductor strain gage transducers can cause a large error in measured stresses.

4.1.5 Rapid Pressurization Response for Senso-Metrics Prototype Transducer

Senso-Metrics transducer S/N 6918 (2,000-psi diaphragm) was chosen for rapid pressurization testing. The objective of the test was to measure the response characteristics of the design under ignition-type loading rates as well as its accuracy in pressure measurement. The test vehicle chosen was a

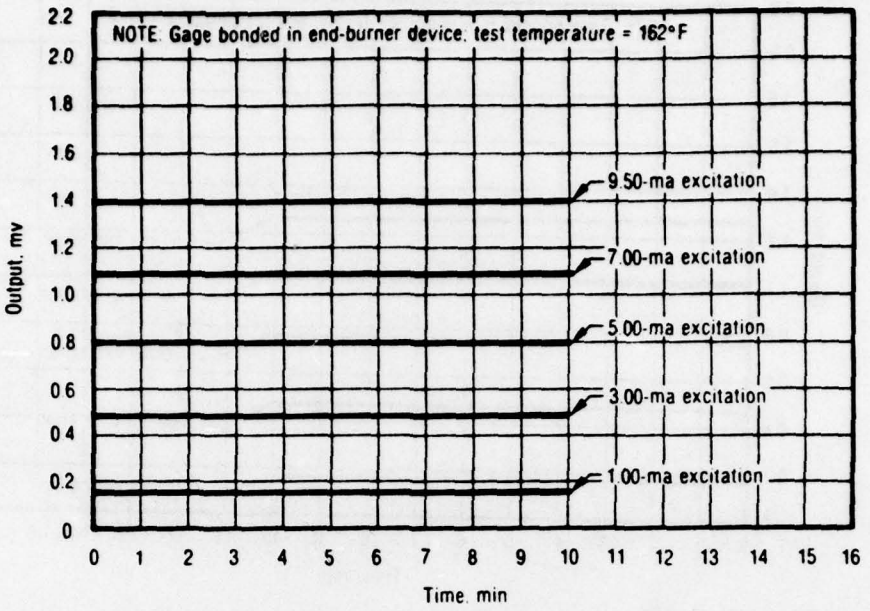


Figure 90. Senso-Metrics Transducer S/N 6918 - 2,000-psi Range (Self-Heating Effects on Bare Gage with Gage Bonded in End-Burner Device; Test Temperature = 162°F)

17177

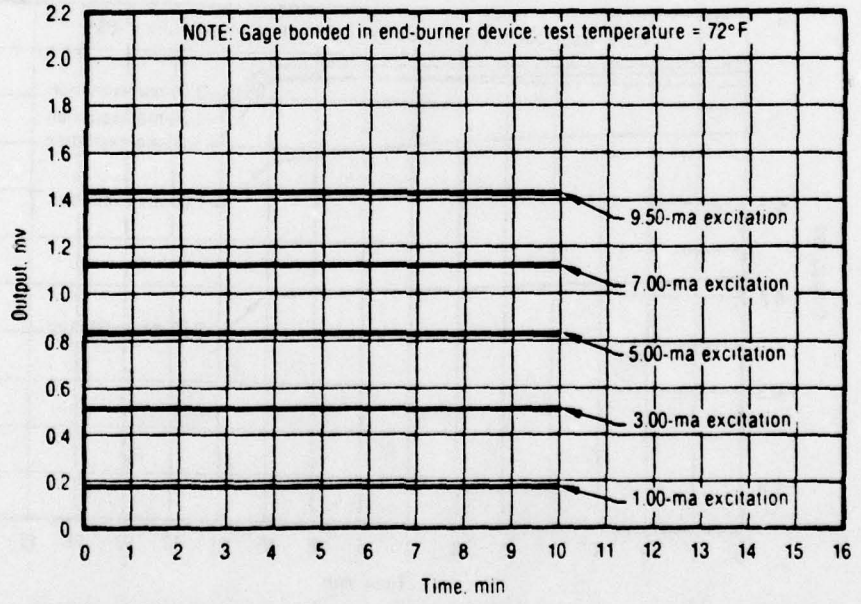


Figure 91. Senso-Metrics Transducer S/N 6918 - 2,000-psi Range (Self-Heating Effects on Bare Gage with Gage Bonded in End-Burner Device; Test Temperature = 72°F)

17178

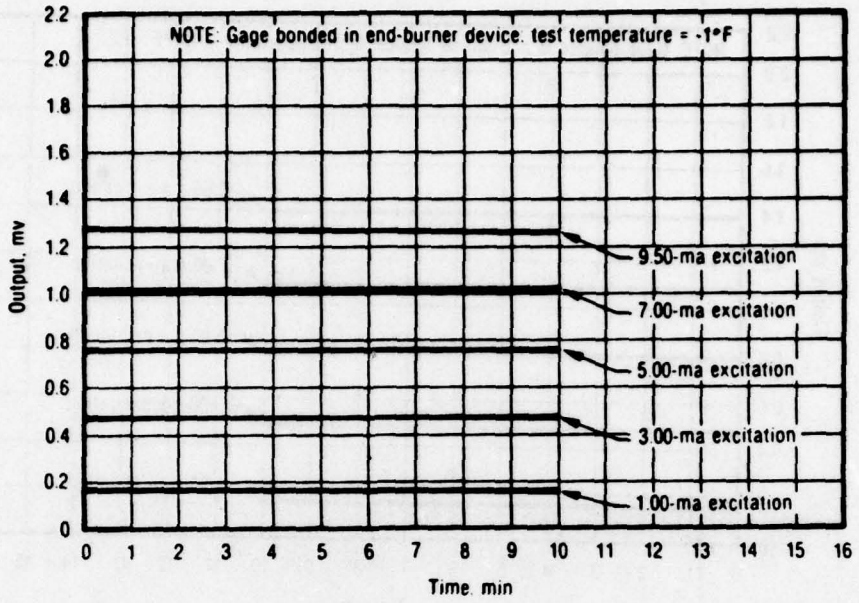


Figure 92. Senso-Metrics Transducer S/N 6918 - 2,000-psi Range (Self-Heating Effects on Bare Gage with Gage Bonded in End-Burner Device; Test Temperature = -1°F)

17179

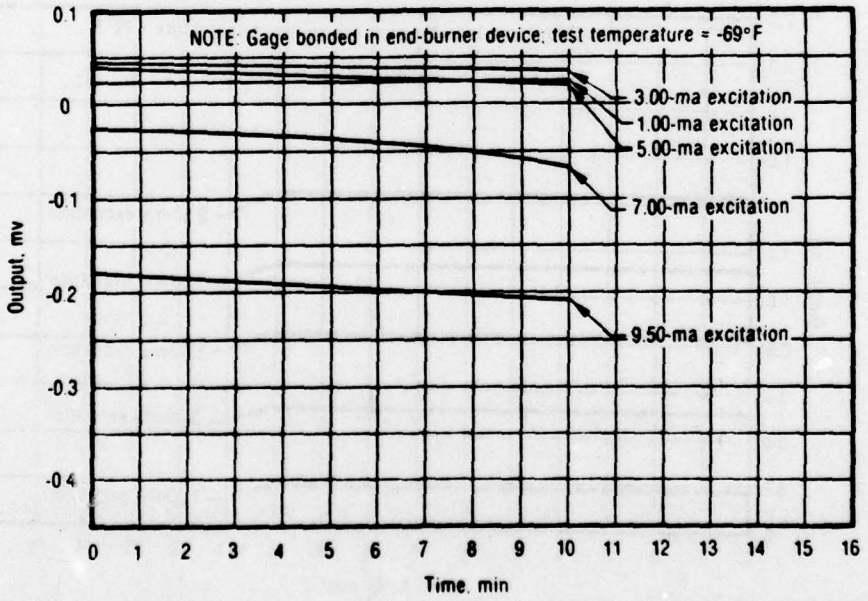


Figure 93. Senso-Metrics Transducer S/N 6918 - 2,000-psi Range (Self-Heating Effects on Bare Gage with Gage Bonded in End-Burner Device; Test Temperature = -69°F)

17180

large end-burner (Figure 94). The vehicle was approximately 10 in. in ID and 10-in. deep. The transducer was bonded on the geometrical center of the base. The top of the vessel was closed with a pressure seal plate. The transducer first was subjected to bare gage testing. The vessel was filled with silicone fluid and dry nitrogen was used for the rapid pressurization. All testing was conducted at 73°F. Several tests were run at ramp times varying between 29 msec and 1.07 sec. Data were recorded on a high speed oscillograph. Table 25 presents the data summary for these tests. The gage response varied an average of 2.03% from the applied pressure measured by the Taber pressure transducer.

After the bare gage tests were completed, the end-burner device was filled with propellant. After cure, high rate tests again were conducted. A copper-constantan thermocouple was mounted in the vehicle approximately 1 in. away from the transducer. The purpose of this thermocouple was not only to measure the test temperature, but also to record any compression heating during rapid pressurization. All data were again recorded on an oscillograph and resolution of the thermocouple signal was approximately 10°F/chart-in. No discernible change in test temperature was measured during the rapid pressurization tests. Graphical data from the pressurization tests are presented in Figures 95 through 97. The raw pressure applied was measured by a Taber pressure transducer; this pressure then was corrected to get the pressure actually present at the transducer location. The transducer recorded pressure is shown along with its corrected value accounting for disturbance and interaction. The corrected transducer stress varies from the corrected Taber pressure by an average of 3.3% at peak pressure over the three loading rates.

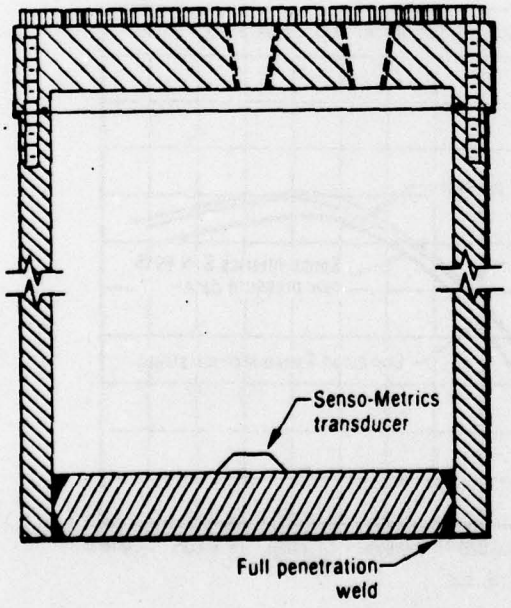


Figure 94. Transducer/Propellant Test Fixture

17168

TABLE 25. HIGH RATE PRESSURIZATION RESPONSE (WITHOUT PROPELLANT) FOR SENSO-METRICS STRESS TRANSDUCER (S/N 6918; 2,000-PSI DIAPHRAGM GAGE)

T4581-D

Test Date	Test No.	Ramp Time, sec	Taber Pressure, psi	Senso-Metrics Pressure, psi	% Pressure Deviation, Senso-Metrics/ Taber
9-1-77	1	0.0288	1,172.30	1,180.66	0.71
9-1-77	2	0.0302	1,237.56	1,247.15	0.77
9-1-77	3	0.0402	778.53	756.50	-2.83
9-1-77	4	0.0679	888.79	868.02	-2.34
9-1-77	5	0.0993	848.29	820.88	-3.23
9-1-77	6	0.1109	897.79	876.60	-2.36
9-1-77	7	0.3992	920.29	900.19	-2.18
9-2-77	8	0.6474	884.03	894.06	1.12
9-2-77	9	0.8510	886.29	901.68	1.71
9-2-77	10	0.9126	863.74	892.81	3.26
9-2-77	11	1.0659	906.59	923.80	1.86

NOTE: Test temperature = 73°F

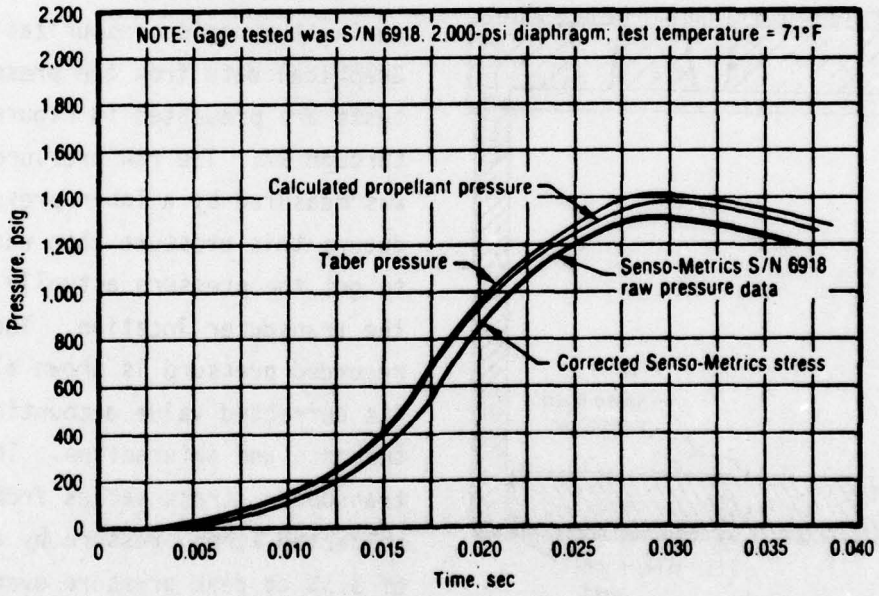


Figure 95. Pressure vs Time for High Rate Pressure Test of the End-Burner Device with Embedded 2,000-psi Transducer

17164

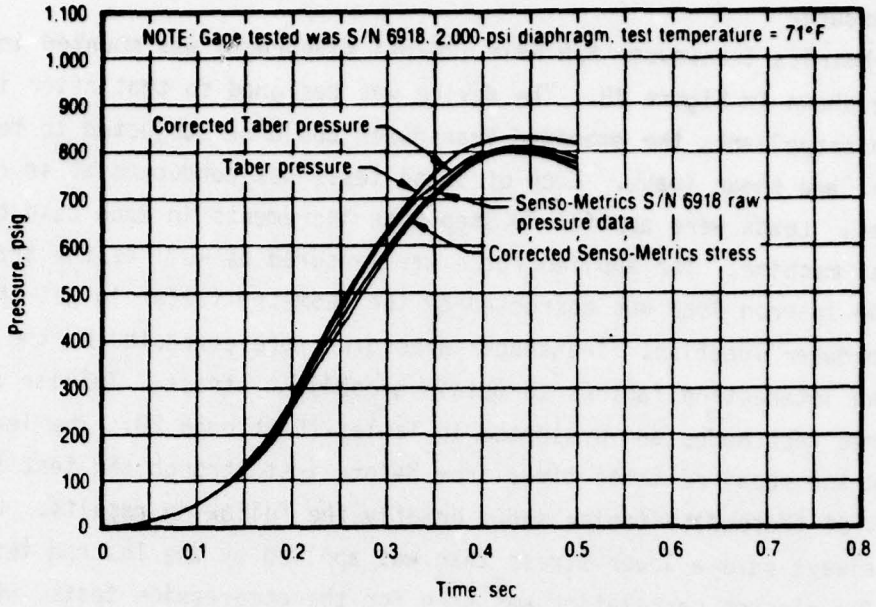


Figure 96. Pressure vs Time for High Rate Pressure Test of the End-Burner Device with Embedded 2,000-psi Transducer

17165

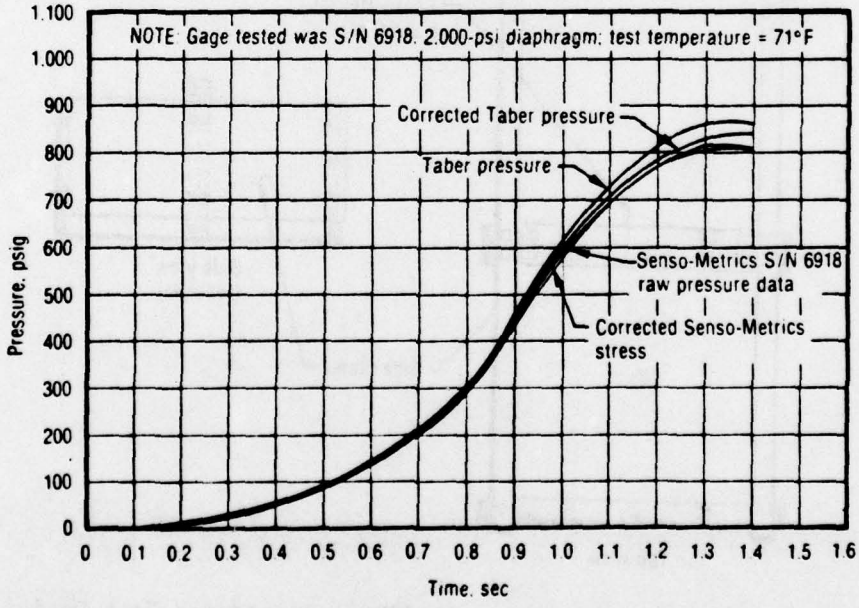


Figure 97. Pressure vs Time for High Rate Pressure Test of the End-Burner Device with Embedded 2,000-psi Transducer

17166

4.1.6 Tests in Tension/Compression/Shear Device for Senso-Metrics Prototype Transducer

Senso-Metrics transducer S/N 6916 (25-psi diaphragm) was mounted in the test device shown in Figure 98. The device was designed so that after it was filled with propellant, the embedded transducer could be subjected to tension, compression, and shear loads. Each of these tests was conducted at several temperatures. Loads were applied in step-wise increments in each case by an Instron test machine. The applied force was measured as well as the transducer output. The Instron load was corrected by the geometry factor to get the stress at the transducer location. Transducer pressures were corrected by the disturbance and interaction factors to obtain propellant stress. Tabular data for all three test modes are presented in Tables 26 through 28. The leadwires were broken and repaired three times from before test through the test sequence. An analysis of these data tables shows briefly the following results. Overall, the gages always gave a lower stress than was applied by the Instron testing machine. The closest correlation was seen for the compression tests, where the gage was only low by about 5%. For the tension test, the gage reading de-

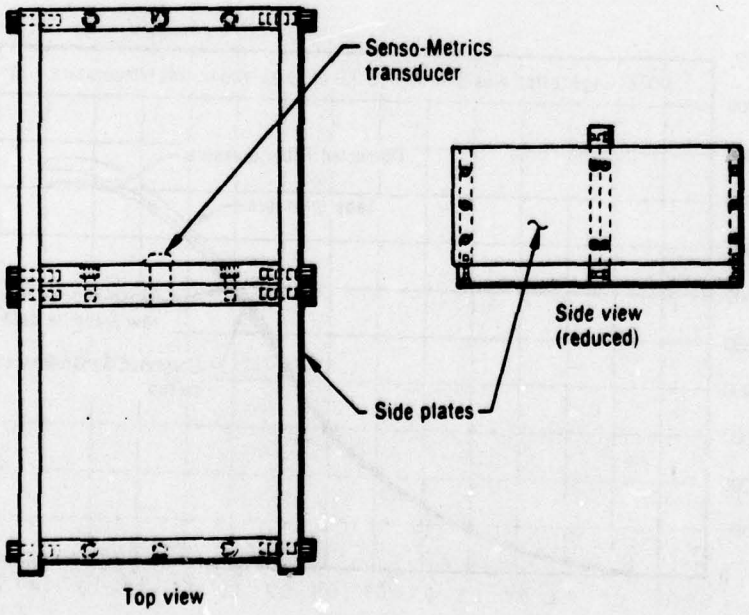


Figure 98. Tension/Compression/Shear Transducer Test Device

17167

TABLE 26. COMPRESSION TEST RESULTS FOR TENSION/COMPRESSION/SHEAR DEVICE

T4578-D

Test Temperature, °F	Average Instron Stress, psi	Corrected Instron Stress,* psi	Uncorrected Transducer Pressure, psi	Corrected Transducer Stress,† psi	Ratio, corrected Instron stress / corrected transducer stress
77	0	0			
	4.94	4.75	4.43	4.10	1.16
	8.03	7.72	7.16	6.63	1.16
	14.89	14.32	14.49	13.41	1.07
	20.69	19.90	20.63	19.10	1.04
120	0	0			
	8.44	8.12	7.39	6.84	1.19
	12.72	12.24	11.67	10.80	1.13
	17.50	16.84	17.43	16.13	1.04
	20.97	20.17	21.28	19.70	1.02
152	0	0			
	8.36	8.04	7.48	6.92	1.16
	12.58	12.10	11.56	10.70	1.13
	16.67	16.04	15.75	14.58	1.10
	20.86	20.07	19.83	18.36	1.09
-1	0	0			
	4.25	4.09	4.07	3.77	1.08
	8.39	8.07	8.32	7.70	1.05
	12.50	12.03	12.88	11.92	1.01
	16.72	16.08	17.49	16.19	0.99
	20.94	20.14	22.14	20.49	0.98
-82	0	0			
	4.36	4.19	2.09	1.93	2.17
	8.61	8.28	4.69	4.34	1.91
	12.72	12.24	7.97	7.38	1.66
	16.78	16.14	11.43	10.58	1.53
	20.92	20.13	15.01	13.89	1.45

NOTE: Gage tested was S/N 6916, 25-psi diaphragm Senso-Metrics prototype

* Corrected Instron stress = (average Instron stress) (0.962), where 0.962 is the average stress correction factor for a pressure load

† Corrected transducer stress = (uncorrected transducer pressure) (0.9257), where 0.9257 = (transducer interaction factor) (transducer disturbance factor) for a pressure load

TABLE 27. TENSILE TEST RESULTS FOR TENSION/COMPRESSION/SHEAR DEVICE

T4579-D

Test Temperature, °F	Average Instron Stress, psi	Corrected Instron Stress, psi	Uncorrected Transducer Pressure, psi	Corrected Transducer Stress,† psi	Ratio, correct corrected	Instron stress transducer stress
69	0	0				
	2.00	1.92	1.62	1.50		1.28
	6.31	6.07	5.10	4.72		1.29
	8.36	8.04	6.98	6.46		1.24
	10.42	10.02	8.86	8.20		1.22
-5	0	0				
	2.11	2.03	1.74	1.61		1.26
	4.25	4.09	3.50	3.24		1.26
	7.25	6.97	5.33	4.93		1.41
	8.53	8.21	6.98	6.46		1.27
	9.92	9.54	8.21	7.60		1.26
-67	0	0				
	2.44	2.35	1.20	1.11		2.12
	4.36	4.19	2.23	2.06		2.03
	6.44	6.20	3.57	3.30		1.88
	8.50	8.18	4.89	4.53		1.81
	10.53	10.13	6.32	5.85		1.73

NOTE: Gage tested was S/N 6916, 25-psi diaphragm Senso-Metrics prototype

* Corrected Instron stress = (average Instron stress)(0.962), where 0.962 is the average stress correction factor for a pressure load

† Corrected transducer stress = (uncorrected transducer pressure)(0.9257), where 0.9257 = (transducer interaction factor) (transducer disturbance factor) for a pressure load

TABLE 28. SHEAR TEST RESULTS FOR TENSION/COMPRESSION/SHEAR DEVICE T4580-D

Test Temperature, °F	Average Instron Stress, psi	Uncorrected Transducer Pressure,* psi
72	1.03	0.22
	2.10	0.38
	3.13	0.43
	4.15	0.39
	4.86	0.35
-4	2.07	0.59
	4.15	0.67
	6.25	0.24
	8.33	0.46
	10.43	0.80
-75	4.19	0.33
	6.28	0.51
	8.35	0.58
	10.39	0.55

NOTE: Gage tested was S/N 6916, 25-psi diaphragm Senso-Metrics prototype

* Transducer pressure recorded was a normal pressure

noted a stress about 25% lower than the Instron. And, at the coldest test temperature, the differences ranged from 45% to 117%. The difference between tension and compression results may be ascribed to some local unbonding around the diaphragm. With a local unbond (not a void), the gage would read correctly in compression but incorrectly in tension since in tension only some of the propellant stress would be transferred to the diaphragm surface.

A more critical look at the compression data was taken in Figure 99 where the corrected Instron and gage stresses are plotted against one another. In this plot, it can be seen that the high temperature data are quite good if a slight offset at the zero loading condition is assumed. Note particularly the 77 and 120°F data fit quite well to a 45° line with an offset of 1 psi. This offset is logical when considering the difficulties in performing this experiment. A very large, heavy, and cumbersome test sample had to be fit in the Instron machine and could easily have been slightly misaligned to cause this initial shift. This explanation would also befit the low temperature data (-82° F) since the effect is purely a function of strain. All tests were performed to a constant stress of

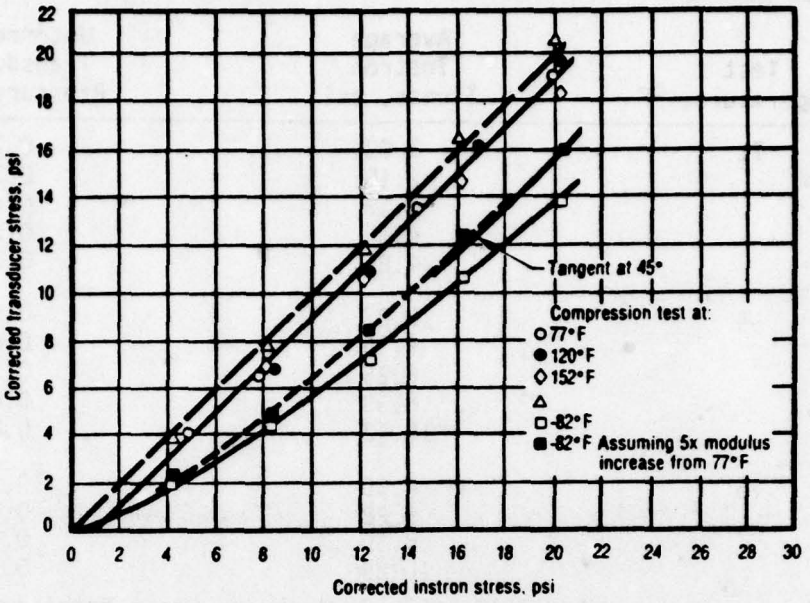


Figure 99. Compression Test Results in Compression/Tension/Shear Device, Preliminary Gage Design

18511

about 20 psi, so at the cold temperature the strain would be much lower due to the increased propellant modulus. The curve for this -82°F data is shown to be approaching the 45° tangent line (direct correlation). If this hypothesis of an experimental test set up shift is correct, then the data are quite good.

It may also be noted that the disturbance and interaction factors applied to the gage data were based on finite element calculations at a constant propellant modulus. However, increasing this modulus by a factor of 5 to simulate the cold temperature tests would change the final results by about 7%, giving even better correlation for this data, as plotted by the "tangent line" in Figure 99.

4.2 PRODUCTION TRANSDUCER CALIBRATIONS

4.2.1 Gaseous Nitrogen Calibrations for Senso-Metrics Production Transducers

Sixteen production stress transducers were manufactured by Senso-Metrics; they are summarized in Table 29.

TABLE 29. SENSO-METRICS PRODUCTION TRANSDUCERS

T4577-D

Transducer S/N	Range, psi	Characteristics
B381	25	Diaphragm, side exit leads
B382	25	
B383	25	
B384	25	
B385	25	
B386	25	
B387	25	
B388	25	
B389	2,000	
B390	25	
B391	2,000	
B392	25	
B393	2,000	
B394	2,000	
B395	2,000	
B396	25	Diaphragm, side exit leads

The transducers were subjected to gaseous nitrogen calibration at several temperatures. Constant current excitation of 5 mA was used for all testing. A Taber pressure transducer was used to monitor the applied pressure which was increased from 0 psig to full scale and back in 20% of full-scale increments (11-point calibration). A 33-point calibration was performed at ambient temperature. The Taber output, transducer output, excitation (including excitation voltage drop and precision 10-ohm resistor), temperature, and ambient atmosphere pressure were recorded. The pressure vessels were filled with Shell Diala oil to minimize temperature fluctuations during pressurization. The data were normalized to 5 mA constant current and 14.7 psia barometric pressure. The sensitivity and zero offset as a function of temperature for each transducer are presented in Figures 100 through 115. Notice that these data show a zero offset at 14.7 psia which is partially the result of the transducers being electrically compensated as an absolute pressure gage (e.g., 0 mV output for 0 psia). It may also be seen in these curves that the range of variation of sensitivity and zero offset as a function of temperature is greater than for the transducers calibrated earlier in this program. This

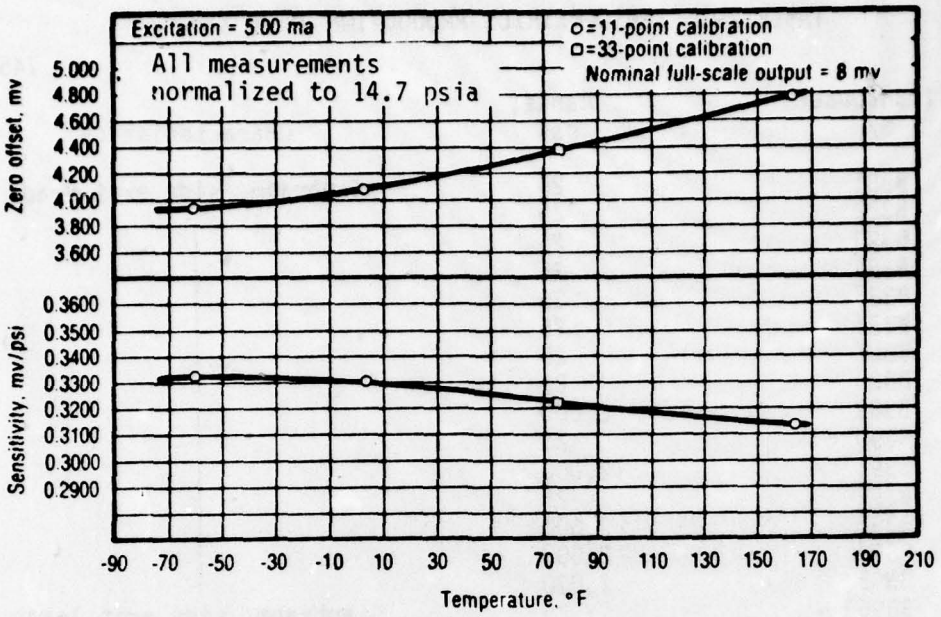


Figure 100. Senso-Metrics Transducer S/N B381 - 25-psi Calibration Data

17195

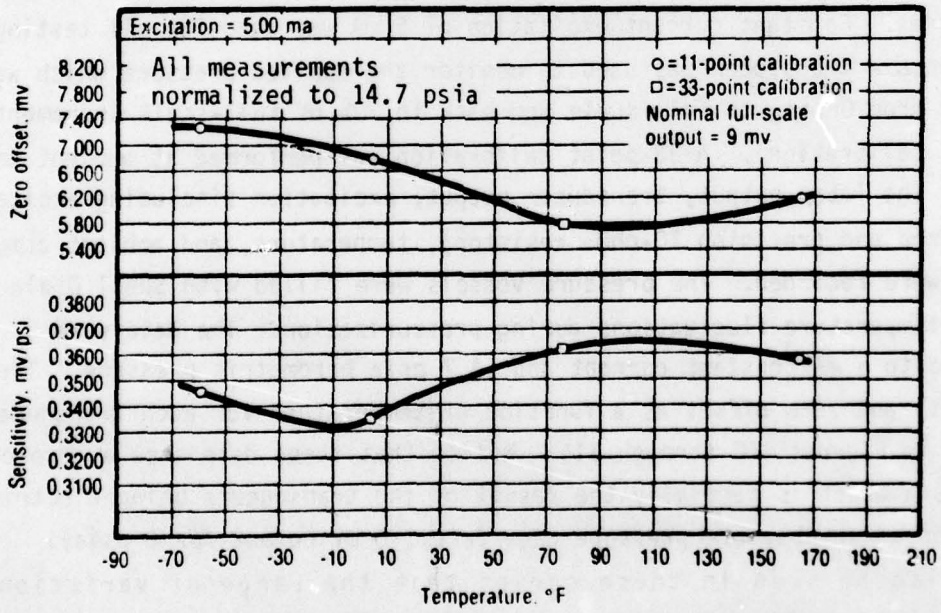


Figure 101. Senso-Metrics Transducer S/N B382 - 25-psi Calibration Data

17194

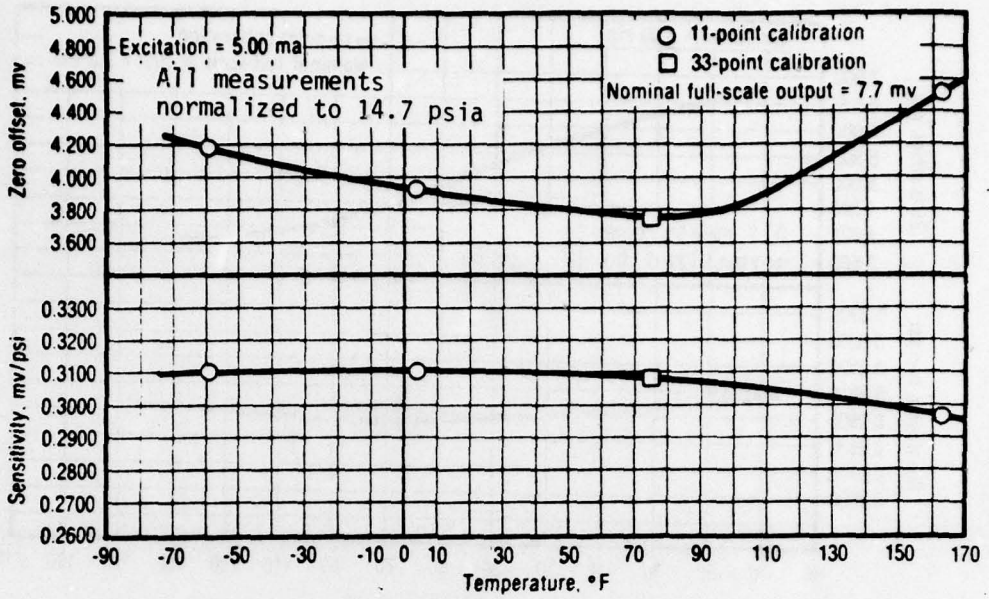


Figure 102. Senso-Metrics Transducer S/N B383 - 25-psi Calibration Data

17193

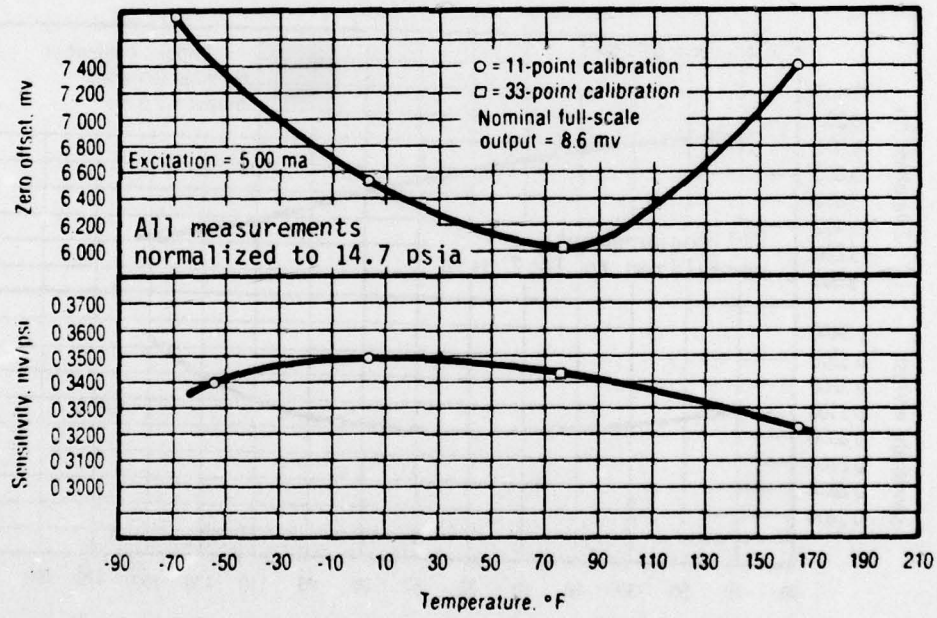


Figure 103. Senso-Metrics Transducer S/N B384 - 25-psi Calibration Data

17192

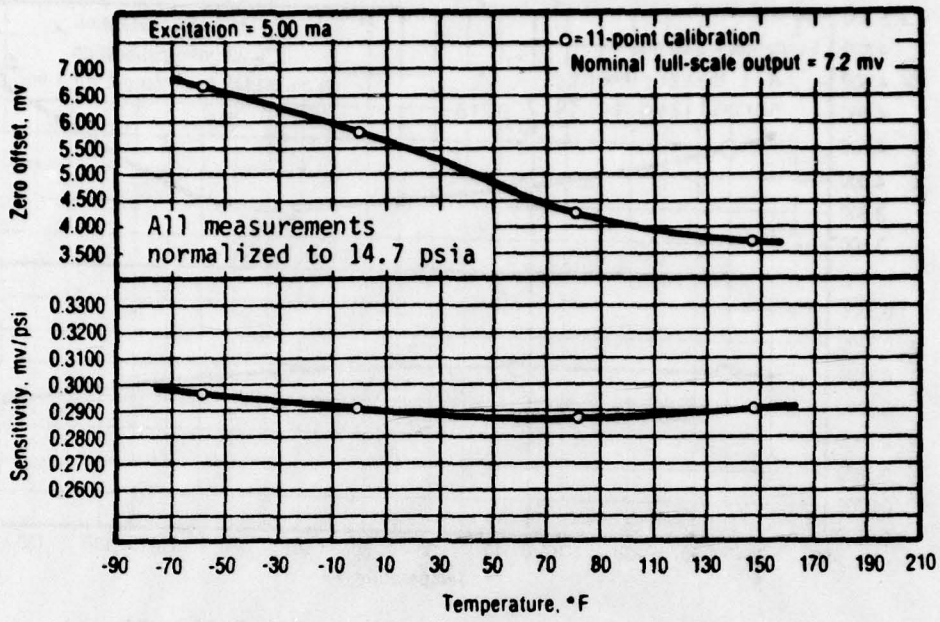


Figure 104. Senso-Metrics Transducer S/N B385 - 25-psi Calibration Data

17191

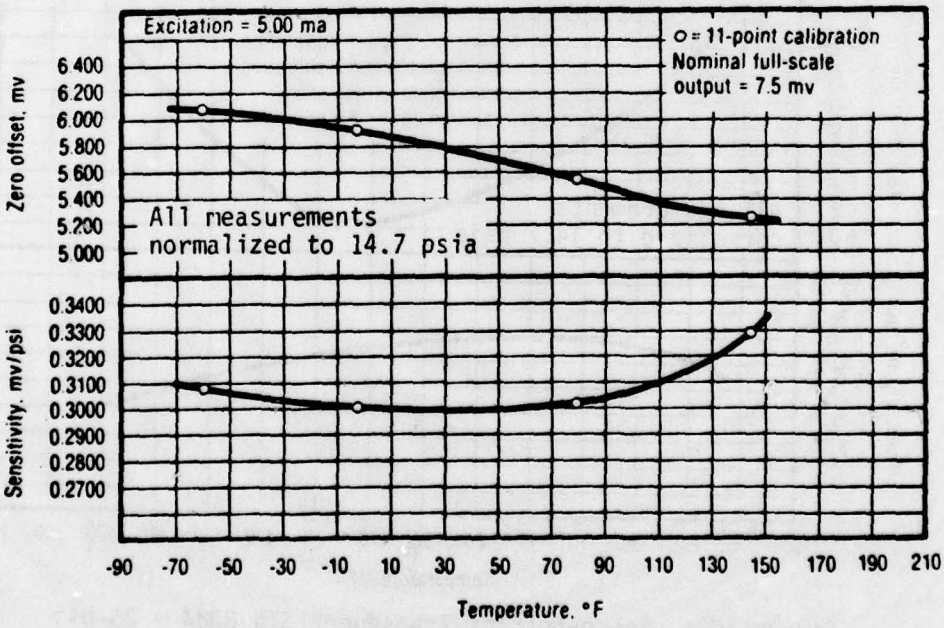


Figure 105. Senso-Metrics Transducer S/N B386 - 25-psi Calibration Data

17190

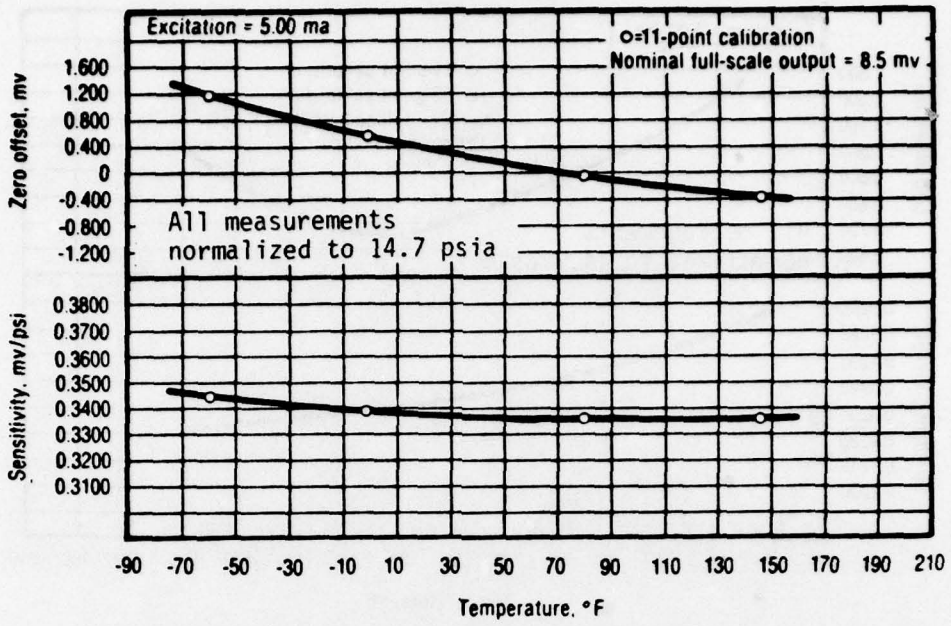


Figure 106. Senso-Metrics Transducer S/N B387 - 25-psi Calibration Data

17189

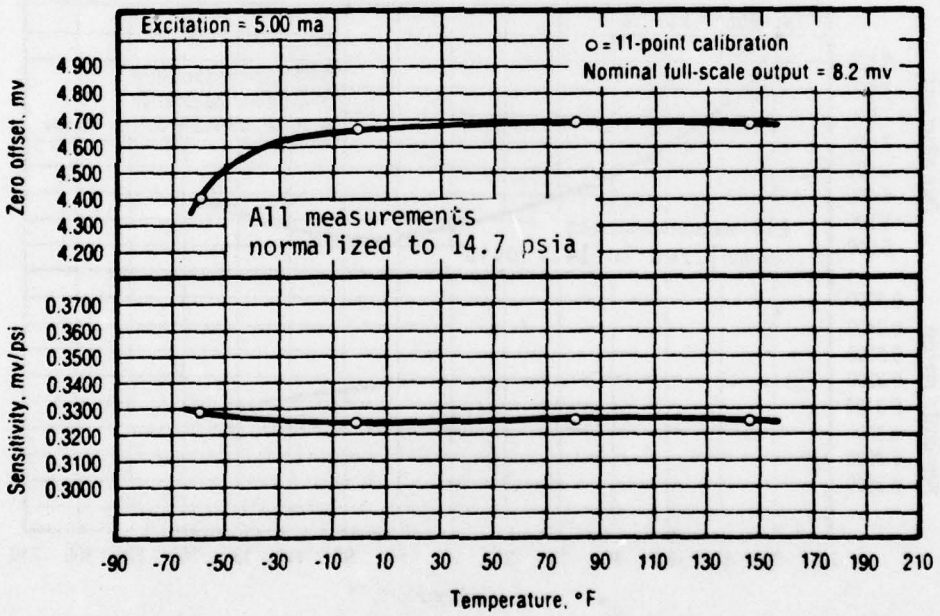


Figure 107. Senso-Metrics Transducer S/N B388 - 25-psi Calibration Data

17188

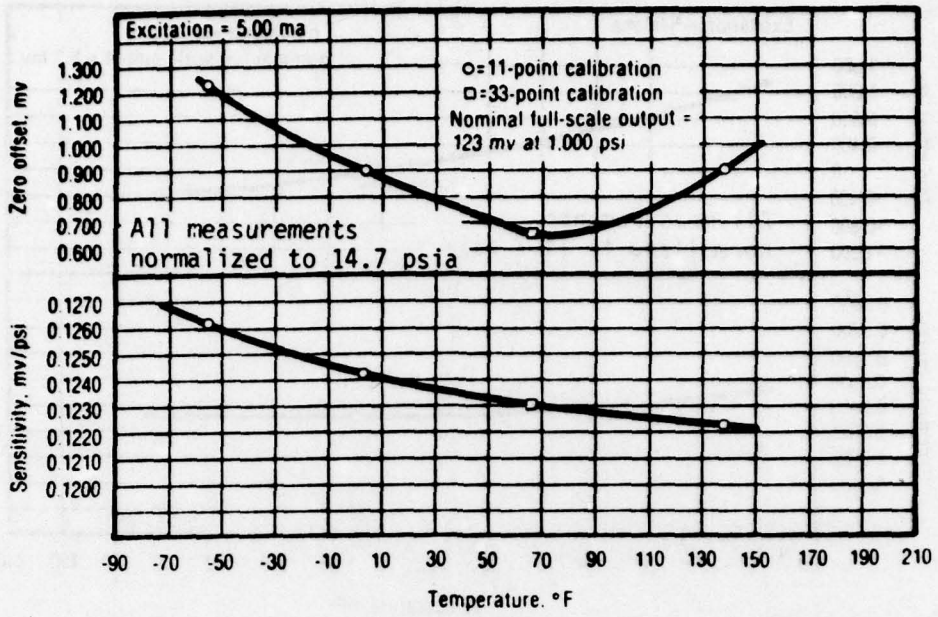


Figure 108. Senso-Metrics Transducer S/N B389 - 2,000-psi Calibration Data

17187

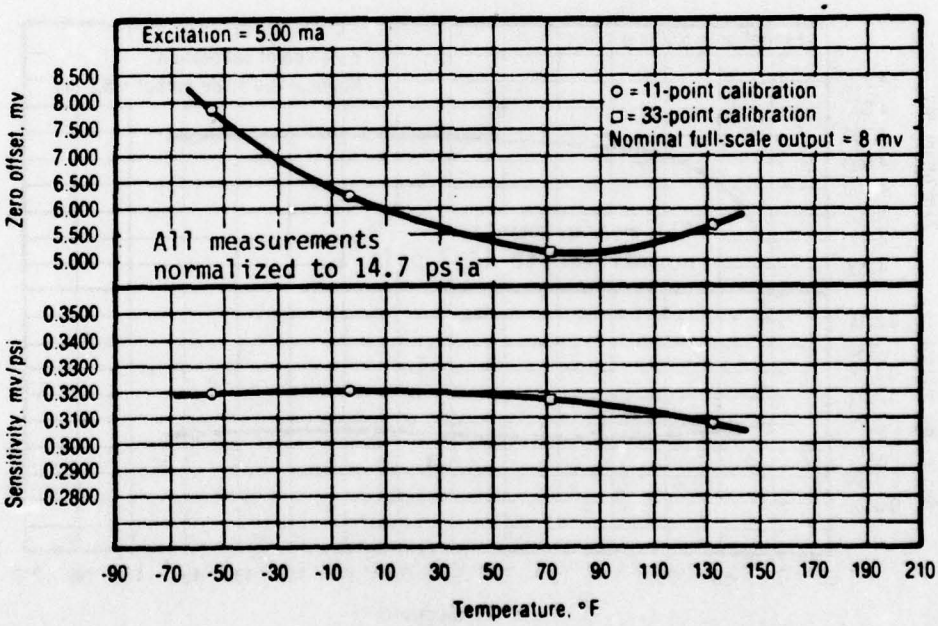


Figure 109. Senso-Metrics Transducer S/N B390 - 25-psi Calibration Data

17186

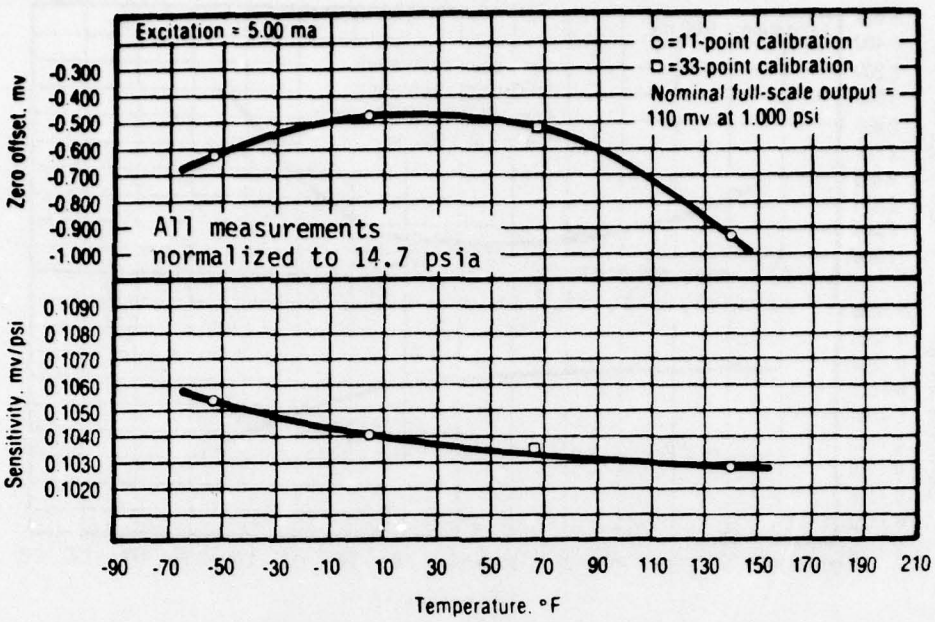


Figure 110. Senso-Metrics Transducer S/N B391 - 2,000-psi Calibration Data

17185

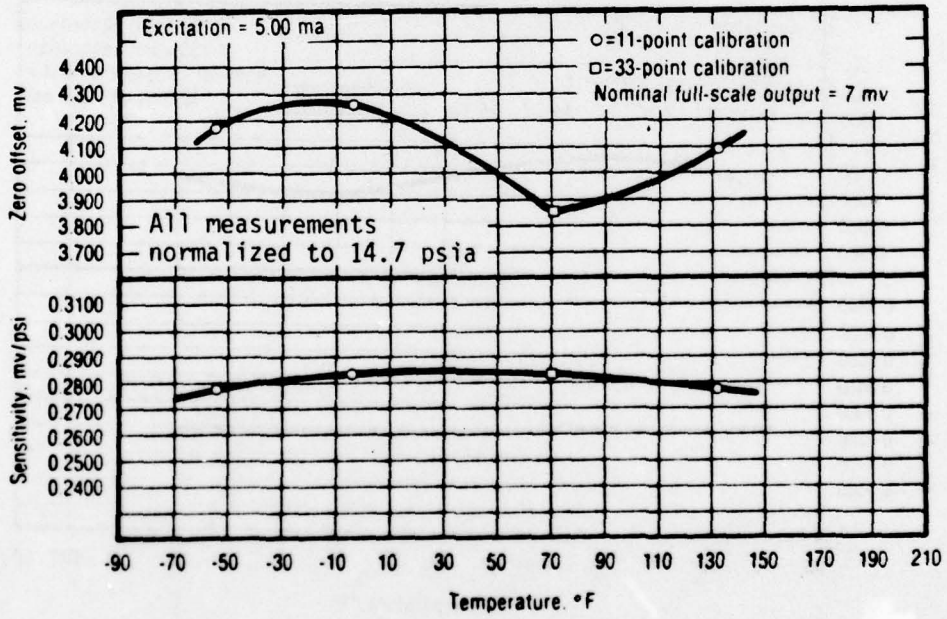


Figure 111. Senso-Metrics Transducer S/N B392 - 25-psi Calibration Data

17184

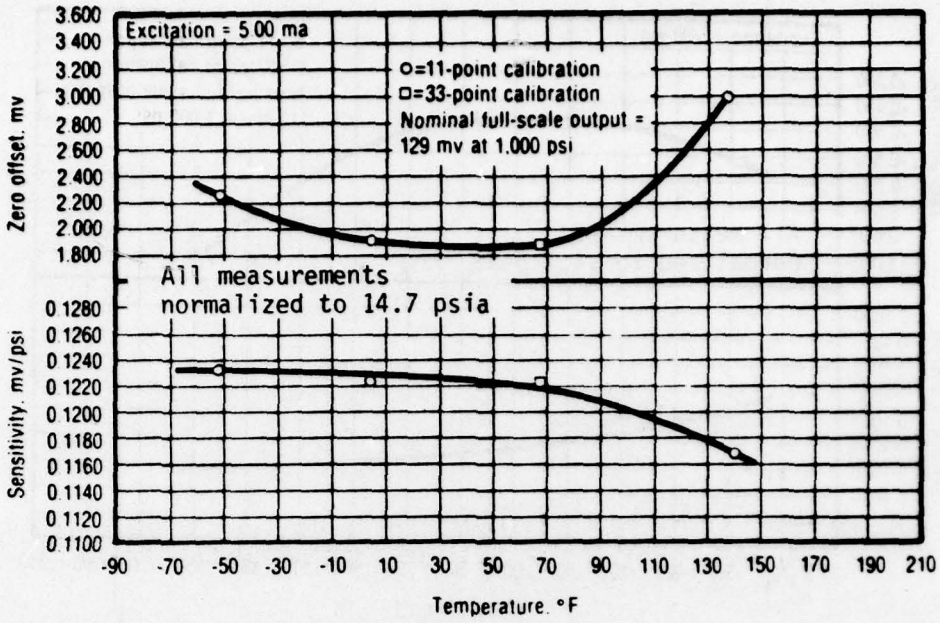


Figure 112. Senso-Metrics Transducer S/N B393 - 2,000-psi Calibration Data

17183

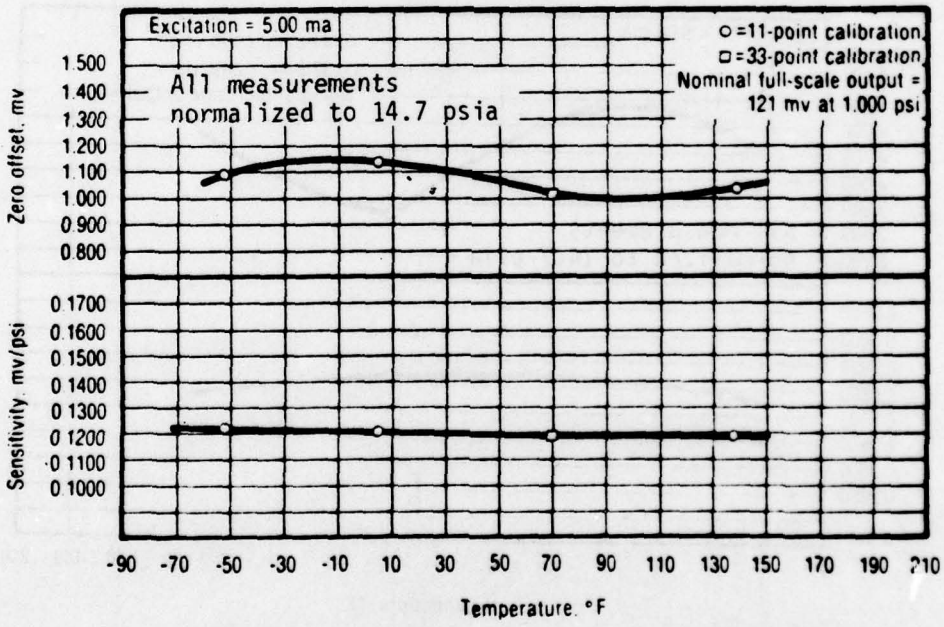


Figure 113. Senso-Metrics Transducer S/N B394 - 2,000-psi Calibration Data

17182

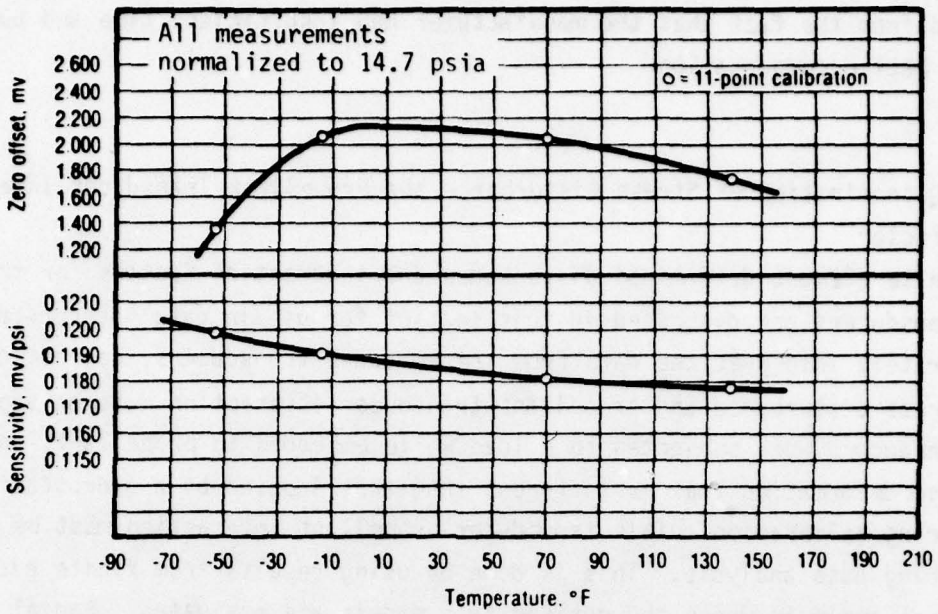


Figure 114. Senso-Metrics Transducer S/N B395 - 2,000-psi Calibration Data

17241

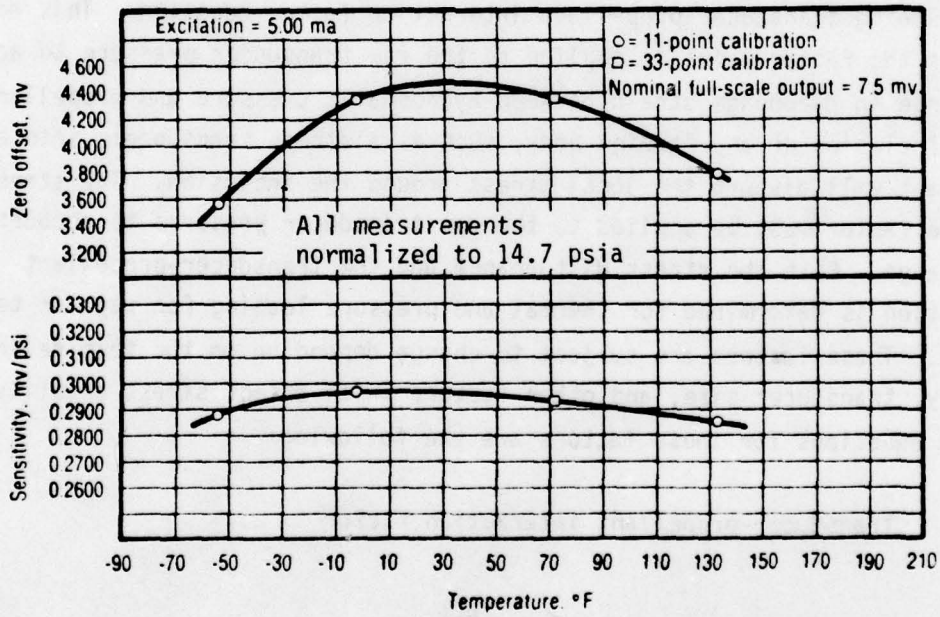


Figure 115. Senso-Metrics Transducer S/N B396 25-psi Calibration Data

17181

resulted from the fact that the manufacturer had insufficient time and budget to achieve better compensation.

4.2.2 Determination of Stress Disturbance and Propellant-Transducer Interaction Factor

Finite element determined disturbance and interaction factors for the production transducers are discussed in this section for use in data interpretation. To accurately interpret the data from the embedded transducers, corrections for both stress disturbance and propellant-transducer interaction must be applied. The transducer, when subjected to a load while embedded in propellant, undergoes diaphragm deformation that is different than that induced by a hydrostatic pressure during calibration. This transducer-propellant interaction must be considered during data analysis. This is done by using results from finite element structural analysis where the desired test models are evaluated. Radial strain in the transducer diaphragm (and, therefore, strain gages) is calculated by the computer. The absolute value of the average integrated radial strains are used in the following transducer-propellant interaction factor equation. This equation produces the factor which is applied to the raw transducer pressure to account for change in diaphragm strain between hydrostatic pressure and propellant pressure. Inclusion of any foreign body, such as a stress transducer, into a mass of propellant will disturb the local stress around the inclusion. The stress disturbance factor must be applied to the raw transducer pressure to account for this change. Both the stress disturbance and the transducer-propellant interaction is determined for thermal and pressure loading for regular test applications. These factors are subject to change depending on the test device goemetry, transducer size, and other factors which affect stress axiality. The general equations for these factors are the following:

A. Transducer-propellant interaction factor

$$I_f = \frac{\epsilon_r + \sigma_{z1}}{\epsilon_f + \sigma_f} \qquad (7)$$

B. Transducer stress disturbance factor

$$D_f = \frac{\sigma_{z2}}{\sigma_{z1}} \tag{8}$$

where

ε_r = average integrated radial strain in diaphragm for a particular loading

σ_{z1} = average integrated stress on diaphragm for a particular loading

ε_f = average integrated radial strain in diaphragm for a hydrostatic load

σ_f = average integrated stress on diaphragm for a hydrostatic load

σ_{z2} = average integrated stress in propellant at diaphragm location, without gage

Use of these two factors to convert from transducer pressure to propellant stress is shown in the following equation:

$$\sigma_{PROP} = \frac{(O.P.) - (Z.O.)}{Se} (I_f)(D_f) \tag{9}$$

where

O.P. = transducer electrical output at temperature T, mV

Z.O. = transducer zero offset at temperature T, mV

Se = transducer sensitivity at temperature T, mV/psig

σ_{PROP} = corrected propellant stress at diaphragm location

The magnitude of the transducer stress disturbance factor varies according to the type of loading for the transducer and solid propellant test device. Figure 116 shows the stress gradients along the Z-axis normal to the stress transducer bonded in the tension/compression/shear device and subjected to a compressive pressure load of 10 psi. Inclusion of the transducer causes the stress to increase at the diaphragm location. As the distance from the transducer location increases, the disturbance lessens until the stresses are equal. The magnitude of this pressure disturbance factor (equation 8) is 0.9744, meaning the transducer pressure readout must be corrected by 2.56% to obtain the stress that would exist without the gage.

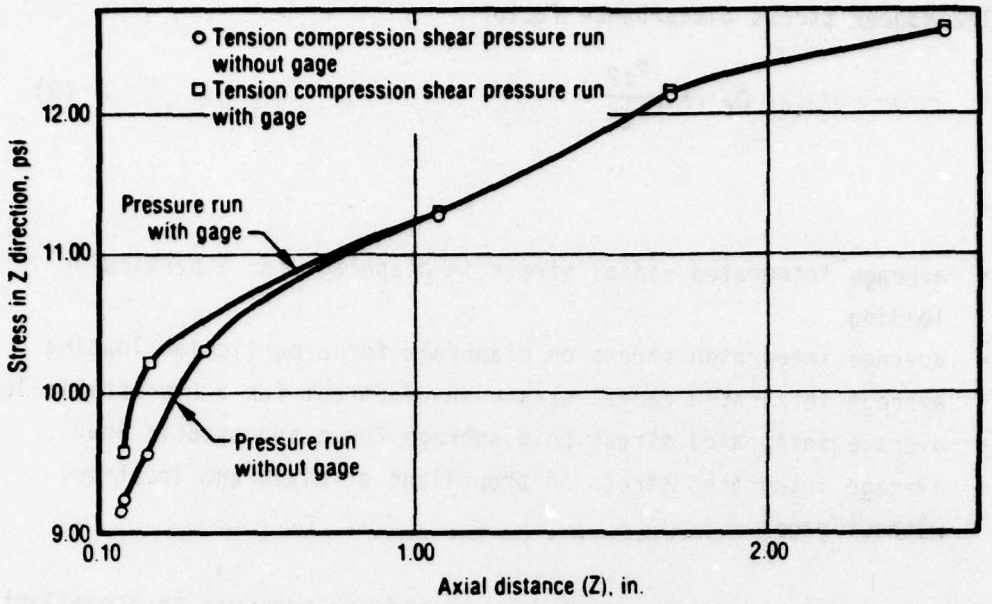


Figure 116. Stress Gradients Along Z-Axis Normal to Senso-Metrics Low Profile Stress Transducer Mounted in Tension/Compression/Shear Device and Subjected to a Pressure Load of 10-psi 17274

Figure 117 shows the stress gradients for the same transducer and tension/compression/shear device subjected to a thermal load of -100°F. Here the effect is reversed. Inclusion of the gage causes the thermal stress to decrease below the stress present without a gage so that the raw transducer pressure must be increased. This thermal disturbance factor is 2.42.

Figure 118 shows stress gradients for the low profile transducer located in the TM-1 subscale motor at midcase and subjected to a thermal load of -100°F. Again, the transducer causes the local stress to drop below the stress present without a transducer present. The thermal disturbance factor here is 1.23 meaning the raw measured transducer pressure must be increased by 23% to obtain the correct propellant stress.

In summary, thermal stress disturbance is much greater than pressure disturbance. Also, under pressure loadings, the presence of the transducer causes the local stress to increase while, under thermal loads, presence of the transducer

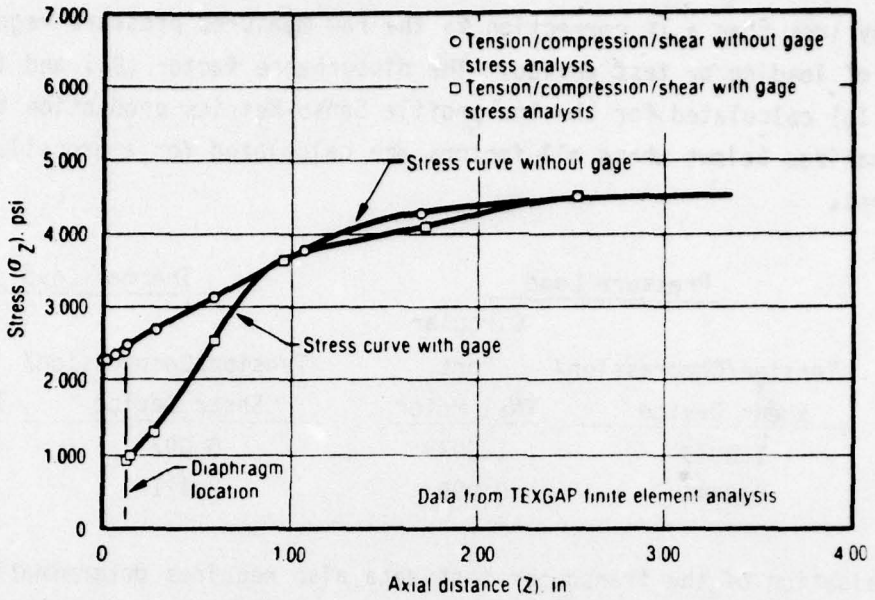


Figure 117. Stress Gradients Along Z-Axis Normal to Senso-Metrics Low Profile Stress Transducer Mounted in Tension/Compression/Shear Device and Subjected to a Thermal Load of -100°F

17273

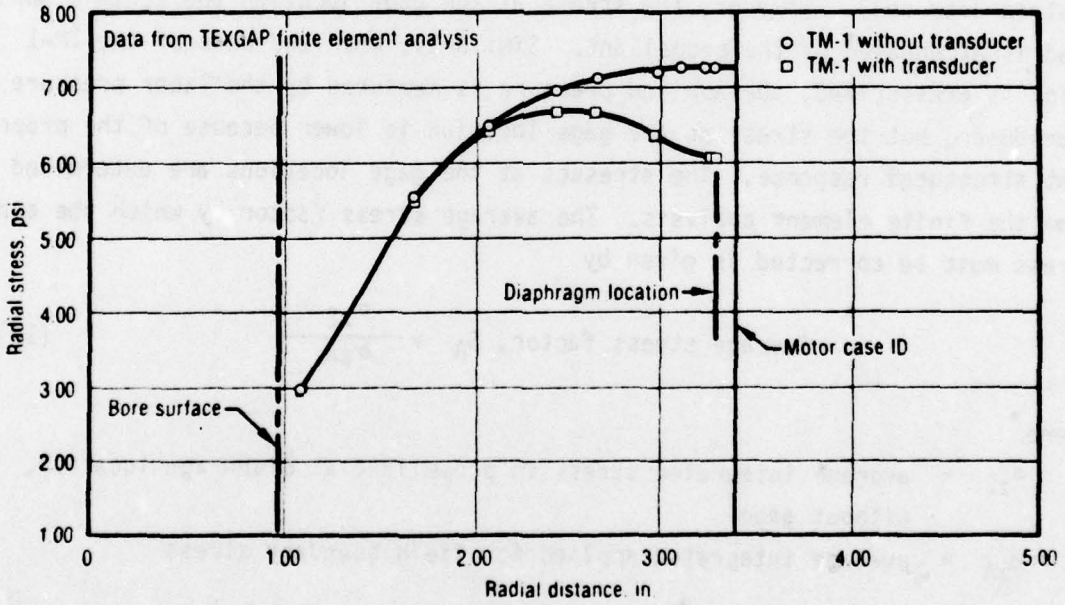


Figure 118. Stress Gradient Along R-Axis Normal to Senso-Metrics Low Profile Stress Transducer Mounted in TM-1 Subscale Motor and Subjected to a Thermal Load of -100°F

17272

causes local stress to decrease. The transducer-propellant interaction factor is generally less than a 1% correction to the raw measured pressure regardless of type of loading or test device. The disturbance factor (D_f) and interaction factor (I_f) calculated for the low profile Senso-Metrics production transducers are summarized below, where all factors are calculated for a propellant modulus of 500 psi.

	Pressure Load		Thermal Load	
Factor	Tension/Compression/ Shear Device	Circular Port TM-1 Motor	Tension/Compression/ Shear Device	Circular Port TM-1 Motor
I_f	1.0073	1.0073	0.997	0.997
D_f	0.9744	0.996	2.421	1.237

Evaluation of the transducer test data also requires determination of the actual stress at the gage location (without transducer) due to the applied load on the test device. When tension, compression, or shear is applied externally to the tension/compression/shear device, the applied load is measured by the Instron load cell. However, the stress at the gage location due to this applied load is attenuated by the propellant. Similarly, when the bore of the TM-1 motor is pressurized, the applied pressure is measured by the Taber pressure transducer, but the stress at the gage location is lower because of the propellant structural response. The stresses at the gage locations are determined from the finite element analysis. The average stress factor by which the applied stress must be corrected is given by

$$\text{Average stress factor, } S_A = \frac{\sigma_{z2}}{\sigma_{zA}} \qquad (10)$$

where

σ_{z2} = average integrated stress in propellant at diaphragm location, without gage

σ_{zA} = average integrated applied for field boundary stress

This factor is used to convert from the external applied stress to the local stress where the transducer is embedded. The external load or stress

is measured by a testing machine load cell or external pressure transducer. These finite element-derived corrected stress values should be equivalent to the actual transducer stress as shown in the following equations:

$$\sigma_{PROP} = (F/A)(S_A) \tag{11}$$

where

F = measured applied force, lb

A = cross-sectional area of sample, $in.^2$

σ_{PROP} = corrected propellant stress at diaphragm location

therefore

$$(F/A)(S_A) = \left[\frac{(O.P.) - (Z.O.)}{Se}\right] (I_f)(D_f) \tag{12}$$

A summary of the average stress factors for the low profile transducers mounted in the tension/compression/shear device and TM-1 and subjected to pressure loads is presented below.

	Pressure Load	
	Tension/Compression/	Circular Port
Factor	Shear Device	TM-1
S_A	0.9169	0.9887

All data presented in this section have had the appropriate corrections applied.

4.2.3 Senso-Metrics Production Transducers, Testing in Tension/Compression/ Shear Device

Senso-Metrics transducer S/Ns B381, B382, B384, and B386 were mounted in the tension/compression/shear device as shown in Figure 119 and 120. This is the same device as that used for prototype transducer testing. The test load was applied by an Instron testing machine and transducer output was recorded on a

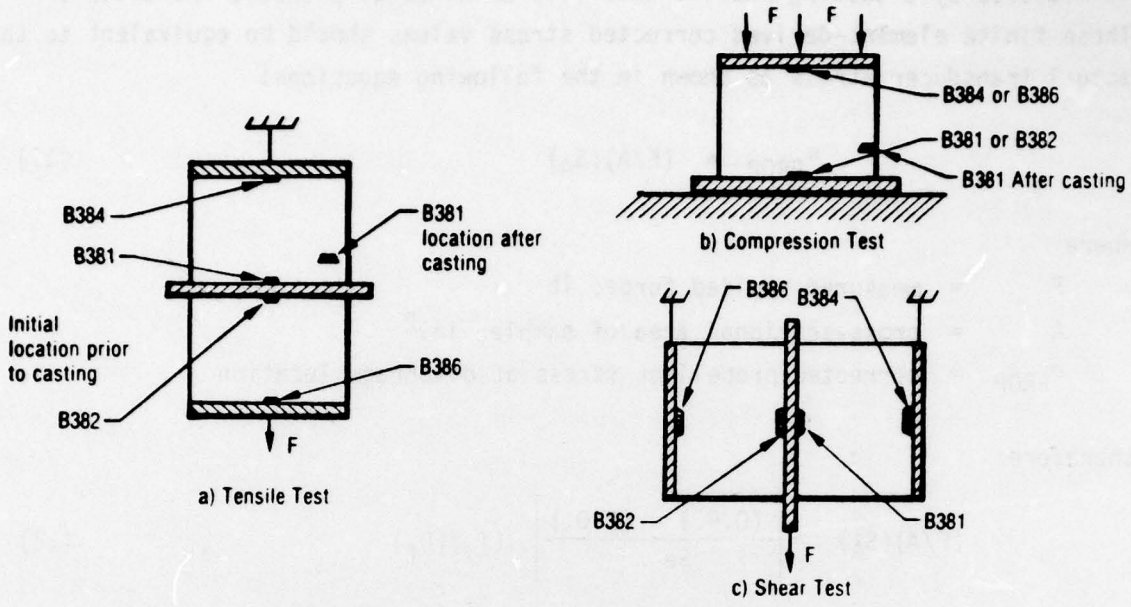


Figure 119. Test Configuration for Tension/Compression/Shear Device
17277

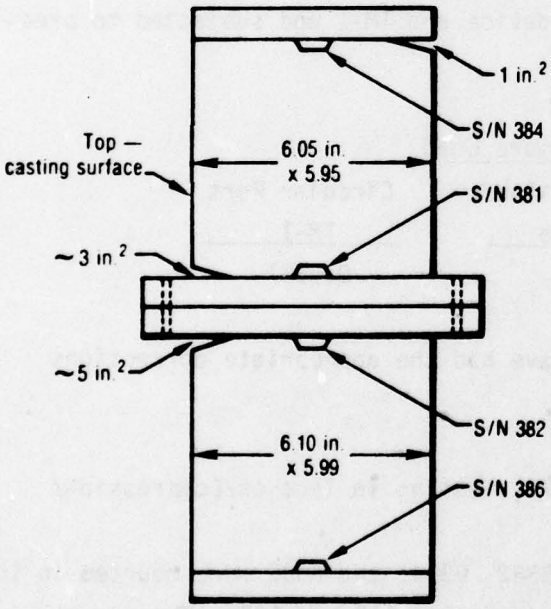
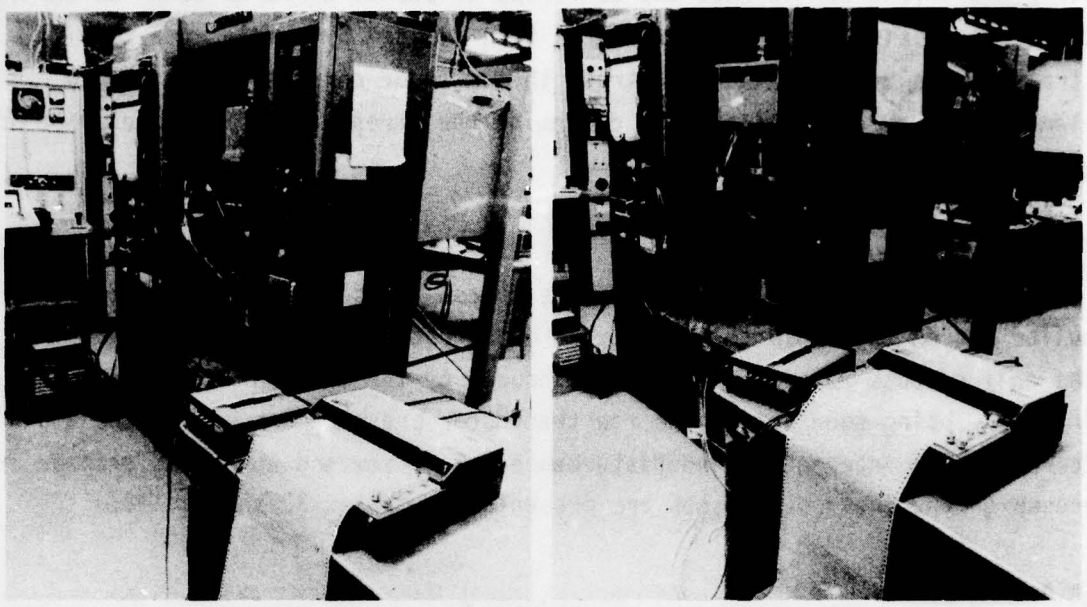


Figure 120. Unbond Areas in Shear Fixture with Final Gage Designs
17225

strip chart recorder. Figure 121 shows photographs of the test setups. Stepwise loading tests were run at several temperatures over the range of 140° to -65°F. All thermal loads on the transducers were nulled out electrically so that only the applied compressive tensile or shear loads were recorded.

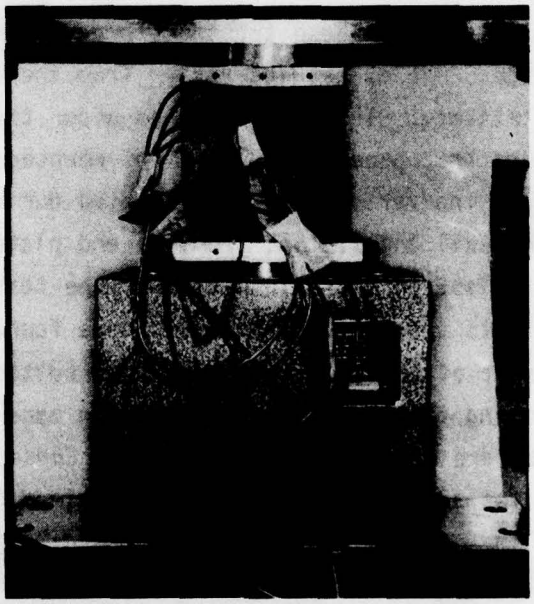
Instron Stress Calculation

The Instron load recording apparatus is a 10-in. full-scale strip chart recorder. The range of full-scale loads available is from 20 to 1,000 lb (20, 50, 100, 200, 500, 1,000). To derive external stress as applied by the Instron machine, the deflection on the



a. Tension

b. Shear



c. Compression

Figure 121. Test Shop for Tension/Compression/Shear Device Transducer Testing

17278

strip chart recorder is read and converted to pounds of force based on the full-scale range being used. This force is then divided by sample area to give stress. This average external stress then must be corrected by a finite element-derived stress factor to determine the stress at the gage location if no gage was in the test device.

Transducer Output Recording

The thermally induced loads on the stress transducers were electrically nulled out on the strip chart recorder being used to record gage outputs. Thus, the only outputs recorded were those induced by the Instron machine mechanical loading. Using equation 9, the raw transducer pressure was calculated and then corrected for interaction and disturbance. Both raw and corrected transducer pressures and Instron stresses are presented in Tables 30 through 42.

Data Summary

Corrected stress values from gage S/Ns B382, B384, and B386 are generally within a few percent of the corrected Instron stress for the testing cycle for tension and compression tests. These transducers gave some response proportional to shear loading. Gage S/N B381 results varied from the other three transducers over the entire test history. It was discovered after the completion of all the testing in this fixture that gage S/N 381 was not mounted on the end plate as assumed but had somehow inadvertently been relocated during casting to a position about 1.0 in. from the wall and 1.5 in. from the end plate of the fixture as shown in Figure 119. Also, on close inspecton of the test fixture after completion of these tests, several unbond areas were found. These areas were only visible as a result of the fixture having been tested at -75^{o}F. The unbonds were caused by processing personnel applying masking tape to the inside of the tooling immediately before casting the propellant. Consequently, the unbond regions were present for all the testing of the sample and the areas might have grown as a result of the testing loads. The estimated regions of unbond are shown in Figure 120. The unbond labelled 1 in.^{2} is only in a corner, the 3-in.^{2} unbond extends approximately one-half the distance across the top of the fixture, and the 5-in.^{2} unbond crosses the entire top of the sample.

TABLE 30. COMPRESSION TEST RESULTS AT 144°F
SENSO-METRICS, INC. PRODUCTION TRANSDUCERS

T4642-D

S/N	Test Temperature, °F	Average Instron Stress, psi	Corrected Instron Stress,* psi	Uncorrected Transducer Pressure, psi	Corrected Transducer Stress,† psi	Ratio‡
B381	144	0	0	0	0	-
		5.00	4.58	4.87	4.78	0.958
		10.00	9.17	10.33	10.14	0.904
		15.03	13.78	16.62	16.31	0.845
		20.06	18.39	22.44	22.03	0.835
		25.00	22.92	28.43	27.90	0.822
B382	144	0	0	0	0	-
		5.03	4.61	4.58	4.50	1.024
		10.00	9.17	9.01	8.85	1.036
		15.00	13.75	13.35	13.10	1.050
		20.78	19.05	19.11	18.76	1.015
		25.00	22.92	22.61	22.20	1.032
B384	144	0	0	0	0	-
		5.00	4.58	5.36	5.26	0.871
		10.00	9.17	10.08	9.89	0.927
		15.03	13.78	14.92	14.64	0.941
		20.06	18.39	19.85	19.48	0.944
		25.00	22.92	24.57	24.11	0.951
B386	144	0	0	0	0	-
		5.03	4.61	4.44	4.36	1.057
		10.00	9.17	8.36	8.20	1.118
		15.00	13.75	12.58	12.35	1.113
		20.78	19.05	17.69	17.36	1.097
		25.00	22.92	21.39	21.00	1.091

* Corrected Instron stress = (average Instron stress)(0.9169), where 0.9169 is the stress correction factor for all transducers due to their location in the test device; these factors determined from TEXGAP finite element analysis

† Corrected transducer stress = (uncorrected transducer pressure)(0.9815), where 0.9815 is the product of transducer interaction factor and transducer disturbance factor for a pressure load; these factors determined from TEXGAP finite element analysis

‡ $\frac{\text{Corrected Instron Stress}}{\text{Corrected Transducer Stress}}$

TABLE 31. COMPRESSION TEST RESULTS AT 98°F
SENSO-METRICS, INC. PRODUCTION TRANSDUCERS

T4643-D

S/N	Test Temperature, °F	Average Instron Stress, psi	Corrected Instron Stress,* psi	Uncorrected Transducer Pressure, psi	Corrected Transducer Stress,† psi	Ratio‡
B381	98	0	0	0	0	-
		5.00	4.58	6.25	6.14	0.746
		10.00	9.17	12.23	12.00	0.764
		15.14	13.88	18.81	18.46	0.752
		20.06	18.39	25.01	24.55	0.749
		25.06	22.98	-	-	-
B382	98	0	0	0	0	-
		5.03	4.61	4.65	4.56	1.011
		10.03	9.20	9.58	9.40	0.979
		15.06	13.81	14.88	14.61	0.945
		20.06	18.39	19.72	19.35	0.950
		25.03	22.95	23.86	23.42	0.980
B384	98	0	0	0	0	-
		5.00	4.58	4.89	4.80	0.954
		10.00	9.17	9.55	9.37	0.979
		15.14	13.88	14.53	14.26	0.973
		20.06	18.39	19.57	19.21	0.957
		25.06	22.98	24.61	24.16	0.951
B386	98	0	0	0	0	-
		5.03	4.61	4.96	4.87	0.947
		10.03	9.20	9.43	9.25	0.995
		15.06	13.81	14.25	13.99	0.987
		20.06	18.39	19.34	18.99	0.968
		25.03	22.95	24.04	23.60	0.972

* Corrected Instron stress = (average Instron stress)(0.9169), where 0.9169 is the stress correction factor for all transducers due to their location in the test device; these factors determined from TEXGAP finite element analysis

† Corrected transducer stress = (uncorrected transducer pressure)(0.9815), where 0.9815 is the product of transducer interaction factor and transducer disturbance factor for a pressure load; these factors determined from TEXGAP finite element analysis

‡ $\frac{\text{Corrected Instron Stress}}{\text{Corrected Transducer Stress}}$

TABLE 32. COMPRESSION TEST RESULTS AT AMBIENT TEMPERATURE
SENSO-METRICS, INC. PRODUCTION TRANSDUCERS

T4644-D

S/N	Test Temperature, °F	Average Instron Stress, psi	Corrected Instron Stress,* psi	Uncorrected Transducer Pressure, psi	Corrected Transducer Stress,† psi	Ratio ‡
B381	76	0	0	0	0	-
		5.03	4.61	6.25	6.13	0.752
		10.00	9.17	12.19	11.96	0.767
		15.03	13.78	18.80	18.45	0.747
		20.06	18.39	25.28	24.81	0.741
		23.14	21.22	29.20	28.66	0.740
B382	72	0	0	0	0	-
		5.28	4.84	4.86	4.77	1.015
		10.06	9.22	9.91	9.73	0.948
		15.06	13.81	14.71	14.44	0.956
		20.03	18.37	19.33	18.97	0.968
		25.03	22.95	23.79	23.35	0.983
B384	76	0	0	0	0	-
		5.03	4.61	5.24	5.14	0.897
		10.00	9.17	9.85	9.67	0.948
		15.03	13.78	14.74	14.47	0.952
		20.06	18.39	19.63	19.27	0.954
		23.14	21.22	22.56	22.14	0.958
B386	72	0	0	0	0	-
		5.28	4.84	5.26	5.16	0.938
		10.06	9.22	10.15	9.96	0.926
		15.06	13.81	15.09	14.81	0.932
		20.03	18.37	19.91	19.54	0.940
		25.03	22.95	24.74	24.28	0.945

* Corrected Instron stress = (average Instron stress)(0.9169), where 0.9169 is the stress correction factor for all transducers due to their location in the test device; these factors determined from TEXGAP finite element analysis

† Corrected transducer stress = (uncorrected transducer pressure)(0.9815), where 0.9815 is the product of transducer interaction factor and transducer disturbance factor for a pressure load; these factors determined from TEXGAP finite element analysis

‡ $\frac{\text{Corrected Instron Stress}}{\text{Corrected Transducer Stress}}$

TABLE 33. COMPRESSION TEST RESULTS AT AMBIENT TEMPERATURE
SENSO-METRICS, INC. PRODUCTION TRANSDUCERS

T4645-D

S/N	Test Temperature, °F	Average Instron Stress, psi	Corrected Instron Stress,* psi	Uncorrected Transducer Pressure, psi	Corrected Transducer Stress,† psi	Ratio‡
B381	73	0	0	0	0	-
		4.47	4.10	5.16	5.06	0.810
		10.03	9.19	11.12	10.91	0.842
		15.11	13.86	17.13	16.81	0.825
		20.08	18.41	23.79	23.35	0.788
		25.50	23.38	-	-	-
B382	73	0	0	0	0	-
		5.03	4.61	4.45	4.37	1.055
		10.06	9.22	9.19	9.02	1.022
		15.06	13.81	14.01	13.75	1.004
		20.06	18.39	18.99	18.64	0.987
		25.22	23.13	23.94	23.50	0.984
B384	73	0	0	0	0	-
		4.47	4.10	4.30	4.22	0.972
		10.03	9.19	9.41	9.24	0.995
		15.11	13.86	14.44	14.17	0.978
		20.08	18.41	19.70	19.34	0.952
		25.50	23.38	25.28	24.81	0.942
B386	73	0	0	0	0	-
		5.03	4.61	4.70	4.61	1.000
		10.06	9.22	9.29	9.12	1.011
		15.06	13.81	14.05	13.79	1.001
		20.06	18.39	19.38	19.02	0.967
		25.22	23.13	24.77	24.31	0.951

* Corrected Instron stress = (average Instron stress)(0.9169), where 0.9169 is the stress correction factor for all transducers due to their location in the test device; these factors determined from TEXGAP finite element analysis

† Corrected transducer stress = (uncorrected transducer pressure)(0.9815), where 0.9815 is the product of transducer interaction factor and transducer disturbance factor for a pressure load; these factors determined from TEXGAP finite element analysis

‡ $\frac{\text{Corrected Instron Stress}}{\text{Corrected Transducer Stress}}$

TABLE 34. COMPRESSION TEST RESULTS AT 0°F
SENSO-METRICS, INC. PRODUCTION TRANSDUCERS

T4646-D

S/N	Test Temperature, °F	Average Instron Stress, psi	Corrected Instron Stress,* psi	Uncorrected Transducer Pressure, psi	Corrected Transducer Stress,† psi	Ratio‡
B381	0	0	0	0	0	-
		5.17	4.74	9.42	9.25	0.512
		10.11	9.27	14.41	14.14	0.656
		15.31	14.03	20.17	19.80	0.709
		20.11	18.44	25.93	25.45	0.725
		25.06	22.97	30.73	30.17	0.761
B382	0	0	0	0	0	-
		5.08	4.66	3.43	3.37	1.383
		10.08	9.24	7.08	6.94	1.331
		15.06	13.81	11.66	11.45	1.206
		20.03	18.37	16.61	16.31	1.126
		25.03	22.95	21.63	21.23	1.081
B384	0	0	0	0	0	-
		5.17	4.74	4.92	4.83	0.981
		10.11	9.27	9.47	9.29	0.998
		15.31	14.03	14.47	14.20	0.988
		20.11	18.44	19.17	18.81	0.980
		25.06	22.97	24.15	23.70	0.969
B386	0	0	0	0	0	-
		5.08	4.66	4.73	4.64	1.004
		10.08	9.24	9.38	9.21	1.003
		15.06	13.81	14.44	14.17	0.975
		20.03	18.37	19.70	19.33	0.950
		25.03	22.95	25.15	24.69	0.930

* Corrected Instron stress = (average Instron stress)(0.9169), where 0.9169 is the stress correction factor for all transducers due to their location in the test device; these factors determined from TEXGAP finite element analysis

† Corrected transducer stress = (uncorrected transducer pressure)(0.9815), where 0.9815 is the product of transducer interaction factor and transducer disturbance factor for a pressure load; these factors determined from TEXGAP finite element analysis

‡ $\frac{\text{Corrected Instron Stress}}{\text{Corrected Transducer Stress}}$

TABLE 35. COMPRESSION TEST RESULTS AT -61°F
SENSO-METRICS, INC. PRODUCTION TRANSDUCERS

T4647-D

S/N	Test Temperature, °F	Average Instron Stress, psi	Corrected Instron Stress,* psi	Uncorrected Transducer Pressure, psi	Corrected Transducer Stress,† psi	Ratio‡
B381	-61	0	0	0	0	-
		5.17	4.74	5.02	4.92	0.963
		10.11	9.27	9.57	9.39	0.987
		15.14	13.88	13.63	13.37	1.038
		20.00	18.34	17.24	16.93	1.083
		25.14	23.05	20.87	20.49	1.125
B382		Transducer leadwire tube broken during handling				
B384	-61	0	0	0	0	-
		5.17	4.74	2.38	2.33	2.034
		10.11	9.27	4.73	4.64	1.998
		15.14	13.88	7.38	7.24	1.917
		20.00	18.34	9.90	9.72	1.887
		25.14	23.05	12.70	12.46	1.850
B386		Transducer leadwire tube broken during handling				

* Corrected Instron stress = (average Instron stress)(0.9169), where 0.9169 is the stress correction factor for all transducers due to their location in the test device; these factors determined from TEXGAP finite element analysis

† Corrected transducer stress = (uncorrected transducer pressure)(0.9815), where 0.9815 is the product of the transducer interaction factor and the transducer disturbance factor for a pressure load; these factors determined from TEXGAP finite element analysis

‡ $\frac{\text{Corrected Instron Stress}}{\text{Corrected Transducer Stress}}$

TABLE 36. TENSILE TEST RESULTS AT 140°F SENSO-METRICS, INC. PRODUCTION TRANSDUCERS

T4648-D

S/N	Test Temperature, °F	Average Instron Stress, psi	Corrected Instron Stress,* psi	Uncorrected Transducer Pressure, psi	Corrected Transducer Stress,† psi	Ratio‡
B381	140	0	0	0	0	-
		2.03	1.86	1.95	1.91	0.974
		4.00	3.67	3.89	3.82	0.961
		6.03	5.53	5.70	5.59	0.989
		8.03	7.36	7.62	7.48	0.984
		10.03	9.20	9.81	9.63	0.955
B382		Transducer leadwire tube broken during handling				
B384	140	0	0	0	0	-
		2.03	1.86	1.98	1.94	0.959
		4.00	3.67	3.91	3.84	0.956
		6.03	5.53	5.95	5.84	0.947
		8.03	7.36	7.96	7.81	0.942
		10.03	9.20	10.07	9.88	0.931
B386	140	0	0	0	0	-
		2.03	1.86	1.85	1.82	1.022
		4.00	3.67	3.61	3.54	1.037
		6.17	5.68	5.40	5.30	1.072
		8.11	7.44	7.04	6.91	1.077
		9.19	8.43	8.18	8.03	1.050

* Corrected Instron stress = (average Instron stress)(0.9169), where 0.9169 is the stress correction factor for all transducers due to their location in the test device; these factors determined from TEXGAP finite element analysis

† Corrected transducer stress = (uncorrected transducer pressure)(0.9815), where 0.9815 is the product of transducer interaction factor and transducer disturbance factor for a pressure load; these factors determined from TEXGAP finite element analysis

‡ $\frac{\text{Corrected Instron Stress}}{\text{Corrected Transducer Stress}}$

TABLE 37. TENSILE TEST RESULTS AT AMBIENT TEMPERATURE
SENSO-METRICS, INC. PRODUCTION TRANSDUCERS

T4649-D

S/N	Test Temperature, °F	Average Instron Stress, psi	Corrected Instron Stress,* psi	Uncorrected Transducer Pressure, psi	Corrected Transducer Stress,† psi	Ratio‡
B381	75	0	0	0	0	-
		2.03	1.86	2.14	2.10	0.886
		4.03	3.70	4.28	4.20	0.881
		6.03	5.53	6.47	6.12	0.904
		8.00	7.34	8.67	8.20	0.895
		10.00	9.17	10.87	10.67	0.859
B382	75	0	0	0	0	-
		2.03	1.86	1.75	1.72	1.081
		4.03	3.70	3.39	3.33	1.111
		6.03	5.53	5.27	5.17	1.070
		8.00	7.34	7.00	6.87	1.068
		10.00	9.17	8.72	8.56	1.071
B384	75	0	0	0	0	-
		2.03	1.86	1.74	1.71	1.088
		4.03	3.70	3.50	3.44	1.076
		6.03	5.53	5.26	5.16	1.072
		8.00	7.34	7.14	7.01	1.047
		10.00	9.17	9.02	8.85	1.036
B386	75	0	0	0	0	-
		2.03	1.86	1.87	1.84	1.011
		4.03	3.70	3.52	3.45	1.072
		6.03	5.53	5.22	5.12	1.080
		8.00	7.34	6.96	6.83	1.075
		10.00	9.17	8.77	8.61	1.065

* Corrected Instron stress = (average Instron stress)(0.9169), where 0.9169 is the stress correction factor for all transducers due to their location in the test device; these factors determined from TEXGAP finite element analysis

† Corrected transducer stress = (uncorrected transducer pressure)(0.9815), where 0.9815 is the product of transducer interaction factor and transducer disturbance factor for a pressure load; these factors determined from TEXGAP finite element analysis

‡ $\frac{\text{Corrected Instron Stress}}{\text{Corrected Transducer Stress}}$

TABLE 38. TENSILE TEST RESULTS AT 16°F SENSO-METRICS, INC. PRODUCTION TRANSDUCERS

T4650-D

S/N	Test Temperature, °F	Average Instron Stress, psi	Corrected Instron Stress,* psi	Uncorrected Transducer Pressure, psi	Corrected Transducer Stress,† psi	Ratio‡
B381	16	0	0	0	0	-
		2.17	1.99	2.32	2.28	0.873
		4.27	3.92	4.56	4.48	0.875
		6.40	5.87	6.80	6.67	0.880
		8.54	7.83	9.00	8.84	0.886
		10.66	9.77	11.15	10.95	0.892
B382	16	0	0	0	0	-
		2.17	1.99	3.41	3.34	0.596
		4.27	3.92	6.79	6.66	0.589
		6.40	5.87	10.08	9.89	0.594
		8.54	7.83	13.27	13.03	0.601
		10.66	9.77	16.41	16.10	0.607
B384	16	0	0	0	0	-
		2.17	1.99	2.10	2.06	0.966
		4.27	3.92	4.09	4.01	0.978
		6.40	5.87	5.93	5.82	1.009
		8.54	7.83	7.97	7.83	1.000
		10.66	9.77	9.82	9.64	1.013
B386	16	0	0	0	0	-
		2.17	1.99	1.23	1.21	1.645
		4.27	3.92	2.99	2.93	1.338
		6.40	5.87	4.98	4.89	1.200
		8.54	7.83	6.94	6.81	1.150
		10.66	9.77	8.76	8.60	1.136

* Corrected Instron stress = (average Instron stress)(0.9169), where 0.9169 is the stress correction factor for all transducers due to their location in the test device; these factors determined from TEXGAP finite element analysis

† Corrected transducer stress = (uncorrected transducer pressure)(0.9815), where 0.9815 is the product of transducer interaction factor and transducer disturbance factor for a pressure load; these factors determined from TEXGAP finite element analysis

‡ $\frac{\text{Corrected Instron Stress}}{\text{Corrected Transducer Stress}}$

TABLE 39. TENSILE TEST RESULTS AT -63°F
SENSO-METRICS, INC. PRODUCTION TRANSDUCERS

T4651-D

S/N	Test Temperature, °F	Average Instron Stress, psi	Corrected Instron Stress,* psi	Uncorrected Transducer Pressure, psi	Corrected Transducer Stress,† psi	Ratio‡
B381	-63	0	0	0	0	-
		2.89	2.65	2.83	2.78	0.953
		4.06	3.72	4.20	4.12	0.903
		6.03	5.53	6.48	6.36	0.869
		8.11	7.44	9.03	8.86	0.840
		10.08	9.24	11.54	11.33	0.816
B382		Transducer leadwire tube broken during handling				
B384	-63	0	0	0	0	-
		2.89	2.65	3.35	3.29	0.805
		4.06	3.72	4.81	4.72	0.788
		6.03	5.53	7.38	7.25	0.764
		8.11	7.44	10.16	9.97	0.746
		10.08	9.24	12.73	12.49	0.740
B386		Transducer leadwire tube broken during handling				

* Corrected Instron stress = (average Instron stress)(0.9169), where 0.9169 is the stress correction factor for all transducers due to their location in the test device; these factors determined from TEXGAP finite element analysis

† Corrected transducer stress = (uncorrected transducer pressure)(0.9815), where 0.9815 is the product of transducer interaction factor and transducer disturbance factor for a pressure load; these factors determined from TEXGAP finite element analysis

‡ $\frac{\text{Corrected Instron Stress}}{\text{Corrected Transducer stress}}$

TABLE 40. SHEAR TEST RESULTS AT 136°F
SENSO-METRICS, INC. PRODUCTION TRANSDUCERS

Transducer S/N	Test Temperature, °F	Average Shear Stress, psi	T4652-D Uncorrected Transducer Shear Stress, psi
B381	136	1.00	-1.75
		2.00	-3.89
		3.00	-5.97
		4.00	-8.16
		5.00	-10.55
B382	Transducer leadwire tube broken during handling		
B384	136	1.00	-0.15
		2.00	-0.30
		3.00	-0.49
		4.00	-0.49
		5.00	-0.58
B386	Transducer leadwire tube broken during handling		

The test device was temperature conditioned for approximately 16 hr at each temperature before testing. This may not have been adequate time for reaching complete thermal equilibrium. The stability of the colder temperatures during the compression tests was not as good as the temperature stability of the tensile tests due to the nature of the conditioning box used for the compression tests. The tubes containing the leadwires for transducer S/Ns B382 and B386 were broken part way through the testing; this caused the leadwires to break also. The breaks occurred between the embedded transducer sensor and the hermetic glass-to-metal seal some inches away from the sensor and external to the propellant mass. No effort was made to reconnect the wires after they broke due to the safety hazard and because the internal vacuum of the sensor was lost.

The partial unbonding of the propellant may account for some of the small difference between the measured and reported stress. This partial unbonding of the propellant and test fixture probably occurred during the initial testing at the elevated temperature as this is where the lowest bond capability exists. All further testing with the tension/compression/shear device would experience

TABLE 41. SHEAR TEST RESULTS AT AMBIENT TEMPERATURE
SENSO-METRICS, INC. PRODUCTION TRANSDUCERS

T4653-D

Transducer S/N	Test Temperature, °F	Average Shear Stress, psi	Uncorrected Transducer Shear Stress, psi
B381	79	1.01	-1.66
		2.06	-3.60
		3.01	-5.22
		4.00	-7.22
		5.00	-9.38
B382	79	1.01	-0.56
		2.06	-0.56
		3.01	-0.37
		4.00	-0.40
		5.00	-0.56
B384	79	1.01	0.11
		2.06	0.28
		3.01	0.65
		4.00	0.79
		5.00	0.82
B386	79	1.01	0.17
		2.06	0.59
		3.01	1.12
		4.00	1.36
		5.00	1.52

some deviation from expected conditions because of this phenomenon. The overall measured stress gage performance is good in the tension/compression/shear device when actual testing considerations are included in the interpretation.

For these tests the same comments that were made about the prototypes would apply, section 4.1.6, particularly with regard to errors in determining stresses in tension with an unbonded sample. Looking at the compression data for the two best gages, S/N B302, S/N B304, for all but the coldest test temperature, it can be seen that results correlated with the measured Instron stress to about ±3%. For the shear tests, the data for gages 384 and 386 seem to increase slightly with applied load. This result led to some speculation that the gages may not have been mounted in the exact center of the end plates. Normal stress increases

TABLE 42. SHEAR TEST RESULTS AT -3°F
SENSO-METRICS, INC. PRODUCTION TRANSDUCERS

T4654-D

Transducer S/N	Test Temperature, °F	Average Shear Stress, psi	Uncorrected Transducer Shear Stress, psi
B381	Output recording device malfunctioned		
B382	Transducer leadwire tube broken during handling		
B384	-3	1.03	0
		2.01	0
		3.01	0
		4.01	0.23
		5.10	0.29
B386	-3	1.03	-0.13
		2.01	-0.23
		3.01	-0.26
		4.01	-0.23
		5.10	-0.23

rapidly away from the axial centerline, being about 50% of shear stress 1.0 in. from the centerline. When a shear load was applied to the fixture due to the unbond areas shown in Figure 120, the state of stress was considerably distorted from that analyzed. This distortion occurred on only one side of each gage and had the net effect of moving the gage off the axial centerline into an area with a component of normal stress. Therefore, the data shown in Tables 40 through 42 are probably real stresses, and do not represent sensitivity to shear. Gage S/N 381, being mounted near the edge of the sample, was obviously in a region of high normal stress as can be seen from the fixture analysis, Figure 120.

4.2.4 Senso-Metrics Production Transducers in Circular Port TM-1 Motors

Four Senso-Metrics production transducers were tested in two TM-1 motor cases. One TM-1 motor case was instrumented with two 25-psi gages (S/Ns B392 and 396) mounted at the case midpoint on the inside wall. Gage sensing surfaces were facing each other mounted 180° apart on the same plane. The gages were epoxied in place according to the gage mounting procedure presented in section 7.0. Two 2,000-psi gages (S/Ns B391 and B393) were instrumented as above in another TM-1 motor case. This CSD test motor (Figure 122) is a routinely cast

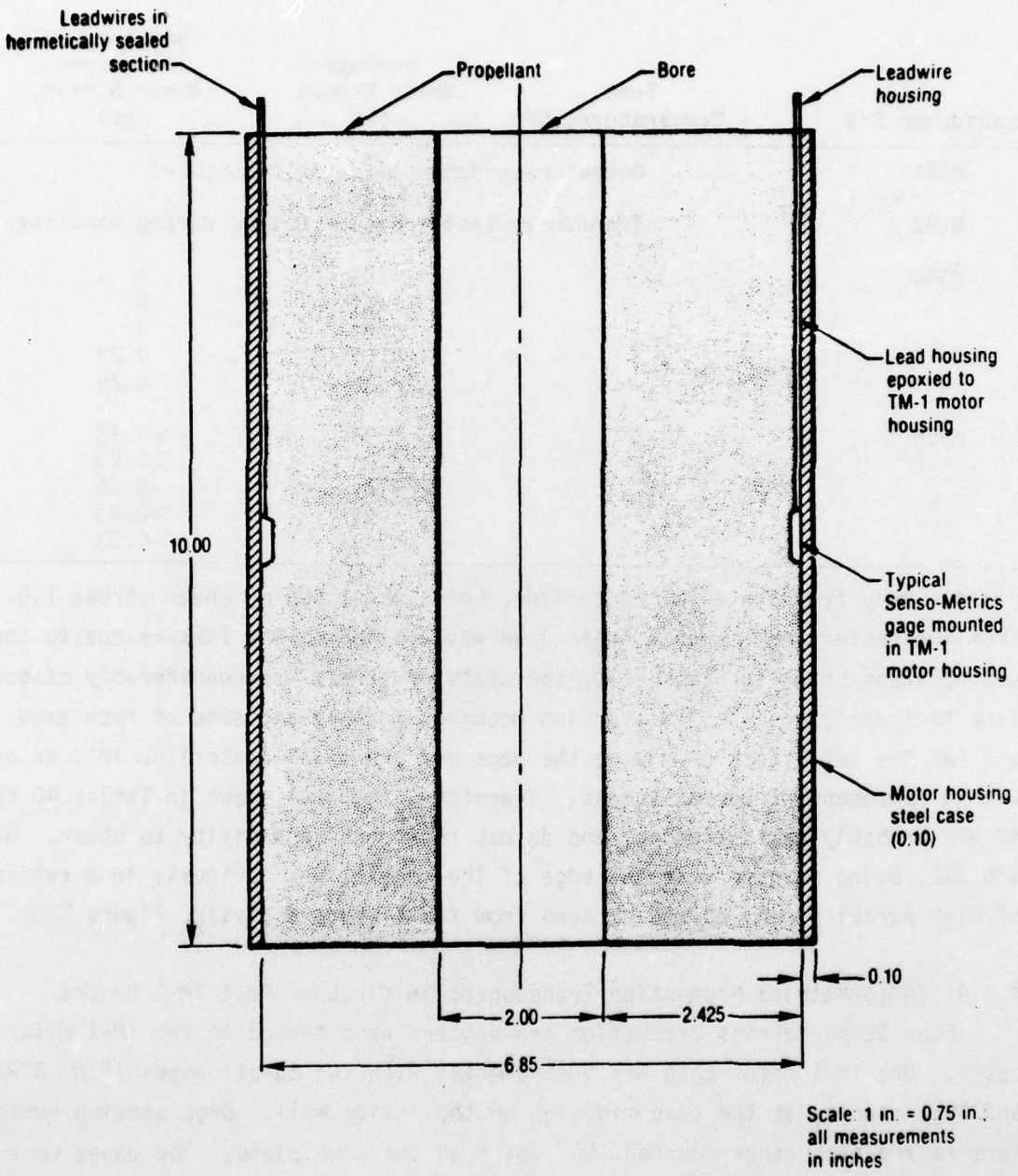


Figure 122. Cross Section of TM-1 Motor

17279

and tested motor. The TM-1 case has a 0.10-in.-thick wall, a length of 10 in., ID of 6.85 in., and B/A of 3.425 (2.00-in. bore), where B is the outer diameter of the grain (6.85 in.) and A is the bore diameter (2.0 in.).

The TM-1 Senso-Metrics instrumented motors were thermal cycled six times between approximately 115°F and ambient temperature. Strain measurements were taken by an Intermik gage at each temperature. Bore hoop strain measurements were recorded after temperature stabilization had occurred. The bore hoop strain versus test temperature is presented in Figure 123.

After the cycling tests were completed, the motor was step-cooled to -65°F. Continuous hourly transducer data were recorded and bore measurements and inspections were performed at each temperature level. No bore cracks or bond failures occurred during the thermal testing. The maximum bore strain was slightly more than 7%.

The data for corrected transducer bond stress versus temperature are presented in Figure 124. The upper curve in this figure is the maximum measured stress at each temperature increment before relaxation. The lower curve is the bond stress after approximately 20 to 21 hr at each temperature. The maximum stress occurred at 6 to 8 hr after change of temperature. Figure 125 shows typical stress and temperature versus time during a cooldown cycle. Typical stress relaxation occurred 6 to 8 hr after the initial cooldown cycle. A typical set of temperature and stress versus time curves for a heat-up cycle are shown in Figure 126.

After the instrumented 2,000-psi motor reached ambient temperature, it was subjected to high rate pressurization. The motor was placed in a pressure vessel and filled with silicone oil before pressurization. Applied pressure was monitored with a CSD calibrated pressure transducer (Taber, 0 to 2,000 psi). Corrected Taber pressure and measured Senso-Metrics transducer stress versus pressurization ramp time for two different loading rates are presented in Figures 127 and 128. At peak pressure the transducer varies from the corrected Taber stress by only 0.7%. Propellant stress response was slightly behind the Taber fluid pressure response as expected for a viscoelastic structural response.

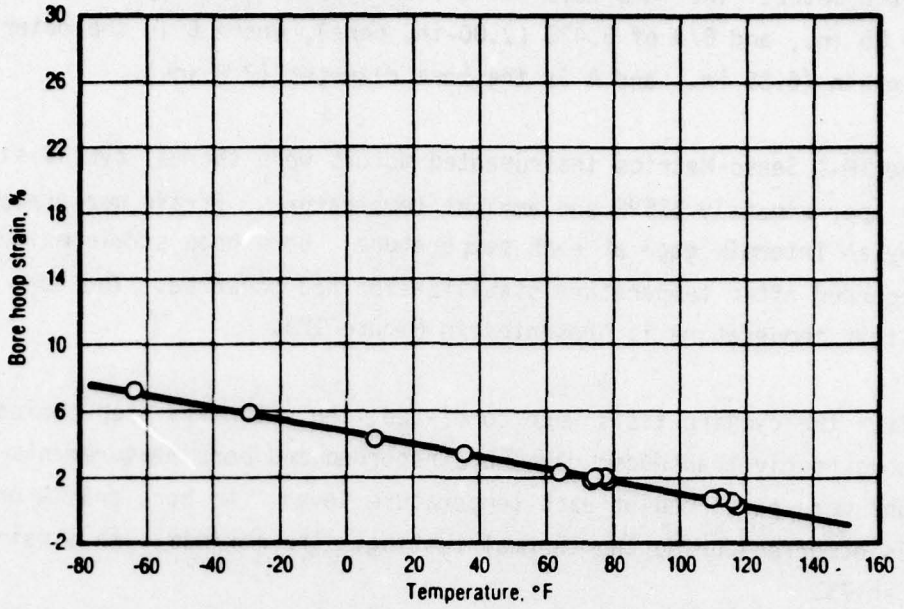


Figure 123. Strain vs Temperature for 25-psi TM-1 Motor

17280

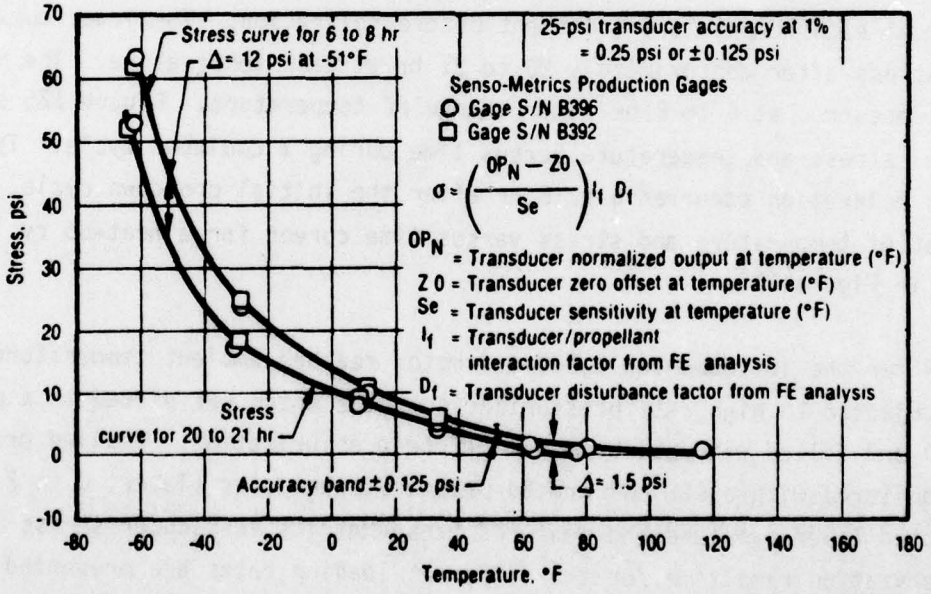


Figure 124. Maximum Stress vs Temperature for Thermal Testing of TM-1 Motor with 25-psi Gage

17281

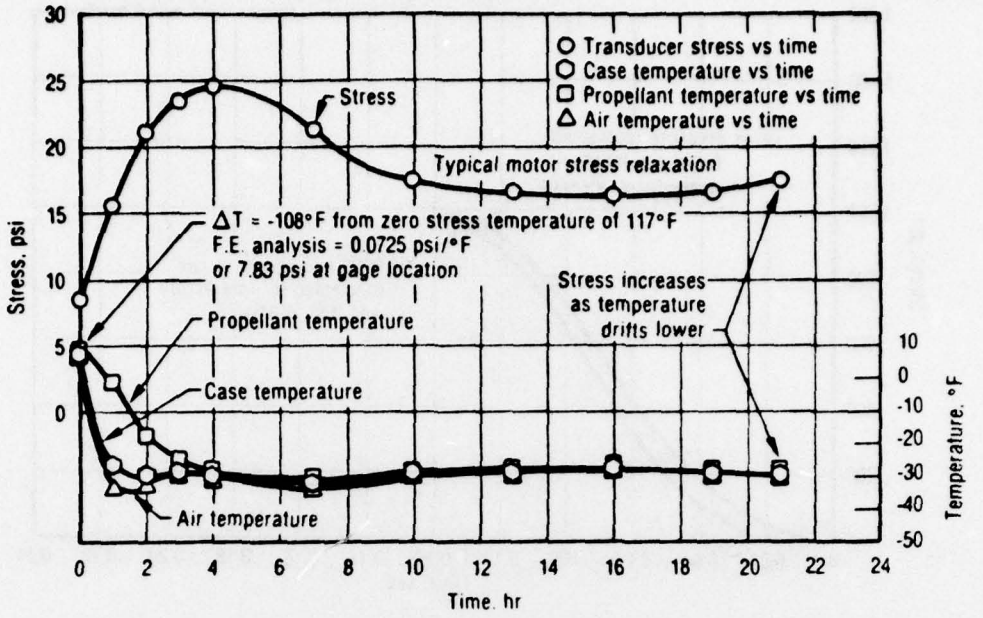


Figure 125. Typical Step Cooldown - Stress vs Temperature for TM-1 Motor (Transducer S/N B396)

17282

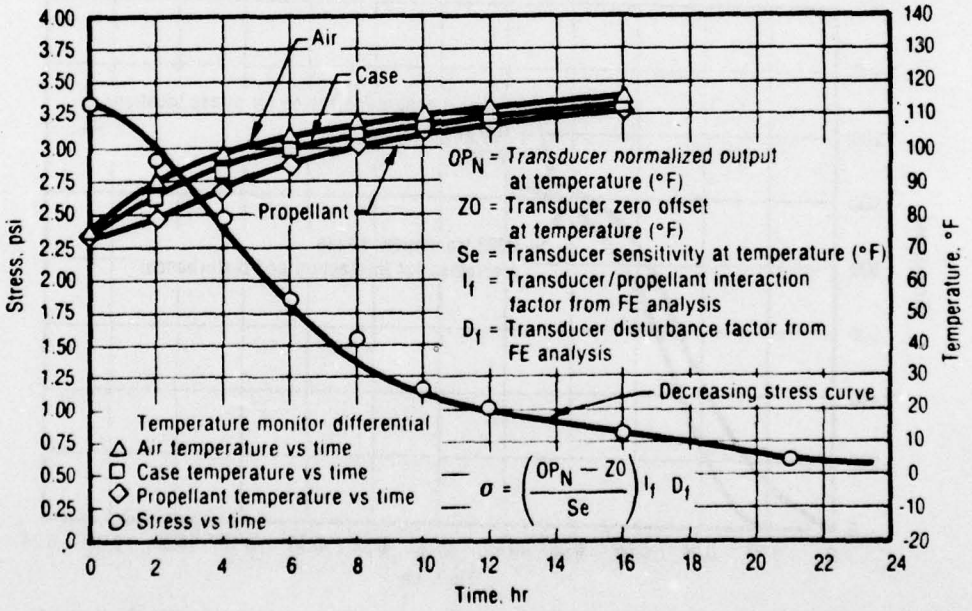


Figure 126. Typical TM-1 Motor Warmup Stress Gage Response (Transducer S/N B396)

17283

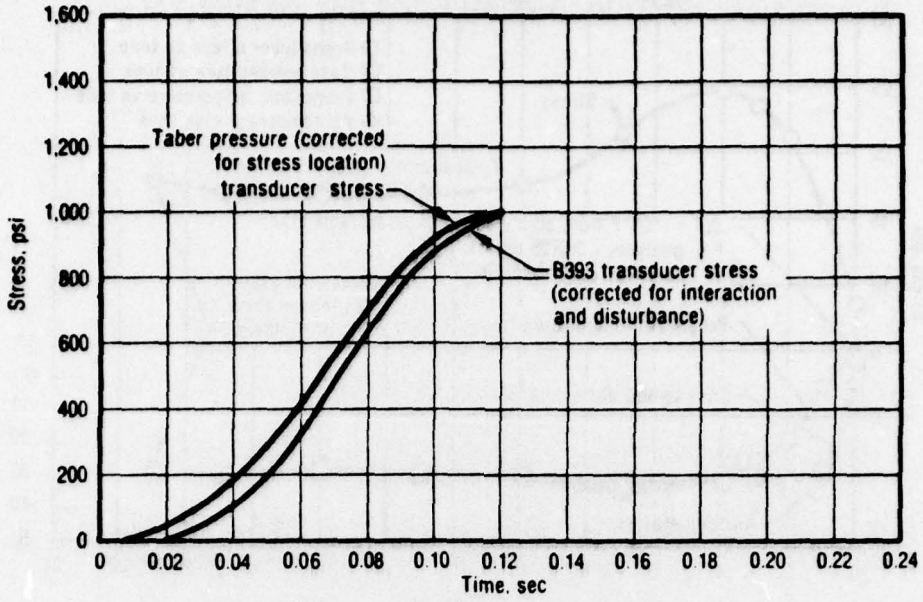


Figure 127. High Rate Pressurization Response in TM-1 Motor (Transducer S/N B393; 2,000 psi)

17284

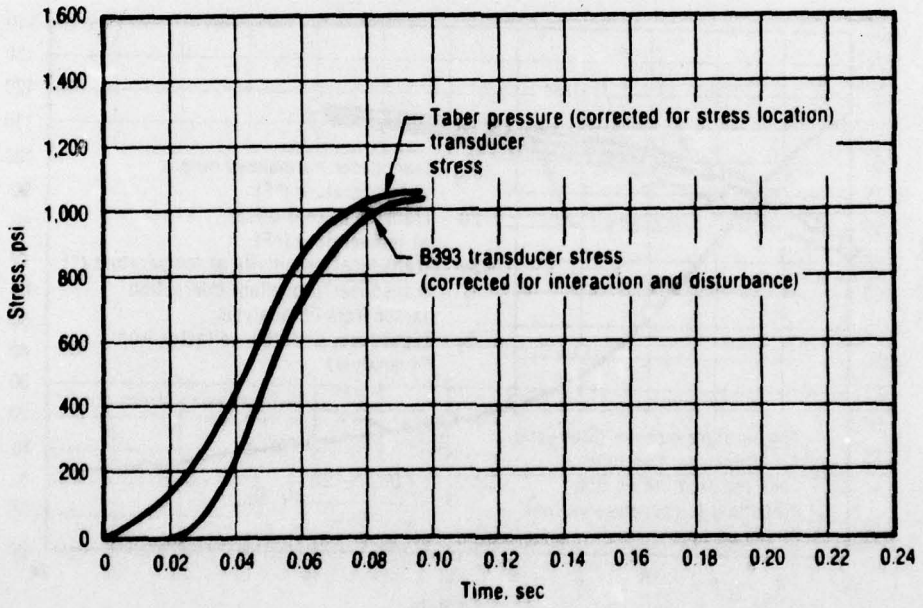


Figure 128. High Rate Pressurization Response in TM-1 Motor (Transducer S/N B393; 2,000 psi)

17285

After pressurizing to approximately 1,000 psi, inspection showed no motor failure, debonding, or crack propagation. The motor was then cooled down in steps to -52°F. Stress transducer output and excitation were monitored continuously. The maximum transducer stress versus temperature for the entire thermal test is presented in Figure 129. The upper curve is the maximum stress (6 to 8 hr into test) before relaxation occurred. The lower curve is the 24 hr data. Figure 130 shows a typical cooldown plot of stress and temperature versus time for this motor.

Comparison of Figures 124 and 129 shows that the two gages compare well in stress measurements at the lower test temperature where gage output is greater. At warm temperatures the 2,000 psi transducer reads a higher stress than the low range gage; however, its design accuracy is ±10 psi.

4.2.5 Theoretical Thermal Stress Predictions for TM-1 Motor Cooldown

The stress transducer data from the TM-1 motor with 25 psi stress gages is compared with theoretical stress predictions in this section. Linear viscoelastic analysis was conducted using the method outlined in CPIA No. 230. This linear viscoelastic analysis was also modified using a thermal-mechanical interaction parameter (A_F) which was extensively evaluated on the AFRPL-CSD Failure Mechanisms Program.

Stress calculations for a thermorheologically simple material with a thermal-mechanical interaction coefficient A_F and temperature-dependent shift factor A_T begins with the following equation:

$$\sigma = E_e (\varepsilon - \alpha\Delta T) + A_F \int_0^t \Delta E (\xi - \xi') \frac{d(\varepsilon - \alpha\Delta T)}{d\tau} d\tau \qquad (13)*$$

* Equation (4), Page 5-111, CPIA Publication 230, "JANNAF Solid Propellant Structural Integrity Handbook", Sept. 1972.

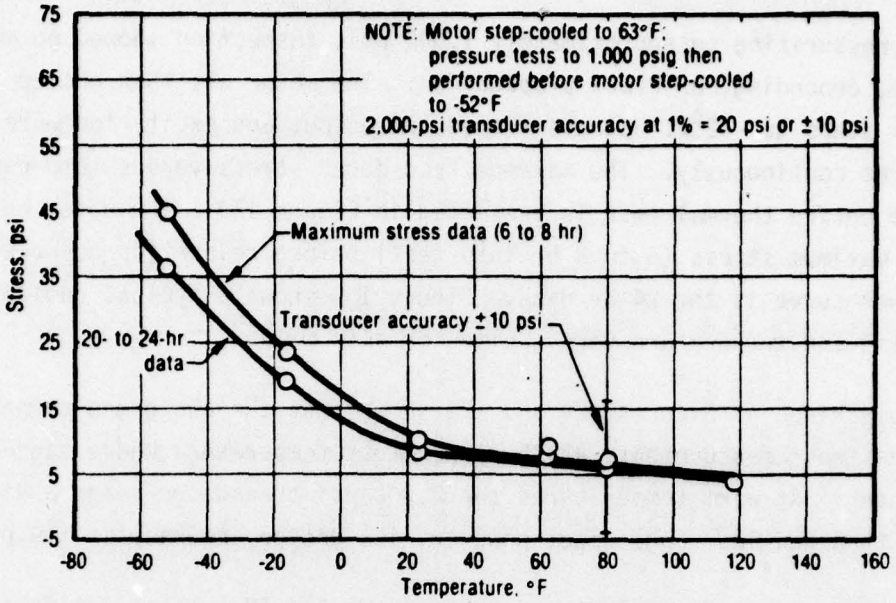


Figure 129. Maximum Stress vs Temperature for Step-Wise Cooldown Test (Transducer S/N B393 in TM-1 Subscale Motor)

17286

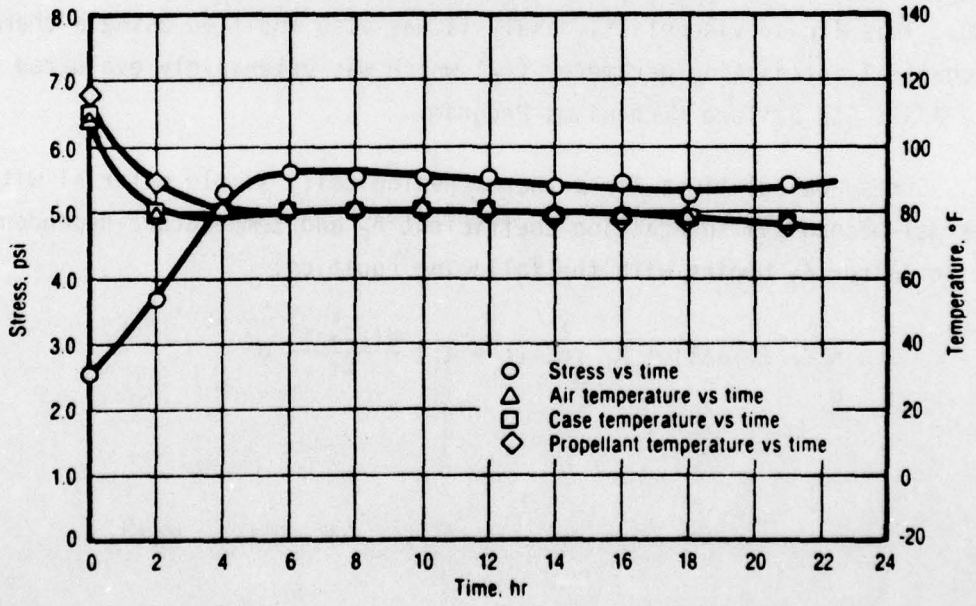


Figure 130. Cooldown Stress vs Time in TM-1 Motor (Transducer S/N B393; 2,000 psi)

17287

E_e = Equilibrium modulus

ϵ = mechanical strain

$\alpha\Delta T$ = thermal strain

α = linear coefficient of thermal expansion

$\Delta T = T - To$ = applied temperature change

T = current temperature

To = stress free temperature

$\Delta E(\xi) = E(\xi) - E(\xi')$ = transient component of modulus

$(\xi - \xi')$ = temperature reduced times

τ = integrating time variable

$$\xi(t) \equiv \int_0^t dt'/A_T, \quad \xi' \equiv \xi(\tau) \equiv \int_0^\tau dt'/A_T \tag{14}$$

Equation (13) becomes effective modulus for constant rates of straining and cooling

$$E_{eff} = \frac{\sigma}{\epsilon - \alpha\Delta T} = E_e + \frac{A_F}{t} \int_0^t \Delta E(\xi - \xi')d\tau \tag{15}$$

$$E_{eff} = E_e + \frac{A_F}{t} \int_0^t \Delta E(\xi)d\tau \tag{16}$$

with ΔE and A_T expressed in power laws.

$$\Delta E = E_1 (\xi)^{-n} \tag{17}$$

$$A_T = \left(\frac{T_R - T_a}{T - T_a}\right)^m \tag{18}$$

and E_1, n, m, T_a, T_R are determined from curve fitting the master modulus and the A_T data. Using the Power law representation equation 16 is rewritten after integrating as

$$E_{eff} = E_e + \frac{A_F E_1(\xi)^{-n}}{1-n} = E_e + \frac{A_F E_1 (t/A_T)^{-n}}{1-n} \qquad (19)$$

and the final effective modulus is expressed in terms of an I_T factor which is related to the stress ratios of stress from a simultaneous straining cooling test and a constant strain rate test at a constant temperature and is evaluated from the unbounded elliptical integral:

$$I_T \equiv \frac{1-n}{(m+1)^{1-n}} \left(-1 - \frac{1}{\Delta T}\right)^{1-n} \int_{(\Delta T_n+1)^{m+1}}^{1} (1-x)^{-n}$$

$$x \left(\frac{m}{m+1} + n - 2\right) dx \qquad (20)^*$$

These results are expressed in terms of the normalized temperature change, ΔT_n, defined as

$$\Delta T_n = \frac{T - T_o}{T_o - T_a} \qquad (20a)^*$$

$$\therefore E_{eff} = \frac{A_F I_T E (t/A_T)^{1-n}}{1-n} + E_e \qquad (21)$$

Using the above analytic expressions (equation 21), the effective modulus for the slowly cooled instrumented TM-1 motor was calculated and used to predict the radial bond stress.

The determination of A_F (thermal-mechanical interaction factor) comes from the comparison of the isothermal secant modulus to that of the measured effective modulus from simultaneous straining-cooling experiments. The ratio between the two moduli is, in effect, A_F.

* CPIA Publication 230, page 5-114.

Propellant characterization was done in laboratory conditions to obtain both the simultaneous straining-cooling data and Master Modulus curve. Equations 17 and 18 are the power laws used to fit the experimental data for modulus and the time temperature shift behavior. With the Master Modulus curve, the variables A_T, n, m, and I_T are determined. The value I_T, contains the values n, m, ΔT_n from equation 20. Equation (21) was then used to calculate motor stress for the appropriate cooling rates.

The conventional 3% strain-stress relaxation modulus master curve for UTP-19,360-750/6452 is presented in Figure 131. Simultaneous straining cooling data for the same propellant is presented in Figure 132. Four samples were tested concurrently to obtain the straining-cooling similitude data for evaluating the A_F thermal-mechanical interaction factor.

A comparison of predicted and measured stress graphs is presented in Figure 133. The A_F corrected stress predictions are in excellent agreement with the measured stresses. Conventional viscoelastic analysis underpredicts the actual bond stresses. This underprediction was expected based on results from the Failure Mechanism program which showed that the thermal-mechanical interaction factor A_F is required to obtain accurate effective modulus values for motors that are exposed to a combined straining-cooling histories. Details of the A_F corrected analyses are presented in the final report for the Failure Mechanisms program (CSD 2540-FR).

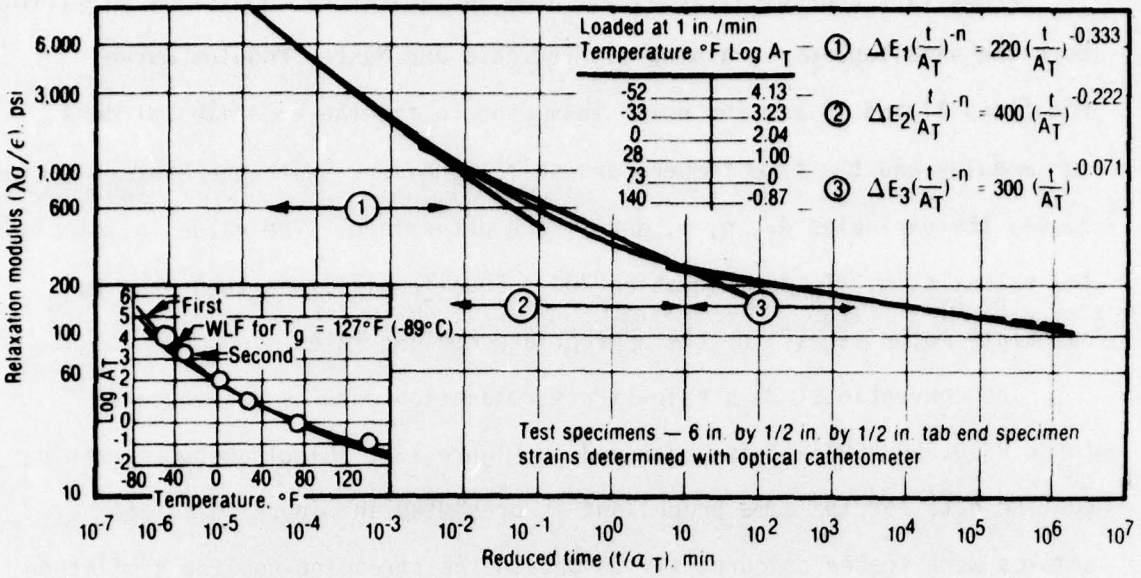


Figure 131. Master Modulus Data for UTP-19,360-750/6452 at 3% Strain
Note: 750/6452 Means Batch Identification

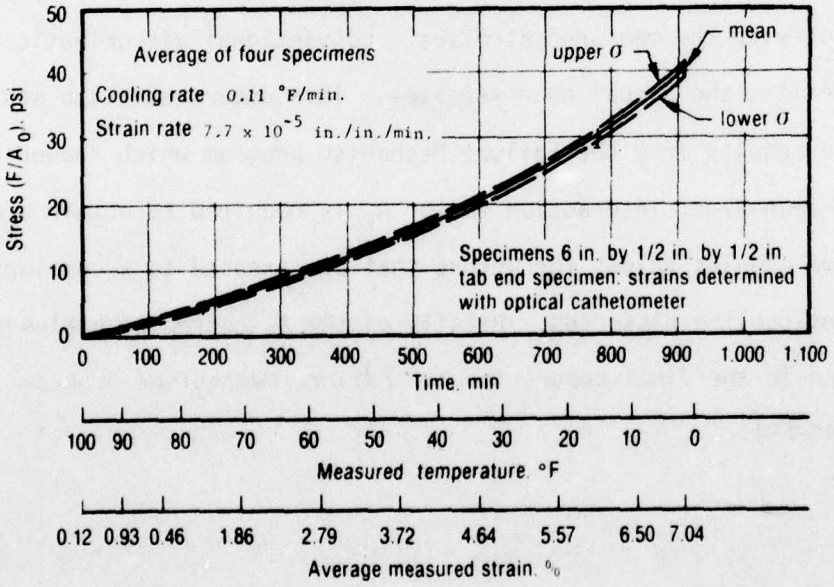


Figure 132. Simultaneous Straining-Cooling Test with Uniaxial Bars of UTP-19,360-750/6452

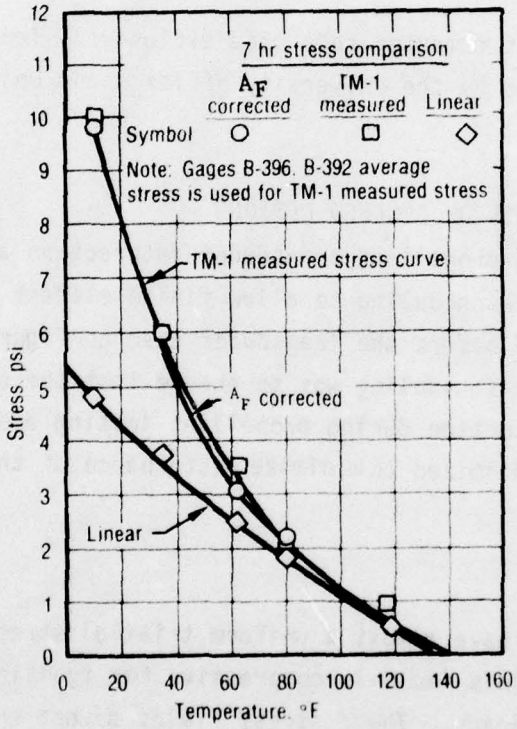


Figure 133. Comparison of Stress Gage Response with Analytical Prediction

5.0 FINITE ELEMENT ANALYSIS OF STRUCTURAL TEST FIXTURES

The structural test fixtures used to evaluate gages in a propellant environment were analyzed by finite element methods. These investigations began by optimizing the structural test fixture designs. The analyses gave stress axialities at gage locations, stress disturbances, and stresses at critical test vehicle locations which could be used to establish limits for temperature or pressure loading based on propellant mechanical properties. Most importantly, the structural test fixture analyses were used to interpret gage response in the embedded conditions characteristic of a solid propellant motor.

The finite element computer code used exclusively for these studies was the TEXGAP 2D developed by the University of Texas and United Technologies Corporation.

5.1 STRUCTURAL ANALYSIS OF CELESCO DESIGNS

Concern about the propellant transducer interaction and stress field disturbance caused some rescheduling to allow finite element analysis runs to be conducted and analyzed before the transducer case configurations were machined. The objective of the rescheduling was to ensure that the case walls were thick enough to prevent distortion during propellant testing and that the transducer external design was optimized to minimize disturbance of the stress field above the transducer.

Grain Simulator

Most SRM designs have almost a uniform triaxial stress field where transducers are located. This field is compressive for ignition loads and tension for thermal cooldown loads. These stress fields do not change significantly unless one approaches a free surface near the bore or bond termination or a grain irregularity. It would be desirable to model these uniform triaxial stress fields for the laboratory evaluation of the transducers. BIT or other similar test fixtures generate a large stress gradient across the gage region,

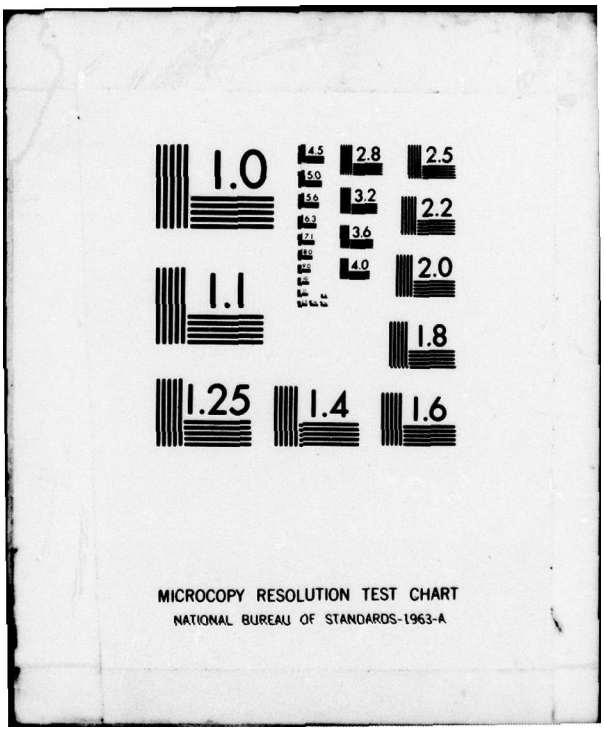
AD-A073 659 UNITED TECHNOLOGIES CORP SUNNYVALE CALIF CHEMICAL SY--ETC F/G 9/1
THE DEVELOPMENT OF IMPROVED NORMAL STRESS TRANSDUCERS FOR PROPE--ETC(U)
JUN 79 E C FRANCIS, R E THOMPSON, W E BRIGGS F04611-75-C-0042

UNCLASSIFIED CSD-2548-FR-VOL-1 AFRPL-TR-79-34-VOL-1 NL

3 OF 3
AD A073659



END
DATE FILMED
10-79
DDC


1.0
1.1
1.25
1.4
1.6
1.8
2.0
2.2
2.5
2.8
3.2
3.6
4.0
4.5
5.0
5.6
MICROCOPY RESOLUTION TEST CHART
NATIONAL BUREAU OF STANDARDS-1963-A

especially for thermal loading conditions. One potential laboratory test design is that of a shallow end burner (Figure 134). This design is wide enough to simulate a large bonded sheet.

In an attempt to obtain a 3D tension stress field for the laboratory transducer evaluation, a grain simulator sample was evaluated (Figure 135). Early analysis for pressure loads showed that a shallow, 3-in. thickness gave a good 3D compressive stress field. However, thermal analysis runs for different design heights show that triaxiality is poor at the gage location for an L/D of 0.3 and 0.8 designs (Table 43). An L/D of 1.5 gave an adequate triaxial thermal stress but the stress amplitudes were too high and could cause propellant unbonding. A compromise L/D design of 1.0 was selected for the transducer analysis. The final simulator design is 10 in. high and 10 in. in diameter with a steel case wall thickness of 1 in.

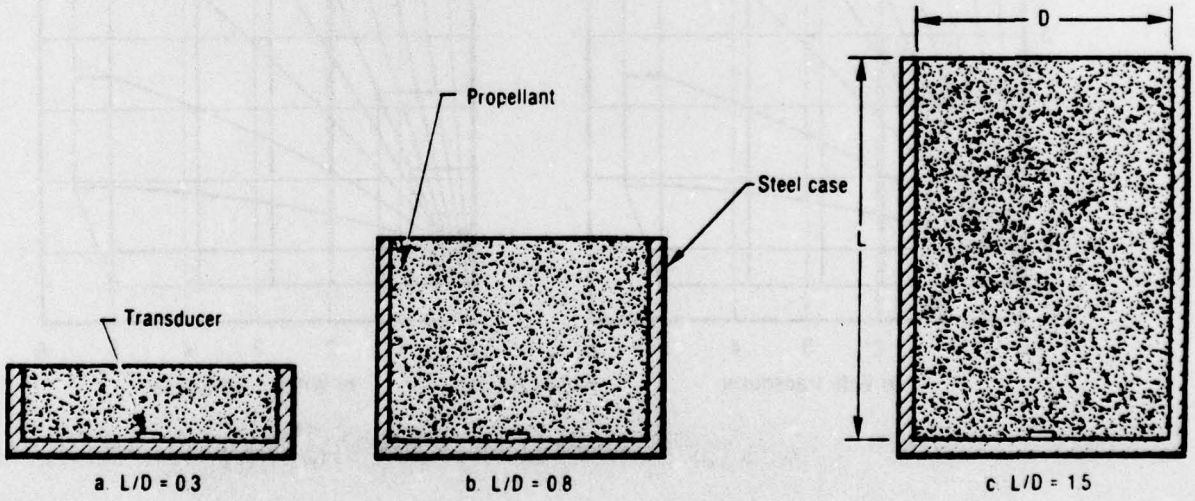


Figure 134. Laboratory Test Simulator Concept

18504

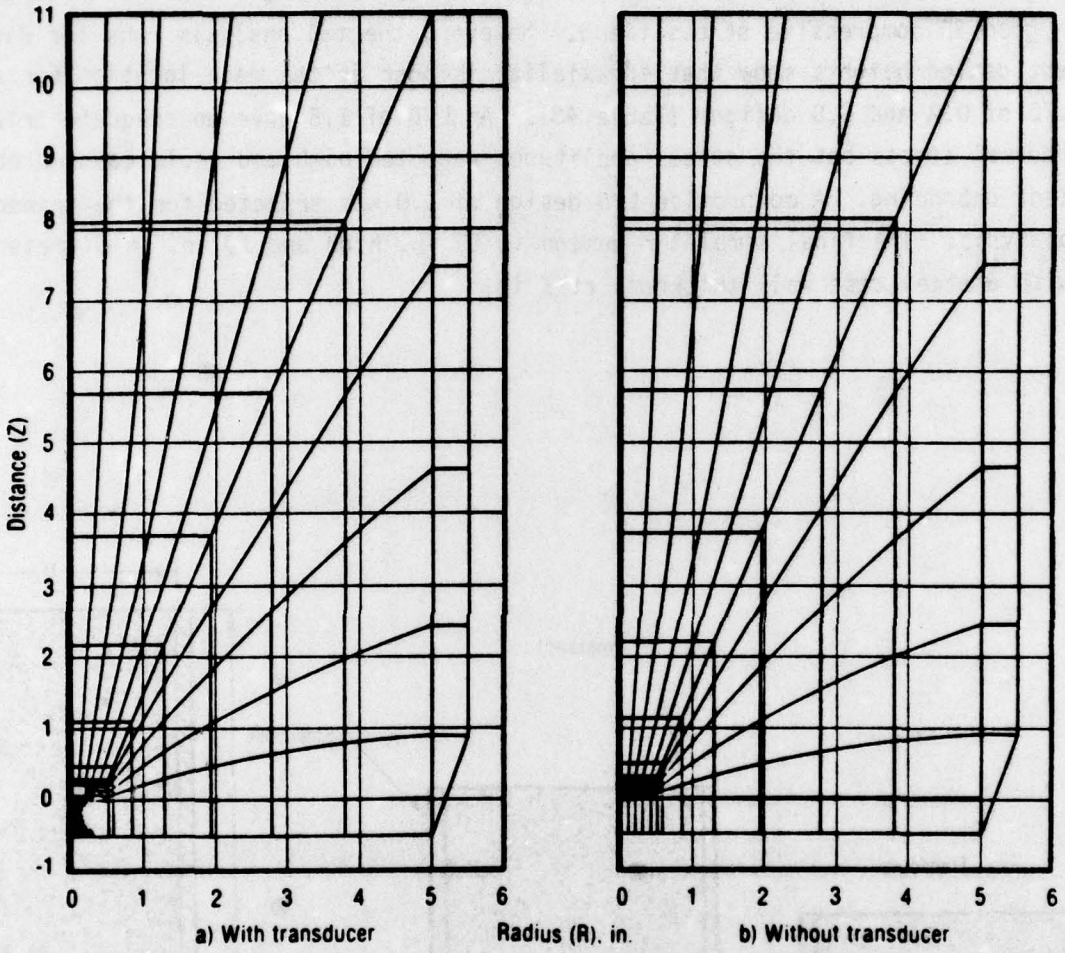


Figure 135. Typical Grain Simulator Sample Grid With and Without Transducer
16513

TABLE 43. STRESS AXIALITY FOR GRAIN SIMULATOR WITHOUT TRANSDUCER - THERMAL LOAD
(E_p = 2,000 PSI; ΔT = -100°F)

T4567-D

L/D and ID No.	R	Z	σ_r	σ_z	σ_θ
L/D = 0.3;	0.08	0.46	22.29	-3.93	22.29
	0.32	0.52	22.83	-4.03	22.81
	0.71	0.58	23.68	-3.96	23.56
	1.23	0.64	25.29	-3.44	25.00
	1.87	0.69	28.16	-1.69	27.77
	2.64	0.76	32.55	3.28	32.85
	3.52	0.84	36.43	16.25	40.74
	4.49	0.94	34.54	38.80	47.75
L/D = 0.8;	0.08	0.54	99.45	56.81	99.54
	0.40	0.68	100.90	57.45	101.47
	1.05	0.82	100.48	167.86	104.59
	1.97	1.02	95.72	92.07	107.79
	2.50	1.14	97.23	107.93	108.01
L/D = 1.5;	0.06	0.44	301.26	261.66	301.42
	0.22	0.56	301.87	261.24	302.13
	0.47	0.67	301.77	262.90	302.18
	0.82	0.80	300.50	268.43	303.65
	1.24	0.96	296.74	278.51	303.88
	1.74	1.28	287.93	290.58	300.62
	2.00	1.50	286.46	296.97	297.04

NOTE: R = radial distance from transducer center; Z = axial distance from transducer center; σ_r = stress in radial direction; σ_z = stress in axial direction; σ_θ = third of the triaxial stresses

Stress Disturbance for Celesco Design Concepts

The stress disturbance for a thermal load is presented in Table 44 where analysis results are presented with and without the transducer in the grain simulator. Side and vertical propellant stress disturbances are limited to less than 2 in. from the transducer center by comparing results with and without the gage at the same location. Stress disturbance at the propellant bondline is shown in Figures 136 through 140. The preliminary square corner design showed a 12% stress concentration at the corner and then reduced stress on the transducer sides for the tensile load in a propellant bar (Figure 136). The 45° corner design (Figures 137 through 140) reduced the corner stress concentration. However, the transducer side thermal stresses were significantly higher than those on top of the diaphragm. The 0.030-in.-radius corner model appeared to improve the corner stresses slightly, but the side thermal stresses were still higher than desired.

TABLE 44. STRESS DISTURBANCE DATA FOR NORMAL STRESS TRANSDUCER IN GRAIN SIMULATOR
(E = 100 PSI; $\Delta T = -100^{o}F$)

T4568-D

		No Gage (Computer ID No. 23)			Gage (Computer ID No. 16)		
R	Z	σ_r, psi	σ_z psi	σ_θ, psi	σ_r, psi	σ_z psi	σ_θ, psi
0.40	0	7.80	6.93	7.80	9.11	8.21	9.11
0.54		7.81	6.94	7.81	8.15	7.27	8.15
0.71		7.83	6.96	7.83	7.98	7.07	7.97
1.07		7.90	7.03	7.90	7.93	7.06	7.92
1.62		8.06	7.19	8.07	8.06	7.19	8.06
2.35		8.41	7.53	8.41	8.41	7.53	8.41
3.28		8.98	8.15	8.99	8.98	8.15	8.98
4.39		10.59	9.69	10.60	10.59	9.69	10.60
0	0.26	8.05	6.77	8.05	6.94	6.02	6.94
	0.29				7.06	5.99	7.06
	0.39	8.15	6.71	8.15	7.59	5.84	7.60
	0.79	8.40	6.56	8.41	8.33	6.08	8.36
	1.65	8.62	6.34	8.64	8.63	6.30	8.64
	2.95	8.40	6.04	8.41	8.40	6.03	8.41
	4.71	7.49	5.19	7.49	7.48	5.19	7.49
	6.91	5.57	3.17	5.62	5.57	3.17	5.62
	9.56	1.41	1.68	1.79	1.41	1.67	1.79
0.54	0.39	8.21	6.79	8.11	8.06	6.96	8.25
0.71	0.79	8.44	6.64	8.45	8.38	6.67	8.47
1.07	1.65	8.66	6.53	8.70	8.64	6.52	8.70
1.62	2.95	8.36	6.40	8.47	8.35	6.40	8.47
2.35	4.71	7.38	5.90	7.60	7.38	5.90	7.60
3.28	6.91	5.47	4.72	5.84	5.47	4.72	5.84
4.39	9.56	3.61	3.88	4.51	3.61	3.88	4.51

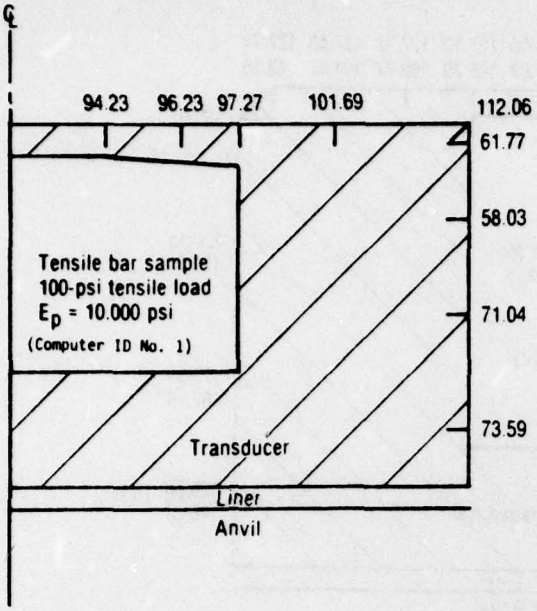


Figure 136. σ_Z Stress Disturbance at Bond Line for Square Diaphragm Transducer with 100-psi Tensile Load
16512

5.1.1 Finite Element Analysis of Celesco Design

Finite element analyses were conducted as shown in Table 45. Element types used for the analyses are shown in Figure 141. Typical diaphragm displacement profiles for Numbers 8 and 9 analysis runs are presented in Figures 142 and 143 for different modulus values and loading conditions. Modulus effects are noted, but they are minor.

Analysis of the cantilevered beam support bending action is shown in Figure 144 as axial displacement along a plane through this support. Displacement over the support area

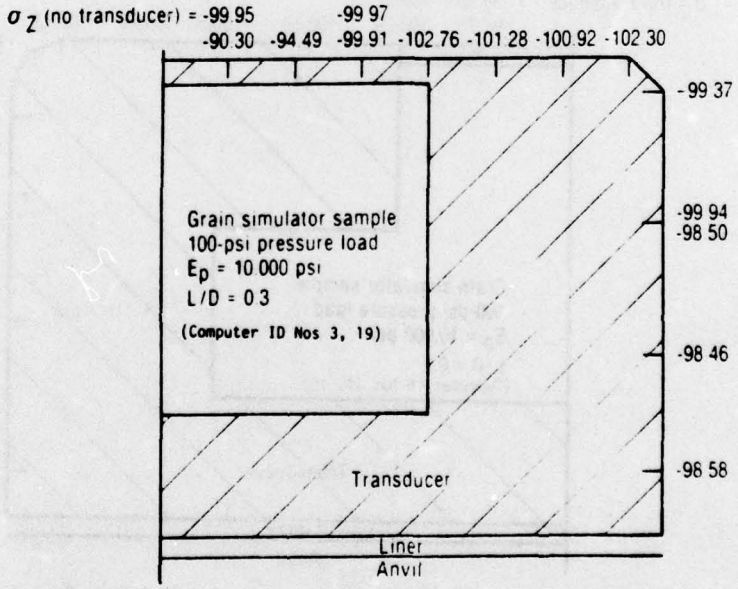


Figure 137. σ_Z Stress Disturbance at Bond Line for 45° -0.016-in. Corner Diaphragm Transducer with 100-psi Pressure Load
16511

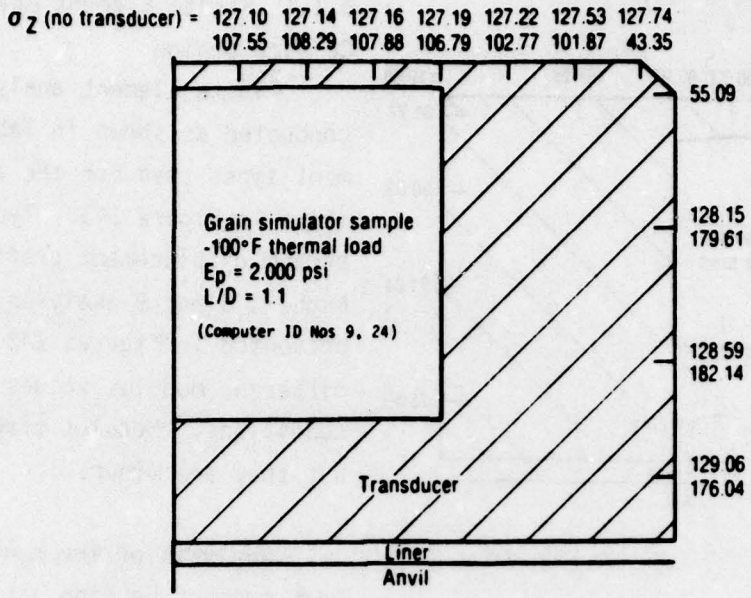


Figure 138. σ_z Stress Disturbance at Bond Line for 45° -0.016-in. Corner Diaphragm Transducer with -100°F Thermal Load

16510

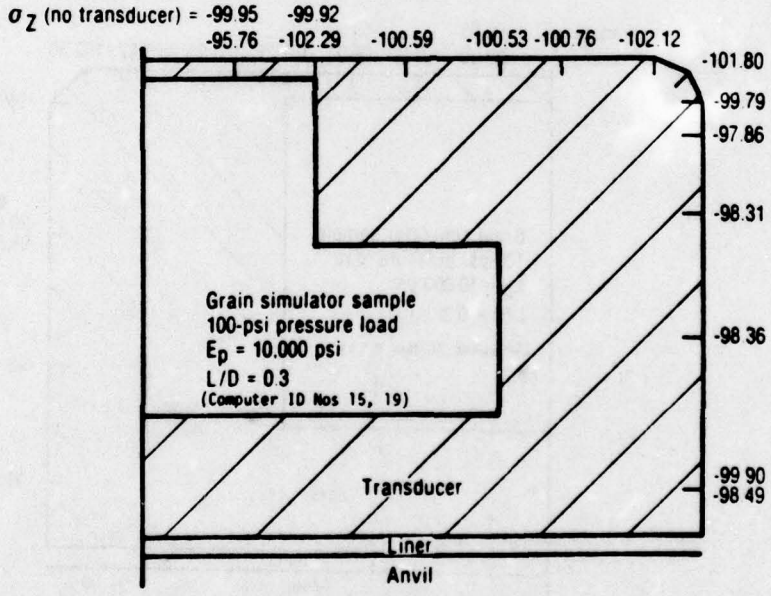


Figure 139. σ_z Stress Disturbance at Bond Line for 0.030-in.-Radius Corner Cantilever Beam Transducer with 100-psi Pressure Load

16509

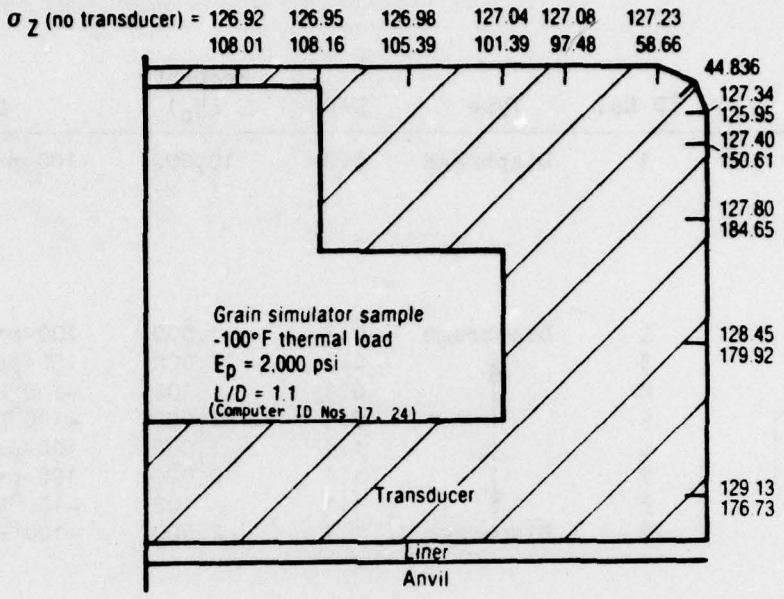


Figure 140. σ_Z Stress Disturbance at Bond Line for 0.030-in.-Radius Corner Cantilever Beam Transducer with -100°F Thermal Load

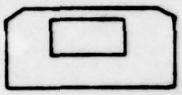
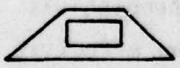
16508

(from a radius of 0.11 to 0.23 in.) is about 10 μ in. which would cause an attached beam to move an additional 9 μ in. at its tip as shown by the dashed line. This amount of displacement was considered to be unacceptable because it reduces gage electrical output as it is mechanically subtracted from the diaphragm displacement by the interior gage linkage. To alleviate this problem, the beam support platform was stiffened by doubling its thickness to 0.101 in. and the transducer sidewall was increased from 0.10 to 0.13 in. thick. The result of this design change is shown in Figure 145 where the beam tip displacement is seen to be 2.5 μ in.

A partial summary of transducer test conditions and computer output is presented in Table 46. Diaphragm center displacements presented are with respect to the bottom outside edge of the transducer. Platform bending was subtracted from the diaphragm center displacement to determine the effective axial displacement for a beam gage which is directly proportional to the amount of strain that the semiconductor elements sense.

TABLE 45. SUMMARY OF NORMAL STRESS TRANSDUCER DESIGNS AND ANALYSIS

T4569-D

Design	ID No.	Type	L/D	Property (E_p)	Load
Preliminary	1	Diaphragm	0.3	10,000	100-psi tensile
					
No. 1	2	Diaphragm	0.3	1,000	100-psi pressure
	3		0.3	10,000	100-psi pressure
	4		0.3	100	-100°F thermal
	5		0.3	2,000	-100°F thermal
	6		1.1	1,000	100-psi pressure
	7		1.1	10,000	100-psi pressure
	8		1.1	100	-100°F thermal
	9	Diaphragm	1.1	2,000	-100°F thermal
No. 2	10	Cantilever beam	0.3	1,000	100-psi pressure
	11		0.3	10,000	100-psi pressure
	12		0.3	100	-100°F thermal
	13		0.3	2,000	-100°F thermal
No. 2 - Stiffened with 0.030-in.-radius on corner	14		0.3	1,000	100-psi pressure
	15		0.3	10,000	100-psi pressure
	16		1.1	100	-100°F thermal
	17	Cantilever beam	1.1	2,000	-100°F thermal
No. 3 - 45° champhered sides	18	Diaphragm	0.3	1,000	100-psi pressure
					

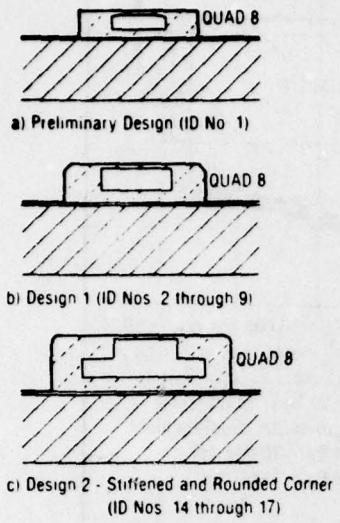


Figure 141. Finite Element Modelling Configurations

17146

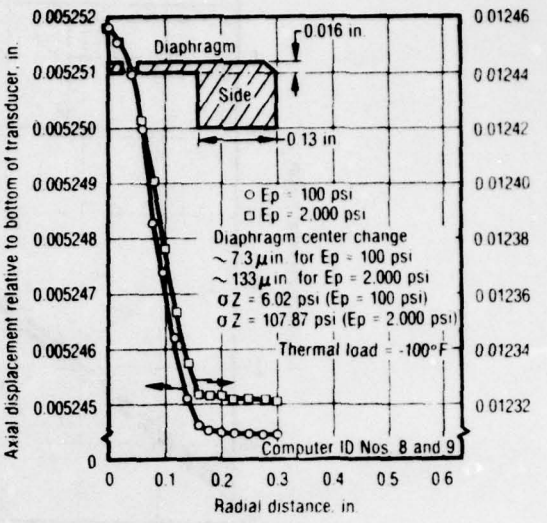


Figure 142. Axial Displacement Values for Transducer in Grain Simulator Sample - Thermal Loading

16504

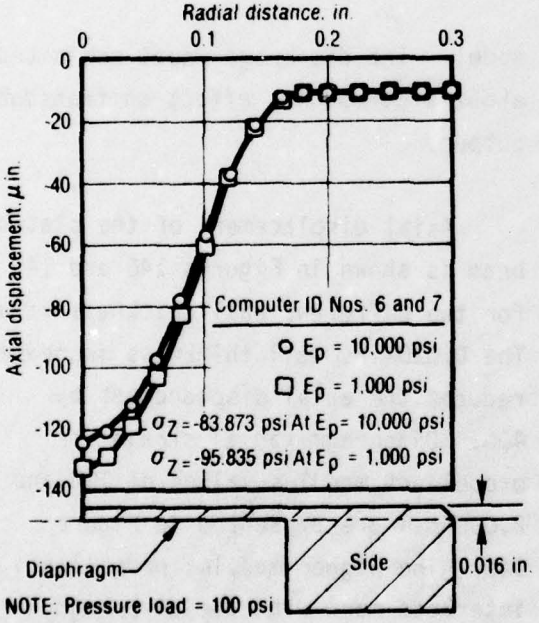


Figure 143. Axial Displacement Values for Transducer in Grain Simulator Sample (L/D = 1.1) - Pressure Loading

16505

Normalized data for both the diaphragm and cantilevered beam models are presented in Tables 47 and 48. Note that these results are for two different L/D grain simulators. Stress distrubance above the transducers varied between 10% and 20% depending on the propellant modulus and loading condition. Modulus effect on this stress disturbance appears to be about 5%. Both transducer models appear to produce about 15% to 17% higher output for the pressure load than for the thermal load condition. Modulus effect on the transducer output was less than 1% for the cantilevered beam

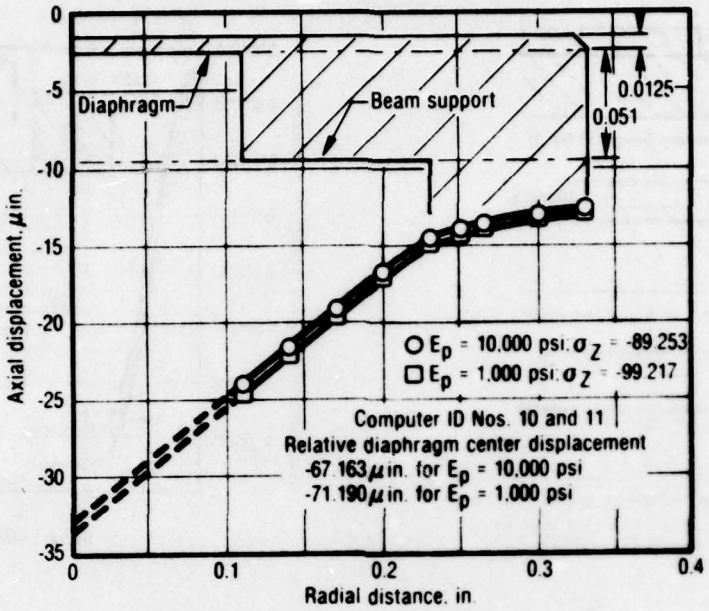


Figure 144. Cantilevered Beam Platform Bending Data (p = 100 psi, L/D = 0.3) 16506

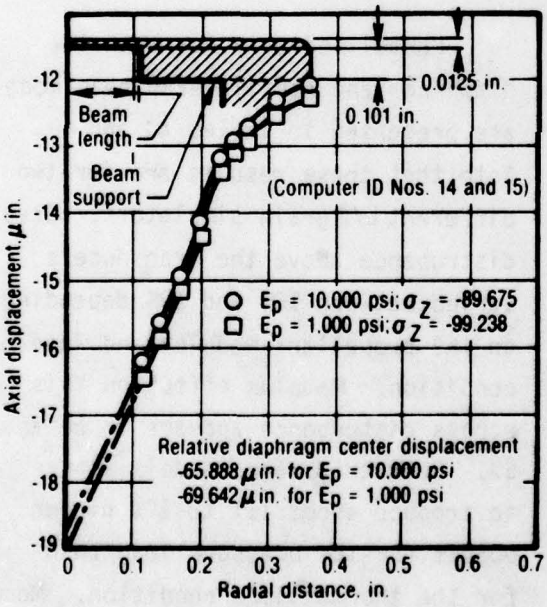


Figure 145. Improved Cantilevered Beam Platform Bending Data (P = 100 psi; L/D = 0.3) 16507

model. The diaphragm model exhibited about a 6% modulus effect on transducer output.

Axial displacement of the platform beam is shown in Figures 146 and 147 for two different wall thickness values. The 0.030-in. wall thickness increase reduced the axial displacement by 40%. Diaphragm radial strain for propellant modulus values of 100 and 2,000 psi are presented in Figure 148. The higher modulus propellant interacts more with the diaphragm and causes a larger strain concentration at the diaphragm edge.

TABLE 46. PARTIAL SUMMARY OF COMPUTER DATA

T4570-D

ID No.	Diaphragm Radius, in.	Diaphragm Thickness, in.	Diaphragm Center Strain, μ-strain	Diaphragm Center Displacement U_z Reliability, μin.	Platform Bending, μin.	Effective Axial Displacement	Load	Modulus, psi	Stress at Diaphragm Top, psi	L/D
1	0.122	0.016/ 0.021	-47.561				Tensile 100 psi	10,000	93.112	Tensile bar
2	0.163	0.016	127.26				Pressure 100 psi	1,000	-99.133	0.3
3	0.163	0.016	117.25				Pressure 100 psi	10,000	-88.90	0.3
4	0.163	0.016	1.425				Thermal -100°F	100	-0.822	0.3
5	0.163	0.016	30.249				Thermal -100°F	2,000	-17.69	0.3
6	0.163	0.016	123.05				Pressure 100 psi	1,000	-95.835	1.1
7	0.163	0.016	110.69				Pressure 100 psi	10,000	-83.873	1.1
8	0.163	0.016	-7.2955				Thermal -100°F	100	6.02	1.1
9	0.163	0.016	-129.91				Thermal -100°F	2,000	107.87	1.1
14	0.113	0.011		-69.64	-2.2	-67.44	Pressure 100 psi	1,000	-99.238	0.3
15	0.113	0.011		-65.89	-2.5	-63.39	Pressure 100 psi	10,000	-89.675	0.3
16	0.113	0.011		4.10	0.46	3.64	Thermal -100°F	100	5.9608	1.1
17	0.113	0.011		75.00	7.5	67.50	Thermal -100°F	2,000	107.07	1.1

NOTE: Rigid-mounted diaphragm has 111-μr at bottom center for 100-psi load from Martin Marietta technical note

TABLE 47. THERMAL AND PRESSURE STRESS DISTURBANCE FOR CANTILEVER TRANSDUCER
T4571-D

ID No.	L/D	Load	Modulus	Stress Disturbance, $\frac{\sigma_z \text{ no gage}}{\sigma_z \text{ gage top}}$	$\frac{U_z \text{ (effective)}}{\sigma_z \text{ gage top}}$	$\frac{U_z \text{ (effective)}}{\sigma_z \text{ no gage}}$
14	0.3	Pressure	1,000	-	0.679×10^{-6}	-
15	0.3	Pressure (100 psi)	10,000	1.114 (25)	0.706×10^{-6}	0.634×10^{-6}
16	1.1	Thermal	100	1.131 (23)	0.611×10^{-6}	0.539×10^{-6}
17	1.1	Thermal ($\Delta T = -100^{o}F$)	2,000	1.183 (24)	0.630×10^{-6}	0.533×10^{-6}

NOTE: Stress disturbance ~11% to 18%; modulus effect on stress disturbance ~5%; modulus effect on thermal U_z/σ_z (no gage) ~0.5%; pressure output ~17% higher than thermal output

TABLE 48. THERMAL AND PRESSURE STRESS DISTURBANCE FOR DIAPHRAGM TRANSDUCER
T4572-D

ID No.	L/D	Load	Modulus, psi	Stress Disturbance, $\frac{\sigma_z \text{ no gage}}{\sigma_z \text{ gage top}}$	$\frac{\varepsilon_r}{\sigma_z \text{ (gage top)}}$	$\frac{\varepsilon_r}{\sigma_z \text{ (no gage)}}$
6	1.1	Pressure	1,000	-	1.283×10^{-6}	-
7	1.1	Pressure (100 psi)	10,000	1.122 (25)	1.302×10^{-6}	1.160×10^{-6}
8	1.1	Thermal	100	1.126 (23)	1.077×10^{-6}	9.56×10^{-7}
9	1.1	Thermal ($\Delta T = -100^{o}F$)	2,000	1.179 (24)	1.207×10^{-6}	1.023×10^{-6}

NOTE: Stress disturbance ~12% to 18%; modulus effect on stress disturbance ~5%; modulus effect on thermal strain/σ_z (no gage) ~6.2%; pressure output ~15% higher than thermal output

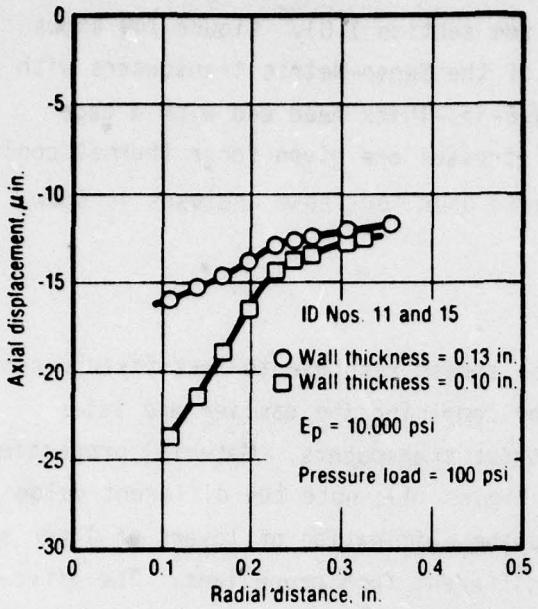


Figure 146. Cantilevered Beam Platform Bending Data (P = 100 psi; L/D = 0.3)

16501

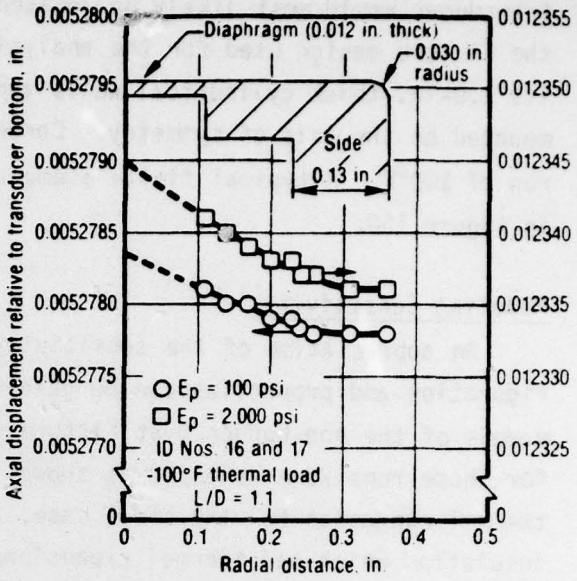


Figure 147. Cantilevered Beam Platform Bending Data

16502

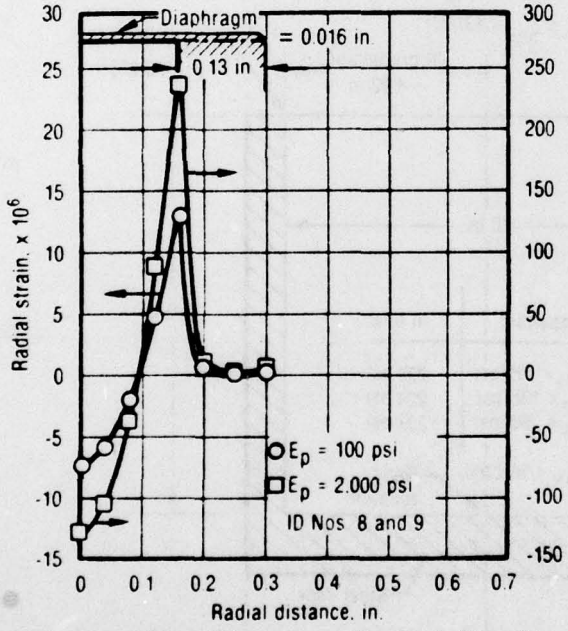


Figure 148. Diaphragm Radial Strain Distribution for Thermal Load Modulus Variation

16503

5.2 END-BURNER TEST FIXTURE FOR SENSOMETRICS, INC., TRANSDUCERS

The primary fixture designed for evaluating gages was an end-burner cylinder. This had the primary advantages of being used readily for rapid pressurization tests and of its axisymmetric geometry being modeled easily for finite element analysis. Preliminary studies of this fixture included varying its L/D ratio from 0.3 to 1.5; from this it was determined that an L/D of at least 1.0 was necessary to achieve stresses at its head end approaching hydrostatic pressure (e.g., analogous to motor conditions where a stress

transducer would most likely be located; see section 1.0). Figure 149 shows the fixture design used for the analysis of the Senso-Metric transducers with its 1.0-in.-thick cylindrical walls and 1.5-in.-thick head end with a gage mounted on the axis of symmetry. Corner stresses are given for a thermal cooling run of 100°F. A typical finite element grid used for these analyses is shown in Figure 150.

Modeling Sensitivity

An appreciation of the sensitivity of stress response to test fixture configuration and properties can be gained by comparing the earlier and later models of the end-burner test fixture without transducers. Material properties for these runs were selected as shown in Figure 149; note the different value of thermal expansion for the steel case, and the elimination of layers of liner and insulation which had thermal expansions different from propellant. The effective change in temperature was reduced from -100° to -70°F. Correcting for this temperature difference, stresses along the sidewalls and head end are compared for the earlier and later analysis in Figure 151. The later model without liner

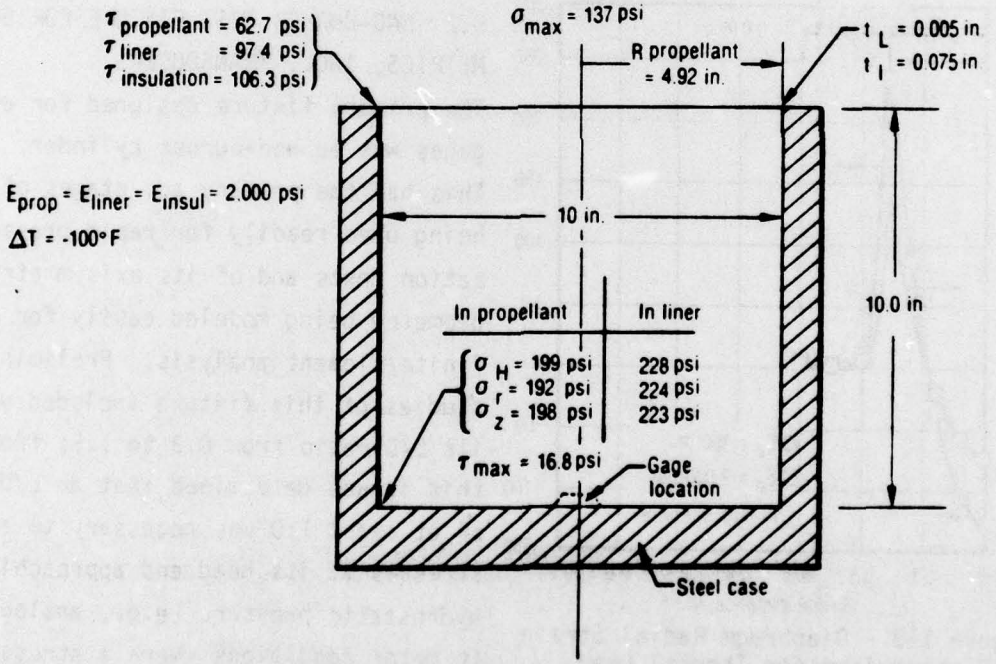


Figure 149. End-Burner Test Fixture

17200

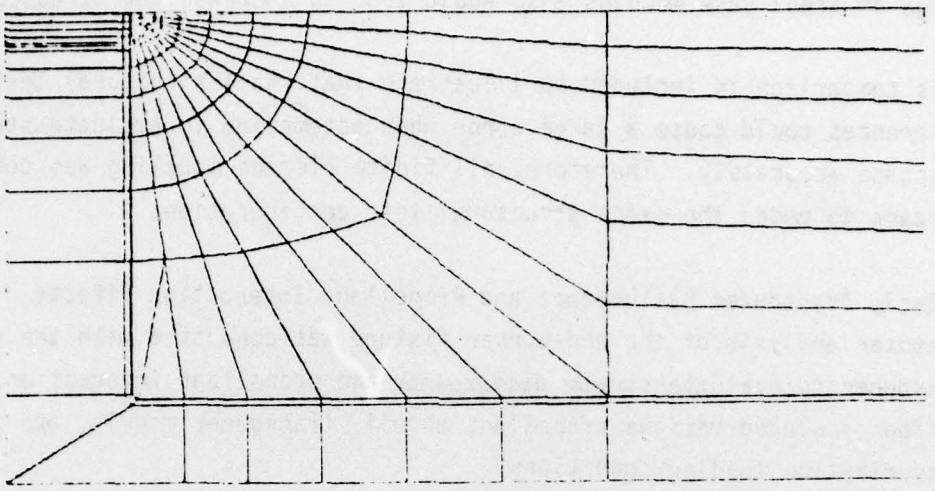


Figure 150. Finite Element Model of Gage in End-Burner Fixture

17199

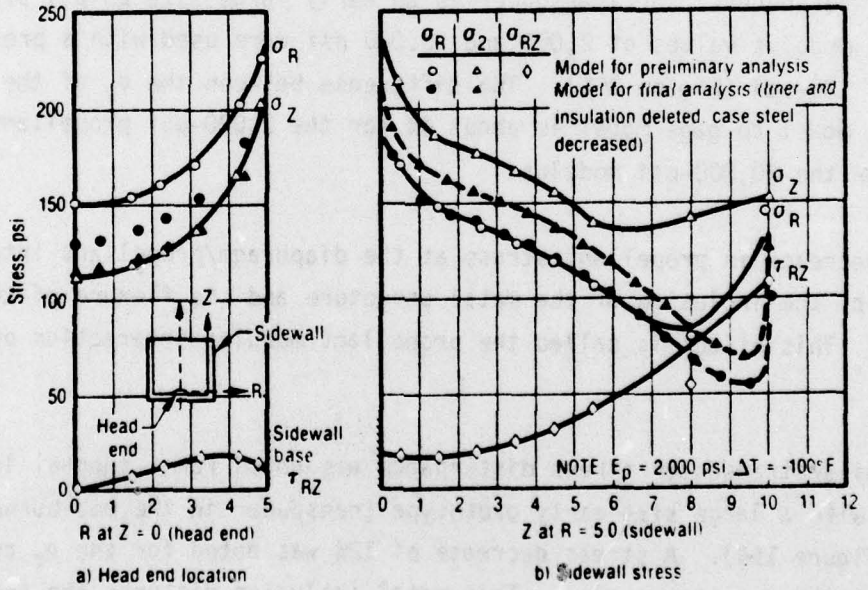


Figure 151. Comparison of Preliminary and Final End-Burner Model Stresses Without Transducers

17201

and insulation (actual test configuration) has about 10% to 15% lower σ_z values along the case wall; and a decrease in σ_r is 10% to 15% lower on the base. This stress change was anticipated because the coefficient of thermal expansion values for the insulation and liner used were double those of the propellant; the change in steel case modulus also would tend to increase the stresses.

This comparison is included to illustrate that small structural test modeling differences could cause a large error when attempting to evaluate stress gage response accurately. Therefore, all finite element modeling was done with extreme care to model the exact structural test configuration.

5.2.1 Early Transducer Disturbance and Propellant Interaction Effects

Computer analysis of the end-burner fixture was conducted with the without the transducer to evaluate stress disturbance and propellant interaction. These calculations included various propellant moduli, transducer models, and thermal and pressurization loading conditions.

5.2.1.1 Stress Disturbance

A typical end-burner stress distribution is shown in Figure 152 with and without a transducer. The transducer is an early large size 25-psi prototype; propellant modulus values of 2,000 and 20,000 psi were used with a pressure loading of 100-psi (Figure 153). The difference between the σ_z of the all-propellant model to gage model is about 4% for the 2,000-psi propellant modulus and 19% for the 20,000-psi modulus.

The decrease in propellant stress at the diaphragm/propellant interface is caused by the inclusion of the metal structure and the flexure of the metal diaphragm. This effect is called the propellant modulus interaction of the tranducer.

A similar transducer stress disturbance was noted for a thermal loading condition with a large size early prototype transducer in the end-burner test fixture (Figure 154). A stress decrease of 12% was noted for the σ_r component and 23% for the σ_z stress value. This metal inclusion disturbs the thermal

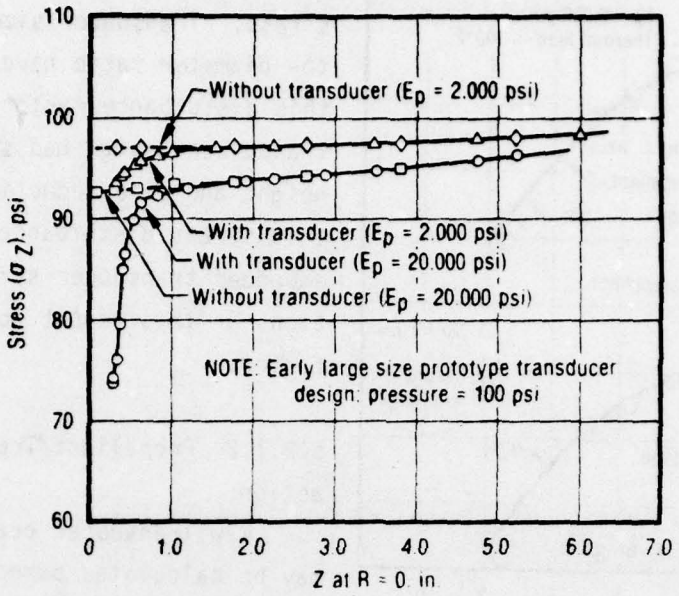


Figure 152. Transducer Stress Disturbance in End-Burner Test Fixture - Pressure Load

17196

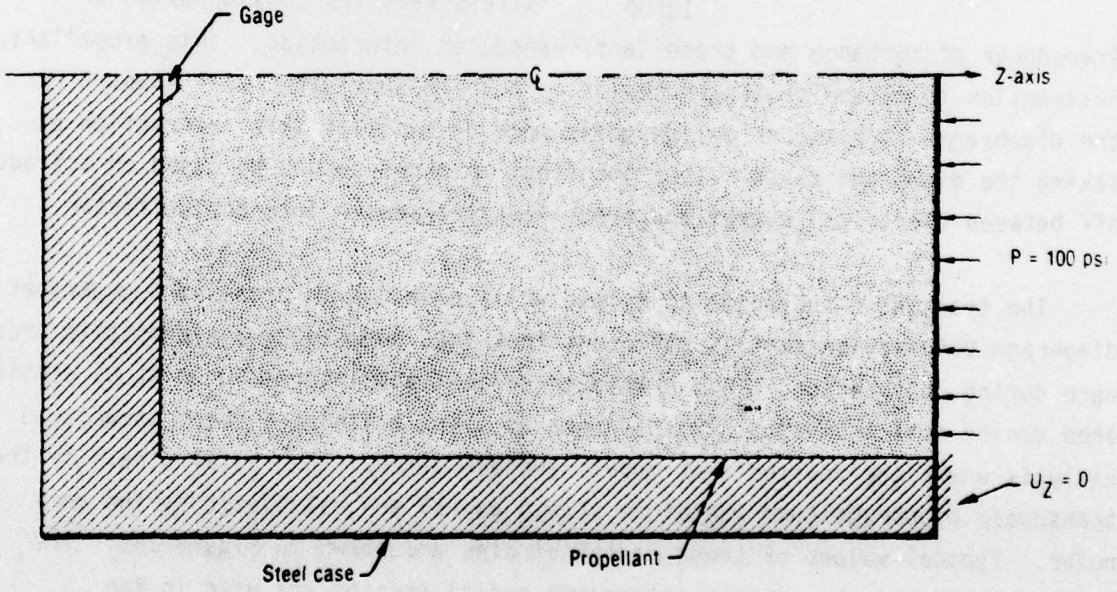


Figure 153. Pressure Loading of End-Burner Fixture

17197

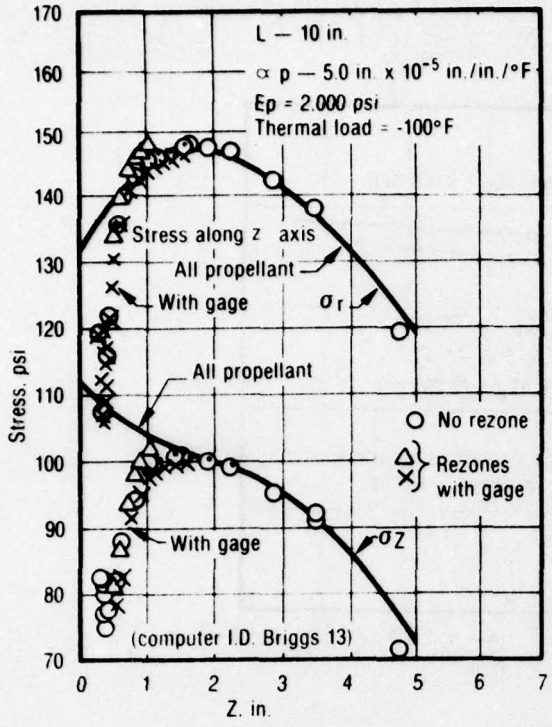


Figure 154. Transducer Stress Disturbance in End-Burner Test Fixture - Thermal Load

18505

stress much more than the pressure stress. Transducer size and height-to- diameter ratio have an effect on this disturbance factor. The finalized transducer design had significant height and size reduction to minimize this stress disturbance factor. All embedded transducer stress interpretations in this report account for this factor.

5.2.1.2 Propellant/Transducer Interaction

Raw transducer pressure values may be calculated based on fluid calibration data after a test is performed in a structural test device. However, conversion to propellant stress requires consideration of transducer disturbance and propellant/transducer interaction. This propellant/ interaction is caused by the propellant providing some structural support for the diaphragm. Transducer design goals were to minimize this interaction by making the diaphragm thicker, but the final thickness would be based on a trade-off between electrical output and propellant/transducer interaction factor.

The transducer subjected to a load while embedded in propellant undergoes diaphragm deformation that is different from that induced by a hydrostatic pressure during calibration. This transducer/propellant interaction must be considered during data analysis. This is done by using a finite element structural analysis where the desired test models are evaluated. The radial strain in the transducer diaphragm (and therefore strain gages) are calculated by the computer. Typical values of these radial strains are shown in Figure 155. The absolute value of the average integrated radial strains are used in the following transducer/propellant interaction factor equation.

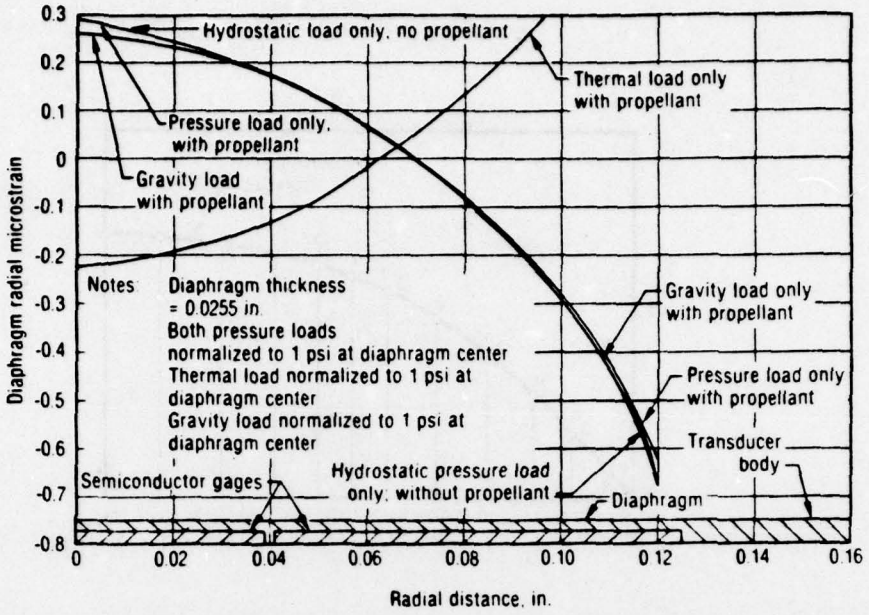


Figure 155. Diaphragm Radial Strain vs Radial Distance for Senso-Metrics Transducers (2,000-psi Range, in End-Burner Device)

14018

Strain versus radial distance on the silicon gage was plotted as shown in Figure 156; this figure is produced from finite element analysis data. Because of the fineness of the grid used in the analysis, 31 strain versus radial distance data points were available. The average integrated strain then was calculated by a computer program based on the following steps:

The computer breaks the ϵ and d data points into groups of three and curve-fits the data between these points; in the second group of three points, the first point is the same as the third point of the previous group; therefore, the slope at matching points from neighboring groups of three are the same. In this manner a very accurate curve fit of the data is performed.

Then a numerical integration of the form

$$\bar{\epsilon} = \frac{\int_{d=1}^{d=n} \epsilon(d)}{d} \qquad (22)$$

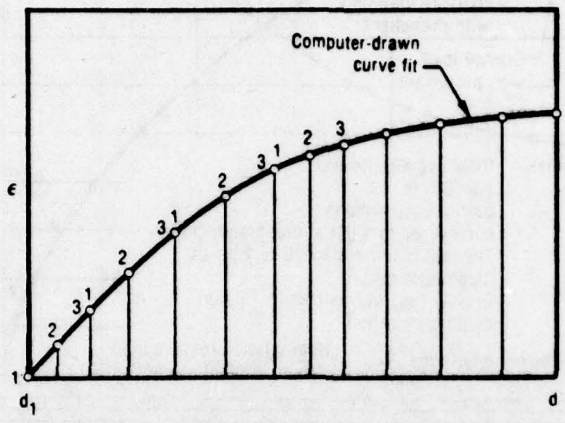


Figure 156. Stain Integrating Model for Evaluating Interaction Factor
17150

is performed to obtain the average integrated strain used for disturbance and interaction calculations.

Both the stress disturbance and the transducer/propellant interaction is determined for thermal, gravitational, and pressure loading for regular test applications. These factors are subject to change depending on the test device geometry, transducer size, and other factors which affect stress axiality. The general equations for these factors are

$$I_f = \frac{\epsilon_r \div \sigma_{z1}}{\epsilon_f \div \sigma_f} \tag{23}$$

for transducer/propellant interaction factor, and

$$D_f = \frac{\sigma_{z2}}{\sigma_{z1}} \tag{24}$$

for transducer stress disturbance factor,
where

ϵ_r = average integrated radial strain in diaphragm for a particular loading

σ_{z1} = average integrated stress on diaphragm for a particular loading

ϵ_f = average integrated radial strain in diaphragm for a hydrostatic load

σ_f = average integrated stress on diaphragm for a hydrostatic load

σ_{z2} = average integrated stress in propellant at diaphragm location, without gage.

Use of these two factors to convert from transducer pressure to propellant stress is shown by

$$\sigma_{prop} = \frac{(OP) - (ZO)}{Se} (I_f)(D_f) \tag{25}$$

where

OP = transducer electrical output at temperature T, mV

ZO = transducer zero offset at temperature T, mV

Se = transducer sensitivity at temperautre T, mV/psig

σ_{prop} = corrected propellant stress at diaphragm location

The applied stress at the exterior of the test device is different from the stress at the transducer diaphragm location in the propellant because the propellant redistributes the internal stress. The stress at the transducer diaphragm location also is different from the stress at the propellant/case interface because of the gage height. Finite element analysis was used to determine these factors for thermal, gravitational, and pressure loadings from the specific test devices used for transducer evaluation.

The following factors are used to convert the external applied stress to the local stress where the transducer is embedded:

Average stress factor,

$$S_A = \frac{\sigma_{Z2}}{\sigma_{ZA}} \tag{26}$$

Bondline stress factor,

$$S_B = \frac{\sigma_{ZB}}{\sigma_{Z2}} \tag{27}$$

where

σ_{Z2} = average integrated stress in propellant at diaphragm location (without gage)

σ_{ZA} = average integrated applied stress to vehicle exterior

σ_{ZB} = average integrated stress at bondline location inside vehicle (without gage)

The external load or stress is measured by a testing machine load cell or external pressure transducer. These finite element derived corrected stress values should be equivalent to the actual transducer stress as shown by

$$\sigma_{prop} = (F/A)\ (S_A) \tag{28}$$

where F = measured applied force (lb); A = cross-sectional area of sample ($in.^2$); and σ_{prop} = corrected propellant stress at diaphragm location. Therefore,

$$(F/A)(S_A) = \frac{(OP - (ZO)}{Se}\ (I_f)(D_f) \tag{29}$$

and the stress at the bondline case is

$$\sigma_{bondline} = (F/A)\ (S_A)\ (S_B) \tag{30}$$

The structural analysis factors for the Senso-Metrics prototype 2,000-psi transducer for the end burner fixture with a propellant modulus of 500 psi are the following:

Factor	Thermal Load	Gravity Load	Pressure Load
I_f, transducer interaction	0.990	0.990	0.996
D_f, transducer disturbance	1.231	0.994	0.995

The thermal stress disturbance of 23% is larger than desirable and was prime motive for further transducer height reduction on the final Senso-Metrics design.

Transducer performance in the end-burner design is sensitive to the propellant modulus as shown in Figure 157. The output ratio, as defined by the inverse of disturbance, or σ_{Z1}/σ_{Z2}, is a measure of propellant/ transducer disturbance and decreases as propellant modulus increases. This decrease in transducer sensitivity has been a major concern in transducer design work. Analytic results in Figure 157 are for propellant modulus values out to 20,000-psi which is excessive for most solid propellant motor applications.

A corresponding analysis for the thermal loading conditon of the Senso-Metrics prototype design was conducted (Figure 158). Thermal loading conditions generate a large stress disturbance (-23%) for both transducer ranges. This is caused by the stress biaxiality and difference in thermal expansion between materials, and stress calculations must take this into account. The actual change in output ratio is about 8% for the 25-psi design over the propellant modulus range of 0 to 10,000 psi.

Corresponding output ratio curves are presented in Figure 159 for the final Senso-Metrics transducer design. The major change with the low profile design is to reduce the thermal load stress disturbance from 23% to 8%. Considerable caution should be used in applying these output ratio curves since they are useful only for the exact conditions analyzed. Results are sensitive to specific test fixture geometry, gage geometry, temperature differences, and material thermal properties used; this is made clear in Figure 160. Recalling from the discussion of the end-burner fixture design, an L/D of 1.0 was selected arbitrarily to simulate typical rocket motor stress fields. Figure 160 shows

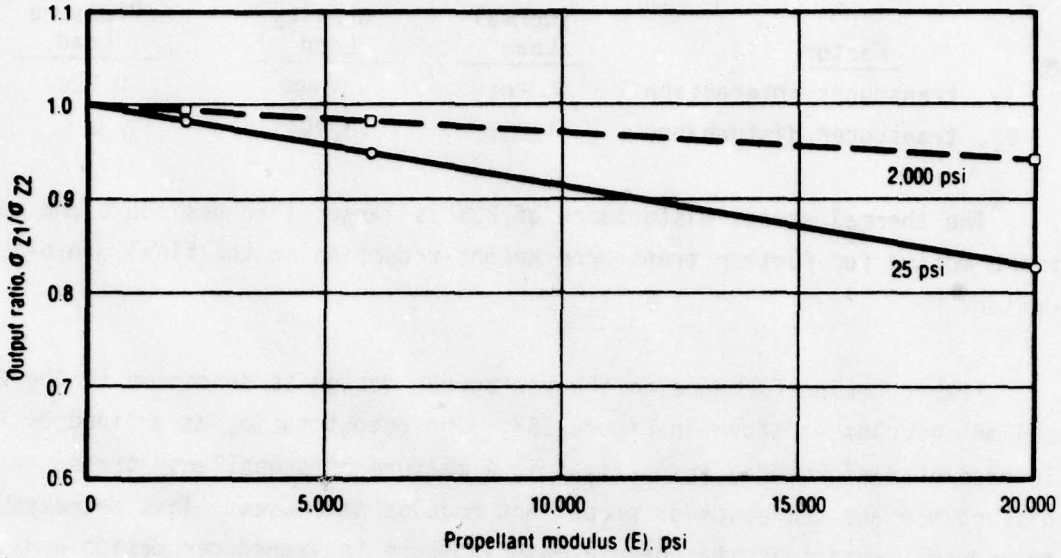


Figure 157. Senso-Metrics Prototype Transducer Output vs Propellant Modulus in End-Burner Fixture for Pressure Load

17204

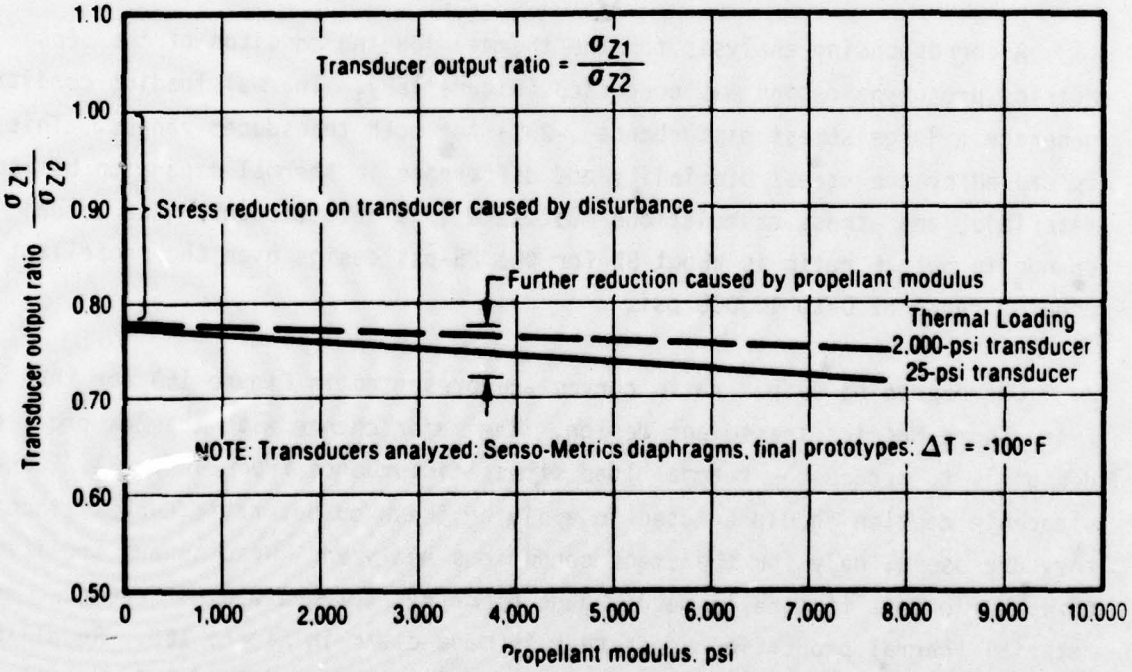


Figure 158. Senso-Metrics Prototype Transducer Output Ratio vs Propellant Modulus in End-Burner Fixture for Thermal Load

17205

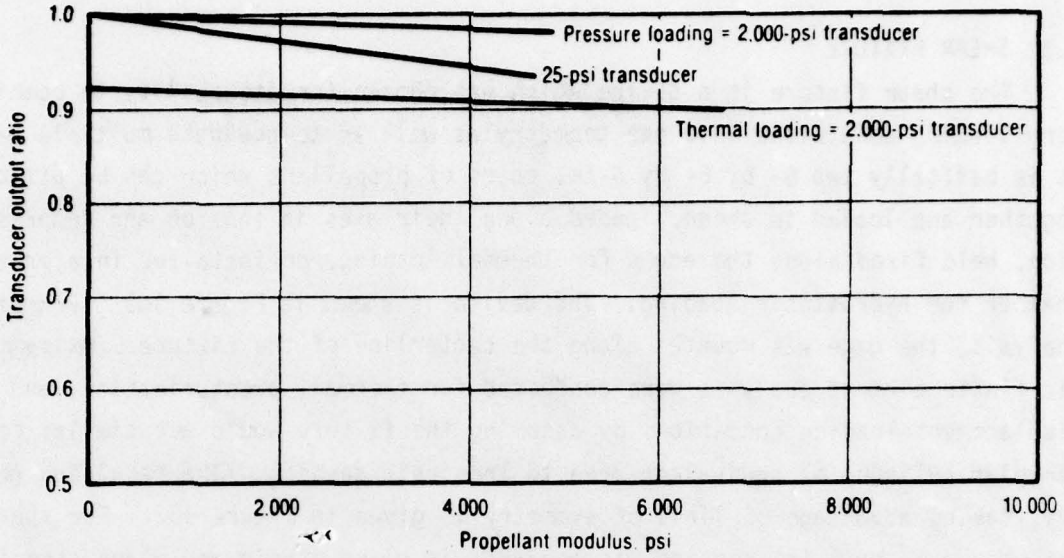


Figure 159. Senso-Metrics Final Design Ratio vs Modulus

17202

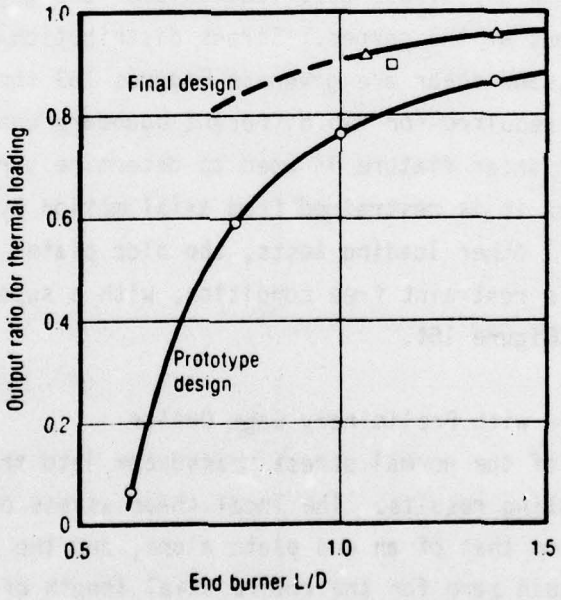


Figure 160. Effect of End-Burner L/D on Transducer Output Ratio for Thermal Load

17203

what happens to thermal disturbance if test fixture geometry or gage design geometry are changed.

5.3 SHEAR FIXTURE

The shear fixture is a device which was chosen for its ability to combine many loading conditions into one geometry as well as to evaluate multiple gages. It is basically two 6- by 6- by 6-in. cubes of propellant which can be attached together and loaded in shear, loaded along their axes in tension and compression, held fixed along the edges for thermal loading, or installed in a pressure chamber for hydrostatic loading. The device is shown in Figure 161. For each analysis, the gage was mounted along the centerline of the fixture. Axisymmetric finite element analyses were conducted for thermal, pressurization, and displacement loading conditions by assuming the fixture would act similar to a circular cylinder of equivalent area to the cubic section. The resulting geometry, taking advantage of lines of symmetry is given in Figure 162. For shear analyses a 6- by 6-in. section was analyzed in plane strain and plane stress.

Results of shear fixture analyses without a transducer were plotted along the end plate to show the stress distribution over the gage loctaion and the stress concentrations at the corner. Stress distribution for thermal loading, axial displacement, and shear are given in Figures 163 through 166. Two thermal loading curves are required for two different boundary conditions. When the tension/compression/shear fixture is used to determine stress free temperature or cooldown stresses it is restrained from axial motion by the side plates, see Figure 161. For all other loading tests, the side plates are removed and stress is determined from a restraint free condition, with a superimposed thermal stress as given by Figure 164.

5.3.1 Shear Fixture with Preliminary Gage Design

The inclusion of the normal stress transducer into the shear fixture model causes some interesting results. The local shear stress on top of the diaphragm is about doubled from that of an end plate alone, and the radial and axial components of stress remain zero for the entire axial length of test fixture. These results are shown graphically in Figure 167. The fact that σ_z remains

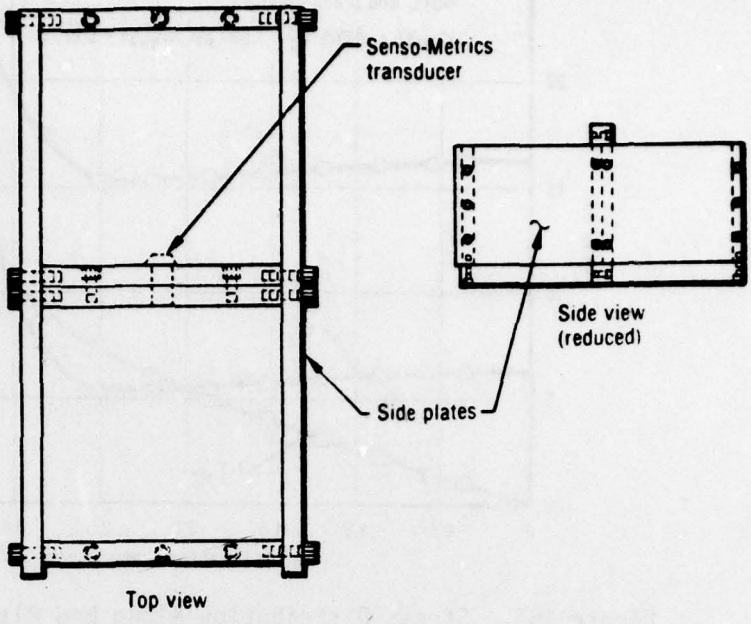


Figure 161. Tension/Compression/Shear Test Device

17167

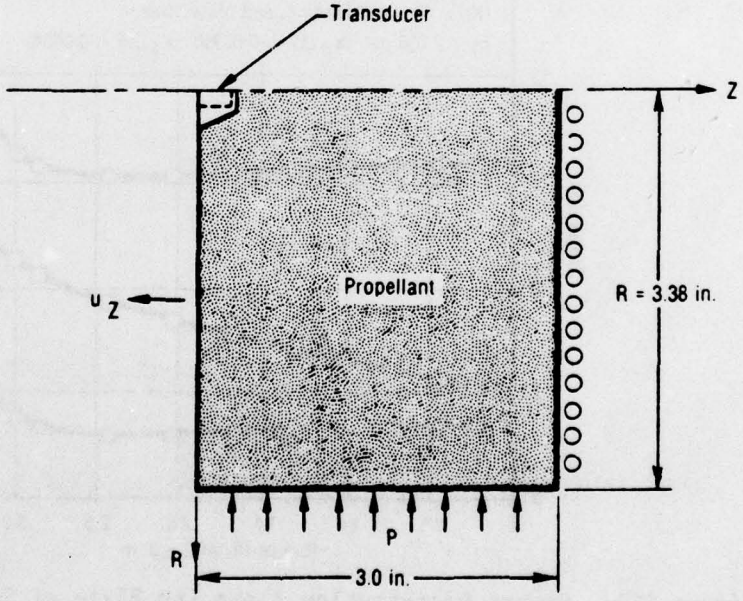


Figure 162. Model of Shear Sample

17221

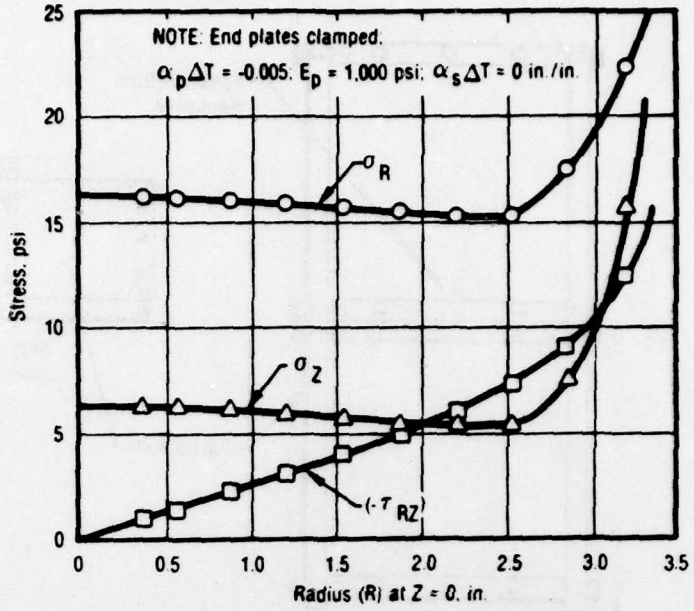


Figure 163. Stress Distribution Along End Plate of Shear Fixture - Thermal Loading

17217

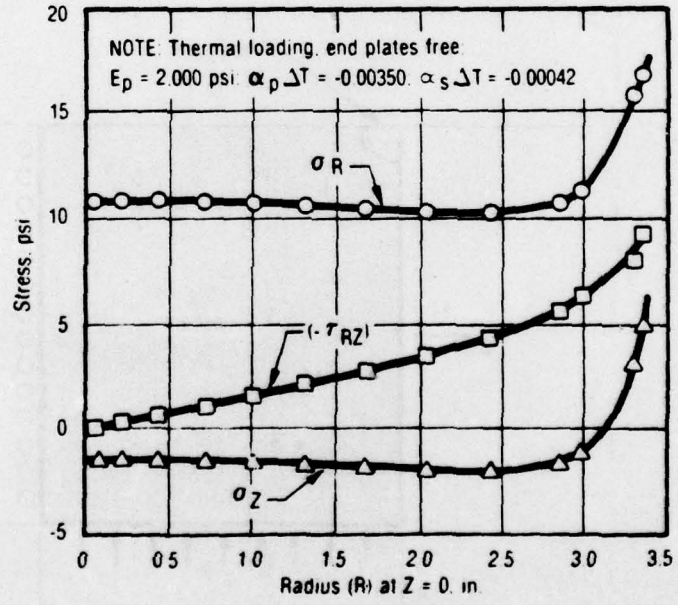


Figure 164. Stress Distribution Along End Plate of Shear Fixture

17218

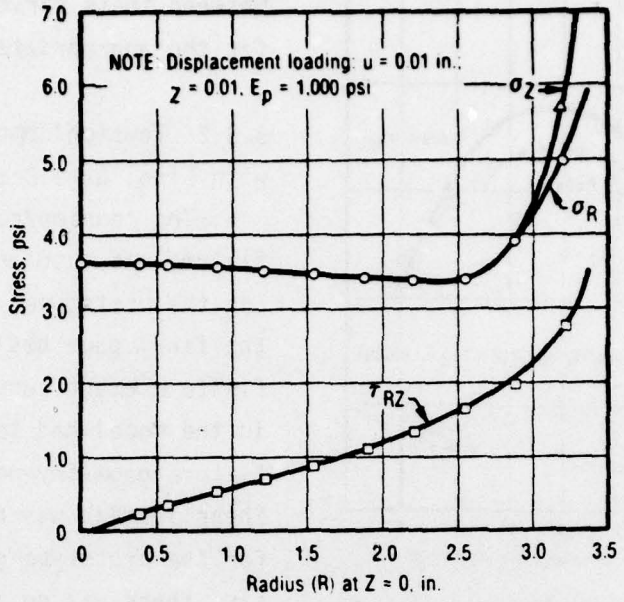


Figure 165. Stress Distribution Along End Plate of Shear Fixture
17219

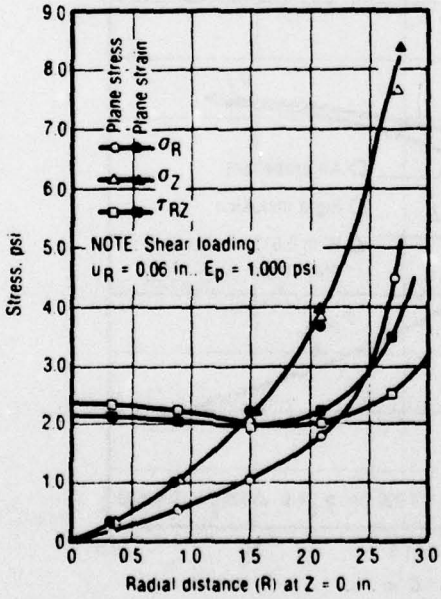


Figure 166. Stress Distribution Along End Plate of Shear Fixture
17220

zero means that this is an ideal fixture for evaluating the sensitivity of the normal gage to a shear stress across its diaphragm surface.

The response of the shear fixture under axisymmetric loads is shown in Figures 168 through 170 for thermal, displacement, and combined pressure loads with displacement. Three conditions are shown in each figure, plotted along the axis of symmetry: (1) a run for the all-propellant analysis; (2) a run including a 25-psi transducer; and (3) a run with the transducer having a very stiff diaphragm (essentially

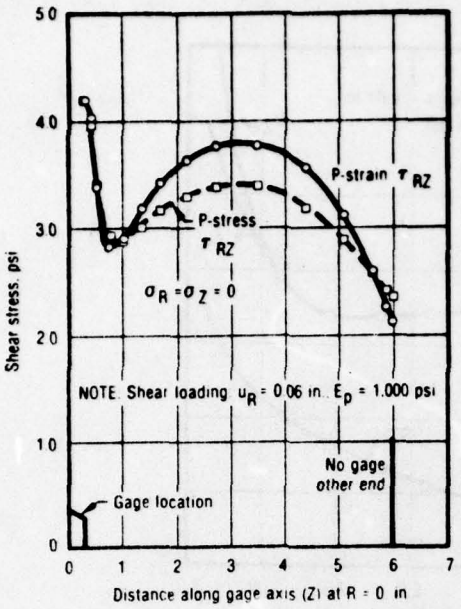


Figure 167. Shear Fixture with Gage, Prototype Design

17213

a rigid inclusion). The difference between these curves is the disturbance for the appropriate loading conditions.

5.3.2 Tension/Compression/Shear Fixture with Final Gage Design

The tension/compression/shear fixture was also analyzed by replacing the prototype gage design with the final gage design geometry. Only finite element runs with the gage in the model had to be made, since fixture geometry remained the same. Shear loading was not analyzed since, for the prototype gage design analysis, there was no normal stress over the diaphragm for this condition.

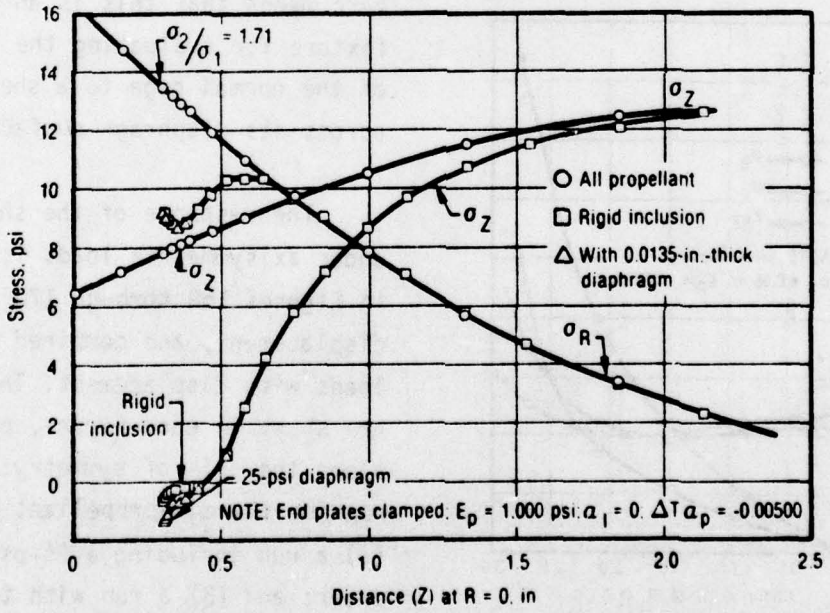


Figure 168. Thermal Loading in Shear Fixture, Prototype Design

17214

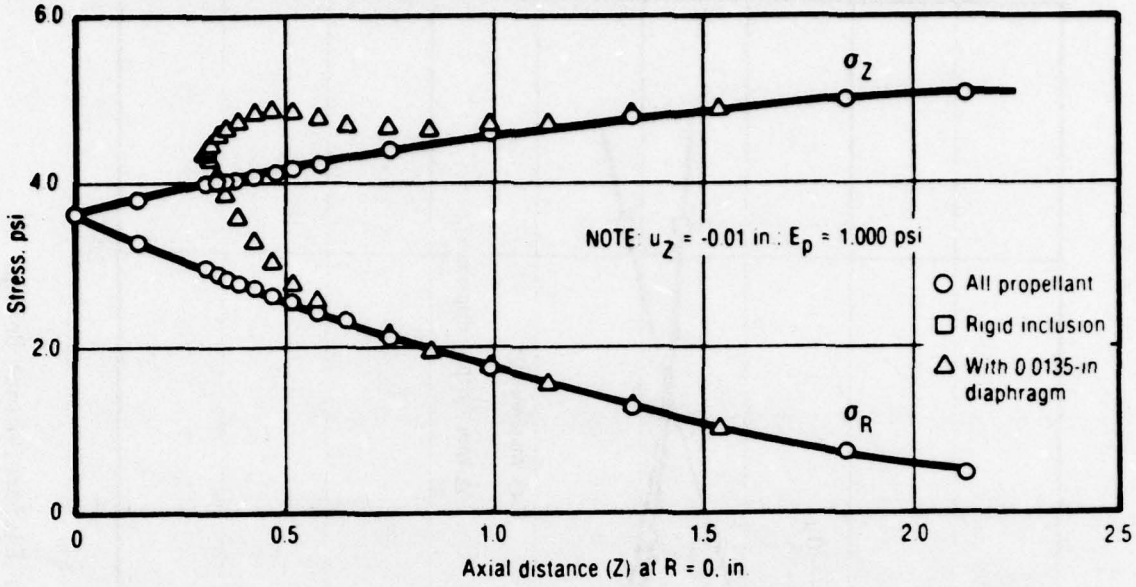


Figure 169. Uniaxial Displacement of Shear Fixture, Prototype Design
17215

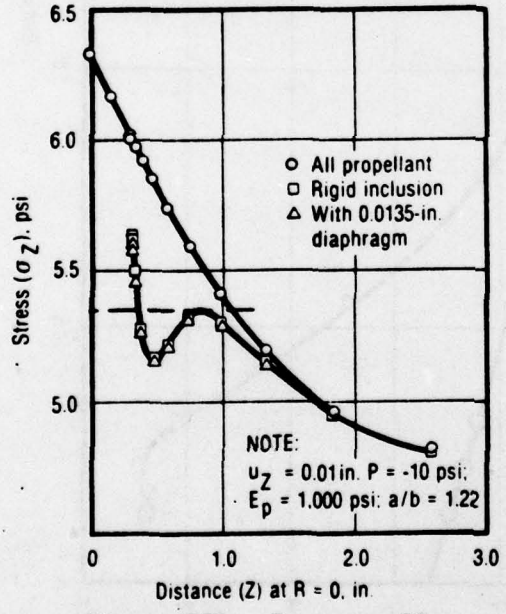


Figure 170. Pressure Plus Displacement Loading in Shear Fixture, Prototype Design
17216

Changing the gage aspect ratio but leaving it on the axial centerline would not change this result.

Thermal loading was analyzed and is plotted in Figure 171. This figure is plotted to the longitudinal center of the test specimen (z = 3.0 in. and R = 0 in.). The solution with a gage present is shown as the dotted line. Note that for these particular conditions, the correction for the gage becomes exceedingly large. As can be seen in the figure, σ_Z, the normal stress that the gage is measuring, is changed from -1.0 psi

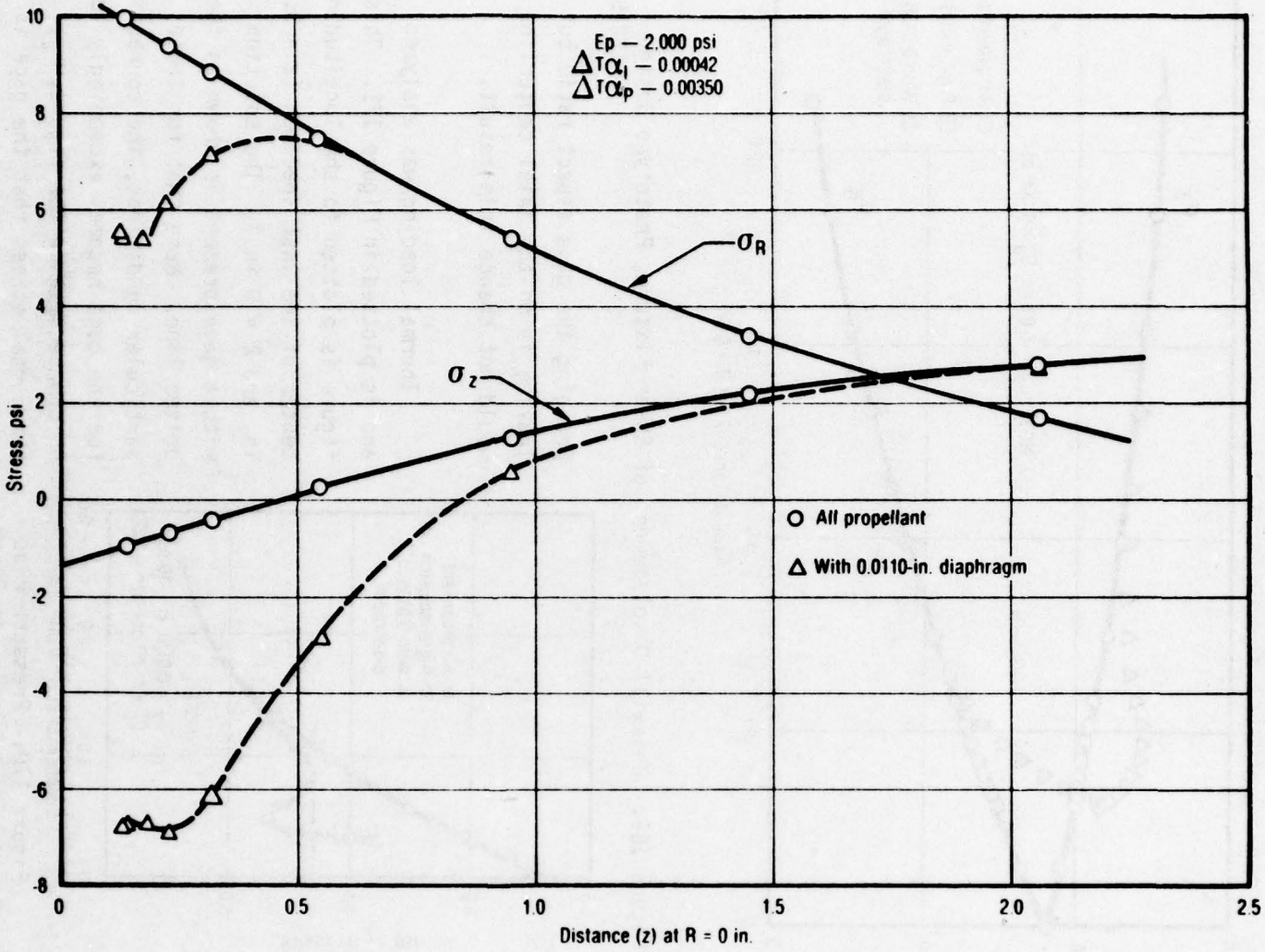


Figure 171. Thermal Loading in Shear Fixture, Final Design

18506

to about -6.8 psi by the presence of the gage in the model. The effect is similar to that noted with the prototype design, Figure 168. Different propellant thermal properties and moduli were used as noted on the figure.

Displacement loading is shown in Figure 172. These results are comparable to the prototype gage, although a different propellant modulus and axial displacement were used.

5.4 CIRCULAR PORT GRAIN

The final gage evaluation tests were conducted using a circular port grain configuration. Finite element analyses were performed on this motor to determine predicted stresses for comparison with gage output. These analyses also were required to determine the factors needed to interpret gage readings. Runs were performed for both thermal and pressure loading to simulate test conditions of the analog grains. These were the final gage evaluation tests and were performed only with the final design, low profile transducers.

The grain configuration is shown in Figure 173. The motor is a circular ported grain with a steel case. Two transducer locations were considered, one on the longitudinal center at 5.0 in. and the other one half the way to an end at L = 2.5 in. Neither liner nor insulation was used in the actual test vehicle or its model. A finite element grid was constructed (Figure 174) to analyze the configuration as an axisymmetric solid. For baseline runs without gages in the model the same grid was used, simply by replacing the gage material properties with propellant properties.

Typical results of a thermal analysis of the circular port test vehicle (without gages) are shown in Figure 175. Inner bore hoop strain at the axial center of the grain was 2.53%. A pressure solution also was made by pressurizing the inner bore to 10 psi with a propellant modulus of 500 psi. This gave a maximum inner bore hoop strain of 0.041%.

Finite element runs using the normal stress transducers in the model posed some unusual problems. The axisymmetric model chosen requires that the gages actually be modeled as rings, since the real geometry is a 3D situation, these

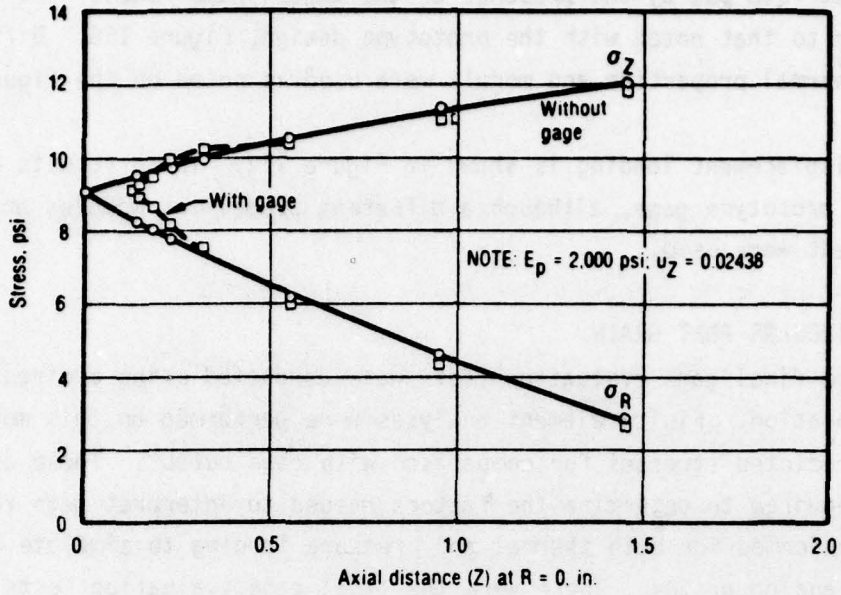


Figure 172. Uniaxial Displacement of Shear Test Fixtures - Final Gage Design

17206

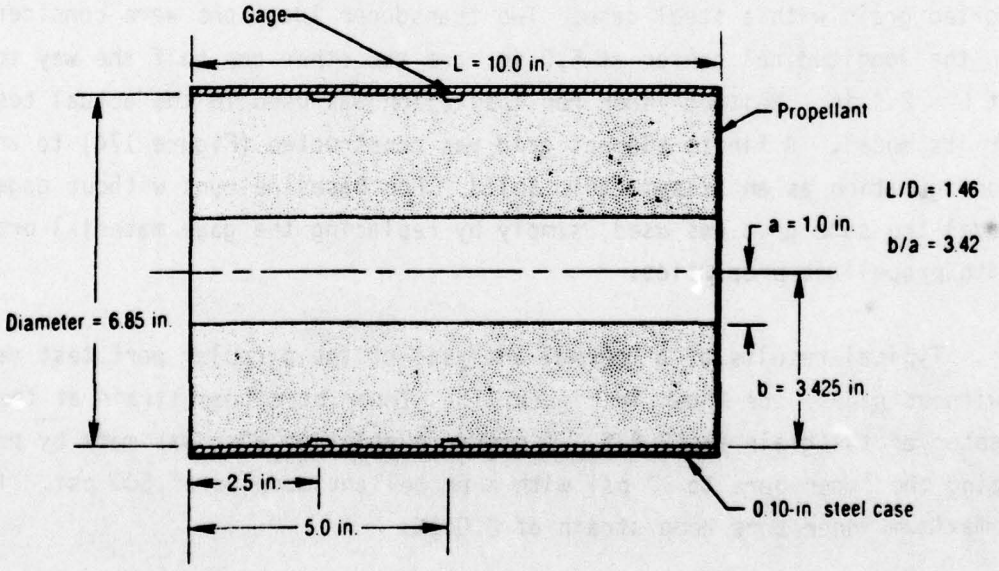


Figure 173. Circular Port Test Motor (TM-1)

17207

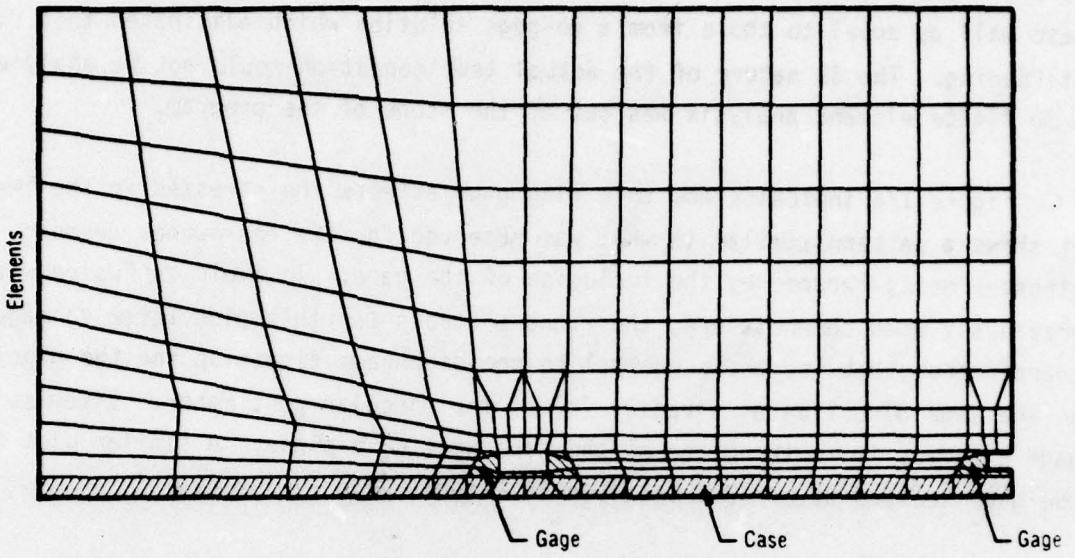


Figure 174. Finite Element Grid for Circular Port TM-1

17208

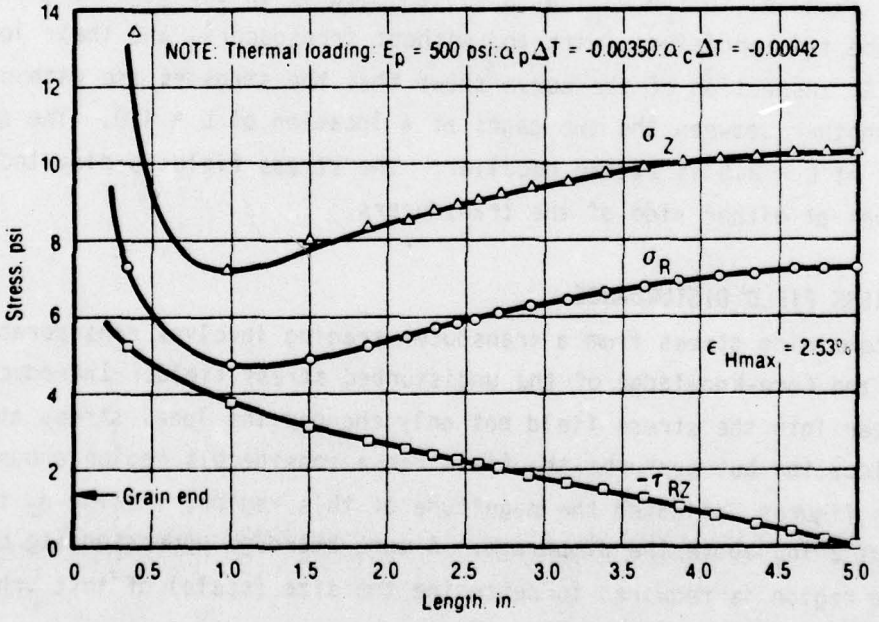


Figure 175. Stresses Along Wall of Circular Port EM-1 Without Gage

17209

rings will not disturb the propellant in exactly the same fashion as a gage. When the steel rings were included in the model their stiffness contributed significantly to that of the case which unrealistically distorted the results. To alleviate this problem. displacement boundary conditions were applied to the case wall as equal to those from a no-gage solution which eliminated this ring stiffening. The 3D nature of the actual test condition could not be analyzed as a 3D finite element analysis was out of the scope of the program.

Figure 176 indicates how this ring gage affects the stresses in the TM-1. It shows a pattern similar to what was observed for the end-burner geometry of stresses being reduced by the inclusion of the gage. To avoid confusion with previously used nomenclature, the r and z stress for this plot refer to gage coordinates; that is, the z (normal to the diaphragm direction for the gage) is in the same direction as a radius (r) of the circular port motor. Likewise the gage r radius is in the plane of the case wall of z-plane. A similar plot for the gage lcoated at L = 2.5 is given in Figure 177.

With two gages in proximity along the wall, it is important that they not disturb one another's respective stress fields. Figure 178 is a plot of stresses parallel to the wall at a distance equal to the gage height from the wall. The two conditions (with and without transducers) and their locations are shown. An inspection of the curve shows that the stresses are within about 1% of one another between the two gages at a location of L = 4.0. The effect about the gage at L = 2.5 is rather peculiar: the stress field is disorted in opposite directions at either side of the transducers.

5.5 STRESS FIELD DISTURBANCE

Determining stress from a transducer reading involves considerable calculations and fore-knowledge of the undisturbed stress field. Introducing the transducer into the stress field not only changes the local stress at the diaphragm location but perturbs the field for a considerble region around the gage. Previous figures indicated the magnitude of this region, showing σ_z to change for about 2 in. above the diaphragm. A more thorough understanding of this disturbance region is required to determine the size (scale) of test vehicles required for accurate gage application.

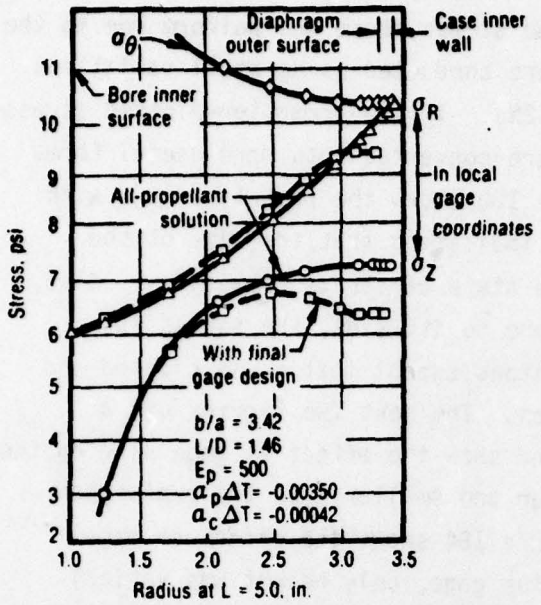


Figure 176. Thermal Stress Analysis of TM-1 Circular Port Motor With and Without Final Gage Design Section at L = 5.0 in.

17210

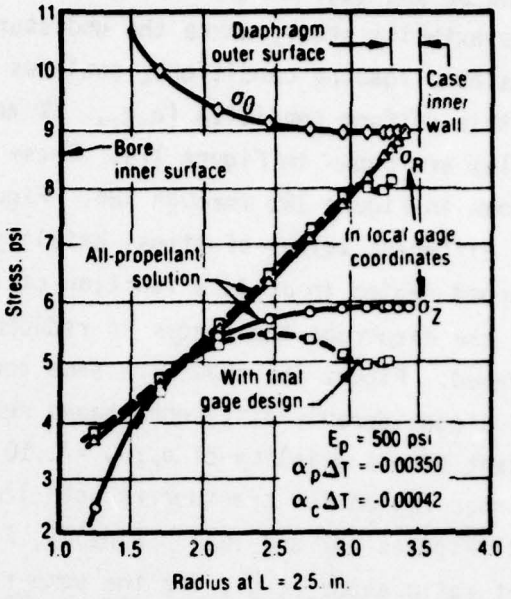


Figure 177. Thermal Stress Analysis of TM-1 Circular Port Motor With and Without Final Gage Design Section at L = 2.5 in.

17211

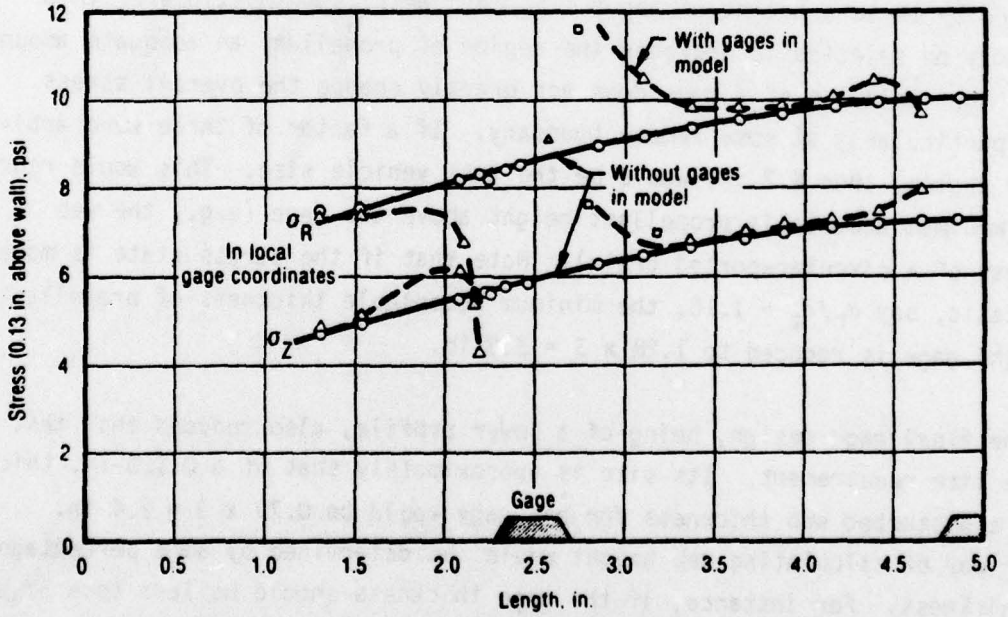


Figure 178. Effect of Gages on Stress Field Along Line Through Diaphragm Outer Surface (TM-1)

17212

The disturbance region or zone-of-influence is defined by using the plot options of the gage analysis program, TEXGAP. Using models similar to the stress axiality study, where the undisturbed stress state was uniform due to the hydrostatic loading conditions, analyses were conducted using small variations from this uniform condition (e.g., 1% and 2%). Typical computer-plotted stress profiles are shown in Figure 179. These were converted into more useful forms as shown in Figure 180 through 184. Figure 180 shows the prototype gage with three different values of stress axiality, indicating that the size of the disturbed region in σ_z is a function of the state of stress biaxiality. Also, above the diaphragm the stress is reduced and to its side, the stress is increased. Figure 181 shows the same conditons except that σ_r is plotted and gives a considerably different shaped region. The next two figures use a constant stress axiality of $\sigma_r/\sigma_z = 1.10$ and show the effect of gage size on the disturbed region for transducers both larger and smaller than the prototype model (Figures 182 and 183). Finally, Figure 184 shows the effect of gage aspect ratio alone (e.g., for the same radius gage, only height was varied). These show that by halving the thickness from 0.128 to 0.064, the disturbed region is reduced only by a small amount. Using the prototype design as an example, Figure 180 shows that with a σ_r/σ_z ratio of 1.20, the stress field is disturbed by 1% to a height of about 1.56 in. Next, some multiple of this number may be selected to increase the region of propellant an adequate amount so that the inclusion of a gage does not greatly change the overall stress state, particularly at some remote boundary. If a factor of three were arbitrarily chosen, then 4.7 in. would be the test vehicle size. This would represent a minimum acceptable propellant height above the gage (e.g., the web thickness of a circular-ported grain). Note that if the stress state is more hydrostatic, say $\sigma_r/\sigma_z = 1.10$, the minimum acceptable thickness of propellant above the gage is reduced to $1.28 \times 3 = 3.8$ in.

The final gage design, being of a lower profile, also reduces this test vehicle size requirement. Its size is approximately that of a 0.128-in.-thick model; a disturbed web thickness for his gage would be $0.79 \times 3 = 2.4$ in. Another way of calculating web height would be determined by some percentage of gage thickness. For instance, if the gage thickness should be less than 5% of the web, then the low profile final gage design would be adequate for a web of 2.4 in.

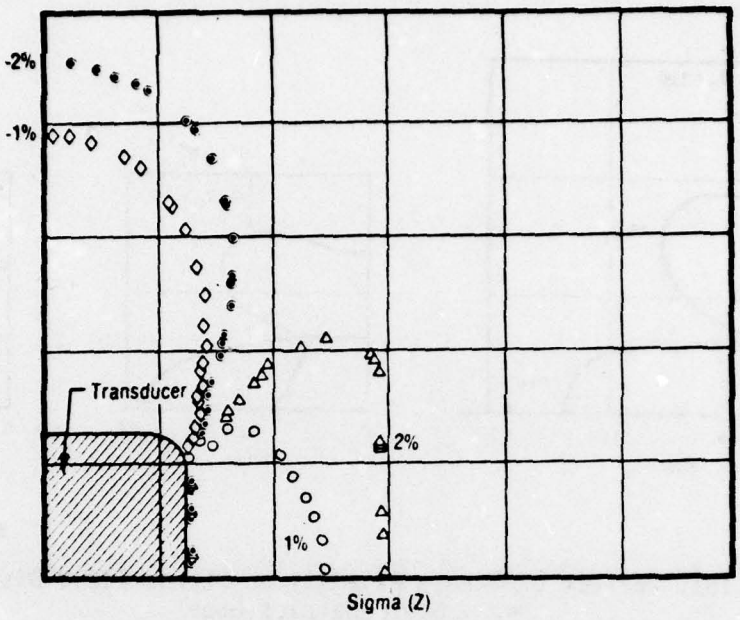


Figure 179. Typical Stress Disturbance Zone

17243

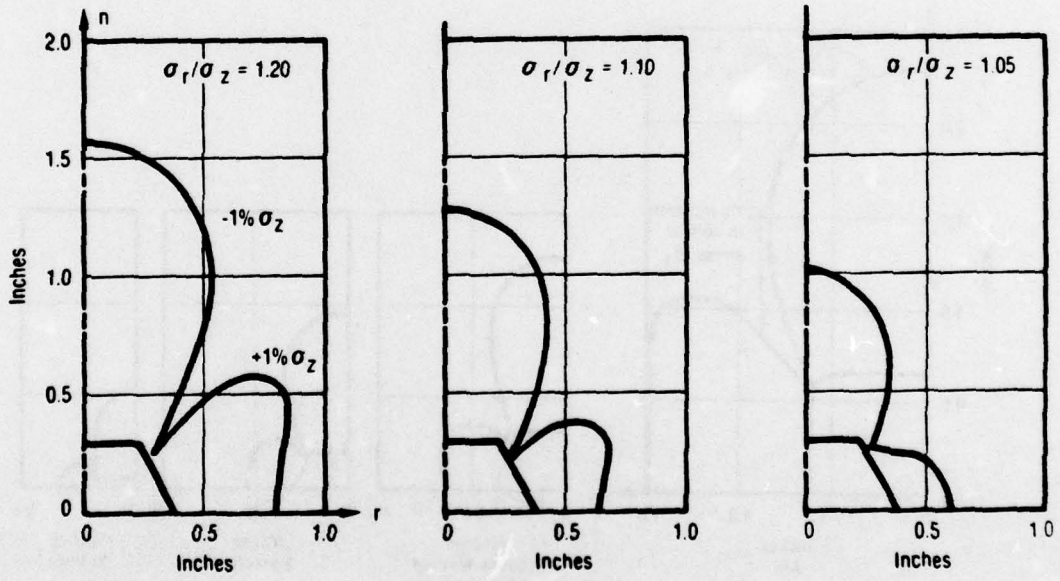


Figure 180. Effect of Stress Axiality on Stress Field Disturbance, σ_n - Senso-Metrics Gage

17248

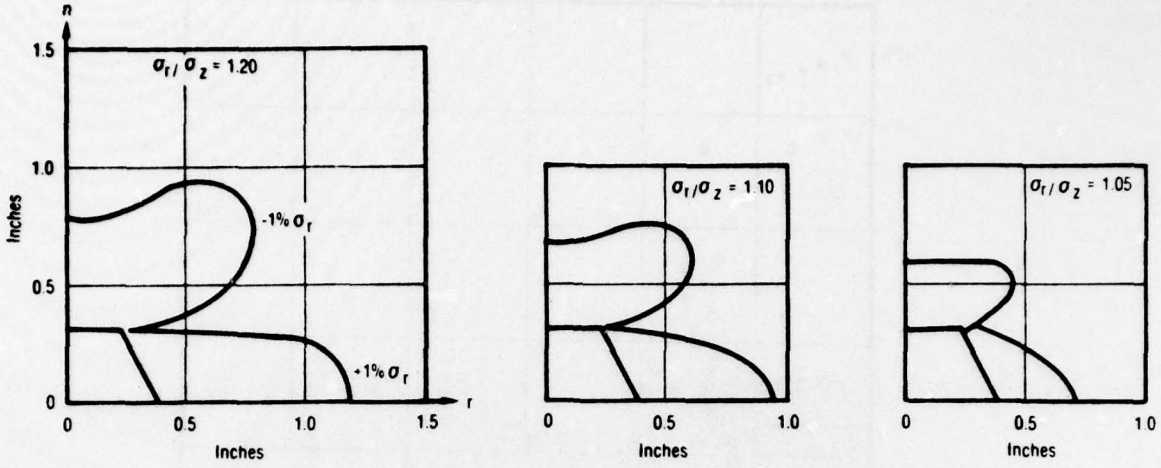


Figure 181. Effect of Stress Axiality on Stress Field Disturbance, σ_r - Senso-Metrics Gage

17247

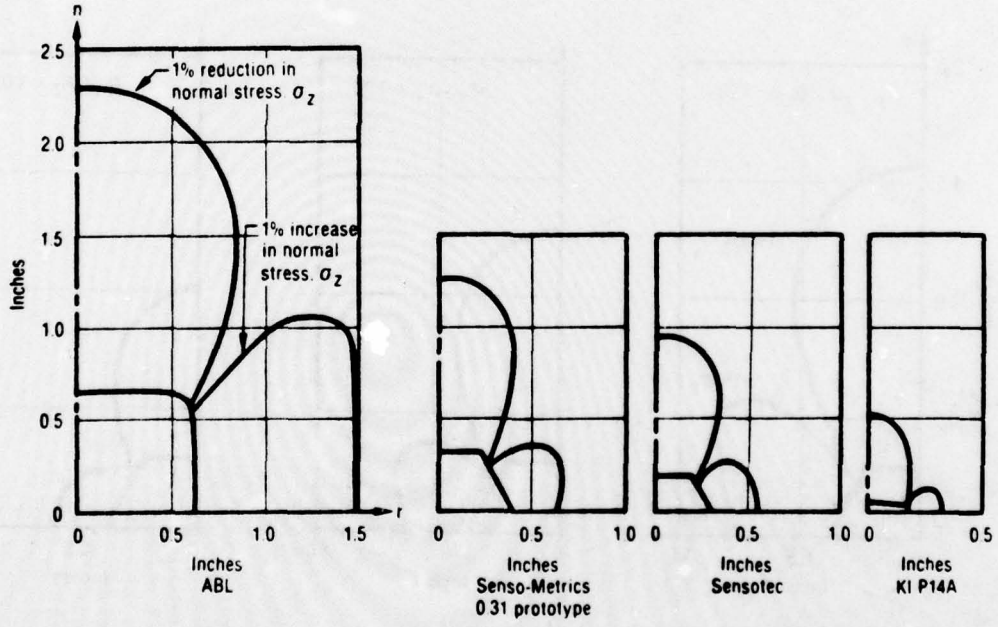


Figure 182. Effect of Gage Size on Stress Field Disturbance, σ_n Uniform Stress Field, σ_r/σ_n = 1.10

17246

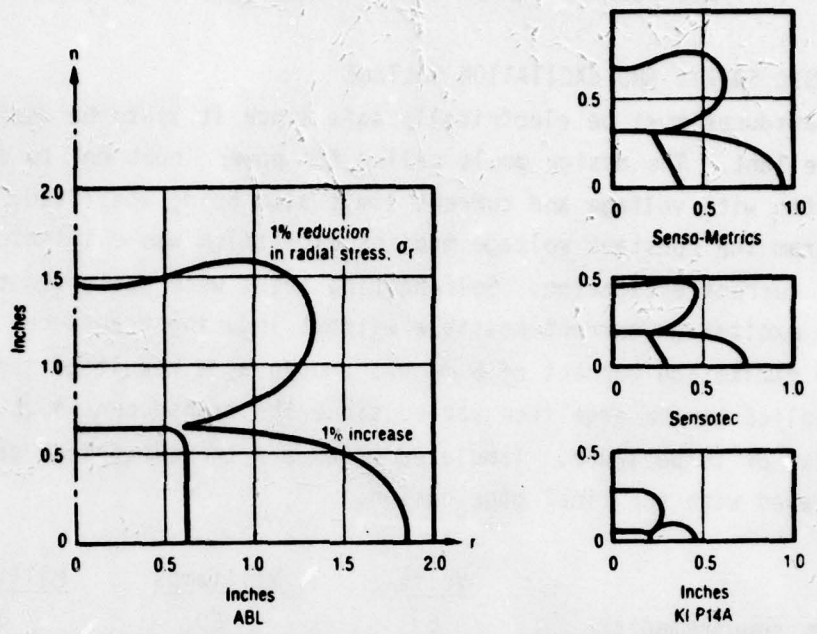


Figure 183. Effect of Gage Size on Stress Field Disturbance, σ_r Uniform Stress Field, σ_r/σ_n = 1.10

17245

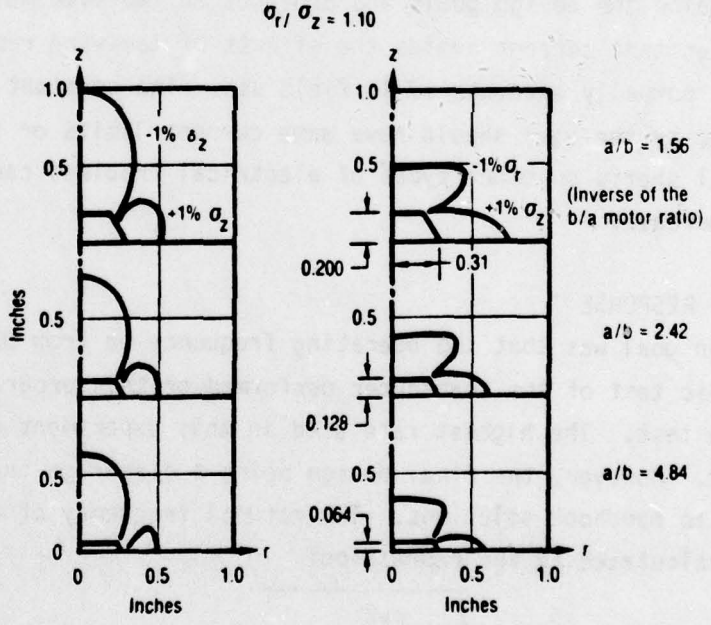


Figure 184. Effect of Gage Aspect Ratio on Stress Field Disturbance

17244

6.0 COMPARISON OF RESULTS WITH DESIGN GOALS

6.1 INTRINSIC SAFETY AND EXCITATION VOLTAGE

The transducer must be electrically safe since it is to be used in solid rocket propellant. The design goals called for power input not to exceed 300 milliwatts with voltage and current limit also being specified. Early in the program the constant voltage mode of excitation was eliminated in favor of constant current excitation. Self-heating tests were performed to determine the highest excitation current possible without inducing transducer electrical change. An excitation current of 5 mA was chosen as a result of these tests. Voltage supplied to the gage then varied since the transducer input impedance is a function of temperature. Tabulated below are the electrical goals and values achieved with the final gage design.

	Volts	Milliamps	Milliwatts
Maximum requirements	6	50	300
Final design	1.2 to 1.8	5	10

All are well below the design goals and provides an improved method of transducer excitation. Constant current avoids the effects of leadwire resistance and contact changes, etc., normally encountered in field use. The constant current power source provided by the user should have some current limits or fuses to ensure that electrical shorts or other types of electrical problems cannot cause a large power increase.

6.2 FREQUENCY RESPONSE

The design goal was that the operating frequency be from DC to 2,000 Hz. The only dynamic test of the transducer performed on this program was the rapid pressurization test. The highest rate used in this experiment was equivalent to about 17 Hz. However, the final design being a diaphragm transducer lends itself easily to handbook solutions. The natural frequency of a clamped membrane may be calculated by the expression:

$$\omega = 11.84 \sqrt{\frac{Et^2}{\rho D^4 (1-\nu^2)}} \qquad (31)^*$$

where E = Youngs modulus, t = diaphragm thickness, ρ = mass density, D = Diaphragm Dia., ν = Poisson's Ratio and 11.84 is a constant for this particular mode.

* Shock and Vibration Handbook; Harris and Crede, Page 1-15.

which gives for the 25-psi transducer a natural frequency of about 21 kHz. Hence, the design goal is substantially exceeded. The natural frequency would, of course, be higher for the 2,000-psi transducer with a thicker diaphragm. Likewise, nonlinearity at large deflections, which is not considered by this equation, gives a higher natural frequency.

6.3 LOW RANGE TRANSDUCER OVERPRESSURE ABILITY

A design goal was that the low range 25-psi transducer be capable of withstanding large overpressures without electrical or mechanical damage that could ignite the surrounding rocket propellant. In section 4.1.2 of this report are test data showing that the low range transducer performed normally at pressures of 500 psi and did not suffer permanent electrical output shift or mechanical damage. Also, appendix H presents the analysis of Dr. David Wood which concludes that a diaphragm 0.005-in. thick and 0.300 in. in diameter, made of 15-5 PH in the H-900 neat treatment condition, will withstand a pressure of at least 4,650 psi; thus, the final production transducer (0.0125-in.-thick diaphragm, approximately 0.250 in. in diameter) would withstand pressures greater than 5,000 psi without metal failure.

The overpressure ability is inherent because of the stiff design which operates below the normal output level to minimize the transducer/propellant interaction factor. Very large overpressures (e.g., 1,000 to 2,000 psi) could generate some zero offset shift, but the transducer diaphragm and body structure will not fail.

6.4 PHYSICAL SIZE

To minimize propellant stress disturbance, the transducer maximum size was placed at 0.75 in. in diameter and 0.34 in. in height. The size of the final Senso-Metrics production transducer is approximately 0.60 in. in diameter at the base and 0.125 in. in height. The stress disturbance zone is minimized as shown in section 5.5.

6.5 OPERATING TEMPERATURE RANGE

The operating temperature range of the transducers was chosen to be 160° to -70°F. The transducers were calibrated and tested over this temperature

range and operated normally. No permanent electrical output shift or mechanical damage occurred as a result of temperature cycling.

6.6 ENVIRONMENTAL PROTECTION

The transducer should not be affected by the corrosive chemical environment of solid propellants. To achieve this goal, the body of the transducer was machined from 15-5 stainless steel and the silicon semiconductor strain gages were placed on the sealed inside surface of the diaphragm out of contact with the corrosive propellant. Numerous tests on transducers embedded in propellant for a period of 3 to 4 months have produced normal transducer responses indicating that the harsh propellant environment is not affecting their performance. All transducer joints were EB welded and their leads were protected by stainless steel tubes.

6.7 AGE AND SERVICE LIFE

The stability and performance of the transducers should not degrade more than 0.2%/year over a minimum service life of 10 years. Since this program did not last 10 years, it is not possible to say at this time that the service life goal has been obtained. However, stability data on the Senso-Metrics models over a period of 1 to 2 years meet the age specification for all 2,000 psi transducers and some 25-psi transducers. These gages will be maintained in periodic stability testing for continuous evaluation for the next 3 years to verify their longer time age performance.

6.8 LEADWIRE CONSTRUCTION

The transducer leadwires should be highly resistant to corrosion, flexible, strong, and small enough to pass through a 0.125-in.-diameter hole. The Senso-Metrics prototype and production transducers have their leadwires encased in a 0.125-in.-diameter stainless steel tube which have been proven and documented as corrosion resistant (appendices E and F). The tube is thin walled enough to be flexible. Its diameter meets the design criteria and it is very strong by virtue of its metal construction.

6.9 COST

The goal of this program was to have a final transducer costing less than $1,000. This goal has been attained: the 1979 price of the Senso-Metrics production transducer is less than $600.

6.10 INSENSITIVITY TO OUT-OF-PLANE STRESSES

The primary purpose of the tension/compression/shear device was to evaluate the sensitivity of the normal stress transducer designs to out-of-plane stresses such as a shear stress across the diaphragm surface. As shown by its finite element stress analysis, the tension/compression/shear device when loaded in the shear mode is ideal for this. This analysis indicated that the normal stress varies over the diameter of the diaphragm from 5% to -5% of the applied shear stress. The calculation of summing diaphragm strains would give almost zero gage output for this type of loading.

Data for the prototype 25-psi gage (Table 28) indicate that while a stress was measured, it did not increase uniformly with the applied load. It appears that the data may simply be offset at a constant 0.5 psi for all applied shear stress levels. This implies an uncertainty in determining the initial no-load state when the device is loaded in the testing machine. Moreover, this assumption is highly probable when considering the weight and cumbersomeness of the fixture. Consequently, the data indicate strongly that a normal stress transducer is insensitive to a shear stress across its diaphragm.

The final design was also tested in the fixture. However, some areas of unbond were found which made the results questionable. The shape of the transducer, being similar to the prototype design, would indicate that the same insensitivity to shear stress would have been demonstrated had the tension/compression/shear device been cast without unbonds.

6.11 TRANSDUCER ACCURACY

The accuracy design goal for these transducers was 1% of full-scale reading. Care must be taken to evaluate this goal under optimum conditions. This requires eliminating errors introduced by experimental setup and measuring equipment. The best data available for this purpose are the 33-point NBS type

calibrations. This entails three sequential up and down calibrations over a short period of time. Using the zero offset and sensitivity values computed from all 33 points, deviations between the computed and measured readings may be plotted as error. Figures 185 through 187 show these data for three 25-psi transducers. The first two transducers are well within the 1% error and the third transducer, S/N 388, is marginal at best and should have been rejected by the manufacturer. It subsequently failed due to faulty leadwires during calibration and was not used in any of the gage evaluation experiments.

Zero offset is also an integral part of the 1% goal. For the NBS results presented above, the zero offset is the error at an applied pressure of zero and is within the error band. However, it should be evaluated with chronologic time since any change in zero offset would be interpreted as an erroneous stress. Again, care must be taken in looking at the data that the measuring instrumentation, temperature control, etc., were very precise. To this end, only data gathered during pressurization calibrations will be discussed. These data are tabulated below for calibrations over a 3-month period.

ZERO OFFSET STABILITY

Date	Temperature, ° F	S/N 383, ZO-mV	Maximum Change, Δ mV	S/N 385, ZO-mV	Maximum Change, Δ mV	S/N 388, ZO-mV	Maximum Change, Δ mV
5/26/78	75	3.749	0.106	4.241		4.678	
6/2/78	80	3.855		4.475		4.906	0.370
8/1/78	72	3.794		4.751	0.517	5.048	
8/2/78	72	3.795		4.757		5.018	
8/9/78	72	3.799		4.758		4.914	

One percent accuracy can be expressed in terms of change in zero offset by

$$0.32 \text{ mV/psi} \times \pm 0.25 \text{ psi} = \pm 0.080 \text{ mV} \qquad (32)$$

or a change in output of 0.160 mV. Looking at the value reported, only gage S/N 383 meets this criterion. A detailed inspection of gage data sheets shows

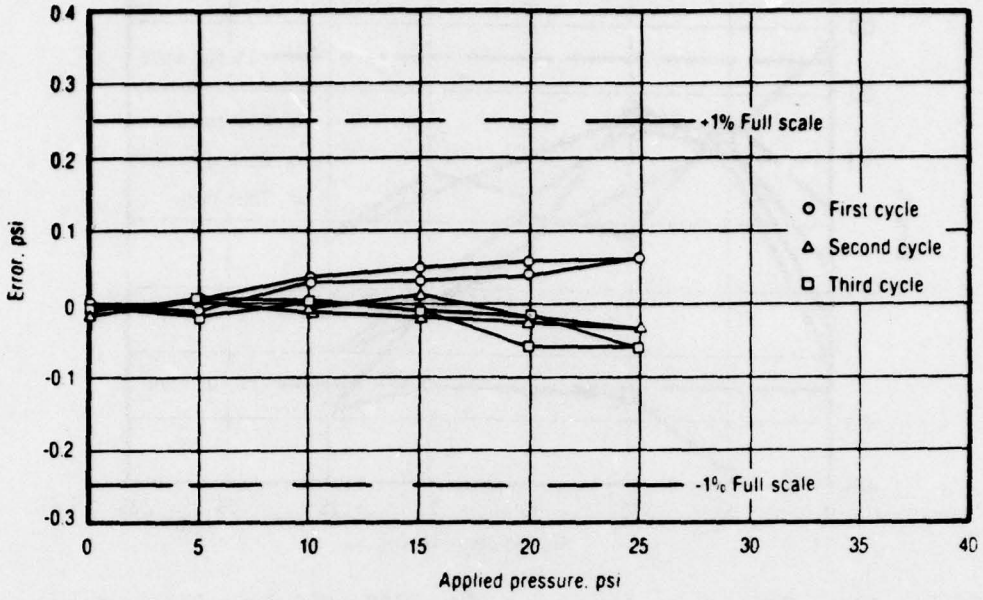


Figure 185. Transducer Accuracy - S/N B383, NBS-Type Calibration

17222

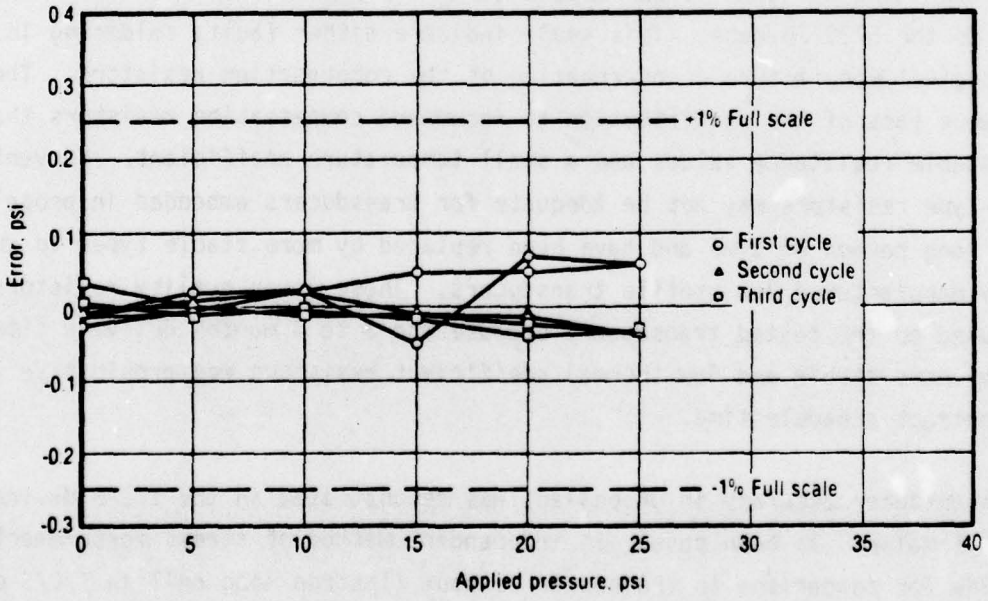


Figure 186. Transducer Accuracy - S/N B385, NBS-Type Calibration

17223

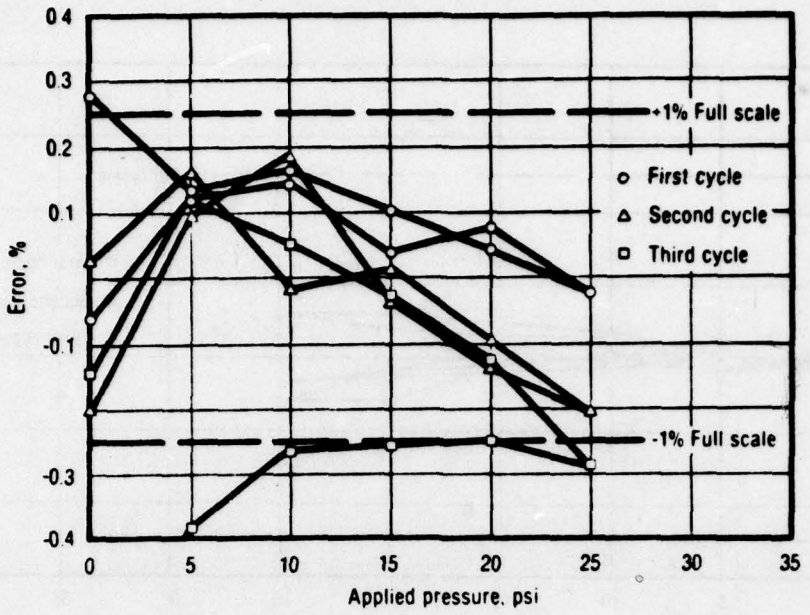


Figure 187. Transducer Accuracy - S/N B388, NBS-Type Calibration
17224

that for S/N 385, the zero offset jumped 0.130 mV while unsoldering and resoldering leadwires when it was assembled in the pressure chamber which was prior to the 5/26/78 date. This would indicate either faulty soldering in the original manufacture or overheating of the compensation resistors. These data were part of the justification to recommend compensation resistors that have stable resistance values and a small temperature coefficient. Conventional RN 55-type resistors may not be adequate for transducers embedded in propellant for a long period of time and have been replaced by more stable types in currently manufactured low profile transducers. These lower quality resistors were used on the tested transducers because the 3 to 4 months delivery time for the more stable and low thermal coefficient resistors was prohibitive within the contract schedule time.

Transducer accuracy in propellant was demonstrated in the T/C/S device and TM-1 motor. In both cases, an independent method of stress measurement was made for comparison to transducer readout (Instron load cell in T/C/S device

and Taber pressure transducer for TM-1 motors). The production model 25-psi transducers in the T/C/S device compared within 3% of the Instron load cell but debonds in the device may have influenced these results. The 2,000-psi transducers in the TM-1 motor compared with 0.7% of the Taber pressure transducer.

7.0 TRANSDUCER CALIBRATION AND APPLICATION TECHNIQUES

Transducer calibration techniques developed on this program were tailored to the specific requirements for accurate evaluation of the improved stress transducers. This required the following equipment:

A. Digital meter accurate to 50 μV and resolution of 10 μV
B. Constant current source (5 mA)
C. Precision, accurate and stable 10-ohm resistor to monitor excitation current
D. Wallace-Tiernan model FA129 absolute pressure gage
E. Taber pressure transducer (Model 217-SA or 227-SA, depending on pressure range required) with special calibration at selected pressure levels (linearity corrections supplied at each 20% of full scale measurement)
F. Thermocouple for temperature measurements
G. Standard resistor for meter check
H. Standard voltage cell for meter check
I. Detailed procedure to ensure quality of laboratory measurements
J. Statistical data reduction techniques for data evaluation and interpretation.

7.1 HARDWARE DESCRIPTION

Several pieces of test hardware were used for stress transducer no-load offset and pressure calibration measurements. Pressure vessels capable of withstanding 2,000 psi pressure and equipped with Conax fittings for leadwire feed through were used to test the stress transducers. A stable constant current power supply was used for transducer excitation (nominally 5 mA). A reference pressure transducer (Taber) was used to measure the pressure applied to the stress transducer inside the pressure vessel. A copper-constantan thermocouple was used for temperature measurement inside the pressure vessel. For bench testing of no-load outputs, a Cu-Co thermocouple or a glass bulb total immersion thermometer was used for temperature measurement. A Wallace-Tiernan absolute pressure meter was selected for measuring barometric pressure. Pressurized dry nitrogen and a pressure regulator were used along with the necessary pressure tubing to apply test pressure to the transducer pressurization vessel. A

temperature conditioning box and hot and cold sources were used for temperature tests other than ambient temperature. Lastly, an accurate digital multimeter, such as a Fluke 8800A, was used to measure the electrical test data. Table 49 lists the measurement instruments used by CSD and their accuracy.

7.2 TEST TECHNIQUES

7.2.1 No-Load Zero Offset Measurements

Before any measurement, a systems check on the Fluke 8800A digital multimeter used to record data was performed. The input leads were shorted with the instrument in a DCV (direct current volts) function and the display adjusted to read 0 V. The standard voltage cell and standard resistor were used for a meter check before proceeding with the gage measurements. Any inability to zero the meter or read the correct reference ohms and volts required the operator to send the instrument to CSD's calibration laboratory for recalibration. At all times the instrument was maintained in current calibration as defined by the CSD calibration sticker on the instrument. After the DVM was determined to be accurate, the no load output of the transducers was measured. Excitation to the transducer was supplied by a multichannel adjustable constant current power supply. A precision stabilized 10-ohm resistor was placed in the excitation leadline and the voltage drop across this resistor was measured. In this manner the excitation current (nominally 5 mA) was calculated precisely. For each gage the value of the precision 10-ohm resistor, the voltage drop across the resistor, and the gage output were measured and entered in the data form shown in Figure 188. Ambient temperature also was recorded as measured by copper-constantan thermocouples and total immersion thermometers. The ambient pressure was recorded by a Wallace-Tiernan absolute pressure meter and entered on the data sheet.

Figure 189 is a photograph of the no-load data acquisition system. Data reduction techniques will be discussed later in this section.

7.2.2 Pressure Calibration Measurements

The transducers were placed in a pressure vessel and the vessel was filled with Shell Diala oil. This fluid minimized temperature effects due to pressurization. Excitation to the transducers was supplied with the adjustable

TABLE 49. EQUIPMENT MEASUREMENT ACCURACIES

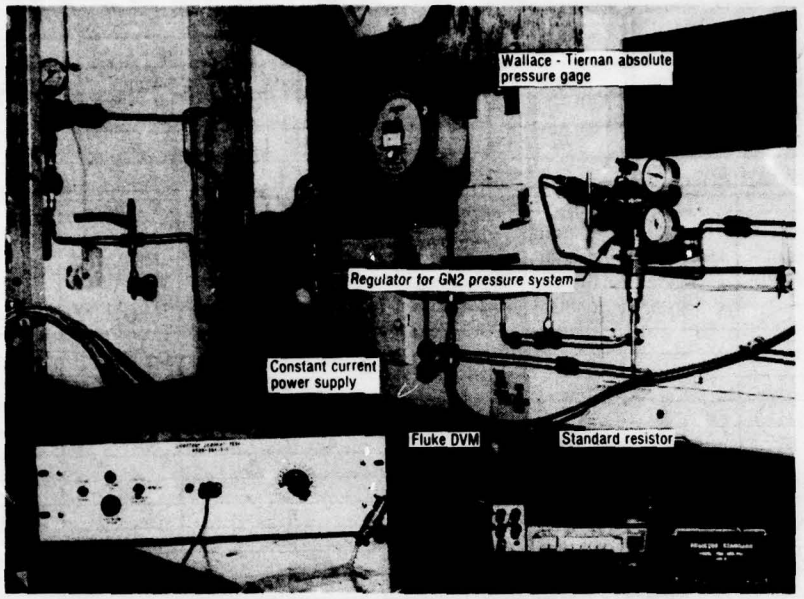
T4555-D

Instrument	Parameter	Accuracy
Fluke 8800A DVM	Normalized gage output, mv/ma	0 to 200 mv range accuracy: 0.005 mv + 0.008% of input, 0.005 ohm + 0.01% of input
Reference transducer (Taber) (0 to 50 psig Model 227-SA and 0 to 2,000 psig Model 217-SA)	Pressure (psig) using internal CSD calibration data	± 0.05% of full scale
Constant current supply (CSD-assembled using Calex programmable constant current modules and 28-v power supply)	Excitation current (ma) across a measured 10-ohm resistor	0.0014 ma at 5-ma excitation
Thermocouple (copper-constantan)	Test temperature	± 2°F
Wallace-Tiernan model No. FA129 absolute barometer gage (0 to 20 psi at 0.02-psi resolution)	Atmospheric pressure (psia)	0.02 psi

Manufacturer_____ Model No._____ S/N_____ Range_____ psia_____

Test Parameter	Manufacturer		CSD			
			First Wiring		Second Wiring	
	Date	Value	Date	Value	Date	Value
Ambient full-scale output, mv						
Ambient sensitivity, mv/psig						
Ambient zero offset, mv						

Test Date	Ambient Temperature, °F	Barometric Pressure (B_p), psia	Standard Resistor Cell, ohms	Input Excitation Resistance (R_{EX}), ohms	Voltage Drop (V_{EX}), mv	Note (1) Excitation Current (I_{EX}), ma	Measured Zero Offset (ZO_M), mv	Note (2) (ZO_{MCN}), mv	Note (3) (ZO_C), mv



11617-6

Figure 189. No-Load Offset Data Acquisition System

17253

multichannel constant current power supply and data were recorded on the Fluke 8800A DVM. The transducers were allowed to condition in the fluid filled pressure vessel for a minimum of 4 hr at 70°F before pressure calibration. The DVM was subjected to the same systems checks of its accuracy before testing as during the no-load output measurements. Pressure was applied to the transducers with a regulated bottle of dry nitrogen. The applied pressure was measured with a Taber pressure transducer supplied by CSD's instrumentation department. The stress transducer excitation requirements were the same as for the no-load measurements.

CSD's calibration department performed a special calibration on the Taber pressure transducer before its use. Rather than supplying a single output in mV at a specific pressure range of approximately 50% of full scale. These data, plus correction factors for linearity and hysterisis at each 20% increment of full scale, were supplied. The stress transducers were pressurized from 0 psia to full scale and back at 20% increments. Each 0-psia data point was recorded with the pressure vessel vented to the atmosphere. A total of 33-points were recorded during the calibration at ambient temperature. An 11-point calibration

was performed at other temperatures. The significance of the 33- and 11- point calibrations are explained in the data reduction section.

The precise value of the 10-ohm precision resistor in the power supply was measured before the pressure run, and at each pressure increment the transducer output and voltage drop across the precision resistor were measured and recorded. In addition the Taber was measured and recorded at each pressure level. The barometric pressure was measured and recorded at the beginning and ending of the pressure series. A copper-constantan thermocouple was located inside the pressure vessel to monitor temperature which was recorded three times during the test. The total pressure calibration system is shown in Figure 190; all data were recorded on the data form shown in Figure 191. Data reduction techniques will be discussed later in this section.

7.3 DATA REDUCTION TECHNIQUES

7.3.1 No-Load Zero Offset Data Reduction

Upon completion of all raw data acquisition, the excitation current was calculated using the relationship

$$I_{ex} = V_{ex}/R_{ex} \tag{33}$$

where I_{ex} is the excitation current, V_{ex} is the measured voltage drop across the 10-ohm resistor, and R_{ex} is the precise value of the 10-ohm resistor. The next step was to normalize the measured transducer output based on an excitation current of exactly 5 mA:

$$ZO_{mcn} = (ZO_m/I_{ex})\ 5 \tag{34}$$

where ZO_{mcn} is the no-load voltage output measured and current normalized, ZO_m is the measured no-load voltage output, and I_{ex} is the excitation current. The final calculation normalized the data to 14.7 psia ambient pressure:

$$ZO_c = ZO_{mcn} + (14.7 - B_p)(S_e) \tag{35}$$

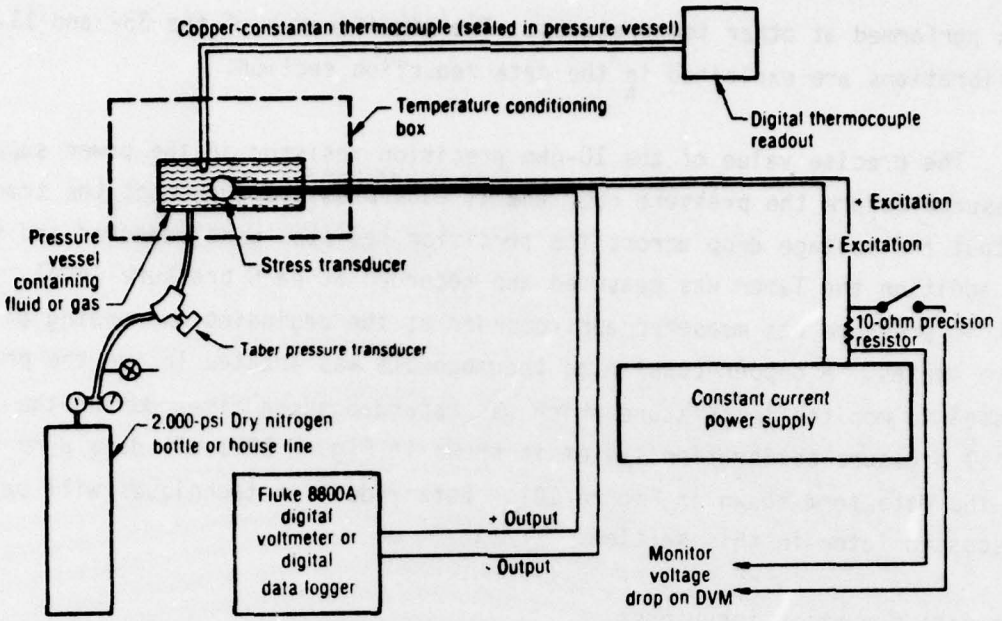


Figure 190. Stress Transducer Calibration and Data Acquisition System
14011

where ZO_c is the final corrected no-load voltage output, ZO_{mcn} is the current normalized no-load voltage output, B_p is the measured barometric pressure, and S_e is the transducer sensitivity.

7.3.2 Pressure Sensitivity Data Reduction

Originally, four methods of transducer sensitivity data reduction were considered. A summary of the four methods is given below.

Method 1*

This method calculates gage sensitivity and a 95 percentile confidence level for gage sensitivity. This method uses a least squares fit of 33 data points of reference pressure versus gage electrical output to determine gage sensitivity. Small variations in excitation current are corrected for by normalizing the gage electrical output to 5-mA excitation.

*Natrella, M.G., "Experimental Statistics," National Bureau of Standards Handbook 91, August 1963.

Manufacturer _____ Model No. _____ S/N _____ Range _____ psia

Stress transducer: Excitation _____ ma Output Air _____ mv Oil ____ mv Excitation resistance _____

Standards check: DVM S/N _____ Make _____ Standard cell of ____ ohms reads ____ ohms

	Test Date	Test Date	Test Date
Taber calibration:			
50% shunt, psig:			
50% shunt, mv:			
Excitation, v:			

Test Conditions	Percent of Full Scale	Taber Output, mv	Stress Transducer Output, mv	Stress Transducer Excitation, ma
B_p = _____	0			
_____ °F	20			
(initial)	40			
	60			
Oil temperature	80			
_____ °F	100			
	80			
B_p = _____	60			
_____ °F	40			
(final)	20			
	0			
B_p = _____	0			
_____ °F	20			
(initial)	40			
	60			
Oil temperature	80			
_____ °F	100			
	80			
B_p = _____	60			
_____ °F	40			
(final)	20			
	0			
B_p = _____	0			
_____ °F	20			
(initial)	40			
	60			
Oil temperature	80			
_____ °F	100			
	80			
B_p = _____	60			
_____ °F	40			
(final)	20			
	0			

Comments:

Sample Printout of Reduced Data from H-P 9825 Calculator

```
Semicond rice

E303    25 mil
72 F

CURVE FIT
# DATA PTS     11

5*OFF    3.811451
5*SE Sen 0.312416
5*SE Se  0.000145
```

Where: 5 X off = Computer calculated zero offset at 5 ma excitation

5X SE Sen = Computer calculated standard deviation of the sensitivity at 5 ma excitation

5X Sen = Computer calculated sensitivity at 5 ma excitation

Figure 191. Stress Transducer Calibration Data Sheet

16999

The 33 data points are collected from three successive step-wise pressurizations at 20% intervals. Gage sensitivity is defined as the slope of the curve fit solution.

Method 2*

This method is an extension of the NBS Handbook 91 method which uses 33 data points. In addition to the data supplied in method 1, gage repeatability at particular pressure levels is given. Repeatability is equivalent to the standard deviation of the data scattered about the curve-fit calculated values. At each 20% pressure level interval, the observed value is subtracted from the value calculated by the curve-fit solution, then squared. The squared deltas are summed and divided by one less than the number of data points at the particular pressure level. This method is routinely used at AFRPL's calibration facilities.

The square root of this value represents a 1-σ uncertainty for a gage output measurement at a particular pressure level. The method is described in the equations below and is shown graphically in Figure 192.

$$U_s = \left\{ \frac{\sum_{i=0}^{i=n} \left(OP_{calc} - OP_{obser}\right)^2}{n-1} \right\}^{1/2} \qquad (36)$$

where

U_s = uncertainty of the gage output at a particular pressure level, mV/mA
OP_{calc} = gage output calculated from a 33-point least squares fit, mV/mA
OP_{obser} = gage output observed at a particular pressure level, mV/mA
n = number of gage output data points at a particular pressure level

*Abernathy, Dr. R. B., et al., "ICRPG Handbook for Estimating the Uncertainty in Measurement Made with Liquid Propellant Rocket Engine Systems," CPIA No. 180, AD855130, April 1969. See also Abernathy, Dr. R. B., and J. W. Thompson, Jr., "Handbook, Uncertainty in Gas Turbine Measurements," AEDC TR-73-5 (AD755356); and Abernathy, Dr. R. B., et al., "Tutorial, Test Measurement Accuracy," ISBN-87664-369-1, ISA Presentation, Las Vegas, NV, 1977.

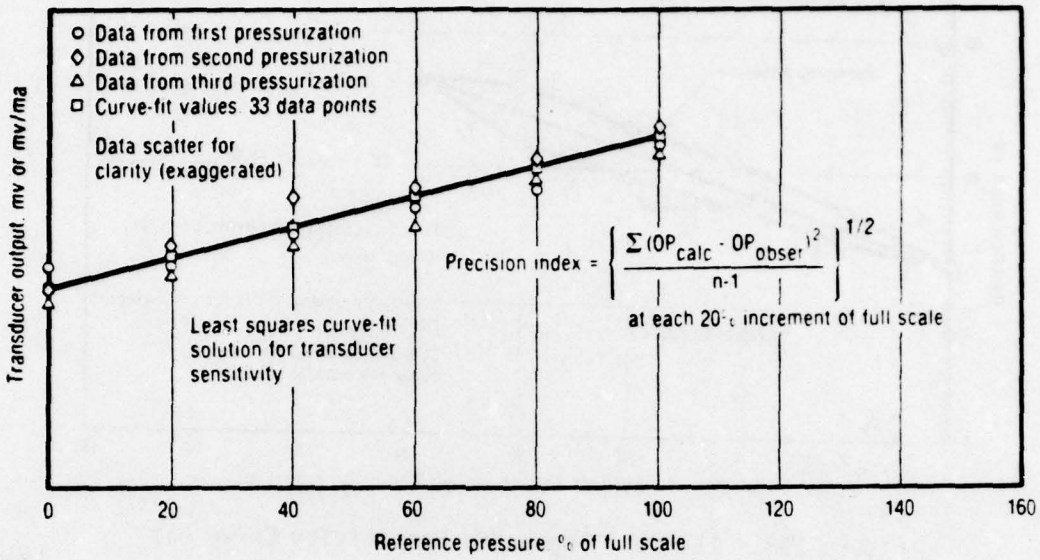


Figure 192. Data Reduction Calculation of Transducer Sensitivity and Uncertainty (Method No. 2)

17252

The uncertainty of gage output can be related to gage full-scale uncertainty by dividing the uncertainty of gage output by the full-scale output of the gage in mV/mA. The authors, Dr. R. B. Abernathy et al. of Pratt and Whitney Aircraft, recommend that the largest uncertainty for any of the 20% pressure levels be considered as a 1-σ uncertainty of the calibration. All stress transducer sensitivity numbers at ambient temperature were obtained using method 2.

Method 3 (Segmented Curve Fit)

This method produces a value for gage sensitivity and an estimated value for the uncertainty of gage sensitivity. The slope of gage output (mV/mA) versus reference pressure between successive pressure levels is calculated. This procedure is used for all the data available. Gage sensitivity is defined as the averaged slope. The standard deviation of the average represents an uncertainty value for gage sensitivity. This uncertainty value is not a 1-σ value, but compares more to the 95% confidence interval of method 1. This method is demonstrated in Figure 193, and was used for the 11-point calibrations at temperatures other than ambient.

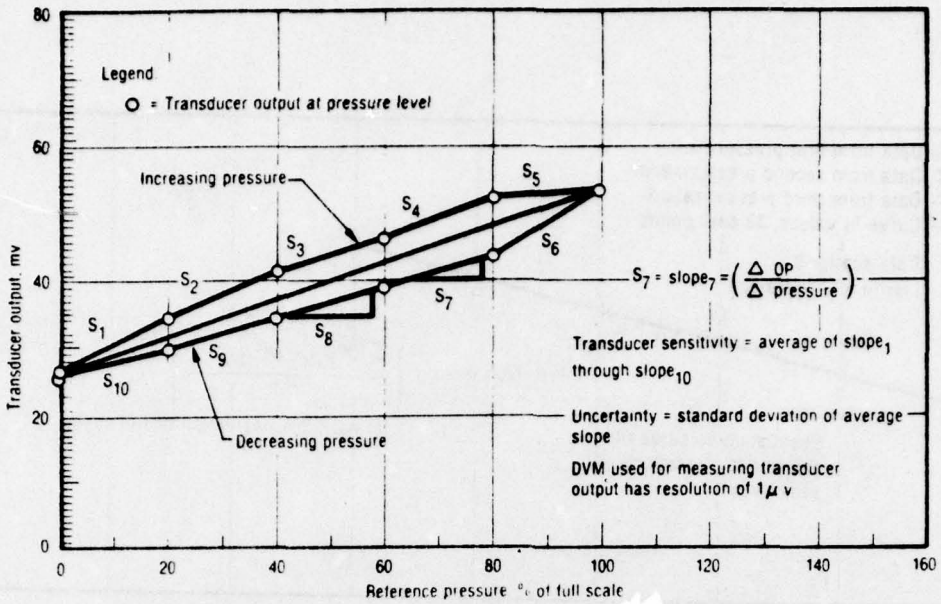


Figure 193. 11-Point Segmented Sensitivity Curve Fit

17000

Method 4 (Straight-Line Approximation)

This method is least accurate and is used primarily to confirm gage operation. It consists of defining sensitivity as the slope between no-load and full-scale transducer output. Usually the approximation of gage performance is made by considering the deltas between the observed value and the calculated value at 50% or 75% of full scale. This method is routinely used by transducer manufacturers for QC purposes. This method is not recommended for detailed transducer evaluations. Method 4 is shown in Figure 194.

7.4 STRESS TRANSDUCER INSTALLATION PROCEDURE

In order to routinely install stress transducers in rocket motor cases after laboratory calibration is finished, the following procedure was developed and followed by CSD personnel.

A. Preparation of Motor Case

1. Thoroughly sandblast the entire inside of the metal motor case.
2. Wash the inside of the motor case with a solvent such as MEK.

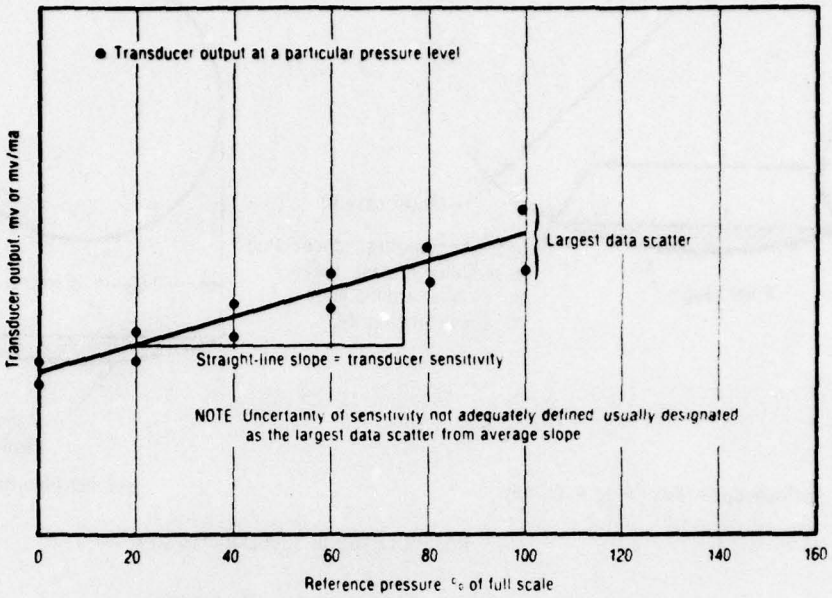


Figure 194. Straight-Line Approximation to Calculate Transducer Sensitivity (Method No. 4)

17251

3. If the motor case must be stored before transducer installation, seal it in a plastic bag to keep out moisture; take care not to touch the inside of the case with hands.

B. Transducer Preparation

1. Calibrate bare stress transducer at several temperatures covering the testing range for the motors.
2. Since the back of the transducer is flat and the inside of the motor case is curved, fabricate a filler plug from either 15-5 or 17-4 stainless steel (see Figure 195 for details on this filler plug).
3. Using a Versamid Epon two-part epoxy mixed in equal portions by weight (or any equivalent epoxy), attach the flat portion of the filler plug to the back surface of the transducer.
4. Place a wooden block on top of the transducer so that a countersunk hole in the block fits over the diaphragm and rests on the sloping sides of the transducer; place a small weight (2 to 3 lb) on the top

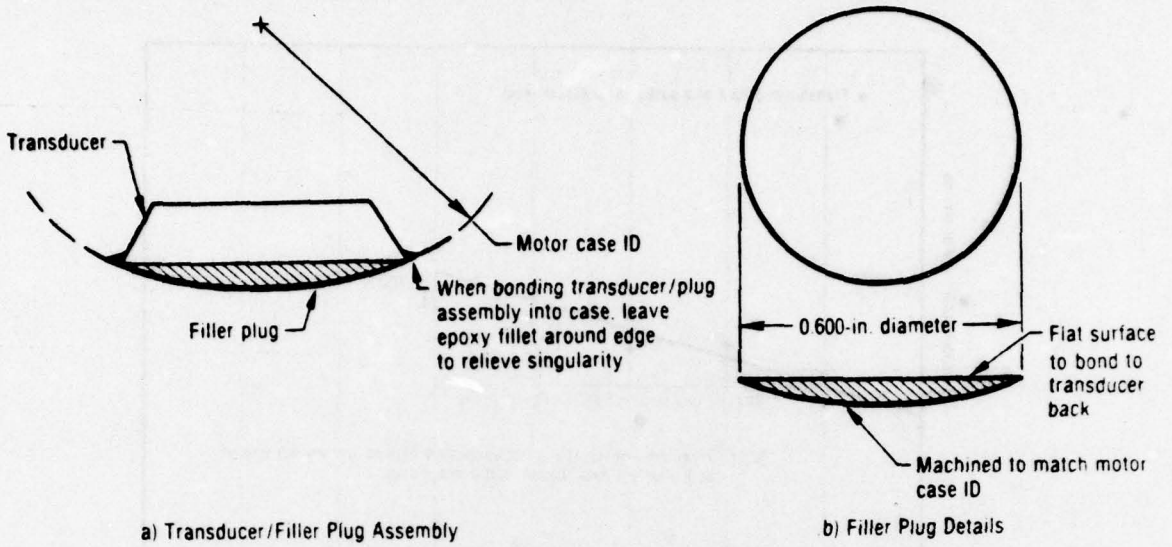


Figure 195. Filler Plug Details

17250

of the block to hold the transducer and filler plug together (since the bottom portion of the plug is rounded, side supports must be placed around the transducer/plug to keep it from tilting).

5. Place the transducer/plug in an oven and cure epoxy 24 hr at 140°F.

C. Transducer Installation in Motor Case

1. Procure a turnbuckle small enough to fit inside the diameter of the motor case; threaded stock may be screwed into each end of the turnbuckle and wooden pads attached to the threaded stock; one pad should have a countersunk hole in it so that it fits over the transducer diaphragm and rests against the sloping sides of the transducer.
2. Prepare the epoxy (CSD uses a Versamid-Epon two-part epoxy mixed in equal portions by weight; pot life of this epoxy is greater than 30 min).
3. Coat the back of the transducer/plug with epoxy and place this assembly on motor case wall at desired location; insert turnbuckle in motor case and place pad with countersunk hole over transducer; rotate

turnbuckle until opposite pad comes in contact with opposite side of the motor case; transducer is now fixed in the desired location and is being held firmly against the motor case (see Figure 196 for turnbuckle/case details).

4. Smooth leadwire tube against the motor case from the transducer to the end of the case; epoxy the tube to the case wall.
5. Place motor case in an oven and cure epoxy for 24 hr at 140°F.
6. At end of epoxy cure, motor and bonded transducer must be conditioned at several temperatures covering the desired testing range to obtain bonded transducer zero offset data; case and transducer must be conditioned at least 2 hr at each temperature before the offset is recorded. The bonded zero offset data for the Senso-Metrics production transducers in the T/C/S and TM-1 devices is presented in Figures 197 through 200. If liner is to be used in the motor, it may be applied directly over the transducer but offset data must be taken after liner application. If insulation is used in the motor it must be applied to the case first and then the transducer bonded to the insulation.

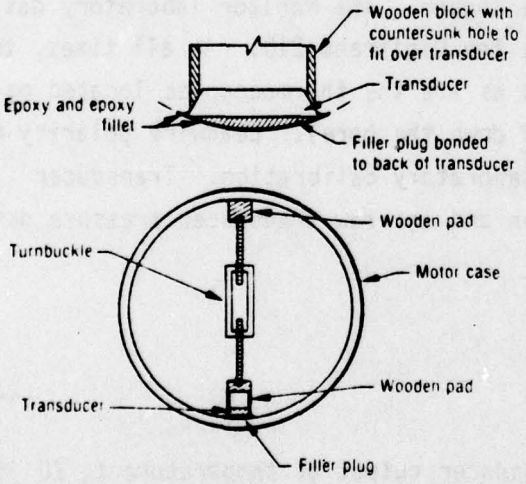


Figure 196. Turnbuckle Details
17249

Pressure calibrations may be performed after transducer installation although previous experience involving the prototype transducer response in the end-burner fixture showed that sensitivity does not change after transducer bonding if epoxy is kept off the diaphragm.

7.5 FIELD MEASUREMENT OF STRESS TRANSDUCER OUTPUT

The techniques of measuring stress transducer outputs that are from case-bonded transducers located in the field differ from laboratory measurements. Usually it is desirable to record the transducer ouptut continuously in order to monitor propellant temperature and

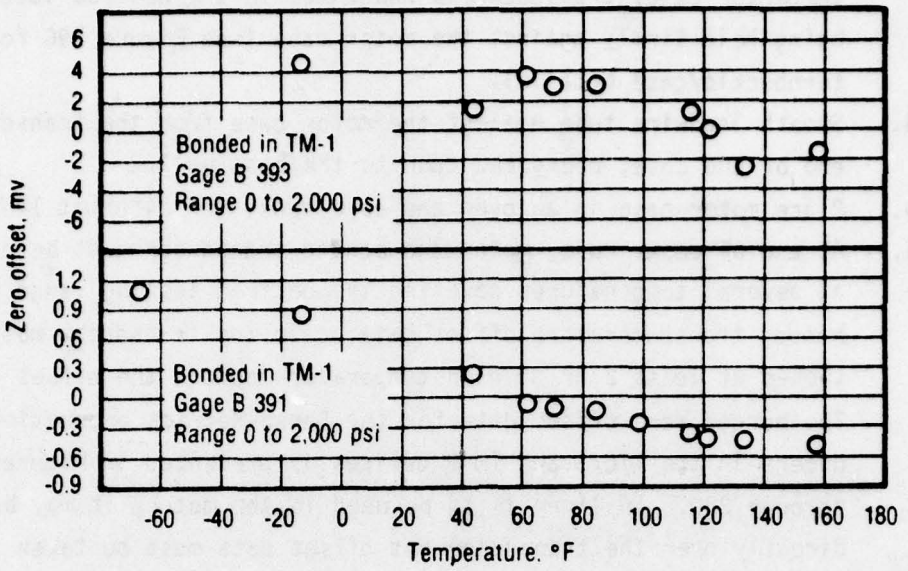


Figure 197. Zero Offset for Senso-Metrics, Inc. Production Transducers Bonded in Test Devices

18510

stress data variances due to thermal cycling and storage loadings. To do this, a periodic continuously recording digital data logger is used. CSD uses either a Doric 210 or a Monitor laboratory data logger. The Monitor laboratory data logger has a resolution of 10 μV as does the Digitrend 210. At all times, transducer excitation and output are recorded as are the thermocouples located on the motor case (in the air near the case and down the bore). Leadwire polarity must be maintained the same as that used in laboratory calibration. Transducer outputs are normalized to 5-mA excitation and the raw transducer pressure data are obtained from

$$P = \frac{(OP_N) - (ZO)}{Se} \qquad (37)$$

where OP_N is the current normalized transducer output at temperature t, ZO is the laboratory measured bare gage zero offset at temperature t (measured prior to installation), and Se is the laboratory measured bare gage sensitivity at

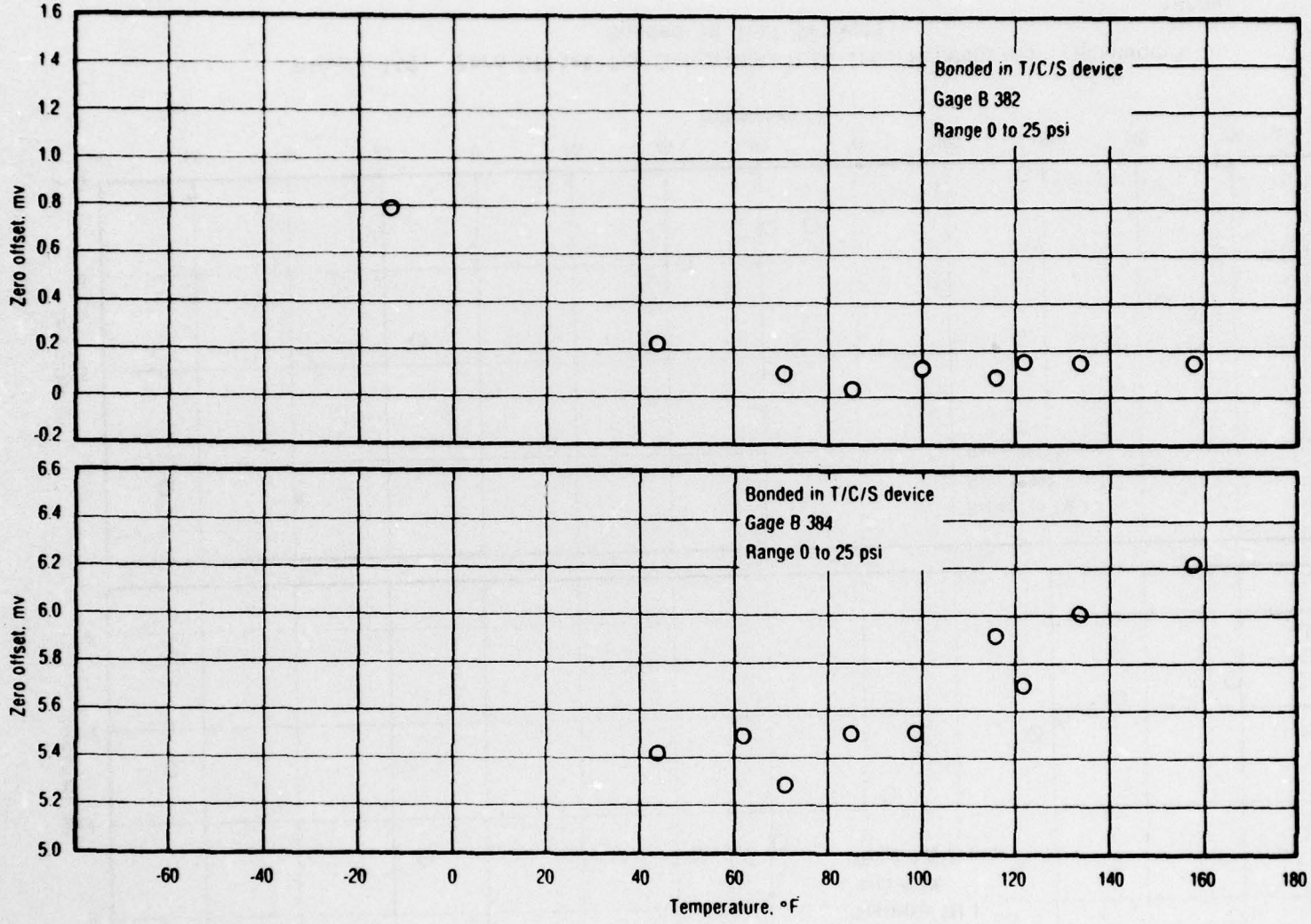


Figure 198. Zero Offset for Senso-Metrics, Inc. Production Transducers Bonded in Test Devices

18509

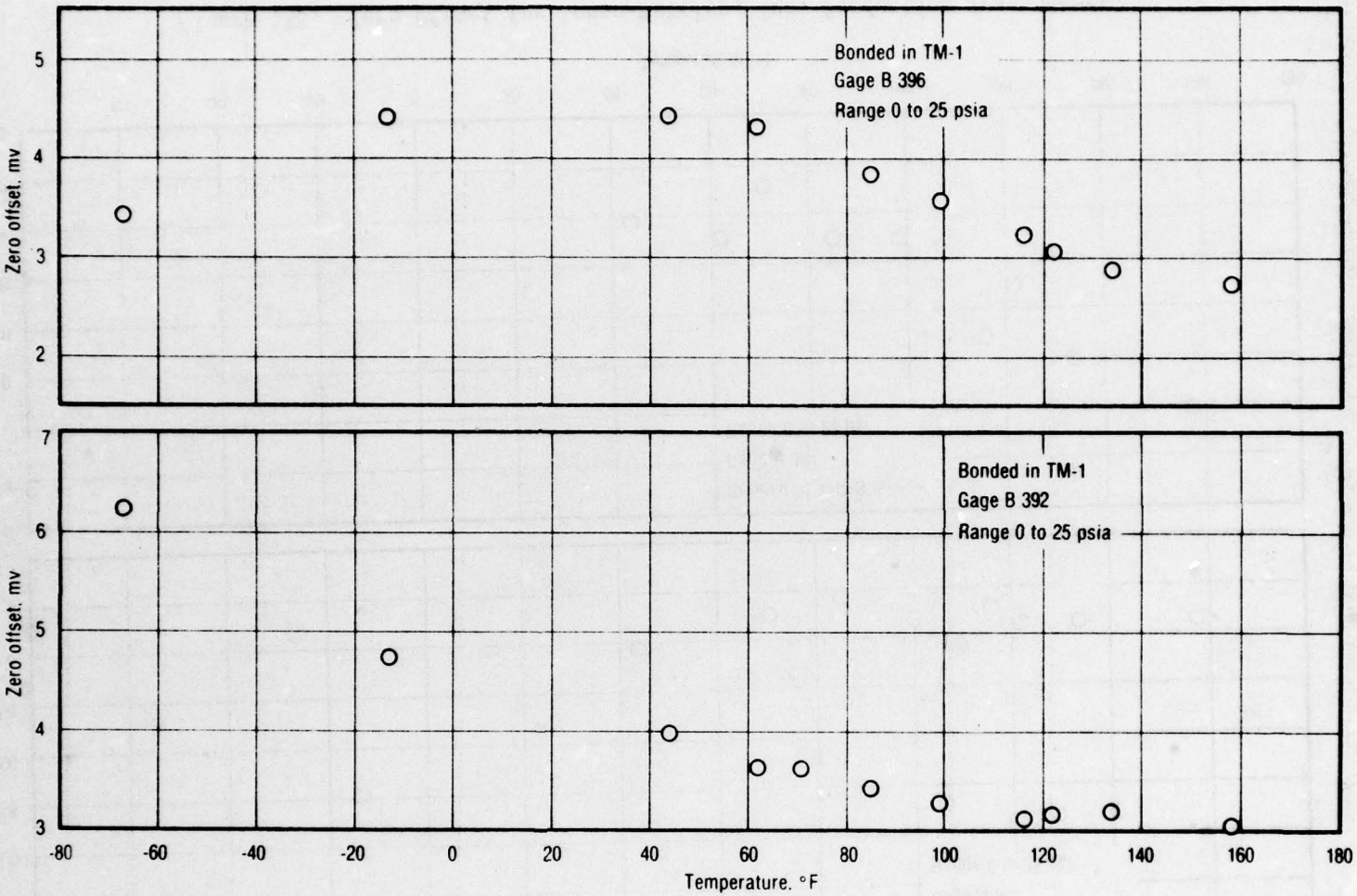


Figure 199. Zero Offset for Senso-Metrics, Inc. Production Transducers Bonded in Test Devices

18508

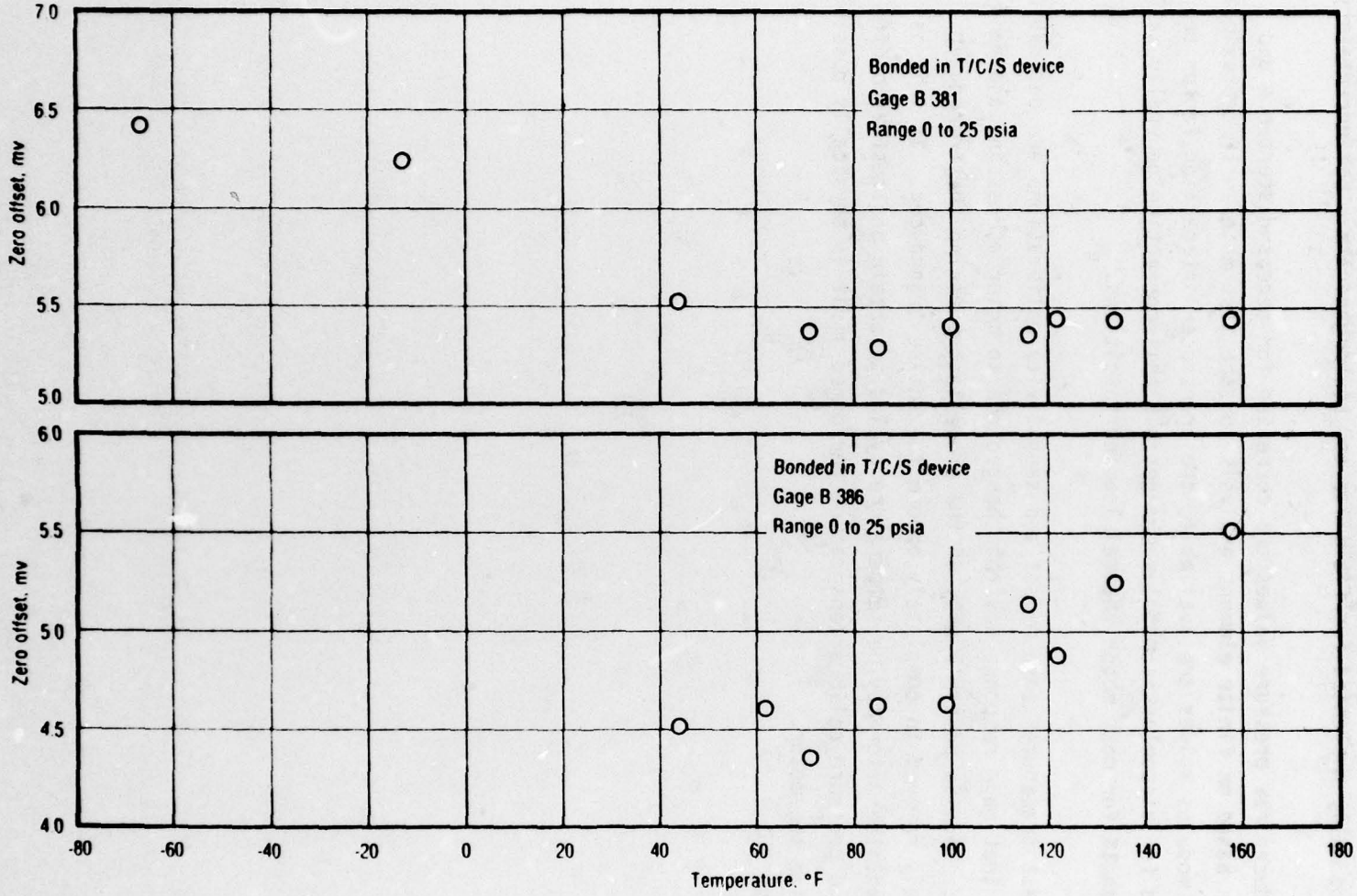


Figure 200. Zero Offset for Senso-Metrics, Inc. Production Transducers Bonded in Test Devices

18507

temperature t (also measured prior to installation). Barometric presure variations are normally neglected for field use and could generate a psi uncertainty.

Transducer raw pressure values are corrected for stress disturbance and interaction based on finite element analysis for the test motor. If approximate propellant modulus values are available, the transducer interaction factor can be adjusted for viscoelastic modulus changes but this correction generally will be less than 1% for most motor thermal loading conditions.

Posttest transducer zero offset and sensitivity calibrations are desirable to confirm that gage response was not changed due to motor processing and handling abuse. This is possible only if the propellant covering the transducer can be safely removed to completely expose the entire transducer. If this is accomplished, the motor may be temperature cycled to obtain posttest zero offset data and pressure calibrations can be performed if it is physically possible to pressurize the motor.

8.0 CONCLUSIONS AND RECOMMENDATIONS

The "Improved Normal Stress Transducer Program" was a comprehensive effort to improve the "state-of-the-art" in motor stress measurements.

8.1 GENERAL CONCLUSIONS

A. An improved stress transducer was designed, manufactured and evaluated for measurement of normal bond stresses in solid propellant rocket motors.

B. The state-of-the-art was improved by using new design concepts, fabrication procedures, evaluation techniques, and analytic considerations.

C. The transducer-propellant interaction was reduced by analytic design procedures.

D. By using finite element analysis, stress disturbance and transducer-propellant interaction can be independently determined and applied in transducer design.

E. The final transducer design provides chemical protection and reduced propellant application difficulties.

F. Transducer and instrumented beam one-year aging tests show good stability.

G. Uncertainty analysis used for planning the instrumented beam tests and transducer evaluation indicated better equipment, test procedures, and analytic interpretation than normally anticipated are required.

H. Embedded stress transducer evaluation in solid propellant show reasonable agreement between predicted and measured stresses for pressure, mechanical and thermal loading conditions.

I. Finite element analysis is required for gage interpretation in specific motor applications.

8.2 DESIGN TRADEOFF AND FABRICATION CONCLUSIONS

A. Chemical protection from the corrosive solid propellant environment can be achieved by using electron-beam welded seals and a glass-to-metal header for wire exits.

B. Use of high resistance stainless steel lead wires may cause temperature compensation, safety, stability and reliability problems. These potential problems were avoided by using low resistance copper wire in the critical part of the transducer circuit and providing chemical protection with a stainless steel protective tube.

C. Complete transducer fabrication by the manufacturer under carefully controlled laboratory conditions using selected components and procedures can reduce transducer field application problems.

D. The cantilevered beam design could not be manufactured without a large mechanical strain offset due to manufacturing difficulties.

E. Tradeoff studies showed that constant current excitation (as compared to constant voltage excitation) provided more safety, compensation, and application advantages.

F. A miniature glass-to-metal header was successfully designed and used in the stress transducers for providing a positive metal-to-metal seal.

G. Long-time chemical stability and wide temperature range requirements dictated the need for an absolute pressure transducer.

H. Optimum transducer design should be as small as feasible consistent with manufacturing limitations.

8.3 METAL STABILITY STUDY CONCLUSION

Literature surveys and analytic studies highlighted a number of metal considerations which have not been considered in previous transducer designs. Some of these specific conclusions are presented below.

A. Metallurgy studies showed that 15-5 stainless steel was better than 17-4 or other metals for the transducer application because of uniformity of properties, and reduction of metal occlusions by a double vacuum melt process.

B. Most metals exhibit significant creep which can be neglected for conventional structural applications, but which is an important consideration in the design and fabrication of a stable stress transducer.

C. Metal creep can be maintained below one microstrain if the metal stresses are relieved and maintained below the precision elastic limit of the metal. (This is about 10% of the yield limit with stainless steel.)

D. Machining of any miniature metal transducer structure generates surface metal stresses which exceed the precision elastic limit and may be near the yield stress. This high stress condition can cause continuous metal creep which would appear as transducer instability.

E. The long-time metal creep problem can be avoided by stress relieving and stabilizing processes after the all-metal machining is completed.

F. Consideration of metal and epoxy creep phenomena in transducer design, fabrication and application has improved transducer stability.

8.4 EPOXY ADHESIVE CONCLUSION

Epoxy used for semiconductor strain gage bonding (like all epoxies) is inherently sensitive to creep phenomena, especially at elevated temperatures. Some conclusions about this specific epoxy behavior are presented below.

A. A survey of the published and unpublished strain gage adhesive data indicates that both foil and semiconductor strain gages experience creep phenomena.

B. Epoxy creep phenomena can be reduced by curing the epoxy completely which generally means some curing at 350^{o}F for strain gage applications.

C. Finite element analysis showed that reducing the epoxy thickness will reduce the effect of the epoxy creep.

D. Epoxy thickness can be reduced by controlling filler particle size or by filtering out the large particles before strain gage bonding.

E. Finite element structural analysis showed that epoxy thickness should be less than 0.001 in.

F. Reductions in epoxy thickness were achieved by reducing metal surface roughness.

8.5 BEAM TEST CONCLUSIONS

A. Literature survey showed that meaningful semiconductor strain gage stability data did not exist before this program.

B. Calibrated temperature accuracies of 0.05^{o}F are required to accurately measure semiconductor strain gage stability.

C. Uncertainty analysis showed that even under the best conditions the daily temperature variations cause significant semiconductor

resistance change and therefore must be considered in the data interpretation.

D. One-year beam stability measurements show no significant strain change at 160^{o}, 120^{o} and 90^{o}F.

8.6 FINITE ELEMENT ANALYSIS CONCLUSIONS

An in-depth study of transducer-propellant interaction and disturbance and gage internal and external design features was conducted using the TEXGAP finite element analysis computer code. Specific conclusions are presented below.

A. The propellant-transducer interaction is critical with the 25 psi transducer because of the thin diaphragm.

B. The 2,000 psi transducer is stiff enough to minimize the propellant-transducer interaction.

C. Finite element analysis showed that the final 25 psi transducer design has propellant-transducer interaction less than one percent for normal thermal loads.

D. Finite element analyses shows that the final stress transducer design generates a thermal stress disturbance of 10% or more. For a pressure load, the disturbance is less than 1%.

E. Analysis showed that the optimum (producing minimum propellant stress concentration) transducer external geometry was achieved with 60^{o} sloping external side.

8.7 TRANSDUCER APPLICATION CONCLUSION

Transducer testing was conducted in propellant in three different types of test vehicles: end burner configuration, tension-compression-shear fixture, and circular port test motors. The stress gages worked successfully in all three geometric conditions and specific conclusions from these tests are presented below.

A. Excellent agreement between predicted and measured thermal stresses was achieved for the circular port test motors.

B. Stress gage evaluation in the tension/compression/shear device showed reasonable correlation between the calculated mechanical stresses and the stress gage measurements.

C. Calibration and interpretation analysis for the stress gages must be carefully conducted with adequate equipment and finite element analysis to yield accurate stress values.

D. Thermal stress gage response in a circular port motor exposed to incremental thermal steps show the expected stress relaxation after each new temperature load.

E. Self heating studies with bare and embedded transducers over the 160^{O} to -65^{O}F temperature range showed a minimal zero shift at -65^{O}F due to self heating at 5 milliamps excitation. Higher temperature tests showed stable transducer electrical output up to 5 milliamp excitation.

F. Self heating and diode effect tests showed a definite diode effect and nonlinear zero offset versus constant current excitation level. Excellent transducer performance can be obtained by maintaining constant transducer excitation levels and polarity.

G. Day to day barometric pressure variations cause notable transducer zero offset changes. Accurate transducer output measurements must be corrected for barometric pressure changes.

H. Constant current power supplies exhibited enough long time drift in field applications to require monitoring the excitation current along with each transducer output measurement. All transducer measurements should be normalized to a constant excitation level.

I. Pressure calibration of the stress transducers should be conducted with the transducers submerged in a suitable liquid medium to minimize thermal stabilization times.

J. A Fluke 8800A (5-1/2 digit) meter was found to be stable and accurate enough for transducer and beam stability test measurements.

8.8 RECOMMENDATIONS

The final low profile transducer design could be improved further, though schedule and cost limitations on this program prohibited such improvements. Some of the potential improvements are listed below:

A. Reduce height and diameter.

B. Reduce EB welding heat by using a laser beam heat source.

C. Consider lower thermal coefficient resistors with ultrastable resistance values.

D. Perform temperature compensation of transducers based on zero voltage output at 14.7 psi rather than absolute zero pressure.

E. For a reduced size transducer one should use 0.040-in. long semiconductor strain gages rather than 0.060-in. gages. This would produce larger average strains in the outside gages and increase output. The gages should be very well matched to reduce zero offset and increase instability.

F. Reduce leadwire protection tube to minimum length for specific applications.

G. Transducer stress interpretation factors were derived for specific test devices and were limited to evaluation using a 2D finite element computer analysis. An in-depth study of 3D effects for both stress disturbance and interaction in a variety of typical motor applications would provide more confidence in general gage usage and interpretation.

H. Stability tests with transducers and instrumented beams should be continued over a sufficiently long period to build confidence in long term gage performance.

ABBREVIATIONS

AFB	Air Force Base
AFRPL	Air Force Rocket Propulsion Laboratory
ASPC	Aerojet Solid Propulsion Co.
BIT	bond-in-tension
CSD	Chemical Systems Division
DVM	digital voltmeter
EB	electron-beam
FE	finite element
FEP	fluorinated ethylene propylene
ID	inner diameter
JANNAF	Joint-Army-Navy-NASA-Air Force Interagency Propulsion Committee
L/D	length-to-diameter (ratio)
OD	outside diameter
PEL	precision elastic limit
SG	semiconductor gage
S/N	serial number
SRM	solid rocket motor
SS	stainless steel
TC	thermal coefficient
T/C/S	tension-compression-shear device
2D	two dimensional
3D	three dimensional
FS	full scale
NBS	National Bureau of Standards
GF	gage factor

LIST OF SYMBOLS

a	radius of bore, in.
b	outer radius of propellant grain, in.
B_p	measured barometric pressure, psi
D	diameter, in.
D_f	disturbance factor
E	Youngs modulus, psi
E_{ex}	excitation voltage, V
E_p	propellant modulus, psi
E_o	gage measured output, V
F_c	compressive force, lb
F_s	shear force, lb
F_T	tensile force, lb
G	gage factor
I_{ex}	excitation current, amps
I_f	interaction factor
L	length, in.
mA	milliamps
mV	millivolts
n	integer number
NOP (o)	voltage and temperature normalized output at initial loading time
NOP (preload)	voltage normalized output before loading
NOP (t)	voltage normalized transducer output at time (t), nondimensional
NOP'(t)	voltage and temperature normalized output at time (t), nondimensional
OP	output voltage, V
OP_{calc}	gage output calculated from a 33 pt least square ft, mV/mA
OP_N	current normalized transducer output at temperature (T)
P	hydrostatic pressure, lb/in^2.
psi	$pounds/in.^2$
R	coordinate direction, radius, in.
R_{CX}	circuit resistance, ohms
S	temperature sensitivity of semiconductor element, $mV/^oF$

LIST OF SYMBOLS (Continued)

Se	gage sensitivity, mV/psi
T	temperature, ^{o}F
t	time, min
t	thickness, in.
u	displacement, in.
U_Z	displacement, in axial direction, in.
U_R	displacement in radial direction, in.
U_S	uncertainty of gage output at a particular pressure level, mV/mA
ZO	gage zero offset, mV
ZO_C	corrected zero offset, mV
α_C	thermal expansion of case, in./in./^{o}F
α_I	thermal expansion of insulation, in./in./^{o}F
α_P	thermal expansion of propellant, in./in./^{o}F
α_S	thermal expansion of steel, in./in./^{o}F
β	angle, degrees
Δ	delta, change (difference)
ϵ	strain, in./in.
ϵ_o	initial strain, in./in.
ϵ_t	strain at time t, in./in.
ϵ_{HMAX}	maximum hoop strain, in./in.
ρ	mass density, lb-sec^2/in.^{4}
σ_R	radial stress, psi
σ_Z	axial stress, psi
τ_{RZ}	shear stress, psi
θ	coordinate direction, rad
μ	micro inches, 10^{-6} in.
ω	natural frequency, radians/sec